MOLECULAR MARKERS OF MECHANORECEPTORS AND POTENTIAL MOLECULES FOR GATING MECHANOTRANSDUCTION

Dissertation to obtain

the academic degree of Doctor rerum naturalium

(Dr.rer.nat)

by

Yinth Andrea Bernal Sierra

Developed in the laboratory of "Molecular Physiology of Somatic Sensation" at the

Max Delbrück Center for Molecular Medicine under the direction of Prof. Dr. Gary R. Lewin

Submitted to the Departament of Biology, Chemistry and Pharmacy

of Freie Universität von Berlin

Berlin, March 2013

1st Reviewer: Prof. Dr. Fritz G. Rathjen

2nd Reviewer: Prof. Dr. Gary R. Lewin

Date of defense: 27.08.2013

ACKNOWLEDGEMENTS

SUMMARY

In somatosensory perception the neurons of the dorsal root ganglia (DRG) are the first responders to the different types of stimuli applied on the skin, and a specific type of stimulus also activates a specific subtype of sensory afferents. Genetic labelling of DRG cell subtypes allows their identification in vivo and in vitro providing a unique opportunity to study the physiology of these cells and could give insights into what makes them modality specific. The first part of this study aimed to use the promoter of the T-type calcium channel subunit 3.2 ($Ca_v3.2$) as a molecular marker for the mechanical ultra sensitive subpopulation of DRG cells, the putative D-hair receptors. Using a knock-in approach two mouse strains were produced. The first strain expresses the GFP protein under the promoter of the $Ca_v3.2$ ion channel ($Ca_v3.2^{GFP}$). Characterization of the $Ca_v3.2^{GFP}$ knock-in mouse using immunofluorescence analysis showed that the promoter of the $Ca_v3.2$ ion channel is strongly activated in the hippocampus in the brain of adult mice. In addition, the activity of the $Ca_v3.2$ ion channel promoter in the DRG was also determined in development. Analysis of GFP expression using immunofluorescence, Western blot and qPCR, showed that GFP protein can be detected at stage E9.5 in some cells of the neuronal crest. At stage E13.5 few GFP$^+$ cells are observed in the DRG, and at stage E18.5 GFP is expressed in 7% of the cells of the DRG. Characterization of sensory afferent subtypes at E18.5 using immunofluorescence showed that GFP$^+$ cells co-stained with TrkB and TrkC and only few GFP$^+$ cells were TrkA positive. The second strain expresses the CRE recombinase under the promoter of the $Ca_v3.2$ ion channel ($Ca_v3.2^{Cre}$). Breeding of the $Ca_v3.2^{Cre}$ mouse with the reporter line Tau$^{(mGFP)}$ permitted the analysis of innervation of the sensory end organs in the skin. GFP$^+$ afferents in $Ca_v3.2^{Cre}$; Tau$^{(mGFP)}$ animals innervated hair follicles and Meissner corpuscles, but not Merkel cells. The GFP signal in $Ca_v3.2^{Cre}$; Tau$^{(mGFP)}$ animals was sufficient for visualization of GFP$^+$ DRG cells in vitro so that electrophysiological characterization of GFP$^+$ DRG cells in cell culture was possible. Whole-cell current clamp recordings showed that about 50% of GFP$^+$ DRG cells have action potential with characteristics of mechanoreceptors and that the other 50% of GFP$^+$ DRG cells showed action potential with characteristics of nociceptors. Although the $Ca_v3.2$ promoter did not show high expression specificity only for D-hair receptors as expected, the strains generated are still very useful tools to study the physiology of cells expressing this subtype of T-type calcium channel and its role in those cells.

In contrast to the large body of information regarding the physiological and anatomical properties of primary afferents and despite the extensive efforts to identify

mechanotransduction genes in mammals, the molecular components of the transduction complex in DRG are still elusive. In mice only the stomatin-like protein-3 (SLP-3) has been shown to be essential for touch sensation. In the second part of this work I screened for a 100 nm long tether protein shown previously in my laboratory to be involved in mechanotransduction by connecting the transduction channel to the extracellular matrix. The tether protein is expressed in DRG but not in SCG, binds to laminin and is cleaved by furing proteinase. A pre-selection of candidate proteins to tether protein were made using a Phython script to search for proteins with a furin cleavage site in the mouse genome. Subsequently the expression of these proteins was determined in DRG vs. SCG using qPCR, and from this analysis only six proteins were selected as potential candidates. Using microcontact printing, it was shown that six tether protein candidates localized to neurites growing on laminin but not on neurites growing on laminin-332. After immunogold labeling and transmission electron microscopy (TEM) of the six protein candidates only two proteins remain promising candidates for the tether protein.

ZUSAMMENFASSUNG

Primär sensorische Neurone, deren Zellkörper in den dorsalen Wurzelganglien liegen, sind die ersten Neurone, die Informationen ueber verschiedene Stimulationen der Haut weiterleiten. Dabei führt ein spezifischer Stimulus zur Aktivierung eines spezifischen Subtyps dieser sensorischen Afferenzen. Mit Hilfe genetischer Marker können die verschiedenen Nervenzelltypen in vitro und in vivo in den dorsalen Wurzelganglien identifiziert werden. Dies ermoeglicht die Untersuchung der Physiologie und der Spezifizität der Modalität dieser Zellen. Im ersten Teil dieser Studie wurde der Promotor des T-Typ Kalzium-Kanals der Untereinheit 3.2 ($Ca_v3.2$) als molekularer Marker für putative D-Haarrezeptoren, die sensitivste Subpopulation mechanischer Zellen der dorsalen Wurzelganglien, verwendet. Zwei knock-in Mausstämme wurden in dieser Studie generiert. Der erste Mausstamm exprimiert grün fluoreszierendes Protein (GFP) unter Kontrolle des Promotors des $Ca_v3.2$ Ionenkanals ($Ca_v3.2^{GFP}$). Durch immunohistochemische Charakterisierung des $Ca_v3.2^{GFP}$ knock-in Mausstamms konnte gezeigt werden, dass im Hippocampus adulter Mäuse der Promotor des $Ca_v3.2$ Ionenkanals sehr stark aktiviert ist. Zusätzlich wurde die Aktivität des Promotors für den $Ca_v3.2$ Ionenkanal im Laufe der Entwicklung bestimmt. Durch die Analyse der GFP-Expression mittels Immunofluoreszenz, Western Blot und qPCR konnte gezeigt werden, dass GFP während des Embryonalstadiums E9,5 in einigen Zellen der Neuralleiste exprimiert wird. Im Embryonalstadium E13,5 konnten nur wenige GFP^+ Zellen in den dorsalen Wurzelganglien lokalisiert werden, während im Embryonalstadium E18,5 GFP in 7 % der Zellen der dorsalen Wurzelganglien detektiert werden konnte. Die immunzytochemische Charakterisierung verschiedener Subtypen sensorischer Afferenzen hat gezeigt, dass die GFP^+ Zellen positiv für TrkB (Mechanorezeptoren) und TrkC (Propriozeptoren) waren und nur wenige positiv für TrkA (Nozizeptoren). Im zweiten Mausstamm wird die Cre-Rekombinase unter Kontrolle des Promotors des $Ca_v3.2$ Ionenkanals ($Ca_v3.2^{Cre}$) exprimiert. Durch die Kreuzung der $Ca_v3.2^{Cre}$ Maus mit der Reportermaus $Tau^{(mGFP)}$ konnte die Innervierung der putativen D-Haarrezeptoren in den Sinnesendorganen der Haut untersucht werden. Eine Innervierung mit GFP^+ Afferenzen konnte in Haarfollikeln und Meissner-Körperchen, jedoch nicht in Merkel-Zellen nachgewiesen werden. Des Weiteren wurden die Zellen der dorsalen Wurzelganglien der $Ca_v3.2^{Cre}$; $Tau^{(mGFP)}$ Maus primaer kultiviert und die GFP^+ Zellen elektrophysiologisch charakterisiert. In Patch-Clamp-Messungen, durchgefuehrt in der Ganz-Zell-Konfiguration, konnte gezeigt werden, dass 50 % der GFP^+ Zellen Aktionspotentiale charakteristisch für Mechanorezeptoren und

50 % solche charakteristisch für Nozizeptoren erzeugen. Obwohl der Ca$_v$3.2 Promotor wider Erwarten nicht spezifisch in D-Haarrezeptoren exprimiert wird, sind die generierten Mausstämme für Untersuchungen der Physiologie dieses T-Typ Kalziumkanals nuetzlich.

Heute existiert ein breites Wissen über die physiologischen und anatomischen Eigenschaften der primären Afferenzen und in der experimentellen Forschung wurden große Anstrengungen zur Identifizierung der an der Mechanotransduktion beteiligten Gene in Säugern unternommen. Jedoch konnten die molekularen Komponenten des Transduktionskomplexes der dorsalen Wurzelganglien bislang nicht identifiziert werden. In der Maus konnte lediglich Stomatin-ähnliches Protein 3 (SLP-3) als für den Tastsinn essentielles Protein gefunden werden. Aus diesem Grund wurde im zweiten Teil dieser Arbeit nach der Identitaet eines 100 nm langen Halteproteins, dessen Existenz zuvor in meinem Labor bewiesen wurde. Dieses Protein ist funktionell an der Mechanotransduktion beteiligt, indem es moeglicherweise den Transduktionskanal mit der extrazellulären Matrix verbindet. Das Halteprotein wird in dorsalen Wurzelganglien, jedoch nicht in den superioren zervikalen Ganglien exprimiert, bindet an Laminin und wird durch Furin-Proteinasen gespalten. Eine Vorauswahl möglicher in Frage kommender Kandidaten wurde durch die Verwendung eines Phython-Skripts vorgenommen, um nach Proteinen mit einer Furin-Spaltstelle im Mäusegenom zu suchen. Anschließend wurde die Expression dieser Proteine mit qPCR in dorsalen Wurzelganglien bestimmt und mit superioren zervikalen Ganglien verglichen. Mittels dieser Analyse wurden sechs potentielle Kandidaten selektiert. Diese wurden durch Mikro-Kontakt-Printing in Neuriten von auf kommerziellem Laminin wachsenden doralen Wurzelganglienzellen lokalisiert. In Neuriten von auf Laminin-332 wachsenden Zellen konnten diese Proteine nicht lokalisiert werden. Durch Immunogold-Färbung und Transmissionselektronenmikroskopie (TEM) konnte ein Teil dieser Protein-Kandidaten subzellulär in Zellen der dorsalen Wurzelganglien lokalisiert werden. Aufgrund dieser Ergebnisse könnten zwei der untersuchten Proteine mögliche Kandidaten für das Halteprotein sein.

TABLE OF CONTENTS

1. PART I: Ca$_v$3.2 CHANNEL PROMOTER AS IN VIVO CELL MARKING

1.1. INTRODUCTION

1.1.1. Somatosensation

The somatosensory system allows living organisms to perceive the physical interaction between them and their surroundings. Somatosensation comprises different modalities: discriminative touch, which is used for recognizing size, shape, texture of objects and their movement upon the skin; nociception, which is used for detecting painful stimuli and temperature; and propioception, which provides information about limb position and muscle forces required by the central nervous system to monitor and execute movements. In order to transmit the diversity of sensations we experience, the somatosensory system has evolved to enable the encoding of the stimuli into four attributes: modality, location, intensity and timing. Perception starts when a stimulus activates specialized receptors that in turn excite the sensory neurons of the dorsal root ganglion (DRG) that encode the sensory information transmitted to the somatosensory cortex in the brain via the spinal cord. Elucidation of the mechanisms underlying the coding of somatosensory stimuli requires the understanding of the cellular and molecular properties of DRG neurons that determine their specialization and selectivity to external stimuli.

1.1.1.1. Dorsal Root Ganglion Neurons

Somatosensory neurons are pseudounipolar neurons with their cell soma located in the dorsal root ganglion. Their axon has two branches, one projecting to the periphery to innervate the skin or specialized sensory end organs, and the other one projecting to the central nervous system. According to the amount of myelination of their axons, DRG neurons are classified into Aα, Aß, Aδ and unmyelinated C-fibers. Myelin thickness determines the velocity at which primary afferents conduct action potentials along the axon. Thus large diameter heavily myelinated Aα-fibers are much faster than unmyelinated C-fibers (Harper and Lawson, 1985; Horch et al., 1977). Considering the long distance action potentials travel along the axon from the stimulation site where the action potential is generated until the second order neuron located in the central nervous system (in

humans it could be longer than 1 meter), fast conduction velocities of sensory afferents guarantees an almost instantaneous perception of the stimuli received. In mice, for instance, conduction velocity of Aß-fibers is in the range of 15 m/s, followed by Aδ-fibers with conduction velocity of approximately 5 m/s and unmyelinated C-fibers being the slowest transmitting action potentials at a speed of 0.5 m/s (Koltzenburg et al., 1997; Milenkovic et al., 2008).

The reason why DRG neurons respond specifically to a particular type of stimulus is related to the morphology of the sensory end organ they innervate and the physiological properties of each sensory neuron subtype. The study of the physiological properties of mouse sensory neurons in vitro as modality, conduction velocity, sensitivity and adaptation has been made possible using the skin nerve preparation. In this methodology the nerve and the patch of the skin which it innervates is isolated and the electrical response of single fibers is recorded during application of a stimulus to the skin (Koltzenburg et al., 1997; Reeh, 1986). Determination of the minimum force required to activate a given sensory afferent allowed a further classification regarding their mechanical sensitivity into low-threshold mechano-receptors (LTM), responding to innocuous forces, and high-threshold mechano-receptors (HTM), which are excited by injurious forces. In general, Aβ fibers which have encapsulated or specialized nerve endings, and high conduction velocities are LTM, and unmyelinated C-fiber nociceptor with no encapsulated endings and slow conduction velocities are HTM and transmit pain sensation. However there is an exception in that one type of C-unmyelinated fiber transmits pleasant touch and is classified as LTM (Löken et al., 2009; Olausson et al., 2002; Vallbo et al., 1999). Aδ-fibers include two subgroups: the LTM D-hair receptors and the HTM A-fiber mechanonociceptors (AM).

Another very important feature of sensory afferents is the way sensory neurons respond to the dynamic and the static phase of mechanical stimulation. Rapidly adapting (RA) afferents fire action potentials only in the dynamic phase of stimulation, whereas slowing adapting receptors (SA) respond to both the dynamic and static phase. Thus, RA afferents sense motion of objects on the skin, the faster the object moves the more action potentials it fires and the duration of the movement signals the duration of the afferent's response. SA afferents give information about the intensity of pressure and the shape of the object, the total number of action potential fired per time unit is proportional to the indentation force (Brown and Iggo, 1967; Leem et al., 1993).

Conduction velocity, sensitivity and adaptation are important properties of dorsal root ganglia neurons for coding somatic sensation, but are not enough to fully describe the modality of the stimulus, the geometry of an object and the location where the stimulus was applied.

1.1.1.2. Sensory End organs

A combination of psychophysical and neurophysiological studies had accumulated evidence that links each afferent type to a distinctly different perceptual function, and shows that the structures associated with the sensory endings are specialized for their assigned functions. These non-neuronal end organs, called sensory end organs, encapsulate the peripheral end of the afferent fiber and function to modulate the response of sensory neurons. They help to determine the afferent's sensitivity, adaptation properties and their receptive field size. Thus the combination of the properties of the afferent together with the anatomical and physiological properties of the sensory end organ determines the kind of modality at to which the afferent responds.

1.1.1.2.1. Merkel cells

Merkel cells appear in clusters which are composed of epithelial cells **Figure 1**. They are located in superficial layers of the skin. Each cluster contains 50-70 Merkel cells innervated by a single myelinated Aβ-fiber. These SA units (sometimes also called type I or SA-I), respond to sustained indentation with a sustained slowly adapting discharge that is linearly related to indentation depth. These afferents are specially sensitive to points, edges and curvature and have the highest spatial resolution of all mechanoreceptors. Individual SA-I afferents can resolve spatial differences as small as 0.5 mm, although their receptive field diameters are 2–3 mm. That is why Merkel cells are very good at encoding the texture, and precise spatial information of the stimulus (Blake et al., 1997; Johnson et al., 2000).

1.1.1.2.2. Meissner Corpuscles

Meissner corpuscles are encapsulated end organs innervated by Aß-fibers that are RA low-threshold mechanoreceptors **Figure 1**. They have a slightly bigger receptive field than SA-I receptors and respond to stimuli relatively uniformly over their entirely receptor field. Thus they havepoor spatial resolution. They selectively respond to dynamic skin

deformation and transmit information about movement across the skin. Meissner corpuscles are well suited for detecting slip between the skin and an object because they are the most effective at signaling sudden forces. For example, they are very responsive to movement of an object held in the hand (Lamb, 1983; Macefield et al., 1996). Thus an important perceptual function of Meissner corpuscles seems to be the relay of feedback signals for grip control.

1.1.1.2.3. Pacinian Corpuscles

Pacinian corpuscles (PC) are also encapsulating sensory end organs. They have an onion-like structure made up of layered lamellae. PCs are innervated by low-threshold RA-Aß afferents **Figure 1**. These afferents are extremely sensitive responding to 10 nm of indentation at 200 Hz (Brisben et al., 1999). This high sensitivity together with their deep location in the dermis and in the subcutaneous tissue are the reasons why Pacinian corpuscles have almost no spatial resolution. The layered lamellae of PCs function as an extremely selective high-pass filters such that the afferent only responds to high frequencies (Bell et al., 1994). They respond to frequencies > 20 Hz with high sensitivity. Because of these properties, the PC population produces a high-fidelity neural image of transient and vibratory stimuli transmitted to the skin by objects (Brisben et al., 1999).

1.1.1.2.4. Ruffini End Organ

Ruffini end organs are SA (sometimes also refered as type-II or SA-II) low-threshold fluid-filled encapsulated corpuscles innervated by an Aß-fiber. Located in the dermis, Aß-fiber endings within Ruffini corpuscles have a large receptive field and respond more sensitively to skin stretch than indentation **Figure 1**. They are involved in perception of the direction of object motion through the pattern of skin stretch (Srinivasan and Dandekar, 1996). It is also believed that they may play a role in propioception because they have receptive fields on the skin over foot joints and respond to joint movement (Leem et al., 1993).
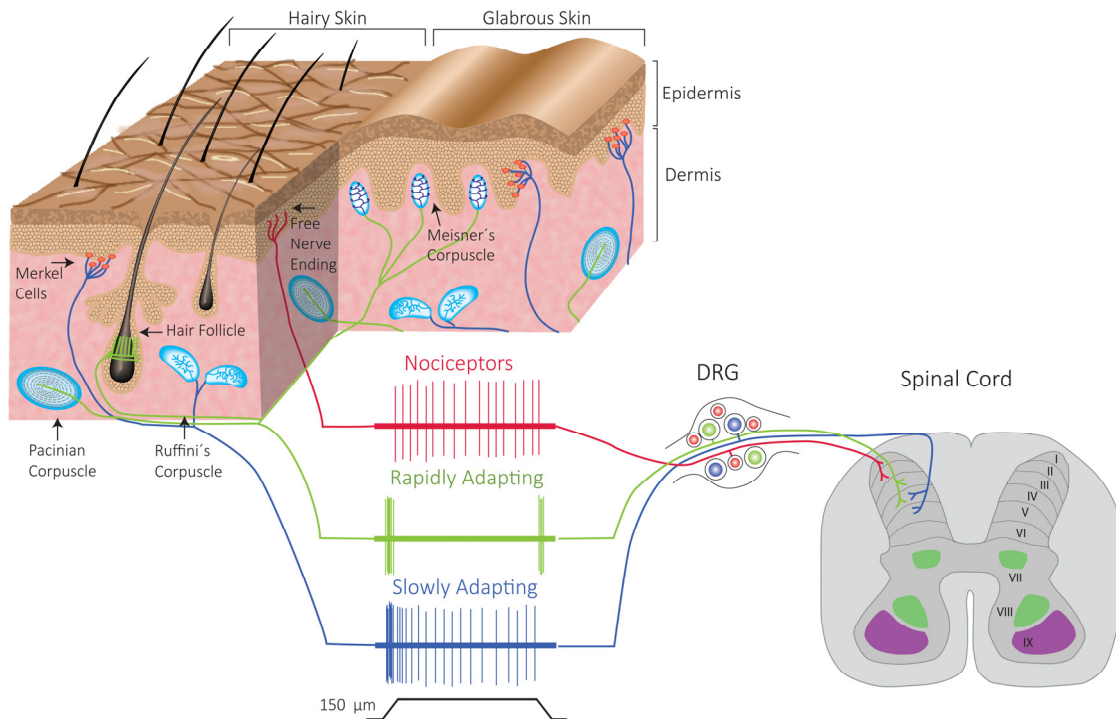
Figure 1. Sensory end organs in the skin and their innervation by sensory afferents. Sensory End organs located in the skin are innervated by specific primary afferents. The cell bodies of the afferents are located in the DRG. The way in which sensory neurons respond to mechanical stimuli depends on the sensory neuron subtype and the morphology of the end organ they innervate. According to the modality they transduce, sensory neurons have different patterns of nerve termination in the spinal cord.

1.1.1.2.5. Hair Follicles

Studies made in cats and rabbits classified the hair follicle afferents as rapidly adapting receptors divided into three groups: down hair afferent (D-hair receptors) each innervated by an Aδ nerve fiber axon, guard hair (G-hair) and tylotrich each innervated by an Aβ nerve fiber. The tylotrich afferents are normally associated with Merkel cells **Figure 1**. They respond to hair displacements and the velocity of the displacement is related to their frequency of discharge in an exponential manner. The D-hair receptors are associated with hairs small in size compared to the other hair afferents and are also the most sensitive, having the lowest mechanical thresholds. Another peculiar characteristic of primary afferents innervating hairs is that normally one myelinated axon supplies many hair follicles and each hair follicle is supply by a number of different axons (Brown and Iggo, 1967). However recently, genetic labelling identified that in the mouse, one type of C-unmyelinated low-threshold receptor (C-LTMR) also innervates hair follicles. Each of the three type of hair follicles found in the mouse is innervated by two or three different sensory afferents. Thus, the Zigzag hairs which are the smallest in mouse skin were

connected to C-LTMR and Aδ-fibers, medium size hairs Awl/Auchene were innervated by C-LTMR, Aδ-fibers and Aβ-fibers, and the biggest hairs G-hairs were innervated by Aβ-fibers and were also associated with Merkel cell complexes which are Aß- SAM (Li et al., 2011a). How this innervation pattern would affect the kind of perception produced by the activation of these receptors is still unknown, but since the common difference between them is the conduction velocity, it might account for the temporal coding of the stimulus when sensory information is integrated and processed in the central nervous system.

1.1.1.2.6. Free Nerve Endings

Only two types of sensory afferent have been observed innervating skin without association to elaborated auxiliary structures: Aδ-fibers and the unmyelinated C-fibers **Figure 1**. In this case the Aδ-fibers are high-threshold SAM and are polymodal, in that they respond to mechanical, chemical and heat stimuli but have a relatively high heat thresholds (>50°C)(Burgess and Perl, 1967). Moreover, another interesting property of these receptors is that if the heat stimulus is maintained, these afferents will subsequently respond at lower temperatures. And most importantly, they will sensitize (the heat or mechanical threshold will drop) in the setting of tissue injury (Treede et al., 1992). C-fibers are SAM that can be further classified into high- and low-threshold mechanoreceptors (HTM and LTM). They are a heterogeneous polymodal population responding to mechanical and/or thermal stimuli, initially identified as the C-mechanoheat (CMH) and the mechano-responsive C-units (CM) (Birder and Perl, 1994). However, later on another C type afferent was added to the classification list, the heat-responsive, but mechanically insensitive, unmyelinated afferents (so-called silent nociceptors) that develop mechanical sensitivity only in the setting of injury (Schmidt et al., 1995). These afferents are more responsive to chemical stimuli (capsaicin or histamine) compared to the CMHs and probably come into play when the chemical milieu of inflammation alters their properties. Subsets of these afferents are also responsive to a variety of itch-producing pruritogens (Schmelz et al., 2003; Wilson et al., 2011). In addition, it was though that C-fibers responded only to noxious stimuli or temperature, but in 2008 it was discovered that an interesting population of C-fibers respond to innocuous stroking of the hairy skin, but not to heat or chemical stimulation. These fibers seem to mediate pleasant touch (Olausson et al., 2008).

1.1.1.2.7. Proprioceptors

Proprioceptors are classified into three groups. The first is the muscle spindle primary ending. These afferents are Aα-fibers, also called Ia afferent fibers. They are exceptionally sensitive to small changes in the length of their parent muscle through the detection of high frequency vibration (Brown et al., 1967). This has led to the general acceptance that the Ia afferent fibers are the principal receptors in mammalian muscles for signaling relative changes in muscle length or muscle stretch velocity. The second group of propioceptors is the muscle spindle secondary endings (II afferent fibers). These are innervated by Aß-fibers and they are an order of magnitude less sensitive to high-frequency vibration, and are often assigned the role of signaling absolute muscle length. Then information conveyed by Muscle spindles is used by the central nervous system to sense relative position of the body segments. The third group of proprioceptors is the Golgi tendon organs, Golgi tendon organs (Ib afferent fibers) are connected to an Aα-fiber, and are also capable of responding to small sinusoidal changes in muscle length (particularly during a contraction), presumably via changes in muscle tension, but are rarely given a role in encoding muscle length and have long been considered simply to signal muscle contraction (Fallon and Macefield, 2007; Fulton and Pi-Suñer, 1928).

1.1.1.3. Somatosensory Pathways

Sensory receptors in the skin have a topographic distribution that informs the central nervous system about the location at which the stimulus was applied. The area of the skin innervated by the nerve fibers coming from a single dorsal root ganglion is called a dermatome. The distribution of dermatomes for all spinal segments are arranged in a caudal-rostral sequence, with the anus and the genitalia most caudally, and the shoulder, neck and dorsum of the head rostrally.

This systematic topographic organization continues in the central nervous system where the central axons of dorsal root ganglion neurons branch extensively and project to nuclei in the spinal gray matter and brain stem. In the spinal cord the gray matter is divided into 10 layers (laminae), each layer contains functionally distinct nuclei that have different patterns of projections. Laminae I-VI correspond to the dorsal horn. Within this region the axons of nociceptive afferents conveying pain and temperature terminate in lamina I-II, low threshold mechanoreceptors terminate in lamina III-V. Lamina VII is roughly

equivalent to the intermediate zone and laminae VIII and IX comprise the ventral horn, where axons from proprioceptive afferents terminate. Lamina X consists of the gray matter surrounding the central canal (Caspary and Anderson, 2003). In addition, the sensory specialization of dorsal root ganglion neurons is preserved in the central nervous system through distinct ascending pathways for the various somatic modalities. The modalities of touch and proprioception are transmitted directly to the medulla through the ipsilateral dorsal columns. Pain and temperature signals are relayed through synapses in the spinal cord to the contralateral anterolateral quadrant, where axons of dorsal horn neurons ascend to the brain stem and thalamus.

1.1.1.3.1. The Dorsal Column-Medial Lemniscus Pathway

Primary afferents mediating tactile sensation and proprioception immediately turn rostral up the spinal cord towards the brain, ascending in the dorsal white matter and forming the dorsal columns. In a cross-section of the spinal cord, at cervical levels, two separate tracts can be seen: the midline tracts comprise the gracile fasciculus conveying information from the lower half of the body (legs and trunk), and the outer tracts comprise the cuneate fasciculus conveying information from the upper half of the body (arms and trunk). The first synapse of the primary afferents is made with second order neurons at the medulla where fibers from each tract synapse in a nucleus of the same name: the gracile fasciculus axons synapse in the gracile nucleus, and the cuneate axons synapse in the cuneate nucleus. The axons of the post-synaptic neurons cross the midline immediately to form a tract on the contralateral side of the brainstem, the medial lemniscus, which ascends through the brainstem to the next relay station in the midbrain, specifically, in the thalamus **Figure 2a** (McGlone and Reilly, 2010).

© 2011 Pearson Education, Inc.
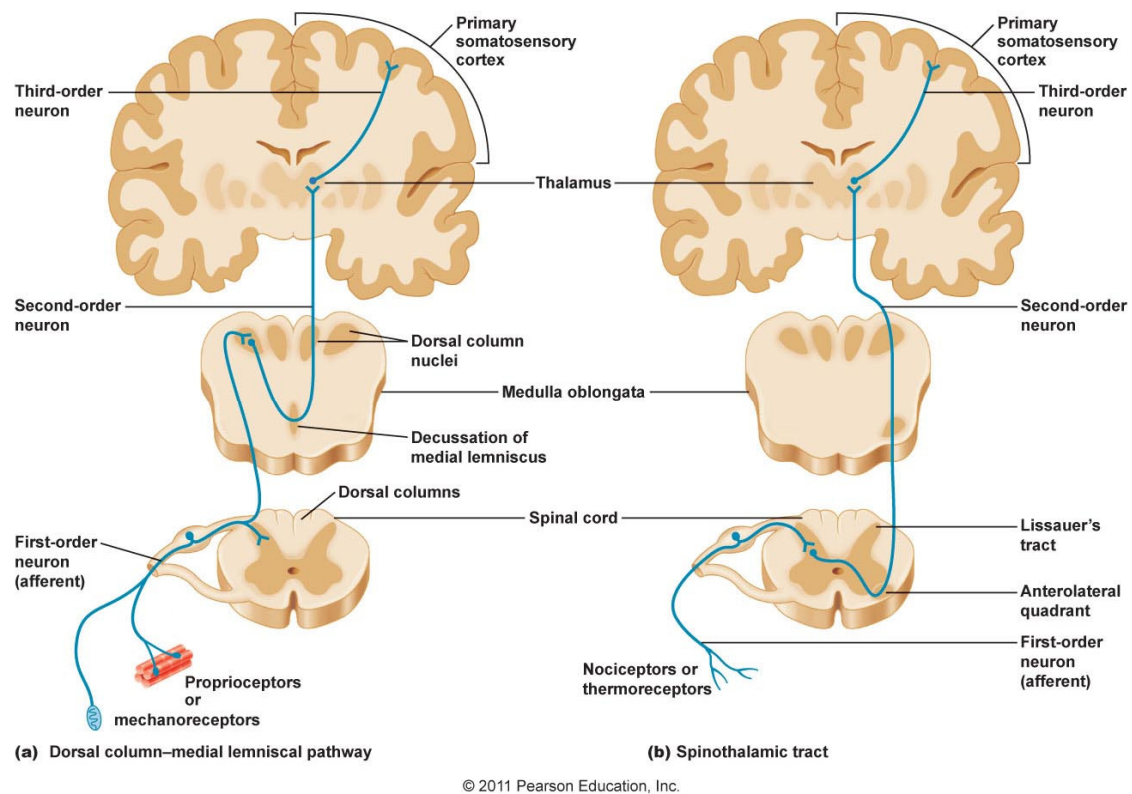
Figure 2. Somatosensory pathways. a) Representation of the dorsal column-medial lemniscal pathway taken by sensory afferents mediating tactile sensation and propioception to send information from the periphery to the brain. b) Representation of the Spinothalamic tract pathway carrying pain and temperature information from the periphery to the central nervous system. Taken from Principles of human physiology. Chapter 10. (5th edition); Stanfield (2012).

1.1.1.3.2. The spinothalamic Pathway

Pain and temperature afferents enter the dorsal horn of the spine and synapse within one or two segments, forming Lissauer's tract. The two types of pain fibers, C and Aδ, enter different layers of the dorsal horn. Aδ fibers enter at the marginal zone (lamina I) and the nucleus proprius (layer IV), and synapse on a second set of neurons which are the secondary afferents which relay the signal to the thalamus. The secondary afferents from both layers send their axons across the midline of the spinal cord to its opposite side and ascend in the spinothalamic tract. C-fibers enter the substantia gelatinosa (lamina II) and synapse on interneurons, which do not project out of the immediate area, but relay to secondary afferents in either lamina I, or lamina IV. The spinothalamic tract ascends the entire length of the spinal cord and the entire brainstem, and on reaching the midbrain is continuous with the medial lemniscus. These tracts enter the thalamus together **Figure 2**. Like axons in the dorsal columns, the axons of the spinothalamic tract are also arranged

somatotopically. Axons entering at each successive spinal segment lie adjacent to those ascending from lower positions of the spinal cord.

It is important to note that although most of the afferents described fit into the architecture-function depicted above, a degree of mixing occurs between the tracts, for example, with some light touch information traveling in the spinothalamic tract, with the result that damage to the dorsal columns does not completely remove touch and pressure sensation. Some proprioceptive information also travels in the dorsal columns, and follows the medial lemniscus to the cortex providing conscious awareness of body position and movement. The pain and temperature system also has multiple targets in the brainstem and other areas(Basbaum et al., 2009).

1.1.2. Development of Dorsal Root Ganglia Neurons

The dorsal root ganglia neurons develop from the neuronal crest cells (NCCs). The NCCs generate many different cell types including sympathetic, glia, endoneural fibroblast and melanocytes. In the mouse, generation of DRG and sympathetic neurons starts at E8.5 when the NCCs start migrating ventrally between the neural tube and the anterior portion of the somite. Within these migrating cells, there is a temporal distinction, an early group begins migrating at E8.5 and gives rise to sympathetic neurons, while the later group starts migrating at E9.5 to become the cells of the DRG at E10.5 (Serbedzija et al., 1990).

Neurogenesis of sensory neurons occurs in three successive waves and is tightly coordinated with cell diversification (Ma et al., 1999). The first wave of neurogenesis, initiated by the basic helix-loop helix transcription factors neurogenin 2 (NGN2), generates mechanosensitive and propioceptive cells which express TrkB and/or TrkC. These cells account for one third of the migrating NCCs and eventually represent about 4% of the adult neurons in the DRG (Rifkin et al., 2000). The second wave of neurogenesis is initiated by neurogenin 1 (NGN1) in SOX10$^+$ multipotent cells and involves two thirds of the migrating NCCs, it occurs in postmigratory NCCs in the ganglion and eventually represent 91% of the DRG population resulting in all subtypes of sensory neurons (Frank and Sanes, 1991). The third and last wave of neurogenesis occurs around E11 in SOX10$^+$/Krox20$^+$ cells yielding manly small diameter TrkA$^+$ nociceptive neurons that will eventually represents 5% of the total DRG cells in the adult mouse (Hjerling-Leffler et al., 2005; Maro et al., 2004).
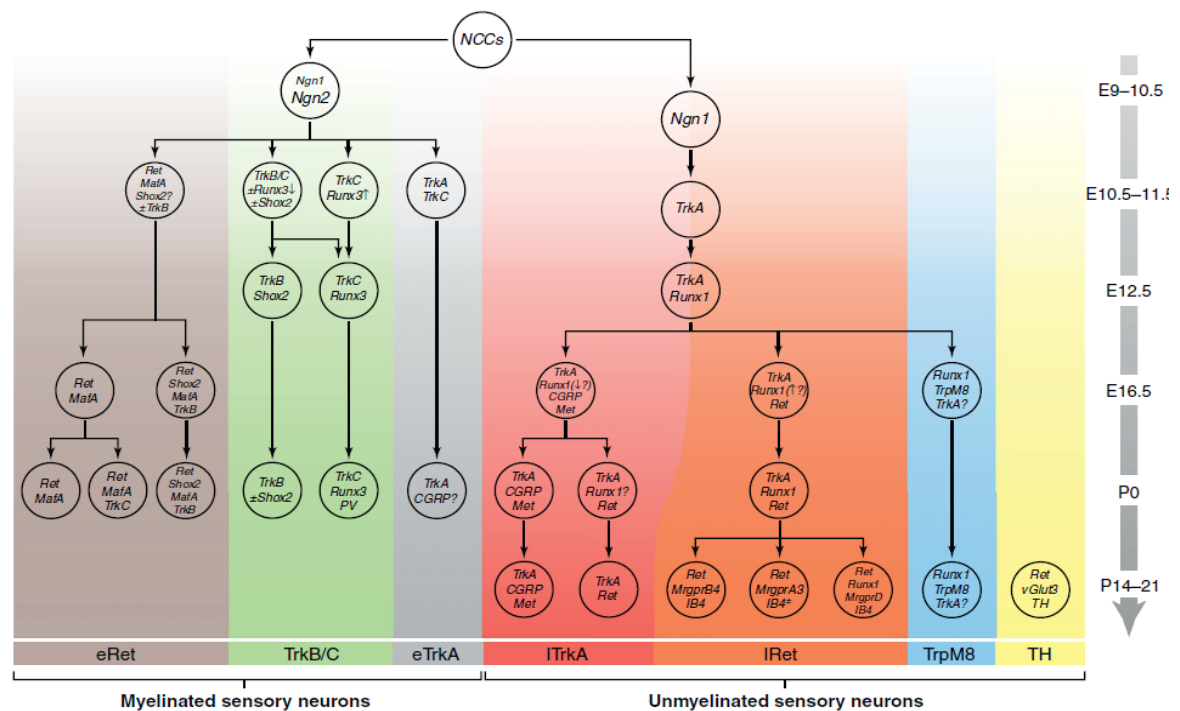
Figure 3. The diversification of sensory neurons during development. Diversification of myelinated and unmyelinated sensory neurons from neuronal crest cells (NCCs), and molecular markers used to identify sensory neurons subpopulations including mechanoreceptors, nociceptors and propioceptors. Diagram taken from Lallemend and Ernfors (2012).

The diversification of sensory neurons into functional subtypes that respondi to specific modalities follows neurogenesis and requires additional specification steps controlled by activation of gene programs together with environmental cues that in a hierarchical process determines cell fate and axonal projections. For example, the transcription factor short stature homeobox 2 (Sox2) is necessary for TrkB expression and suppress TrkC Figure 3. Conditional knock-outs of Sox2 show that it encodes the development of low threshold mechanoreceptive neurons involved in discriminative touch associated with Merkel cells and Meissner corpuscle in the glabrous skin (Abdo et al., 2011; Scott et al., 2011). In addition, signaling of neurotrophin-4 (NT-4) through the TrkB receptor is necessary for survival of sensory neurons upon skin innervation (Rifkin et al., 2000; Stucky et al., 2002). Similarly, the runt-related transcription factor (RUNX) family has key roles in the diversification of sensory neurons. Runx1 and Runx3 are differentially expressed in the DRG, and their non-overlapping expression give rise to two different modalities of sensory neurons. Runx3 is first detected at E10.5 in the DRG and is important for establishment of an early TrkC$^+$ population that will give rise to proprioceptive neurons at birth Figure 3 (Levanon et al., 2002). In Runx3$^{-/-}$ animals proprioceptive afferents fail to project to their targets in the spinal cord as well as those in the muscle (Inoue et al., 2002). Since, Runx3 is

necessary for TrkB repression and expression of TrkC, no signaling of neurotrophin-3 (NT-3) through the TrkB receptor is possible and survival of propioceptive neurons is compromised as seen in NT-3$^{-/-}$ animals (Ernfors et al., 1994; Oakley et al., 2000). On the other hand Runx-1 is specifically expressed in an early TrkA$^+$ population during development, and postnatally its expression is more restricted to a subtype of nociceptors (Chen et al., 2006; Levanon et al., 2001; Marmigère et al., 2006). All the transcription factors, neurotrophic factors and neurotrophic factor receptors described so far underlie the generation of three big groups of sensory neurons, mechanoreceptors (TrkB$^+$), nociceptors (TrkA$^+$) and proprioceptors (TrkC$^+$). However, the diversity of sensory neurons is more extensive than three groups. In this regard, gene screenings and the progress of transgenic technologies as conditional knock-out and inducible Cre animals have made possible the determination of new transcription factors responsible for diversification of even more specific sensory subtype lineages, and at the same time allowed the characterization of the physiological properties of these cells as well as their innervation pattern in the skin and in the spinal cord. This is the case in the recently characterized early Ret (eRet) population which diversifies at later stages into large diameter rapidly adapting low-threshold mechanoreceptors (RA-LTMR) innervating Meissner and Pacinian corpuscles and forming hair follicle lanceolate endings. These eRet neurons selectively express the transcription factor MafA and, at birth have diversified into three types defined as Ret$^+$/MafA$^+$, Ret$^+$/TrkC$^+$/MafA$^+$ and Ret$^+$/TrkB$^+$/MafA$^+$/Shox2$^+$ neurons (Bourane et al., 2009; Luo et al., 2009; Wende et al., 2012). The late Ret neurons (lRet) which are those neurons starting Ret expression in TrkA$^+$ cells at E15 and also depend on Runx1 activity for differentiation, produce three different subtypes, the Ret$^+$/MrgprB4$^+$/IB$_4$$^+$, Ret$^+$/MrgprA3$^+$ and Ret$^+$/Runx1$^+$/MrgprD$^+$/IB$_4$$^+$ (Mrgpr for Mas-related G protein-coupled receptors) **Figure 3** (Chen et al., 2006; Liu et al., 2009, 2008).

Finally, the course of differentiation during development is still not completely clear. Some other molecules have been discovered and proposed as molecular markers for sensory neurons that seem to underlie specific sub-modalities. Tyrosine Hydroxylase (TH) positive cells have been proposed to be identical to low-threshold unmyelinated C-fibers that are negative for TrkA and IB$_4$ and innervate hair follicles and terminate in the lamina II in the spinal cord (Li et al., 2011a). TrpM8$^+$ linage which is activated by cooling and cooling compounds seem to arise from TrkA$^+$/Runx1$^+$ cells (Chen et al., 2006; Takashima et al., 2010).

1.1.3. Voltage-gated Calcium channels

Voltage activated Ca^{2+} channels (VACCs) transduce membrane potential changes into intracellular Ca^{2+} signals in a wide variety of cell types, including nerve, endocrine and muscle cells. Their activation triggers a variety of processes including muscle contraction, chemotaxis, gene expression, synaptic plasticity, and secretion of hormones and neurotransmitters. These channels consist of a principal α_1 subunit and several auxiliary subunits ß, $\alpha_2\delta$, and γ, which have regulatory functions. The α_1 subunit constitutes the pore forming component and contains the voltage sensor and the gating machinery responsible for the basic electrophysiological and pharmacological properties that is been used for classification of the voltage-gated calcium channels family. According to the degree of depolarization required for activation, VACCs have been classified into two big groups, the high voltage activated calcium channels (HVA) that need high depolarizing potentials to open (more positive than -20 mV), and low voltage activated calcium channels (LVA) that are activated by low threshold depolarizing potentials (more positive than -70mV). Further classifications were made according to their current properties and pharmacology, and the names were given according to those characteristics. HVA L-type channels are named so because of their large channel conductance amplitude and slow kinetics of current (L for large and long-lasting) and are sensitive to dihydropyridines 1,4-DHPs (nifedipine, nisoldipine, isradipine) with either inhibitory or activatory action on the channel (Hess et al., 1984). The other subset of HVA channels are specifically expressed in neuronal cells and are distinguished for their sensitivity to peptide toxins isolated from cone snails and spiders. The N-type channel, named N-for neuronal, is sensitive to ω-conotoxin GVIA. The channel sensitive to ω-Aga IVA toxin was named P/Q-type calcium channel (P for Purkinje cells)(Llinás, 1988), and the channels resistant to these toxins were named R-type calcium channel, R for resistant (Ellinor et al., 1993). L-type calcium channels are voltage sensors needed for cell function in skeletal muscle, heart, smooth muscle and neurons. N- and P/Q-type channels are the main subtypes of calcium channel that support synaptic transmission and they are concentrated at nerve terminals. T-type calcium channels are the only group of VACCs belonging to the LVA, and named T be cause they carry transient small currents (Nowycky et al., 1985). T-type channels are expressed throughout the body, including nervous tissue, heart, kidney, smooth muscle, sperm, and many endocrine organs, and have been implicated in a variety of physiological processes including neuronal firing, hormone secretion, smooth muscle contraction, myoblast fusion, and fertilization.

The current nomenclature and classification of VACCs was made after cloning of the α_1 subunit based on sequence similarity and molecular structure **Table 1** (Birnbaumer et al., 1994; Ertel et al., 2000; Hess et al., 1984; Snutch et al., 1990; Tsien et al., 1988).

Table No. 1. Nomenclature of VACCs

		Nomenclature according to [1]	Nomenclature according to [2,3]	Structural nomenclature[4]
HVA	L-type		α_{1S}	$Ca_v1.1$
			α_{1C}	$Ca_v1.2$
			α_{1D}	$Ca_v1.3$
			α_{1F}	$Ca_v1.4$
	P/Q -type		α_{1A}	$Ca_v2.1$
	N-type		α_{1B}	$Ca_v2.2$
	R-type		α_{1E}	$Ca_v2.3$
LVA	T-type		α_{1G}	$Ca_v3.1$
			α_{1H}	$Ca_v3.2$
			α_{1I}	$Ca_v3.3$

[1]Tsien et al., 1988. [2]Snutch et al. 1990 [3] Brinbaumer et al. 1994 [4] Ertel et al. 2000

1.1.3.1. T-type calcium channels

LVA T-type calcium channels were first described in rat and chick sensory neurons (Carbone and Lux, 1984; Nowycky et al., 1985), and subsequently in neurons from the inferior olivary nucleus (Llinás and Yarom, 1986). The T-type calcium channel family is composed of three isoforms with high similarity between their sequences, the subunits $Ca_v3.1$, $Ca_v3.2$ and $Ca_v3.3$. The overall amino acid sequences of the $Ca_v3.1$ and $Ca_v3.2$ channels exhibit 57% homology, and their putative transmembrane segments are 90% identical (Cribbs et al., 2000). The whole amino acid sequence of the $Ca_v3.3$ channel is 59.3% identical with the $Ca_v3.1$ sequence, and 56.9% identical with the $Ca_v3.2$ sequence. Its transmembrane segments are only 80% identical with the transmembrane segments of the $Ca_v3.1$ and $Ca_v3.2$ channels (Lee et al., 1999). The high sequence homology had made the determination of their individual properties and roles in native systems difficult due to a lack of subtype specific pharmacologic tools that enable the separation of individual currents. Nevertheless, expression of every subunit in a heterologous system such as HEK cells and a variety of electrophysiological and computer modelling approaches had helped to investigate their properties and the individual contribution of T-type channel isoforms to neuronal excitability (Cribbs et al., 1998).

T-type calcium channels play an important role in cell excitability, their low voltage threshold for activation make them the first responders to small positive changes in membrane polarization that in turn leads to a further depolarization of the cell membrane causing the firing of Na^+ dependent action potentials. T-type Ca^{2+} channels typically activate at potentials slightly positive to -70 mV and whole-cell currents are usually maximal by ~ -40 mV. T-type Ca^{2+} channels are fully inactivated at potentials more positive than -40 mV, inactivate rapidly in a voltage-dependent manner, and deactivate, or close, relatively slowly. Because these channels are inactivated at positive holding potentials, very negative holding potentials (-80 mV or more negative) are required for full availability of the channels. The kinetics of activation and inactivation of T-type channels also display voltage dependency; rates are slow near threshold potentials and accelerate with increasingly positive potentials (Fox et al., 1987; Nowycky et al., 1985; Perez-Reyes et al., 1998). Another striking property of T-type calcium channel kinetics is the overlapping of their activation and inactivation curves that produces a steady-state "window current" over a negative range of potentials which allows a basal inward flux of calcium ions at membrane potentials close to cellular resting potentials (McRory et al., 2001). T-type calcium channels are thought to contribute to distinct neuronal firing patterns because of their unique biophysical properties including the window current and the fact that their activation-inactivation kinetics is strongly voltage dependent (Cain and Snutch, 2010). For instance, neurons with a depolarized membrane potential (and therefore inactivated T-type channels), or neurons that have a low level of expression of T-type channels are more likely to fire single or tonic action potentials. Burst firing will occur if a high density of T-type channels are present and the neuron is held at a hyperpolarized membrane potential to ensure T-type channels are not inactivated. Slow oscillations occur as a result of bi-stability of particular neurons depending on whether the window current is on or off, however it is also dependent on leak potassium and non-specific cationic conductances (Crunelli et al., 2005).

1.1.3.2. T-type $Ca_v3.2$ calcium channel and its function in the Nervous system

Expression of the $Ca_v3.2$ calcium channel had been observed in central and peripheral nervous systems. In-situ hybridization studies showed localization of the T-type channel subunit 3.2 in the olfactory system, basal forebrain, amygdala, layer V of the neocortex, hippocampus, reticular thalamic nucleus and hypothalamus in the brain, in the external layers of the dorsal horn in the spinal cord and in sensory neurons (Talley et al., 1999). The

same study also showed that co-expression of at least two T-type channel subtypes occurs in many brain regions and that the intensity of the signal found for $Ca_v3.2$ subtype overcomes that of $Ca_v3.1$ only in the hippocampus and in the DRG.

In the brain, the $Ca_v3.2$ calcium channel has been proposed to play a major role in the rhythmic properties of the thalamus. The low threshold spikes produced in the thalamus by T-type calcium channels contribute to rebound burst firing and oscillatory behaviour that maintains normal transitions in sensory gating, sleep and arousal (Crandall et al., 2010; Joksovic et al., 2006; McCormick and Bal, 1997). However, although high expression levels of the mRNA $Ca_v3.2$ calcium channel are observed in cells of the reticular thalamic nucleus, in $Ca_v3.2^{-/-}$ animals there is no complete loss of neuronal firing but only a reduction in tonic firing regularity as well as in the number of burst firing epochs in these neurons (Liao et al., 2011). Thus, the $Ca_v3.2$ ion channel is involved in regulating action potential firing in neurons of the reticular thalamic nucleus, but is not essential for their normal behaviour. In contrast to the $Ca_v3.2^{-/-}$ phenotype, knock-out of $Ca_v3.1$ ionic channel in thalamic neurons completely abolishes burst firing in these neurons (Kim et al., 2001). In the hippocampus, where high $Ca_v3.2$ mRNA also has been reported, and calcium signaling is involve in hippocampal synaptic plasticity, learning and memory, no strong evidence for a penetrant functional role of the $Ca_v3.2$ calcium channel has been found. Only recently one study in $Ca_v3.2^{-/-}$ animals indicated that $Ca_v3.2$ is important for various forms of context-cued memory, but not spatial-cued or trace memory (Chen et al., 2012). Despite the broad expression of $Ca_v3.2$ in the brain, its exact role in neuronal physiology is still unclear because co-expression of the other subunits could mask the phenotype in $Ca_v3.2$ knock-out animals. Conversely, a strong body of evidence has suggested that increased $Ca_v3.2$ calcium channel activity in the brain could underlie neurological disorders such as epilepsy. Thus, increase of expression of $Ca_v3.2$ in neurons can cause changes in the oscillatory burst pattern by increase of T-type calcium currents which in turn lead to seizures (Becker et al., 2008; Powell et al., 2009; Talley et al., 2000). In addition, in humans, gain function mutations in the CACNA1H gene is associated with generalized idiopathic epilepsy (Chen et al., 2003; Heron et al., 2004a). Several missense mutations found in the CACNA1H gene have also been linked to autism spectrum disorder. These mutations were responsible for significantly altering the $Ca_v3.2$ channel activity by causing a positive shift in activation properties, and a reduction in conductance (Splawski et al., 2006).

In sensory neurons, the expression and function of the $Ca_v3.2$ channel has been controversial. T-type calcium currents are concentrated in small and medium diameter rat sensory neurons (Scroggs and Fox, 1992), and seem to be generated in these cells by the subunits $Ca_v3.2$ and $Ca_v3.1$ (Lambert et al., 1998). The controversy comes from studies proposing a role for the $Ca_v3.2$ in nociception vs. a role in the physiology of a specific subpopulation of ultrasensitive mechanoreceptors, the putative D-hair receptors. In-situ hybridization assays and reverse transcription PCR have shown that the subunit 3.2 is mainly expressed in a subset of small-medium diameter dorsal root ganglia cells that correlates with the loss of D-hair mechanoreceptors in NT-4 knock-out adult animals. Also the use of the T-type calcium channel antagonist mibefradil reduced the mechanosensitivity of D-hair receptors (Shin et al., 2003). More recently, characterization of D-hair receptors of $Ca_v3.2$ knock-out mice using the skin nerve preparation revealed that the $Ca_v3.2$ calcium channel is necessary to maintain D-hair receptor mechanosensitivity, and is also important for the temporal coding of these afferents. Sensory impairment was observed only in putative D-hair afferents as shown by the reduction of spikes in response to ramp and hold displacement stimuli in mutants compared to wild-type animals (Wang and Lewin, 2011). In contrast, selective antisense oligonucleotides knock-down of $Ca_v3.2$ in vivo, as well as administration of high doses of mibefradil, antagonizes neuropathic and inflammatory pain after nerve injury (Bourinet et al., 2005), and reverses tactile allodynia and thermal hyperalgesia in rats (Wen et al., 2006). Also, behavioural studies in $Ca_v3.2$ null animals showed attenuated pain responses to acute mechanical, thermal and chemical pain, but not to neuropathic pain (Choi et al., 2006). The main goal of my project is to provide genetic labelling of $Ca_v3.2$ expressing cells to elucidate their physiological properties.

1.1.4. Part I Aims

D-hair receptors are the most sensitive mechanoreceptor in mammals' skin; however its specific function in mechanosensation and what part of the stimulus information is coded by these afferents is still unknown. The objective of the first part of my project was to generate an in vivo cell marker for D-hair mechanoreceptors using the $Ca_v3.2$ channel promoter in order to:

- Identify D-hair afferents in cell culture, and characterize their physiological properties.

- Characterize the D-hair receptor innervation pattern.

- Provide a tool to identify molecules responsible for D-hair receptor properties.

Additionally, because the T-type channel subunit $Ca_v3.2$ is expressed in many different cell types where it appears to play a role in cell excitability, the models developed here may shed light on $Ca_v3.2$ in many cells. The knock-in animals generated here are a very useful tool to investigate the properties of these cells and the specific contribution of this calcium channel to their function.

1.2.   MATERIALS AND METHODS

1.2.1.   Preface

1.2.1.1. Chemicals

Name	Supplier
Agarose, ultra-pure	Invitrogen GmbH, Karlsruhe, Germany
Antibiotic-Antimycotic	Invitrogen GmbH (Life technologies), Karlsruhe, Germany
Ammonium chloride	Carl Roth GmbH & Co. KG, Karlsruhe, Germany
Ampicillin sodium salt	Sigma-Aldrich Chemie GmbH, Schnelldorf, Germany
Aqua-Polymount	Polysciences Europe GmbH
Bovine serum albumin (BSA)	Sigma-Aldrich Chemie GmbH, Schnelldorf, Germany
Bromphenolblue	Carl Roth GmbH & Co. KG, Karlsruhe, Germany
Calcium chloride dihydrate	Merck KgaA, Darmstadt, Germany
Collagenase Type IV	Sigma-Aldrich Chemie GmbH, Schnelldorf, Germany
Dimethyl sulfoxide (DMSO)	Merck KgaA, Darmstadt, Germany
DOC	Invitrogen GmbH, Karlsruhe, Germany
dNTP-Mix	Invitrogen GmbH, Karlsruhe, Germany
DTT	Invitrogen GmbH, Karlsruhe, Germany
EDTA disodium-dihydrate	Carl Roth GmbH & Co. KG, Karlsruhe, Germany
Ethanol	Carl Roth GmbH & Co. KG, Karlsruhe, Germany
Ethidium bromide	Carl Roth GmbH & Co. KG, Karlsruhe, Germany
FBS (fetal bovine serum)	Invitrogen GmbH (Life technologies), Karlsruhe, Germany
D-(+)-glucose	Sigma-Aldrich Chemie GmbH, Schnelldorf, Germany
D-MEM	Invitrogen GmbH (Life technologies), Karlsruhe, Germany
DNAse I	Sigma-Aldrich Chemie GmbH, Schnelldorf, Germany
Ganciclovir	Sigma-Aldrich Chemie GmbH, Schnelldorf, Germany
Glacial acetic acid	Carl Roth GmbH & Co. KG, Karlsruhe, Germany
Glutaraldehyde	Sigma-Aldrich Chemie GmbH, Schnelldorf, Germany
Glycerol	Carl Roth GmbH & Co. KG, Karlsruhe,

	Germany
Horse serum	Invitrogen GmbH (Life technologies), Karlsruhe, Germany
IPTG	Sigma-Aldrich Chemie GmbH, Schnelldorf, Germany
Isopropanol	Carl Roth GmbH & Co. KG, Karlsruhe, Germany
Ketamin 10 %	WDT eG, Garbsen, Germany
ß-mercaptoethanol	Sigma-Aldrich Chemie GmbH, Schnelldorf, Germany
Methanol	Carl Roth GmbH & Co. KG, Karlsruhe, Germany
MgCl2 (50 mM)	Invitrogen GmbH, Karlsruhe, Germany
O.C.T.™ Tissue Tek	Sakura Finetek, Zoeterwoude, Netherlands
Oligo(dT)$_{12-18}$Primer	Invitrogen GmbH, Karlsruhe, Germany
Opti-MEM®	Invitrogen GmbH (Life technologies), Karlsruhe, Germany
Paraformaldehyde	Sigma-Aldrich Chemie GmbH, Schnelldorf, Germany
PBS (10x)	Invitrogen GmbH (Life technologies), Karlsruhe, Germany
PCR Rxn buffer (10x)	Invitrogen GmbH, Karlsruhe, Germany
Penicillin/streptomycin	Invitrogen GmbH (Life technologies), Karlsruhe, Germany
Peptone	Carl Roth GmbH & Co. KG, Karlsruhe, Germany
Poly-L-lysine 0.01 %	Sigma-Aldrich Chemie GmbH, Schnelldorf, Germany
Protease inhibitor tablets complete mini	Roche Pharma AG, Grenzach-Wyhlen, Germany
Proteinase K	Sigma-Aldrich Chemie GmbH, Schnelldorf, Germany
Random Primers	Invitrogen (Size: 9) GmbH (Life technologies), Karlsruhe, Germany
Rompun® (2% Xylazin)	Bayer Vital GmbH, Leverkusen, Germany
Sodium chloride	Carl Roth GmbH & Co. KG, Karlsruhe, Germany
Sodium hydrogen sulphate	Sigma-Aldrich Chemie GmbH, Schnelldorf, Germany
Sodium hydroxide	Sigma-Aldrich Chemie GmbH, Schnelldorf, Germany
Sucrose	Sigma-Aldrich Chemie GmbH, Schnelldorf, Germany
TEA	Sigma-Aldrich Chemie GmbH, Schnelldorf, Germany
TRIS	Carl Roth GmbH & Co. KG, Karlsruhe, Germany
Triton X-100	Sigma-Aldrich Chemie GmbH, Schnelldorf, Germany
Trizol	Invitrogen GmbH (Life technologies), Karlsruhe, Germany

Trypsin-EDTA (0.25 %)	Invitrogen GmbH (Life technologies), Karlsruhe, Germany
Trypsin inhibitor Type I-S (soybean)	Sigma-Aldrich Chemie GmbH, Schnelldorf, Germany
Tween 20	Serva Electrophoresis GmbH, Heidelberg, Germany
X-Gal (bromo-chloro-indolyl-galactopyranoside)	Carl Roth GmbH & Co. KG, Karlsruhe, Germany
Yeast extract	Carl Roth GmbH & Co. KG, Karlsruhe, Germany

1.2.1.2. Buffers and solutions

Name	Composition
0.2M $Na_2H_2PO_4$	15.5% 1M Na_2HPO_4, 4.5% 1M NaH_2PO_4 in MQ, Ph7.4
0.2% Glutaraldehyde	0.2% Glutaraldehyde, 2 Mm MgCl2, 1.25Mm EGTA in PBS. Ph-7.4
4% PFA	4% paraformaldehyde, 2 Mm MgCl2, 1.25Mm EGTA in PBS. Ph 7.2-7.4
10x PBS	80g/l NaCl, 2g/l KH_2PO4, 2g/l KCl, 21.6g/l $Na_2HPO4•7H2O$
50x TAE	242g/l Tris base, 5.71 % (v/v) Glacial acetic acid, 0.05M EDTA, Ph8.0
Blocking buffer for immunostaining	1x PBS with 5% goat serum and 0.1% TritonX-100
LB agar	LB-medium + 1.5% (w/v) agar
LB medium	10g tryptone, 5g yeast extract, 10g NaCl in 1 liter H_2O
SSC 20X	3M NaCl, 300 Mm sodium citrate, Ph 7.0
TBS 10x	0.5M Tris-HCl Ph7.9, 1.5M NaCl
TBS-T	TBS + 0.05% Tween-20
RIPA buffer	50mM Tris-HCl pH7.4, 150mM NaCl, 1mM EDTA, 0.5% DOC, 1% Triton X-100, 0.2% SDS, 1.5mM DTT, Protease inhibitors.
TE buffer	10Mm Tris Ph8.0, 1Mm EDTA
X-gal buffer	35 mM $K_4[Fe(CN)_6]•3H2O$, 35 Mm $K_3[Fe(CN)_6]$, 2Mm $MgCl_2$, 0.02% Nonidet P-40, 0.01% Na deoxycholate, 1 mg/ml X-gal in dimethylformamide in PBS
Patch Clamp Buffer (extracellular solution)	140 mM NaCl, 1 mM $MgCl_2$, 2 mM $CaCl_2$, 4 mM KCl, 4 mM glucose, 10 mM HEPES, pH 7.3, adjusted with NaOH.
Patch Clamp Buffer (intracellular solution)	110 mM KCl, 10 mM Na^+, 1 mM $MgCl_2$, 1 mM EGTA, 10 mM HEPES. pH7.3, pH adjusted with KOH.

1.2.1.3. Bacteria Strains

Name	Genotype
E.coli TOP10	F- mcrA Δ(mrr-hsdRMS-mcrBC) φ80lacZΔM15 ΔlacX74 nupG recA1 araD139 Δ(ara-leu)7697 galE15 galK16 rpsL(Str^R) endA1 λ$^-$
DY380	F- *mcr*A Δ(*mrr-hsd*RMS-*mcr*BC) Φ80d*lacZ* M15 ⊿*lac*X74 *deo*R *rec*A1 *end*A1 *ara*D139 Δ(*ara, leu*) 7649 *gal*U *gal*K *rsp*L *nup*G [λ*cI*857 (*cro-bio*A) <> *tet*]
EL350	F- *mcr*A Δ(*mrr-hsd*RMS-*mcr*BC) Φ80d*lacZ* M15 ⊿*lac*X74 *deo*R *rec*A1 *end*A1 *ara*D139 Δ(*ara, leu*) 7649 *gal*U *gal*K *rsp*L *nup*G [λ*cI*857 [(*cro-bio*A) <> *ara*C-PBAD*cre*]

1.2.1.4. Primers

Name	Sequence 5'-3'
Cre-LF	AGGAGGCGATACTGGCCCAG
Cre-LR	CATGGTGGCAGAGGGCAGCACCTG
Cre-RF	CGCTTCGCCTTCGGCTCCTG
Cre-RA	ACAGGCTAACCCTACCATCTCTGAGA
GFP-LFM	AGGAGGCGATACTGGCCCAGCTC
GFP-LRM	CATGGTGGCAGAGGGCAGCACCTG
GFP-RFM	CGCTTCGCCTTCGGCTCCTG
GFP-RAM	ACAGGCTAACCCTACCATCTCTGAGAAGAAC
CaV-LS	CTCAGGGCCACTCAGAGAATGTAG
CaV-LA	CAGAGAGGCCAATGAGATCACCAAGC
CaV-RS	GATGGCTGTGTAGGGTCAAGGCTACC
CaV-RA	GCAGCTTCTAGTCCAGACCCATC

1.2.1.5. Primary antibodies

Name	Concentration/dilution	Application	Supplier
TH	1:500	ICC/IF, IHC	Invitrogen GmbH (Molecular probes), Karlsruhe, Germany
TrkB	1:2000	ICC/IF, IHC	Invitrogen GmbH (Molecular probes), Karlsruhe, Germany
TrkC	1:2000	ICC/IF, IHC	Jackson ImmunoResearch Europe Ltd., Suffolk, UK
TrkA	1:2000	ICC/IF, IHC	Jackson ImmunoResearch Europe Ltd., Suffolk, UK

GFP	1:1000	WB	Sigma-Aldrich Chemie GmbH, Schnelldorf, Germany
CK20	1:200	IHC, WB	Dako
S100	1:1000	ICC/IF, IHC	Dako
NF-200	1:3000	ICC/IF, IHC	Abcam
ß-gal	1:1000	ICC/IF, IHC	Abcam (ab9361)
Pax-2	1:1000	ICC/IF, IHC	Invitrogen GmbH (Molecular probes), Karlsruhe, Germany
Lmxb-1	1:500	IF	(Müller et al., 2002)
PGP 9.5	1:1000	ICC/IF, IHC	Dako (Z 5116)

1.2.1.6. Secondary antibodies

Name	Concentration/dilution	Application	Supplier
Alexa Fluor 633 goat anti-rabbit IgG	1:1000	ICC/IF, IHC	Invitrogen GmbH (Molecular probes), Karlsruhe, Germany
Alexa Fluor 488 goat anti-mouse IgG	1:1000	ICC/IF, IHC	Invitrogen GmbH (Molecular probes), Karlsruhe, Germany
Cy2 goat anti-rabbit IgG	1:1000	ICC/IF, IHC	Jackson ImmunoResearch Europe Ltd., Suffolk, UK
Cy3 donkey anti-chicken IgG	1:1000	ICC/IF, IHC	Jackson ImmunoResearch Europe Ltd., Suffolk, UK
Goat anti-rabbit-HRP	1:1000	WB	Sigma-Aldrich Chemie GmbH, Schnelldorf, Germany

1.2.1.7. Enzymes for molecular biology

Name	Source
Restriction enzymes	New England Biolabs GmbH, Frankfurt, Germany
T4 DNA Ligase	New England Biolabs GmbH, Frankfurt, Germany
Polymerase, PhusionHF	New England Biolabs GmbH, Frankfurt, Germany
Polymerase, Taq	Invitrogen GmbH, Karlsruhe, Germany
Superscript III	Invitrogen

1.2.1.8. Kits

Name	Supplier
Amersham™ ECL plus WB detection kit	GE Healthcare, Munich, Germany
Pierce® bca Protein Assay Kit	Thermo Scientific, Schwerte, Germany
CloneJET™ PCR Cloning Kit	Fermentas GmbH
Prime-It II Random Primer Labelling Kit	Stratagen GmbH, Waldbronn, Germany
QIAfilter™ plasmid maxi kit	Qiagen GmbH, Hilden, Germany
QIAquick® gel extraction kit	Qiagen GmbH, Hilden, Germany
QIAprep® spin miniprep kit	Qiagen GmbH, Hilden, Germany
TURBO DNA-free™	Applied Biosystems
FastStart Universal Probe Master (Rox)	Roche, Mannheim, Germany
Universal ProbeLibrary System	Roche, Germany

1.2.1.9. Cell culture media

Name	Compositiom
DRG neurone growth medium	DMEM-F12 medium, 100 units/ml penicillin, 100 µg/ml streptomycin, 4 mM L-glutamine, glucose, 10% fetal bovine serum
MEF growth medium	DMEM medium with glutamax, 12% fetal bovine serum, 100µM non essential aminoacids (10mM, 100X), 100 units/ml penicillin, 100 µg/ml streptomycin, 0.1mM mercapto-ethanol
ES cell growth medium	DMEM medium with glutamax, 15% fetal bovine serum, 100µM non essential aminoacids (10mM, 100X), 100 units/ml penicillin, 100 µg/ml streptomycin, 0.1mM mercapto-ethanol, 180µl LIF per 600ml of a total volume (conditioned medium of LIF expressing COS cells).

1.2.2. $Ca_v3.2^{GFP}$ and $Ca_v3.2^{Cre}$ Knock-in mice Generation

1.2.2.1. Molecular Biology

1.2.2.1.1. Amplification of DNA fragments by PCR reaction

All DNA fragments for molecular cloning were amplified from cDNA, BACs or plasmids using Phusion® High-Fidelity DNA polymerase (New England Biolabs). Genotyping of animals, colony and analytical PCR assays were performed with Taq-DNA polymerase (Invitrogen). All primers used in this work were synthesised by Invitrogen.

Standard PCR mix. for Taq polymerase

20-100ng of template

1 x PCR buffer

2mM $MgCl_2$

0.2mM dNTPs

0.5mM primer 3´

0.5mM primer 5´

5U Taq DNA polymerase

H_2O to 30µl reaction volume.

Cycling protocol for Taq polymerase:

Initial denaturation: 94°C 2min

Denaturation: 94°C 30–60sec

Annealing: primer-dependent 30-60sec

Extension: 72°C 30–60sec

Cycles: 25–35

Final extension 72°C 10min

Storage: 4°C

Standard PCR mix. for Phusion®

20-100ng of template

1x HF or GC buffer

0.2mM dNTPs

0.4µM primer 3´

0.4µM primer 5´

1U of Phusion®

H_2O to 50µl reaction volume.

Cycling protocol for Phusion®

Initial denaturation: 98°C 30sec.

Denaturation: 98°C 15sec

Annealing: primer-dependent 20-30sec

Extension: 72°C 30sec/kb

Cycles: 25–35

Final extension 72°C 10min

Storage: 4°C

1.2.2.1.2. Agarose gel electrophoresis

DNA samples were separated on 0.5-2 % agarose gels in the EasyCast™ gel system (Owl Thermo Scientific). Gel was prepared by microwaving the appropriate amount of agarose powder in 1X SB buffer. 0.01 % of SYBR Green (Invitrogen) was added to the pre-cooled agarose solution and the gel was poured into the gel slides and allowed to polymerize. DNA samples were mixed with 6x DNA loading dye and ~200-500 ng of DNA (analytic gels) or 1-4 µg of DNA (preparative gels) per gel pocket. The Smart DNA ladder (Eurogen) was used as a DNA size marker. Electrophoresis was carried out at 70-120 volts for 40-60 minutes and gels were subsequently analysed using the Safe Imager™ blue light (Invitrogen).

1.2.2.1.3. Gel purification of DNA fragments

The QIAquick® gel extraction kit (Qiagen, Germany) was used for extraction of all PCR amplified and enzyme digested fragments after agarose gel electrophoresis. The DNA bands of interest were cut out from 1% agarose gel under the Safe Imager™ illumination and melted in QC buffer at 55 °C. The extraction was performed according to the manufacturer's manual.

1.2.2.1.4. Restriction digestion

Restriction enzyme digestion of DNA was made using specific endonucleases (New England Biolabs, USA). 1 µg of plasmid DNA was mixed with 10 U of the restriction enzyme, 1X final dilution of the required restriction buffer and BSA when needed. The final volume was brought to 30-50 µl with double distilled water and the samples were incubated for 1–2 h at the temperature required for the respective restriction enzyme.

1.2.2.1.5. Ligation of DNA and subcloning

Ligation reaction was carried out as the sticky end ligation with 3-5 fold molar ratios of inserts to vectors. Typical volume for a ligation mixture was 15 µl containing 2000 units (in 1µl) of T4 DNA ligase (New England Biolabs, USA) and 1x ligation buffer. Ligation reaction was carried out at 16° C over night. Three to 5 µl from the reaction mixture was used for transformation into bacteria.

1.2.2.1.6. Electroporation of bacteria for recombineering

DY380 cells containing BAC were inoculated into 20 mL of LB medium and grown over night at 32° C. The next day, 1 mL of the culture (O.D$_{600}$= 1.2) was diluted into 25 mL of LB medium and incubated with shaking until O.D$_{600}$ reached a value of 0.5. Then 10 mL of the cells were transferred into a new 14 mL tube and shaked in a 42°C water bath for 15 minutes. The tube was put in wet ice for 5 min while shaken in order to allow a drop of temperature as soon as possible. The cells were centrifuged at 4000rpm (0°C) for 5 min and resuspended in 888 µL of ice cold water. The suspension was transferred into a 1.5 mL Eppendorf tube and the cells were washed three times as described before. In the last centrifugation step the cells were resuspended in 50µL of ice cold water. In a pre-cooled electroporation cuvette (0.1cm-gap) the cells and 1-2µL of the purified plasmid were mixed. The electroporation was performed in a BIO-RAD electroporator set at 1.75kV, 25µF with the pulse controller set at 200 Ω and time constant set at 3.0. Next 400 µL of SOC medium was added and incubated at 32°C for 1 h. The cells were spread on plates with the appropriate antibiotics.

1.2.2.1.7. Construction of targeting vectors

Gene targeting in embryonic stem (ES) cells is one of the gold standard methods to evaluate gene function in mice. Genomic modifications and very specific mutants can be generated according to the need of the biological question. Knock-in targeting vectors containing the desired modification are made by a non-conventional cloning technique called recombineering. This technique uses homologous recombination to insert functional elements such as recombination sites (loxP or FRT), reporter gene-sequence and selectable markers with precision in almost any DNA sequence (Liu et al., 2003).

In practice, the cassette designed is inserted into a BAC containing the sequence of interest and then this region is excised from the BAC and used to transform ES cells for further recombination. Unfortunately, because of unknown reasons some BAC DNAs are difficult to transform into recombineering-competent bacteria strains, or have rearrangements after transformation. To eliminate these problems a 10-15 kb fragment of BAC DNA containing the Ca$_v$3.2 sequence bearing the insertion site of interest was subcloned into a high-copy pBluescript (pSK$^+$) backbone based plasmid by gap repair.

1.2.2.1.8. Subcloning of Ca$_v$3.2 Sequence by Gap Repair

Subcloning by GAP-repair was made by co-transformation of a BAC bearing the gene of interest with a linearised high-copy plasmid, containing flanking homology sequences to the BAC and selection markers into an *E. coli* strain that expresses λ phage Red proteins (e.g EL350, DY380) (Lee et al., 2001). The next strategy was used to prepare a subcloning vector for the gene targeting. Homology arms (400 bp.) to the Ca$_v$3.2 genomic sequence were inserted into subcloning vector (pDTA) using conventional cloning. The diphtheria toxin A (DTA) is a negative selectable marker against random insertions. Two sets of specific primers containing a new restriction site at the 5′end were used to amplify 400 bp region of the BAC. These two regions will mark the ends of the fragment to be subcloned by gap repair. The PCR products were purified with spin columns and digested with *Spe*I-*Hind*III (left arm) or *Hind*III-*Xho*I (right arm). The digested fragments were again purified and ligated into SpeI-HindIII digested pDTA vector. The resulting plasmid **Figure 4** was used to retrieve a region of Ca$_v$3.2 for knock-in targeting vector construction. EL350 cells co-transformed with BAC were electroporated with 55ng of HindIII digested pDTA linearized plasmid and grown on Amp agar plates for positive selection for at least 15 hours at 30C°. Due to the large size of BACs and absence of selection pressure, initial BAC (chloramphenicol resistance) used for transformation was eliminated. The resulting colonies were tested for correct recombination by restriction profile analysis and sequencing. The plasmid obtained pDTA-Ca$_v$3.2 was used for insertion of targeting cassette.
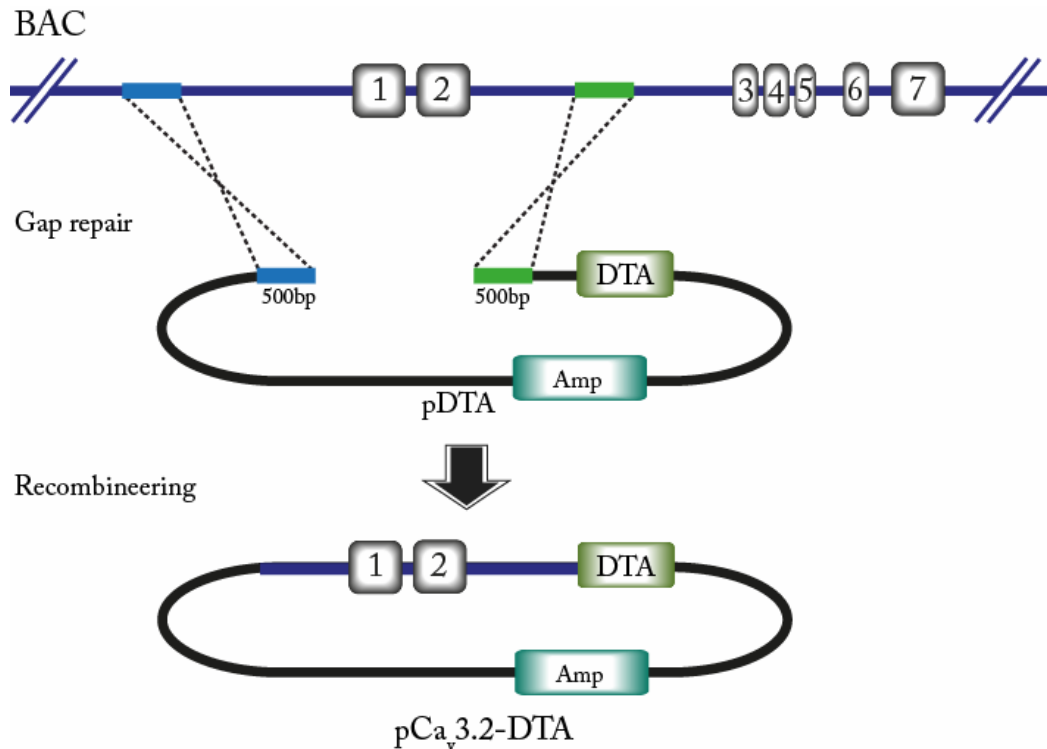
Figure 4. Subcloning of Ca_v3.2 sequence into a multi copy plasmid. The Drawing illustrates the subcloning of the Ca_v3.2 gene region selected from BAC DNA into pDTA plasmid. The short homology arms to the BAC DNA cloned into pDTA vector and necessary for recombineering are depicted in blue and green.

1.2.2.1.9. Construction of targeting cassettes

The targeting cassettes were designed to introduce the enhanced green fluorescence protein (EGFP) or Cre recombinase sequence into the Ca_v3.2 subcloned plasmid. In the first construct the EGFP sequence is followed by a floxed neomycin resistance (Neo) gene for positive selection, and these two elements are flanked by two 400bp BAC DNA homology arms which allow the insertion of the cassette into Ca_v3.2 plasmid by homologous recombination **Figure 5**. To produce the EGFP reporter targeting cassette, two homology arms where cloned into *EGFP-loxP-Neo-loxP* plasmid using conventional cloning. Primers with new restriction sites inserted at the 5´end were used to obtain the left and right homology arms by PCR from BAC DNA. The fragments were purified, digested with KpnI and NcoI (left arm) and SacII- SacI (right arm) and ligated to NcoI-SacII excised *EGFP-loxP-Neo-loxP* cassette into KpnI-SacI digested pBS plasmid.

The second construct had Cre recobinase sequence instead of EGFP, and Neo is flanked by flippase recombination target (FRT) sites to remove the neo cassette following

successful targeting **Figure 6**. The Cre targeting cassette was generated in a similar manner. Cre recombinase sequence was excised from pZero Cre plasmid with *Hind*III and *Pst*I restriction enzymes and inserted into *Hind*III and *Pst*I of pBS-*FRT-neo-FRT* to form pBS-*Cre-FRT-Neo-FRT*. Two 400bp long BAC DNA homology arms were produced using primer pairs engineered to contain *Hind*III and *Nco*I restriction sites flanking the left arm and *Spe*I and *Bst*XI sites flanking the right arm. Introduction of the homology arms into pBS-*Cre-FRT-Neo-FRT* was done by ligating together the *Hind*III-*Nco*I digested left arm, *Spe*I-*Bst*XI digested right arm and *Nco*I- *Spe*I digested *Cre-FRT-Neo-FRT* fragment.

Finally, the targeting vectors were produced by homologous recombination in bacteria between pDTA-Ca$_v$3.2 plasmid and Cre or GFP targeting cassettes. The pCa$_v$3.2^{GFP} targeting vector was made by transforming DY380 cells by electroporation with pDTA-Ca$_v$3.2 plasmid and *EGFP-lox*P-*Neo-lox*P *Sac*I digested fragment as described above. The same methodology was used for the second targeting vector pCa$_v$3.2^{Cre} but in this case the two homology arms *Cre-FRT-Neo-FRT* plasmid were digested with *Hind*III and *Bst*XI restriction enzymes.
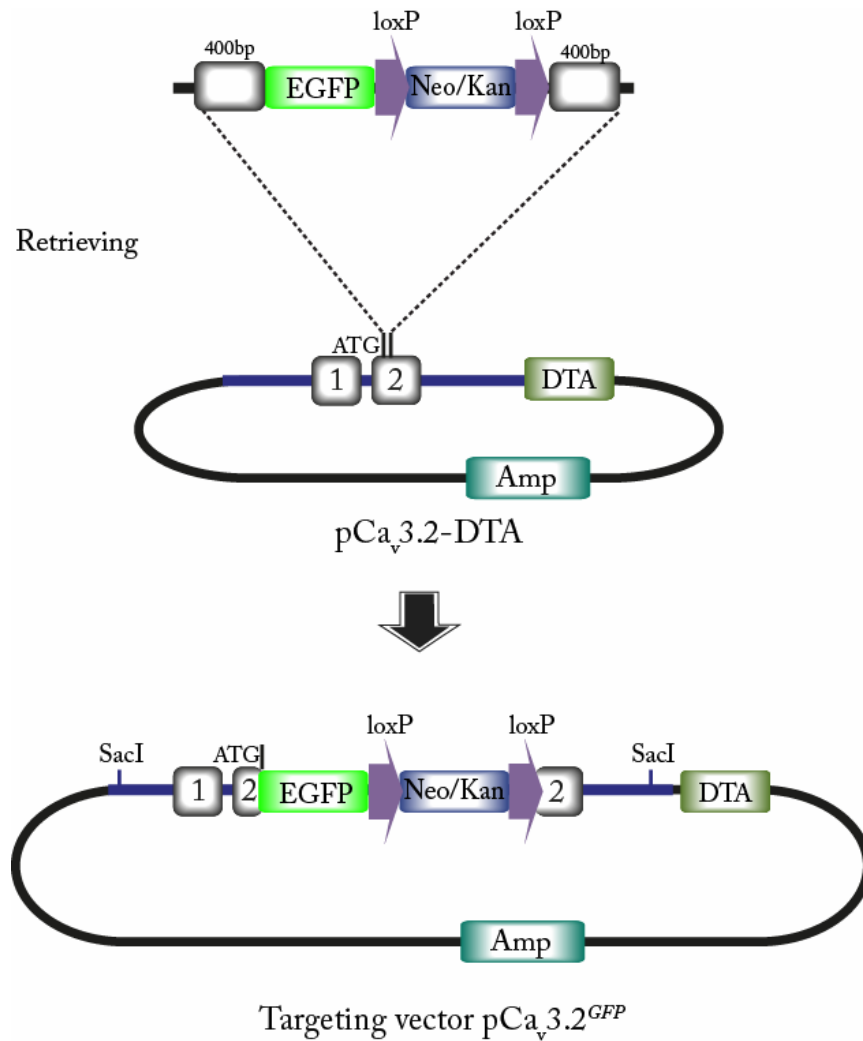
Figure 5. Construction of targeting vector pCa$_v$3.2^{GFP}. The *EGFP-lox*P-*Neo-lox*P cassette was flanked with 400bp homology sequence (represented by the two white boxes) to the insertion site in the pDTA-Ca$_v$3.2 plasmid. EGFP-Neo cassette should be inserted after the ATG translation initiation codon located at the beginning of the exon 2 of the Ca$_v$3.2 channel's sequence. Sac I restriction enzyme's sites are located in the homology arms and where used to excise the *EGFP-lox*P-*Neo-lox*P cassette.
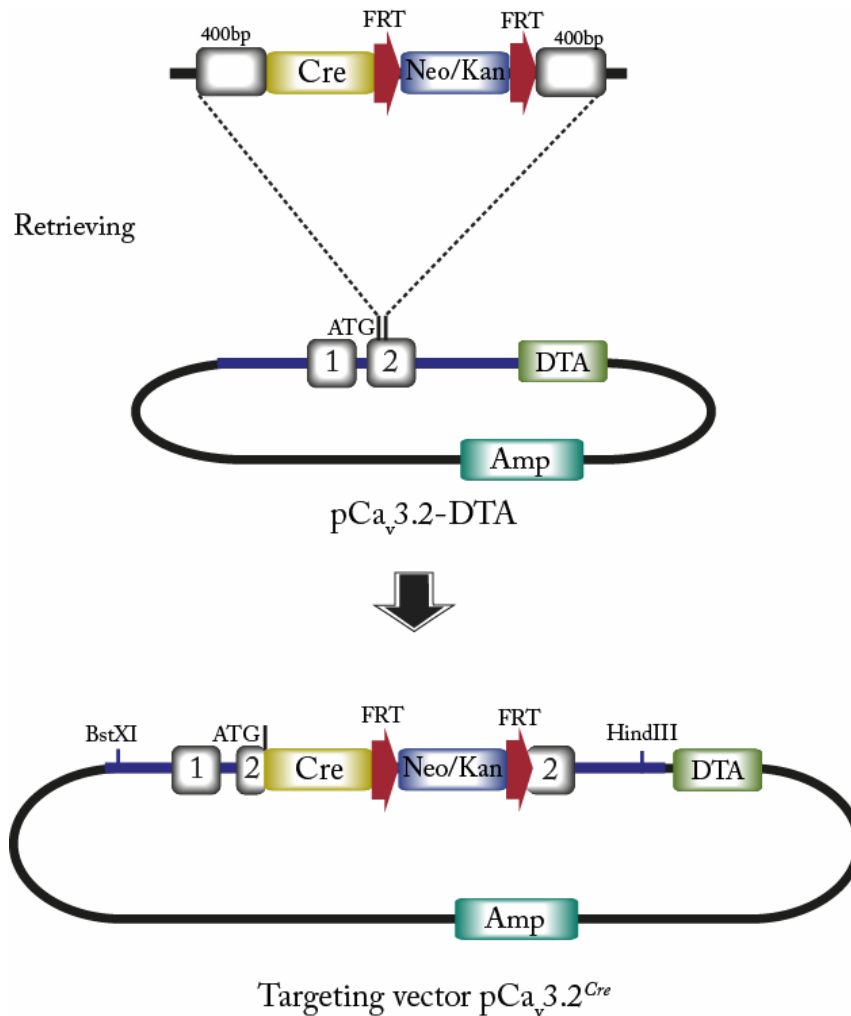
Figure 6. Construction of targeting vector pCa$_v$3.2^{Cre}. The restriction sites BstXI and HindIII located in the homology arms (white boxes) surrounding Cre-Neo were used to release Cre-FRT-Neo-FRT cassette and clone it into pDTA-Ca$_v$3.2 plasmid by homologous recombination.

1.2.2.1.10. Plasmid DNA extraction

Plasmid DNA was extracted using the QIAprep® spin miniprep kit or the QIAfilter™ plasmid maxi kit (Qiagen, Germany). All steps were performed according to the manufacture's protocol. Concentrations of obtained DNA were measured using the GeneQuant 1300 photometer (GE Healthcare). All DNA preparations were stored at -20 °C.

1.2.2.1.11. Sequencing

Sequencing of DNA samples was done by LGC Genomics, Berlin. All sequencing results were analyzed with Vector NTI 11 (Invitrogen) and FinchTV (Geospiza Inc.).

1.2.2.1.12. Linearization of the targeting vector for ES electroporation.

For linearization, 60 μg of the verified and sequenced targeting vector was used. The $pCa_v3.2^{GFP}$ and $pCa_v3.2^{Cre}$ targeting vector were digested with 20U of SwaI endonuclease (New England Biolabs, USA) overnight in 200μl reaction volume containing appropriate buffer and BSA. A small aliquot from the restriction mixture was separated in an agarose gel to verify if the digestion was complete. Afterwards the whole volume of the digested DNA was mixed with 200μl of phenol/chloroform (1:1) and spun in a pre-cooled micro-centrifuge for 15 minutes. The top aqueous layer was carefully transferred to a new tube and mixed with an equal volume of chloroform in order to remove phenol traces. The mixture was centrifuged for 10 minutes more. The top aqueous layer was transferred to the new tube and 25μl of sodium acetate 0,3 M was added followed by addition of 500 μL of ethanol in order to precipitate DNA. The tube was incubated overnight at -20C° and afterwards spun at 14000rpm for 15 minutes at 4C°. The obtained DNA pellet was washed once with ice-cold 70% ethanol, dried and resuspended in 50μl of sterile TE buffer (pH 8).

1.2.2.1.13. Southern blot (alkaline method)

Southern blot was used to screen for recombinant ES-cell clones and genotyping of the resulting mouse lines. DNA probes were designed to observe the 5´ and 3´ insertion end of the targeting vector into the locus of interest as well as for neomycin resistance. Restriction enzyme digested genomic DNA fragments of ES-cell clones or animal tails was separated by electrophoresis on a 0.9% agarose gel using TAE buffer over night at 24 mV. The next day, the gel was incubated in 0.25M HCl for a maximum of 10 min on an orbital shaking platform to depurinate DNA and break large fragments into smaller pieces, which allows more efficient DNA transfer from the gel to the membrane. Neutralization of the gel and denaturation of the DNA into single strands was made by washing the gel with 0.4N NaOH while shaking two times for 15 min. This procedure allows hybridisation of the DNA transferred to the membrane with the probe. Capillary transfer of the DNA from the gel to the nylon membrane was done using 0.4N NaOH as a carrier buffer. After

overnight transfer the membrane was incubated at 80C° for 2 hours in order to fix DNA fragments. The membrane was washed twice in 20X SCC followed by 5 minute incubation in 2X SCC buffer.

1.2.2.1.14. Hybridization with radioactively labelled DNA probes

The DNA sequence used to produce radiolabelled probes were amplified from a BAC containing the gene of interest, gel purified and cloned into pJET1.2 vector from fermentas. When needed, the insert was excised from the vector using restriction enzymes and the radioactive probe was synthesised using a Prime-It II random primer labelling kit (Stratagene) according to the manufacturer's protocol. In all experiments [α− ^{32}P]dCTP isotope (PerkinElmer) was used. Membranes were pre-hybridised in a heated hybridisation buffer (GE Healthcare) for at least 2 hours at 65C° in order to block nonspecific binding. The radioactive probe was boiled for at least 5 minutes, immediately transferred to ice for 5 minutes and added to the hybridisation buffer. Membranes were incubated with the probe overnight at 65C° with constant rotation. After hybridisation the hybridisation buffer was discarded and membranes were washed 2 times for 5 minutes in 2X SSC – 0.1% SDS buffer and 1 time for 30 minutes in the oven with rotation. After this, membranes were transferred into bigger containers with a 0.1 SCC-0.5% SDS buffer and washed 2-3 times in 65C° preheated water-baths. Washed membranes were slightly air-dried, wrapped into plastic and exposed to X-Ray film in exposure cassettes at -80 C°. Exposure time varied from 24 hours to one week.

1.2.2.1.15. Extraction of mRNA from animal tissues and cDNA preparation

Tissues (dorsal root ganglia (DRGs), brain or spinal cord) were dissected and immediately transferred into eppendorf tubes containing an appropriate volume of Trizol reagent (normally 1ml per 100mg of tissue). The samples were homogenised in Precellys®24-Dual homogeniser using 2 steps program. Each step homogenized the sample with a 3D motion speed of 5000 rpm for 25 seconds. Then the samples were incubated for 20-30 minutes at room temperature followed by 2 minutes centrifugation at 13000g. The supernatant was transferred to a new tube and 0.2ml of chloroform per 1ml of Trizol was added; samples were vigorously mixed and incubated for 3 more minutes at room temperature. The tissue homogenate was centrifuged for 10 minutes at 12000g, 4C° and the resulting colourless upper aqueous portion was transferred into a fresh tube. To precipitate RNA, 0.5ml of

isopropanol per 1ml of Trizol volume was added and samples were incubated for 10 minutes at room temperature. Next, RNA was separated by centrifugation at 12000g for 10 minutes, washed with 75% ethanol, air-dried and dissolved in 30μl of RNAse-free water. To eliminate contamination of the RNA with DNA the samples were incubated with DNAase for 30 minutes at 37°C following TURBO DNA-free™ kit's manufacturer recommendations. Two μg of total RNA was used for cDNA synthesis using SuperScript™ III Reverse Transcriptase according to the manufacture's protocol using random primers and Oligo-dT.

1.2.2.1.16. Real Time quantitative PCR

For real time qPCR, 10 μL final reaction volume was used. 1 μl cDNA or water was added to a mix containing: 0.4 μM primers final concentration, 5 μL of universal PCR master mix from Roche and 0.1μL of Probe No. 70 from the mouse Universal ProbeLibrary from Roche. To make an absolute quantification of GFP mRNA, the standard curve was prepared using serial dilutions of pEGFP-N3 plasmid ranging from 5×10^1 to 5×10^8 moles per reaction. Every sample was quantified three times as well as every single point of the standard curve. The samples and standard curve were set up in 384 well-plates and run on ABI Prism 7900 sequence detection system using a two step protocol with a denaturation step at 95°C for 10 min, followed by 95°C for 10 seconds then decrease at 60°C for one minute, 40 cycles. Cycle threshold (CT) values were set manually.

1.2.2.2. Cell biology.

1.2.2.2.1. Preparation of MEF cell culture.

Mouse embryonic fibroblasts (MEFs) were prepared as feeder cells to maintain mouse embryonic stem cells (ES cells) in an undifferentiated state during clone selection.

Prior to MEF preparation, mating of the mice containing neomycin resistance cassette in their genome (e.g. any knock-out mouse line, where a neomycin resistance cassette was used to disrupt a gene sequence), was set up. Mouse embryos from one or two pregnant animals (for one preparation 7 to 9 embryos were used) were dissected aseptically at 14.5-15.5 dpc, cleaned from all membranes and placed in a Petri dish in sterile PBS. Limbs, viscera and brain were removed; the trunks were washed in PBS and DMEM without serum after which they were minced with sterile razor-blades into small pieces and passed

several times through a 10ml glass pipette. The minced embryos were transferred into a 50ml Falcon tube containing 15ml of trypsin/EDTA buffer and incubated at 37C° for 15 minutes while stirring. To reduce viscosity, several drops of DNAse were added to the tissue mixture. After 15 minutes of incubation the tube content was passed several times through a glass pipette and incubated for next 15 minutes while stirring. At the end of incubation time an equal volume of serum-containing medium was added to the trypsinized tissues. The content of the tube was spun at 1000rpm for 10 minutes. The obtained cell pellet was resuspended in a cell culture medium and plated at a rate one dissected embryo per one 15Ø tissue culture dish. On the next day the medium was changed. Fibroblasts were grown to confluence, after which they were split from 1:6 to 1:10 and grown again to confluence. For ES cell cultures, MEFs from the third or later passages were used.

1.2.2.2.2. ES cell cultivation, electroporation and selection of positive clones.

Prior to the ES cell work, a sufficient amount of neomycin resistant MEF cells was prepared as described above. All the cell culture plastic used during ES cultivation was covered with 0.1% gelatine solution in the following way: a sufficient amount to cover a dish surface with 0,1% sterile gelatin was added and incubated for 5 minutes at the room temperature. After incubation the left over liquid was carefully removed with a pipette and covered dishes were covered and left to dry under the hood for at least for 5 minutes.

1.2.2.2.3. Feeder cells preparation for ES cell culture.

Freshly prepared or frozen MEF cells from no more than 4 passages were seeded onto 15cm culture dishes and grown to confluence. The growth medium was changed every second day. Confluent dishes were trypsinized in the following way: the growth medium was aspirated and cells washed once with PBS, 3ml of trypsin/EDTA per 15Ø dish was added and incubated at 37C° until cells detached, 5ml of the medium (containing serum) was added, cells were gently pipetted up and down, transferred into a falcon tube and centrifuged at 1100 rpm for 3 minutes. The cells were resuspended in a feeder growth medium, plated onto three 15cm dishes and grown to confluence. Upon confluence normal feeder medium was substituted with a medium containing mitomycin C (final concentration 0.01mg/ml), and plates were incubated for 2-3 h at 37C°, after that the medium was removed and cells trypsinized as described above. The mitomycin treated cells were seeded onto new dishes and used for ES-cells cultivation for up to 2 weeks.

1.2.2.2.4. Thawing of frozen ES cells and preparation for electroporation with a targeting construct.

A vial of frozen ES cells was thawed at 37C° in a water bath; the cell suspension was transferred to a tube with 10ml of ES cell medium. The tube was swirled several times and centrifuged at 900 rpm for 3 minutes. The cell pellet was thoroughly resuspended in 5 ml of a new ES cell medium to break up all cell clumps. The single-cell suspension was seeded onto a 6cm dish with feeder MEF cells and grown for 2 days. Next, cells were re-plated on one 10cm feeder dish and grown for 2 more days to achieve a dense culture state (but not confluent), when single colonies were round in shape with sharp visible edges. The ES cell colonies were trypsinased with 2.5ml of trypsin/EDTA mixture for 5 minutes at 37C° followed by careful pipetting and centrifugation to achieve full separation of the cells. A number of single cells was estimated, and cell suspension was concentrated to approximately 1.2×10^7 cells in 800µl PBS volume. Twenty to 40µg of linearized targeting vector was mixed with the cells and this mixture was transferred into a cuvette for electroporation. The electroporator parameters used were as follows: impulse length – 2ms, capacity – 1200µF. After electroporation the cuvette was kept on ice for a few minutes for cell recovery. The electroporated cells were transferred to a tube containing 30ml of ES cell medium with LIF and seeded to three 10cm dishes with mitomycin inactivated feeder cells.

1.2.2.2.5. Selection and picking of neomycin resistant ES-cell colonies.

After electroporation the ES-cells grew undisturbed for 48 hours until the medium was changed to one containing G418 (400 µg/ml of active G418). Selection medium was changed once daily over 7 days. On the 8th day single undifferentiated ES cell colonies were picked and cultured for an additional 1-2 days in 96-well plates with feeder cells. ES-cell colonies were trypsinised and split into two new 96-well plates; one plate without feeder cells for screening (replica plate –see below) and a second one with feeder cells for freezing. To freeze ES cells down, 1 volume of ice-cold 2x freezing medium (ES medium with 13.3% DMSO) was added to semi-confluent, trypsinised 96-well plates that contained 1 volume of trypsin in them. The plates were sealed with adhesive PCR film (Thermo Scientific), wrapped in parafilm and gradually frozen to –80°C in Styrofoam boxes. To screen cell clones for homologous recombination, replica plates coated with 0.1% gelatine (Sigma) were made from each 96-well plate. These plates were grown to full confluence and used for DNA preparation and subsequent Southern blot analyses.

1.2.2.2.6. Manipulation of blastocyst and transfer into pseudopregnant mice.

Isolation of blastocysts (C57BL/6 background), and injection of ES cells (129/Ola background) into their inner cavity, and their transfer into uteri of foster mothers in order to create chimeric mice were done in the Transgenic Core Facility (TCF) MDC Berlin-Buch.

1.2.3. Histology.

1.2.3.1. Animal perfusion.

Prior to perfusion, mice were anaesthetised with a Rompun+ Ketavet mixture. 0.5 ml 2% Rompun (20mg/ml Xylazine) and 0.5ml Ketavet (100mg/ml Ketavet) were made in 9.0 ml of PBS, the dose of 0.02 ml/g body weight (~0.45ml) was injected intraperitonealy. Surgical-plane anaesthesia was assured by the absence of toe pinch evoked reflexes. The thoracic cavity was opened by cutting the diaphragm from one lateral aspect to the other lateral aspect. Both lateral aspects of the rib cage were cut in a caudal to rostral direction up to 2nd rib and folded-back to expose thoracic organs. The right atrial-chamber was lacerated with scissors while a 25G perfusion needle attached to a saline syringe was carefully inserted into the left ventricular chamber of the mouse. Mice were perfused with ice-cold PBS until the liver blanching, followed by 4% PFA or 2% PFA / 0.2% glutaraldehyde perfusion during next 20-30 minutes.

At the completion of the perfusion, required tissues were dissected, post-fixed in 4% PFA for 30 min for DRG, 2h for spinal cord, 2h for skin and 6h for brains. Then DRG and spinal cords were dehydrated in 30% sucrose overnight at 4C°, brains were dehydrated in sucrose solution with increasing concentration, of 10%, 20% and finally 30% at 4°C overnight.

1.2.3.2. Whole mount staining and cleaning of LacZ expressing embryos.

After mice were bred, the presence of a vaginal plug was considered as embryonic day 0.5 (E0.5). Timed pregnant mice were killed in a 100% CO_2 chamber, and mouse embryos were dissected into ice cold PBS, and all membranes (including the amnion) were removed. Prepared embryos were fixed for 2-6h in 0.5% glutaraldehyde and rinsed thoroughly in ice-cold PBS. Fresh X-gal buffer was prepared and embryos were incubated in X-gal buffer

overnight at 37C° protected from light. Stained embryos were washed in PBS to remove the rest of the staining solution, and fixed in 4% PFA overnight at 4C°. In some experiments embryos older than 15dpc were skinned prior staining to facilitate staining of internal organs, or viscera was removed to facilitate carcass staining. Embryos were cleared by incubation in a series of solutions containing 20%, 50%, 80% and 100% glycerol (v/v) brought to the final volume with 1% KOH (w/v) at 30C°: Each incubation step last from 4 to 7 days until sinking of the embryos was observed, after which the solution was changed. Cleaned embryos were stored and visualised in 100% glycerol.

1.2.3.3. Preparation of histochemical slices.

Dehydrated DRGs were embedded in O.C.T. Tissue-Teks (Sakura Finetek, Netherlands), frozen on dry ice and stored at -80C° prior to use. Brains, spinal cords and skin were embedded in O.C.T and frozen for a maximum of 20 seconds in dry ice-cooled isopentane and stored at -80°C. For further histochemical experiments, frozen embedded tissues were sectioned on a Cryostat (Leica CM3050S), transferred to slides, and dried at room temperature. The thickness of sections was dependent on tissue type and the type of staining used. For dorsal root ganglia sections thickness was normally about 18μm, brain and spinal cord 16 μm, and 40-50 μm for skin sections.

1.2.3.4. Immunohistochemistry.

Freshly prepared or stored at -80C° slides were washed in 1X TBS and incubation for 2 hours at room temperature in a pre-incubation buffer containing 1% BSA and 0.1% Triton-X-100. After 2 hours the buffer was changed to an incubation buffer containing the first antibody, 5% goat serum and 0.05% Triton-X-100, and incubated overnight at 4C°. Concentrations of the antibodies used were determined empirically for each particular case. The next day sections were washed three times with 1X TBS buffer for 10 minutes followed by incubation with buffer containing secondary antibody applied for 2 hours at room temperature. Finally, slices were washed 3 times with 1X TBS 10 minutes each, the last 10 min wash contained hoesch in a 1:10000 dilution. Then it was washed for 5 min with double distilled water, air-dried and coverslipped.

1.2.4. Protein Analysis

1.2.4.1. Protein isolation and quantification

DRGs or brain regions were isolated and immediately immersed in 2mL CK14 tubes from Precellys® containing RIPA lyses buffer supplemented with a protease inhibitor cocktail (Roche). The samples were homogenised in a Precellys®24-Dual homogeniser using 2 steps program. Each step at 5000 rpm for 25 seconds, and then incubated for 20-30 minutes with rotation followed by centrifugation for 20 minutes at 16000g. The supernatant was transferred into a new tube and centrifuged for 30 more minutes. All the steps were performed at 4C° or on ice to reduce protein degradation. Protein concentrations were estimated using the BCA protein assay kit based on the Biuret reaction. When the protein concentration was obtained, the samples were diluted so that all of them would be in the same concentration.

1.2.4.2. SDS-PAGE and Western blotting

Before separation on SDS gels, protein samples were diluted 1:3 with 4x SDS sample loading buffer and denatured for 5 minutes at 95C°. Cooled samples were then loaded on 13% SDS gel and proteins separated in 1x Tris-glycin buffer at 120-150V on a Mini-PROTEAN III system (BioRad). After separation of proteins, the SDS-PAGE gel was rinsed with distillate to reduce SDS amount, and proteins were blotted on nitrocellulose membrane using wet-blotting Mini Trans-Blot system (BioRad) according to the manufacture's instructions. The membrane was rinsed with 1x TBS buffer and incubated in blocking buffer for non-specific binding of antibody with shaking for 1 hour at room temperature. The blocked membrane was washed 2 times 5 minutes each in 1x TBS-0.5% Tween buffer followed by incubation in the primary antibody diluted in 1x TBS – 0.5% Tween buffer for 1 hour with shaking. In the next step, non-bound antibody was washed from the membrane in   1x TBS – 0.5% Tween buffer (3 times 5 minutes each) and the membrane was incubated in the secondary peroxidase-conjugated antibody pre-diluted in 1x TBS – 0.5% Tween buffer. The membrane was washed again in the same manner and developed with ECL reagent (Pierce). Chemiluminescence signal was detected after exposure of the membranes to ECL films (GE Healthcare).

1.2.5. Physiology

1.2.5.1. DRGs cell culture

Mouse DRGs were dissected from 4 weeks old animals and collected in a 1.5ml tube in PBS on ice. Ganglia were washed once with PBS before incubation with 1μg/ml Collagenase TypeIV in 1ml PBS at 37°C for 25 minutes followed by 3 minutes centrifugation at 170 x g. The supernatant was removed and DRGs were incubated with 100μl 0.5% Typsin in 1ml PBS at 37°C for 20 min. The supernatant was removed and 1ml D-MEM/F12 medium was added. The suspension was passed through a 23G injection needle to dissociate them into single cells, and centrifuged at 170 x g for 4min. The supernatant was removed and cells were resuspended in 1ml culture medium. Cells were plated on laminin (EHS-derived laminins) coated coverslips, which were pre-coated with Poly-L-Lysine (PLL), about 120-150 μl of cell suspension per coverslip. After 4 hours, the cells were floated with 1 mL of DRG medium. Cells were cultured for 24h at 37°C in a Steri-Cult 200 incubator.

1.2.5.2. Electrophysiology

Whole-cell patch clamp recordings were made at room temperature (20–24°C) from cultures prepared as described above. Patch pipettes were pulled from borosilicate glass capillaries (Hilgenberg, Malsfeld, Germany), filled with patch clamp buffer (intracellular solution) and had tip resistances of 4–8 MΩ. The medium of the cell culture was changed for patch clamp buffer (extracellular solution). Recordings were made using an EPC-10 amplifier (HEKA, Lambrecht, Germany) with Patchmaster[©] and Fitmaster[®] software (HEKA). Pipette and membrane capacitance were compensated using the auto function of Patchmaster and series resistance was compensated by 70% to minimize voltage errors.

1.3. RESULTS

1.3.1. The in vivo visualization of D-hair receptors

Down-hair (D-hair) receptors correspond to 6% of the sensory neurons in the DRG, and function as ultra sensitive movement detectors in the skin due to their low mechanical threshold (Brown and Iggo, 1967). D-hairs receptors physiological properties have been well characterised in mice using single fiber recordings in vivo and in vitro. However, although this technique gives us information about the firing pattern of these afferents in response to mechanical stimuli to the skin (Koltzenburg et al., 1997a), the type and properties of the channels responsible for the rapid and specific response of D-hairs receptors to mechanical stimuli can be studied only using patch clamp of DRG neurons in vitro. At the same time, the identification of D-hairs receptors in cell culture is required for studying the effect of molecular factors in D-hairs receptors. That is why a genetic labelling of this subpopulation of sensory neurons would allow a more complete characterization and in addition allow us to unravel D-hair receptors make-up. I used the fact that the $Ca_v3.2$ channel is expressed in the DRG cells only by D-hairs mechanoreceptors (Shin et al., 2003) to produce an in vivo reporter system which uses the promoter of the $Ca_v3.2$ channel to drive the expression of GFP. Generating the $Ca_v3.2^{GFP}$ knock-in mouse would allow a complete description of the spatiotemporal activity of the $Ca_v3.2$ channel in the mouse and at the same time allow the characterization of D-hairs receptors identified. A second knock-in mouse was generated under the same strategy but in this case CRE recombinase would be expressed instead of GFP protein. The $Ca_v3.2^{Cre}$ knock-in mouse would in theory permit the conditional knock-out of genes only in D-hair mechanoreceptors in order to elucidate their effect on the behaviour of this subpopulation of sensory neurons.

1.3.1.1. Generation of $Ca_v3.2^{Cre}$ knock-in mouse

To express cre recombinase in putative D-hair receptors, the targeting cassette containing the sequence of CRE protein was inserted after the star codon of the $Ca_v3.2$ channel gene which is located at the beginning of the second exon **Figure 6**. The insertion of the targeting cassette also produces a knock out of the calcium channel when the locus is targeted because of the stop codon at the end of the Cre recombinase sequence. This

feature is very convenient since it permits us the study of the role of $Ca_v3.2$ channel in these cells.

Confirmation of correct recombination events in ES cells was done by Southern blot as well as the genotyping of offspring chimeras' first generation. The probe 5´ End which binds to the $Ca_v3.2$ channel upstream locus was designed to analyze the upstream region to the insertion site of the targeting cassette. Digestion of genomic DNA with EcoRV restriction enzyme and the use of this probe produce a 22 kb band for the wild type allele and a 17 kb band for the targeted allele **Figure 7**. Efficiency for recombination of 8.7 % can be estimated taking into account that 25 out of 288 ES clones screened with this probe showed a 17kb band in the Southern blot.
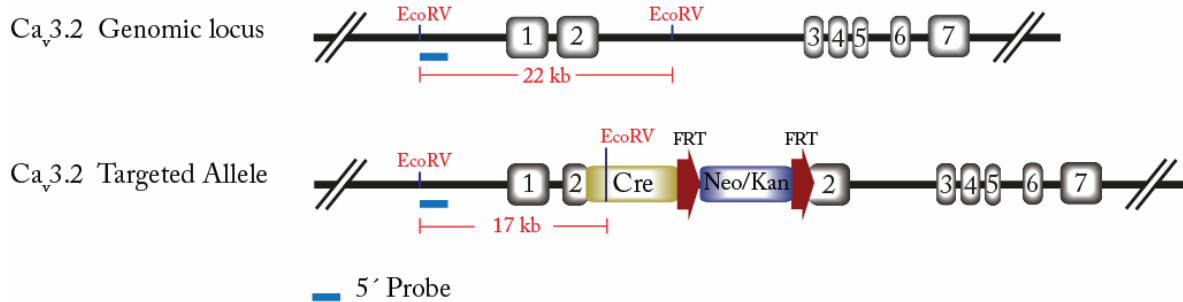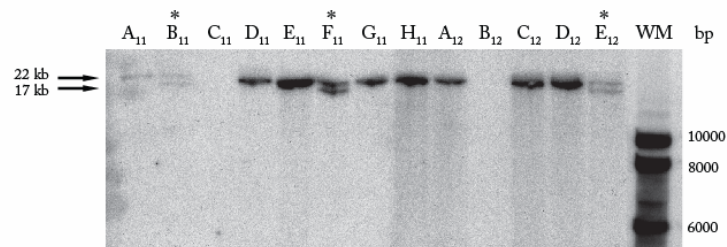
Figure 7. 5´ End Southern blot design for screening of positive ES clones. (A) Representation of $Ca_v3.2$ wild type allele and $Ca_v3.2^{Cre}$ knock-in allele and the band produced when EcoRV is used to digest DNA. The 5´ probe (in blue) binds at the beginning of the DNA sequence. (B) Example of a western blot from ES cell DNA after electroporation with the *Cre-FRT-Neo-FRT* targeting cassette. The wild type allele is recognized by the presence of a 22 kb band while transformed allele shows a 17 kb band. * = $Ca_v3.2^{Cre}$ positive clone.

A second (3´End) probe was use to analyze the downstream region to the insertion site of the targeting cassette. Hybridisation of this probe against EcoRI digested genomic DNA of ES clones produced a 15.5 kb band for the wild type allele and 12 kb band for the targeted allele **Figure 8**. Southern blot of the ES clones being positive for the 5´ End probe were tested using the 3´End probe and as showed in the **Figure 8**, when the

genomic DNA loaded for electrophoresis was enough, the 12 kb band signal showed a correct insertion at the 3´downstrem to the targeting site.
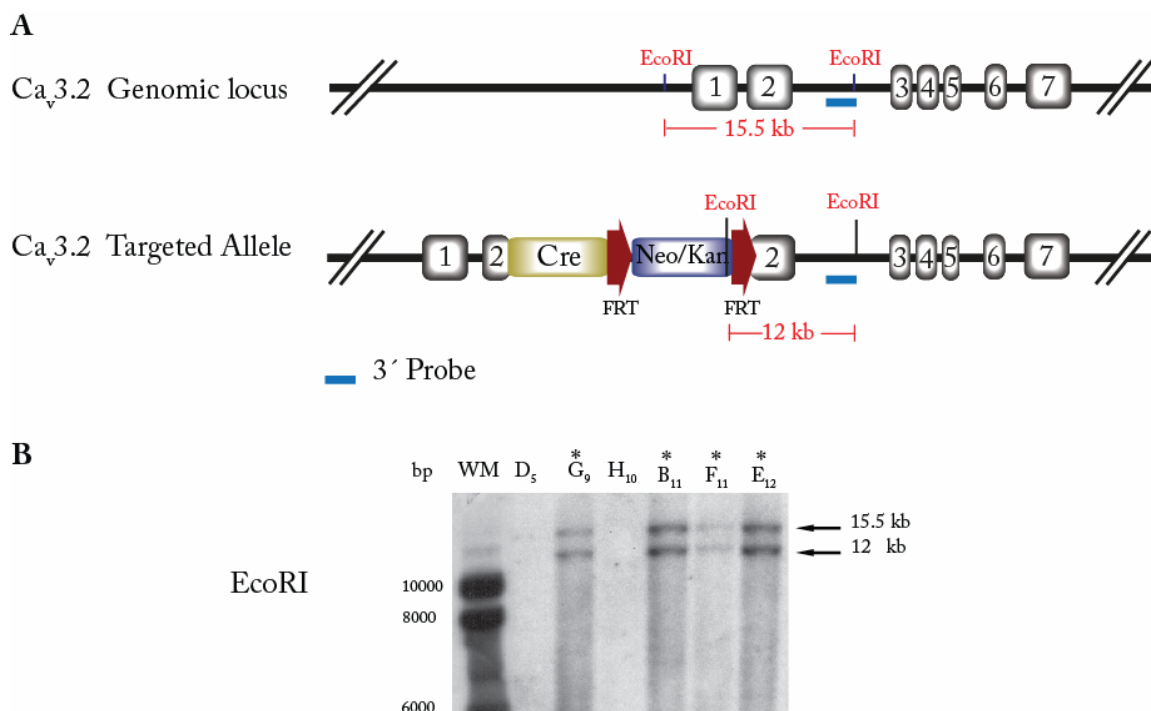
Figure 8. 3´ End Southern blot design for screening of positive ES clones. (A) Shows the design of the 3´End probe (in blue) that will screen for correct insertions to the left side of the insertion site of the targeting cassette. (B) Southern blot analysis of ES clones where the wild type band (15.5 kb) and the knock-in allele band (12 kb) are shown for positive clones when EcoRI restriction enzyme is used. * = positive ES clone.

In order to evaluate if there was any random insertion event in the ES cells' genome, a Southern blot was made using a probe against Neo. Since the bands observed in the Southern blots coming from hybridisation of the membrane with the 5´ End probe or 3´ End probe depend on the DNA sequence selected and the restriction enzymes used, random insertion of the cassette can not be detected using these probes. Hence, hybridisation with a probe against Neo is required.   The binding of the probe is specific for the Neo cassette and in case of random insertion of the Neo cassette in the genome; bands of different sizes than expected from the targeted locus would be observed.

The Neo probe was screened against those knock-in positive clones having a correct insertion of the cassette as observed from analysis of the upstream 5´ end to the insertion site and downstream 3´ end to the insertion site. Four out of six ES clones showed a single

6.5 kb size band indicating no insertions other than those targeted after the initiation codon of the Ca$_v$3.2 channel gene located at the beginning of the second exon **Figure 9**.

Once the *Ca$_v$3.2^{Cre}* mouse line was established the next generations would be genotyped by conventional PCR for the Cre recombinase or a PCR for the Ca$_v$3.2 wild type allele as described in material and methods.
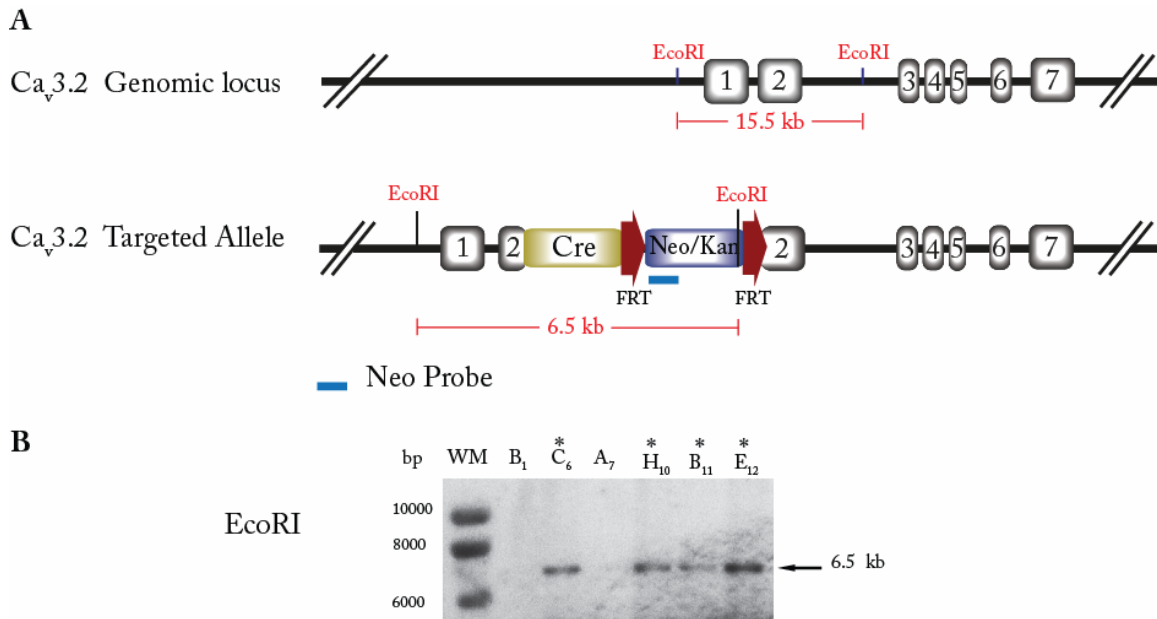
Figure 9. Southern blot design for screening of single insertions of the targeting cassette. (A) Neo probe (in blue) was designed to bind to the beginning of the sequence of the positive selection marker. A single and correct insertion of the targeting cassette would produce a 6.5 kb band. (B) Southern blot analysis of ES clones selected previously with 5′End and 3′End probe were used to test for single targeting cassette insertion. * = positive ES clone.

1.3.2. Characterization of the *Ca$_v$3.2^{Cre}* knock-in mouse

The cre expression pattern in the *Ca$_v$3.2^{Cre}* knock-in mouse was observed by crossing this strain with the reporter lines *Tau^{mGFP}* (*Tau-lox*P-STOP-*lox*P-*mGFP*-IRES-NLS-*LacZ*-pA) or *Rosa26^{LacZ}* (R26R-*lox*P-PKG*neo*4xpA-*lox*P-*LacZ*-pA). In the *Tau^{mGFP}* reporter mouse the expression of myristylated GFP (mGFP) and ß-galactosidase (ß-gal) is activated in neurons once the stop signal flanked by two loxP sites is removed by CRE recombinase. GFP is then sent to the membrane while ß-gal is located in the nucleus of the cell (Hippenmeyer et al., 2005). In the *Rosa26^{LacZ}* reporter line, cytoplasmic ß-gal is ubiquitously expressed in embryos and adult mice upon commencement of activity of Cre (Soriano, 1999).

1.3.2.1. $Ca_v3.2^{Cre}$ knock-in mouse central nervous system

To determine the expression pattern of CRE recombinase in the central nervous system, the $Rosa26^{LacZ}$ reporter line was used because visualization of single cells is possible. The ß-gal expression is restricted to the cytoplasm of the neurons instead of the axon projections as occurs in the Tau^{mGFP} strain. Immunostainings against ß-gal of brain and spinal cord were analysed in 4 weeks old perfused $Ca_v3.2^{Cre}$; $Rosa26^{(LacZ)}$ animals.

Analysis of coronal brain slices shows positive cells for ß-gal in the cortex, hippocampus, cerebellum and brain stem **Figure 10**. The hippocampus was the region with the highest amount of ß-gal positive cells, where cells from the pyramidal layers of fields CA1, CA2 and CA3 as well as cells from the granule cell layer in the dentate gyrus show positive staining **Figure 10,1a**. In the cortex ß-gal positive cells were found in layers I to VI, in the region of the retrosplenial area and somatomotor areas **Figure 10, 1b** and layer V of the somatosensory areas **Figure 10, 1**. Strong staining was also observed in cells of the amygdala in the striatum **Figure 10, 1c**. Although less densely stained, the brain stem also shows some positive cells for ß-gal in the thalamus and hypothalamus **Figure 10, 1** and in the medulla in the hindbrain **Figure 10, 2b**. In the cerebellum, the expression of ß-gal seems to be restricted just to some of the Purkinje cells along the cerebellar cortex **Figure 10, 2a**.
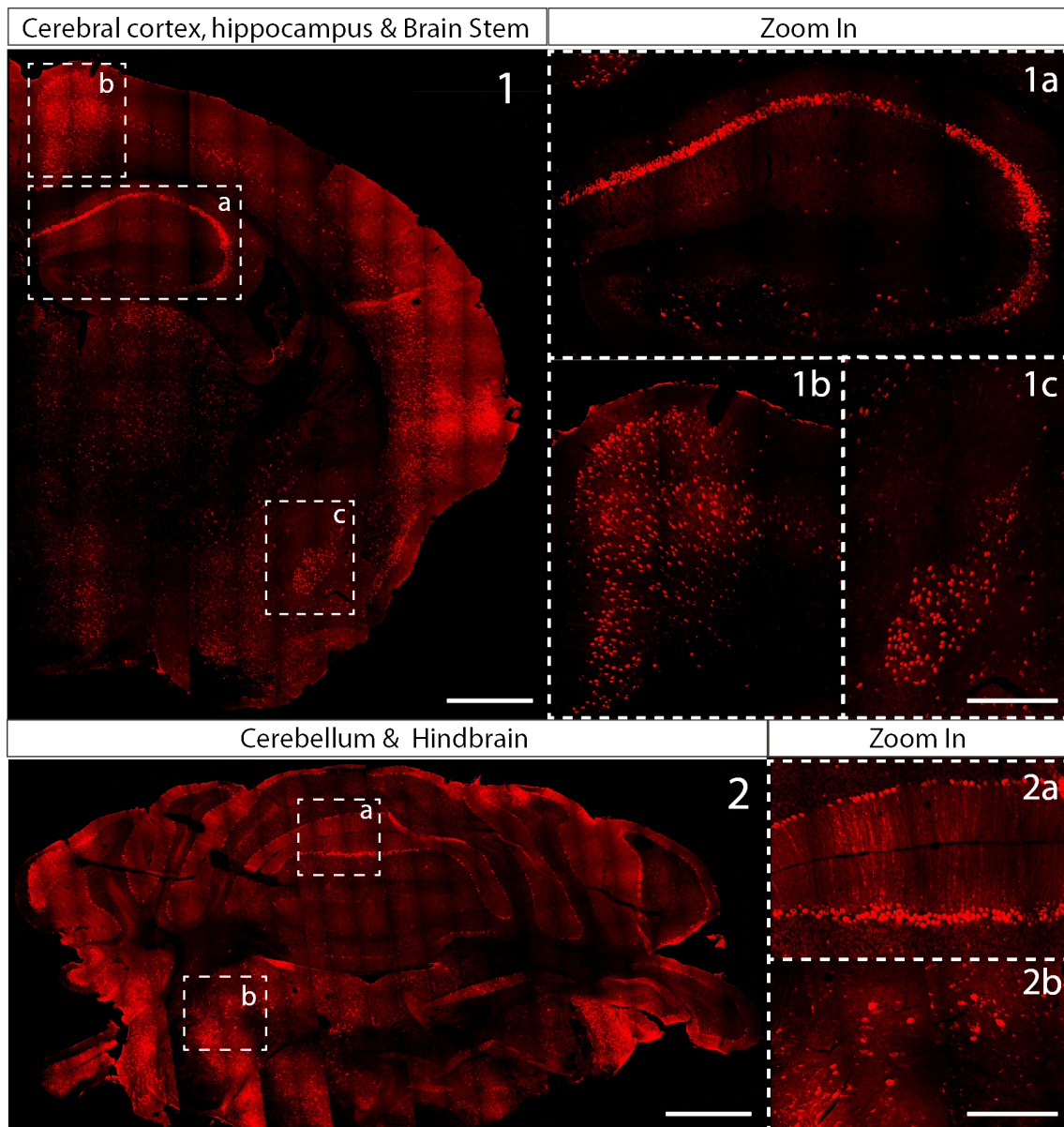
Figure 10. Cre activation in brain of *Ca$_v$3.2^{Cre} ;Rosa26 $^{(LacZ)}$* mice. (1) Coronal section of *Ca$_v$3.2^{Cre}* ; *Rosa26 $^{(LacZ)}$* adult mouse brain stained using antibody against ß-gal. Squares (1a,b and c) show a zoom-in of hippocampus, cortex and amygdala, regions where dense and intense ß-gal signal was observed. (2) Coronal sections of cerebellum and hindbrain. Notice that not every single Purkinje cell of the cerebellum was positive (zoom-in 2a square). 2b zoom-in shows positive staining for ß-gal in some cells of the hindbrain. 1 and 2 scale bar: 600µm. Zoom-in squares scale bar: 300µm.

Interneurons of the spinal cord were ß-gal positive in layers I-X. However, a higher density of ß-gal expressing cells were observed in the dorsal spinal cord compared with those found in the ventral spinal cord where the motor interneurons are located **Figure 11a**. Characterization of ß-gal positive interneurons in the dorsal spinal cord was made using antibodies against Pax2 and Lmxb1 transcription factors which are markers for

GABAergic (inhibitory) and glutamatergic (excitatory) interneurons respectively (Batista and Lewis, 2008)(Cheng et al., 2005). Co-stainings of ß-gal with the interneuron markers showed that Pax2-ß-gal positive cell population **Figure 11b-d** is more prominent than that of Lmxb1-ß-gal positive cells **Figure 11e-g**.
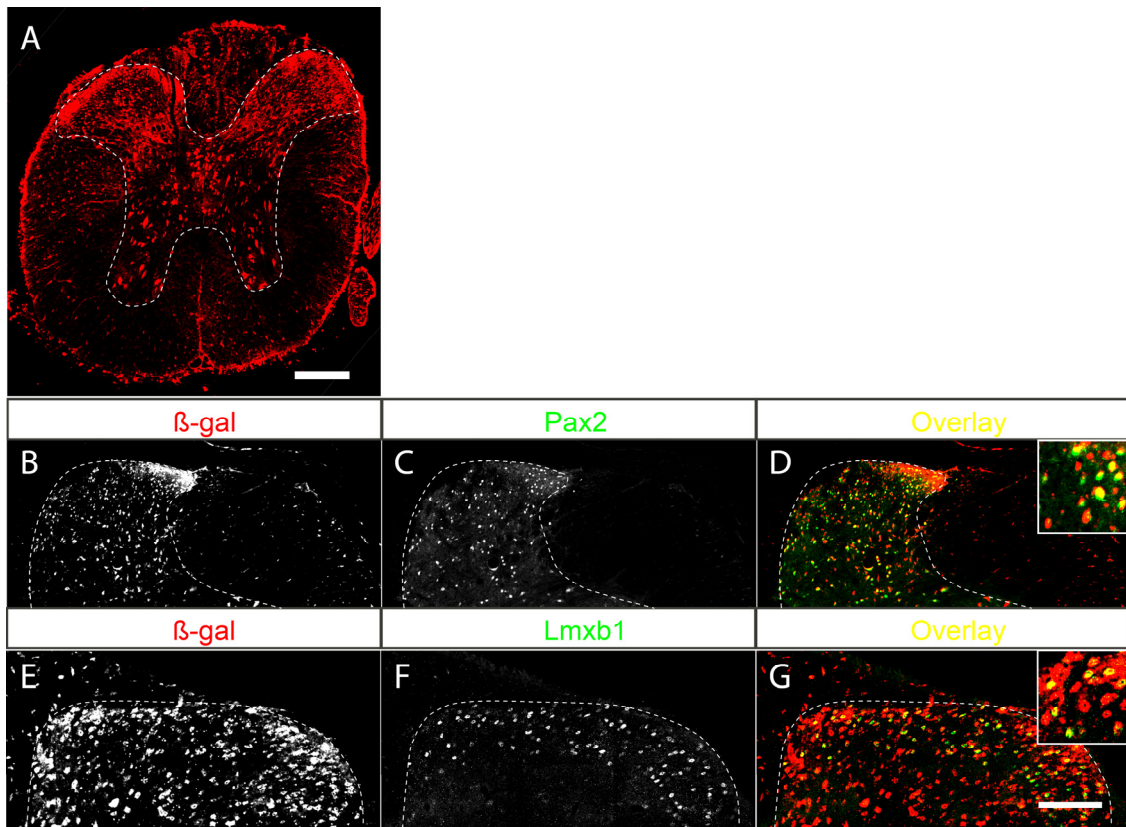
Figure 11. Cre activation in spinal cord of $Ca_v3.2^{Cre}$; $Rosa26^{(LacZ)}$ mice. (A) Whole spinal cord ß-gal staining in adult animals. (B-D) Inhibitory interneurons were stained using an antibody against the transcription factor Pax2. (E-G) Excitatory interneurons were visualized using the transcription factor Lmxb1. Scale bar 200 μm.

1.3.2.2. Cre expressing cells in the DRG

$Ca_v3.2^{Cre}$; $Tau^{(mGFP)}$ adult animals were used to evaluate DRG cells where activation of CRE recombinase took place. Expression of CRE will remove the stop transcription signal that is preventing GFP from being expressed, so that double labeling of GFP with some molecular markers would allow the characterization of cells where the $Ca_v3.2$ channel promoter was activated. Co-staining of GFP with Neurofilament 200 (NF200) allowed the identification of large diameter Aß myelinated afferents which are mechanoreceptors with a low threshold response to mechanical stimuli, and medium diameter Aδ light-myelinated afferents (Bourane et al., 2009a)(Luo et al., 2009a). Co-expression of GFP and NF200 indicates that Aß and Aδ fibers in these animals expressed CRE **Figure 12a-c**. One of the

markers for unmyelinated fibers is the plant lectin isolectin B_4 (IB_4) that binds to small diameter C-fiber nociceptors in the DRG which are the non-peptidergic nociceptors (Silverman and Kruger, 1990). Co-expression of GFP and IB_4 in some DRG cells indicates that the $Ca_v3.2$ channel was also activated in this type of cell **Figure 12d-f**. Tyrosine hydroxylase (TH), a marker for non-peptidergic C, low threshold mechanoreceptors (C-LTMR)(Li et al., 2011a) was used and co-expression of GFP with TH was also abserved **Figure 12g-i**. The broad GFP expression pattern observed in DRGs together with the positive co-expression of GFP and the molecular markers for sensory cell subtypes indicate that the activation of the $Ca_v3.2$ promoter and subsequent CRE recombinase expression took place very early in development. Unfortunately GFP expression seen in animals from breedings between $Ca_v3.2^{Cre}$ with $Tau^{(mGFP)}$ strains do not show a real time activity of the $Ca_v3.2$ promoter because after cre recombination occurs, GFP expression depends on the Tau promoter in these animals.
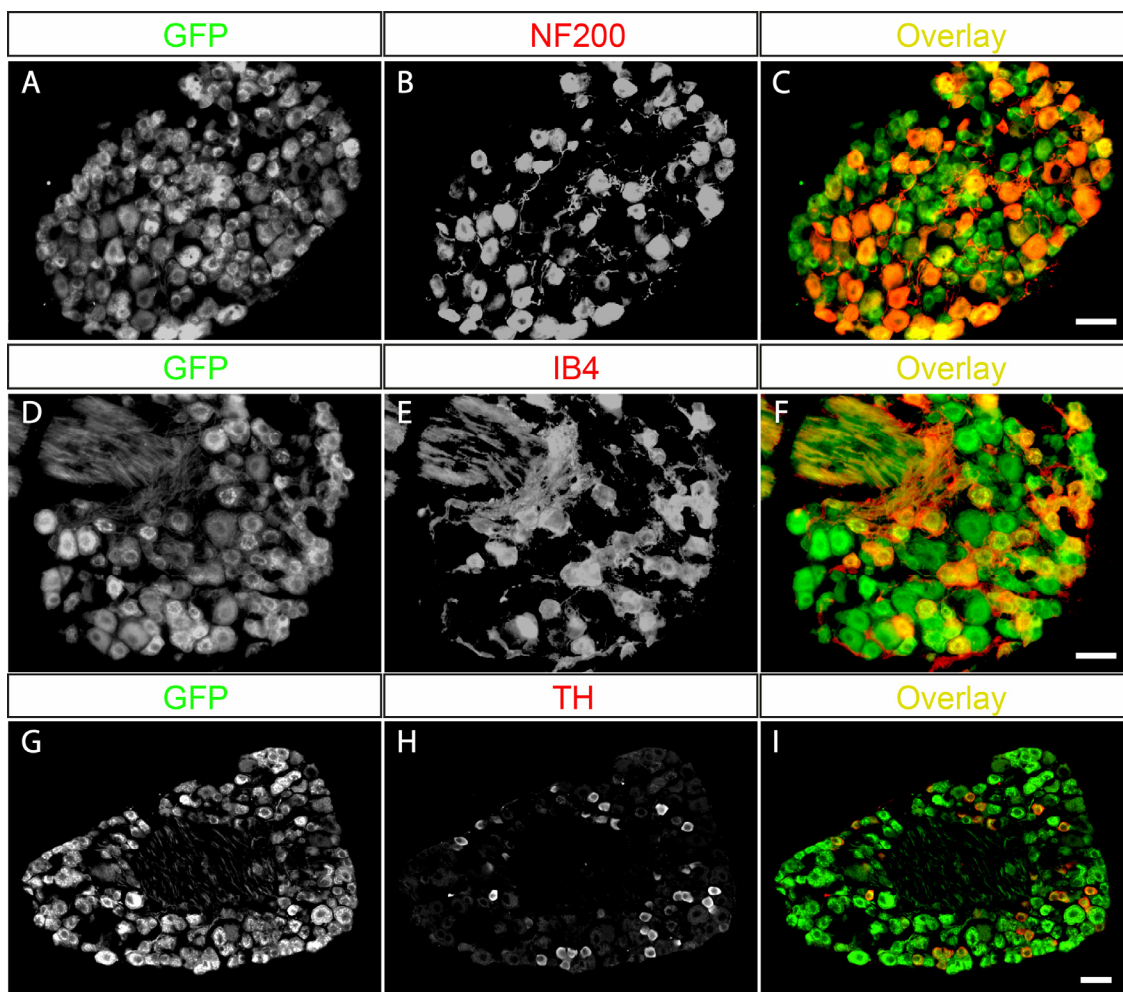
Figure 12. Cre activation in the DRG of $Ca_v3.2^{Cre}$; $Tau^{(mGFP)}$ mice. (A-C) Double immunostaining of GFP and NF200 for identification of Aß and Aδ myelinated afferents. (D-F) Immunostaining of GFP and IB_4 for identification of non-peptidergic unmyelinated noniceptors.

(G-I) Double immunostaining of GFP and TH for identification of non-peptidergic C-LTMR. Scale bar 50 μm.

1.3.2.3. Sensory innervation of the Skin

A special feature of the *Tau*$^{(mGFP)}$ reporter line is that mGFP is a membrane targeted protein and permits tracing of axon projections, allowing analysis of the end-organ innervation in the skin of Ca$_v$3.2^{Cre}; *Tau*$^{(mGFP)}$ animals. Glabrous and hairy skin of the hindpaw of Ca$_v$3.2^{Cre}; *Tau*$^{(mGFP)}$ adult animals were used because of the diversity of touch receptor organs located in the limb. At first it was needed to confirm that the GFP positive fibers observed in the skin were axon projections coming from DRG cells using the protein gene product 9.5 (PGP 9.5) antibody which is a marker for neuronal cells. The co-stainings of GFP and PGP 9.5 showed that all and only the GFP positive structures observed in the skin come from peripheral neurons **Figure 13a-c**.

Afferents innervating the skin can be classified according to their conduction velocity and myelin thickness into large diameter Aß, medium diameter Aδ and unmyelinated small diameter C-fibers (Djouhri and Lawson, 2004). A subset of GFP positive fibers were identified as Aß and Aδ afferents using an antibody against NF-200 **Figure 13d-f**. Additional markers were needed in order to determine the nature of the other GFP positive fibers and to analyse the type of sensory ending organ associated with all GFP positive axons.
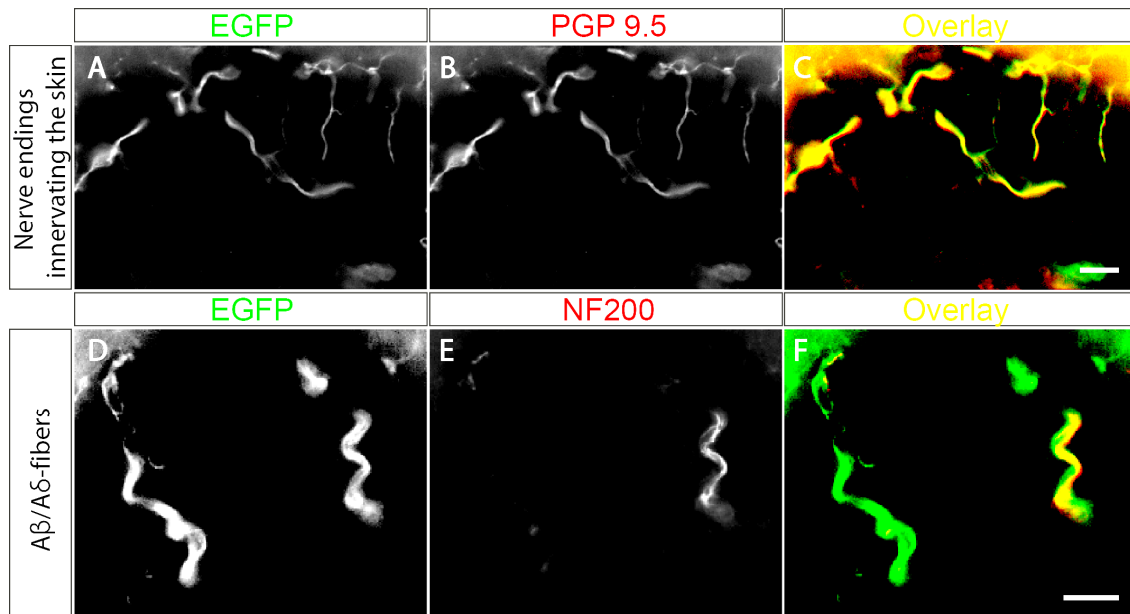
Figure 13. Innervation of DRG cells in the skin of *Ca$_v$3.2^{Cre} ; Tau$^{(mGFP)}$* mice. (A-C) PGP 9.5 staining to visualize nerve endings in the skin. (D-E) NF200 for visualization of Aß and Aδ afferents in the skin. Scale bar 20μm.

In mammals, Aß nerve fiber axons in the skin can innervate Guard-hair follicles (G-hair), Merkel cell neurite complex, Ruffini endings, Meissner corpuscles and Pacinian corpuscles all of which are touch afferents (Lumpkin and Caterina, 2007). Lanceonate and Pilo-Ruffini endings are innervated by axon afferents to hair follicles that respond to light brush stimuli in the skin, and movement of hairs (Brown and Iggo, 1967), and can be visualised using the schwann cell marker S-100 (Luo et al., 2009b). In hairy skin of *Ca$_v$3.2^{Cre}* ; *Tau$^{(mGFP)}$* adult animals, both structures were GFP positive **Figure 14a-f**. However, it is important to mention that although guard hairs (G-hair) as well as down-hairs (D-hair) share the same pattern of innervation, D-hairs are associated with a Aδ-fibers and G-hairs with Aß-fiber, and this difference can not be distinguished using the S-100 antibody.
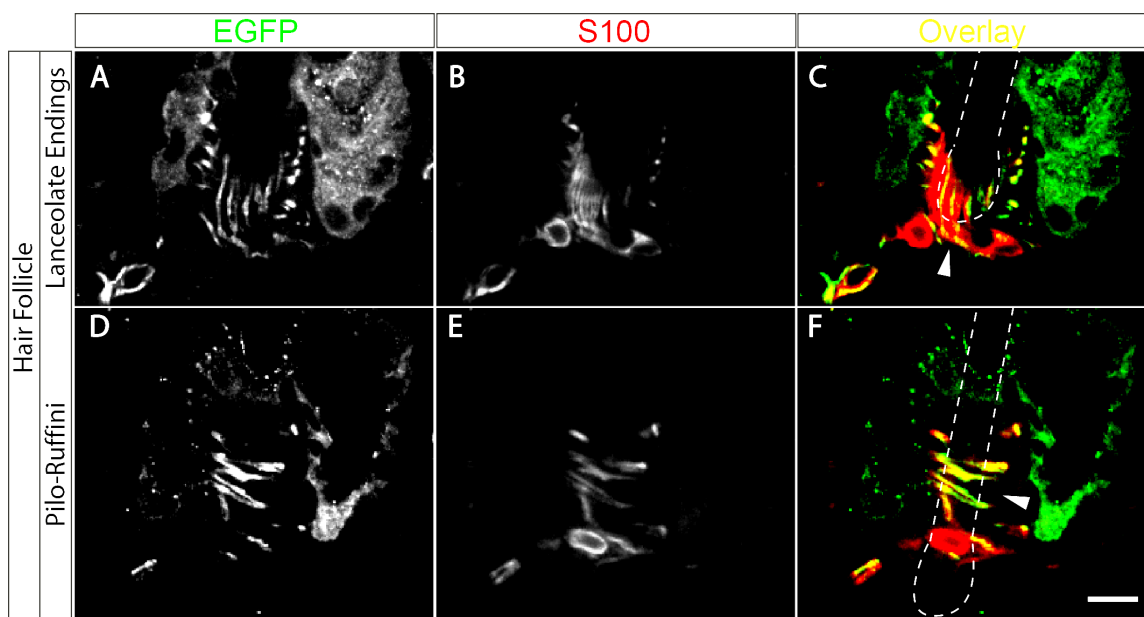
Figure 14. **Hair follicle innervation in the skin of *Ca$_v$3.2^{Cre} ; Tau$^{(mGFP)}$* mice.** Co-immunostaining of GFP and S-100 in hairy skin slices of the mause paw for visualization of lancelonate endings (A-C) and pilo-Ruffini endings (D-F). In C and in D the arrow heads indicate the structure of the nerve innervating the hair follicle. Scale bar 20μm.

Meissner corpuscles are encapsulated end organs present in the dermal papillae of glaborous skin of the palms, soles and lips in mammals (Montagna, 1977). Meissner corpuscles are innervated by Aß fibers and respond to dynamic deformation of the skin (Johnson et al., 1980). These structures were observed as well using S100 antibody stainings in the dermal papillae of footpad skin from *Ca$_v$3.2^{Cre} ; Tau$^{(mGFP)}$* adult mice. Meissner corpuscles showed a normal structure and were also positive for GFP **Figure 15a-f**.

EGFP	S100	Overlay
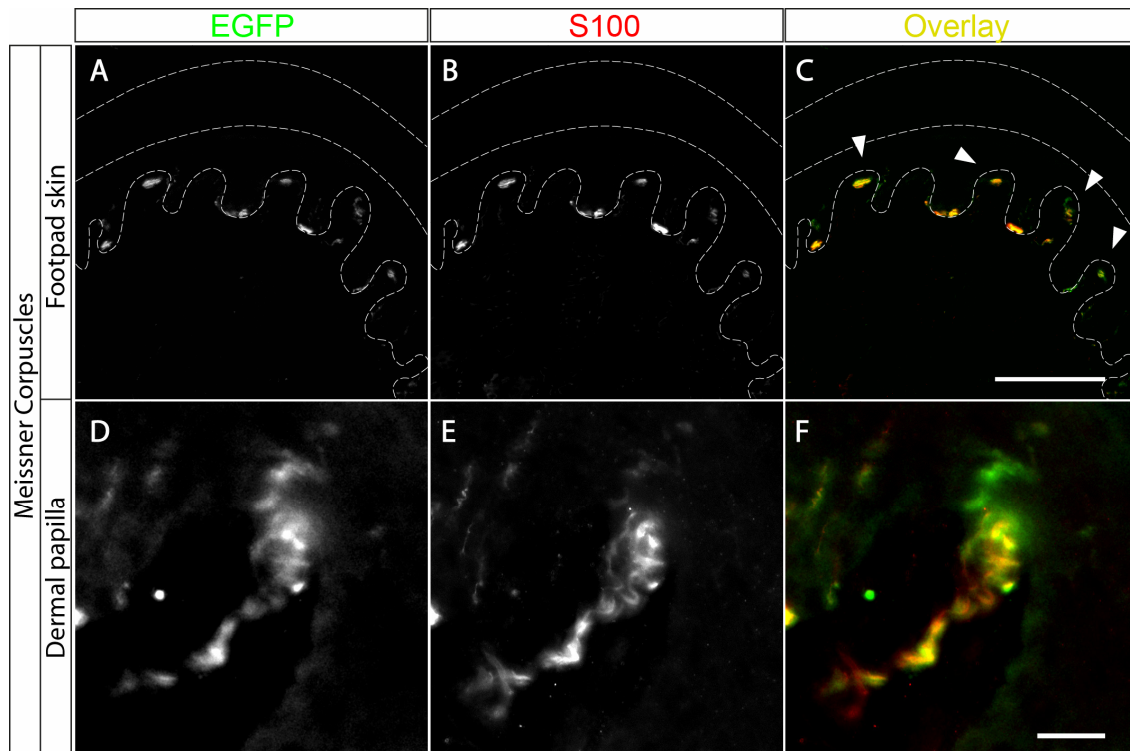
Figure 15. Meissner Corpuscles in skin of $Ca_v3.2^{Cre}$; $Tau^{(mGFP)}$ mice. (A-C) S-100 also permits visualization of Meissner corpuscles in the dermis of glabrous skin of the paw. The dashed lines show the epidermis and dermis. In (C) the arrow heads indicate the location of the Meissner corpuscles. Scale bar 100μm. (D-F) Amplification of the dermal papillae shows a better structure of the corpuscles. Scale bar 10μm.

Merkel nerve endings are located in the basal layer of glabrous skin, and in hairy skin where they group forming special structures called hair disks. They were first described from structure and function in the cat as slowly adapting (SA) mechanoreceptors which respond to skin indentation (Iggo and Muir, 1969), and together with Ruffini corpuscles are the only end organs innervated by an Aß fiber having a slowly adapting response to mechanical stimuli. From a skin staining analysis made on three different animals, Merkel cells were the only touch receptors not innervated by GFP positive axons in $Ca_v3.2^{Cre}$; $Tau^{(mGFP)}$ animals neither in hair disks of the hairy skin **Figure 16a-c** nor in touch domes in glabrous skin **Figure 16d-f**. This result suggest that DRG cells associated with Merkel cells come from progenitors which did not express $Ca_v3.2$ ionic channel at any point during development.
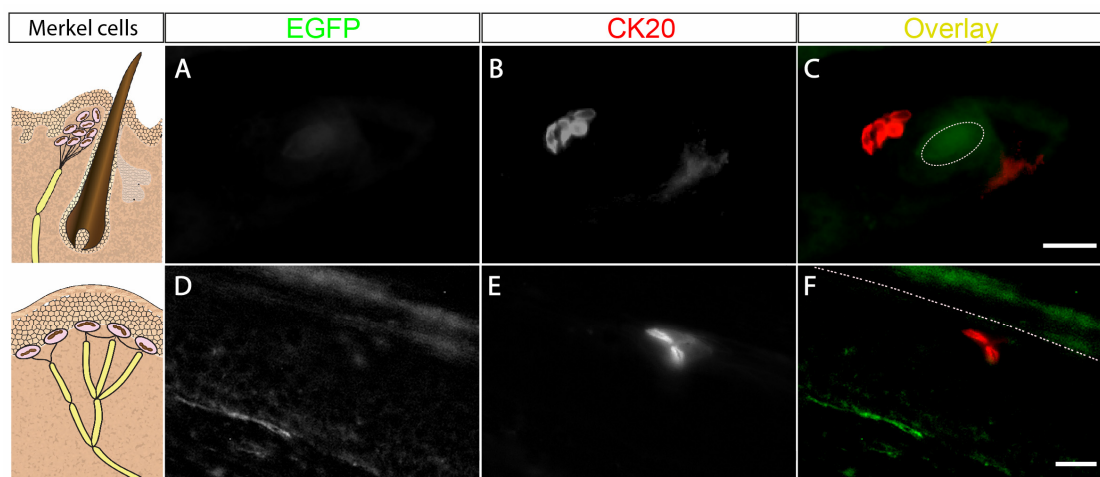
Figure 16. Merkel cells in the skin of $Ca_v3.2^{Cre}$; $Tau^{(mGFP)}$ mice. In the left pannel the localization of Merkel cells is shown in schematic in hairy skin (upper-left) and in the glabrous skin (down-left). Horizontal sections of hairy skin (A-C) and perpendicular sections to the glabrous skin of the mouse paw. The dashed circle in C indicates the transversal section cut of the hair. (D-F) were stained using CK20 to identify the merkel cells at the end of DRG afferents. The dashed line in F indicates the separation between epidermis and dermis. Scale bar 20μm.

1.3.2.4. Activation of $Ca_v3.2$ ion channel promoter during development in $Ca_v3.2^{Cre}$ knock-in mouse

The $Ca_v3.2^{Cre}$ mouse can be used as well to determine when the $Ca_v3.2$ channel promoter turns on expression during development. Breedings between $Ca_v3.2^{Cre}$ and $Tau^{(mGFP)}$ mice were made, and embryos from different stages of development were analysed. Whole embryo x-gal stainings of $Ca_v3.2^{Cre}$; $Tau^{(mGFP)}$ mice showed nuclear ß-gal expression at ages as early as E11.5. At day 11.5 of development, the embryos already have a high ß-gal staining signal in the hind brain, DRGs and spinal cord compared with only few positive cells for ß-gal found in forebrain and midbrain **Figure 17a-c**. As development continues more and more neurons in the brain, DRGs and spinal cord start to express ß-gal **Figure 17d-i**.
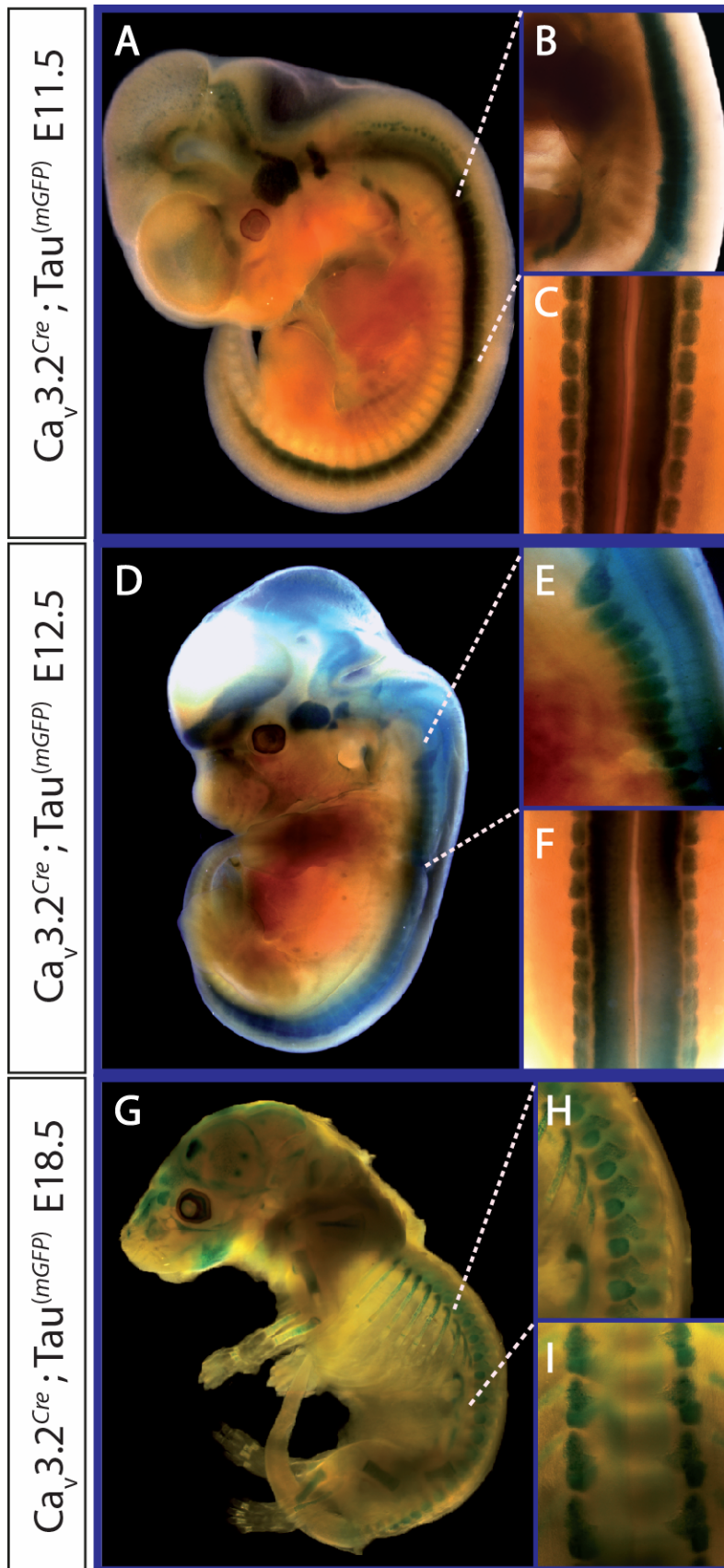
Figure 17. Cre activation in *Ca$_v$3.2^{Cre}* ; *Tau$^{(mGFP)}$* mice in development. ß-gal expression in the nervous system of *Ca$_v$3.2^{Cre}* ;*Tau$^{(mGFP)}$* mice as shown by the blue staining. Embryos at stages E11.5 (A-C), E12.5 (D-F) and E18.5 (G-I) of development. The staining observed in bones in the E18.5 embryos was also observed in negative controls. C, F and I, dorsal view of the spinal cord.

B, E and H, lateral view of the spinal cord. Stronger X-gal staining was observed in the spinal cord and DRGs in early stages compared with brain.

1.3.2.5. Electrophysiological properties of Ca$_v$3.2^{Cre} ; Tau$^{(mGFP)}$ DRG cells in culture

DRG cells in culture retain many of the properties of mechanoreceptors and can respond to mechanical stimuli. Using patch clamp techniques, nociceptors can be recognized in cell culture for having a hump on the falling phase of the action potential and mechanical activated currents with a slowly adapting (SA), intermediate adapting (IA) or rapidly adapting (RA) inactivation kinetics. RA currents in nociceptors are TTX insensitive (Hu and Lewin, 2006)(Rugiero et al., 2010). On the other hand, mechanoreceptors possess narrow action potentials without a hump and possess rapidly adapting currents (RA) that activate and inactivate very quickly to mechanical stimuli (Hu and Lewin, 2006).

Action potentials duration at half peak amplitude, recovery time after hyperpolarization, and shape have been reported by different authors as classification methods for sensory neurons in cell culture (Djouhri et al., 1998; Lawson, 2002; Lechner et al., 2009; Petruska et al., 2000). Since action potentials properties from DRG cells of Ca$_v$3.2 knock-out mice are not different to those from wild type mice (Wang and Lewin, 2011), I used half peak duration and after hyperpolarization duration of DRG action potentials to classify the GFP positive cells of Ca$_v$3.2^{Cre} ; Tau$^{(mGFP)}$ adult mice into mechanoreceptors or nociceptors. Whole-cell current clamp recordings from GFP positive DRG cells in cell culture showed action potential shapes characteristic of mechanoreceptors in some cells and nociceptors in other cells **Figure 18A**. The classification criteria is based on the fact that action potentials without a hump are normally narrow in shape, have short half peak duration and are characteristic of mechanoreceptor cells. In the same manner, humped action potentials with long half peak duration are characteristic of nociceptors. In addition, longer hyperpolarization duration is observed in nociceptors compared to mechanoreceptors (Djouhri et al., 1998). The results showed the existence of two populations of cells according to the grouping and distribution of the data. Approximately 50% of the GFP positive cells can be classified as mechanoreceptors according to their action potential short half peak duration and low τ constant values of hyperpolarization duration. The other 50% of the GFP positive cells had action potentials with higher half peak duration and higher τ constant value **Figure 18C**.
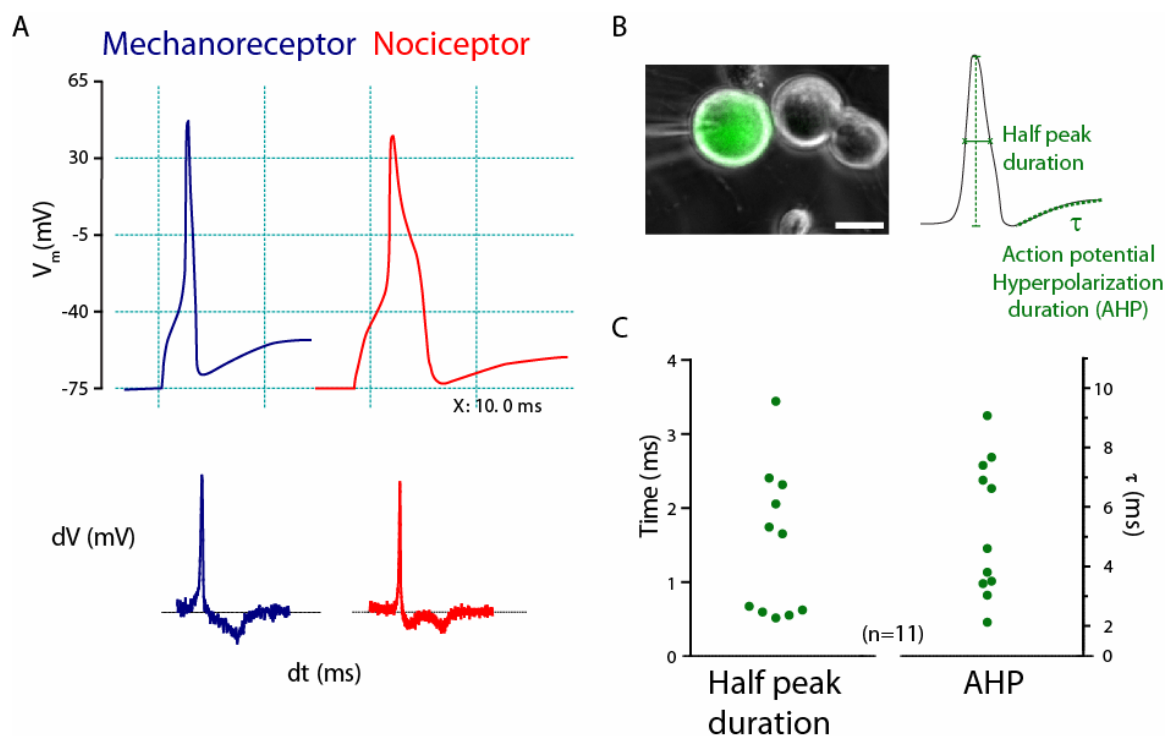
Figure 18. Action potential properties of GFP positive cells from $Ca_v3.2^{Cre};Tau^{(mGFP)}$ animals. (A)Examples of the action potential shape of mechanoreceptors and nociceptors. At the bottom is a graphic of the first derivate dV/dt which shows the presence of one minimum for mechanoreceptors and two minimums for nociceptors. (B) Left side: example of a GFP positive cell in cell culture, scale bar 20 μm. Right side: illustration of the action potential variables measured. (C) Action potential electrophysiological parameters of GFP positive DRG cells in culture, measured in whole cell current-clamp modus. Cells with a half peak duration of less than 1 ms were classified as mechanoreceptors.

1.3.3. Generation of $Ca_v3.2^{GFP}$ knock-in mouse

The $Ca_v3.2^{GFP}$ knock-in mouse shares the same construct design as the $Ca_v3.2^{Cre}$ mouse. The GFP-loxP-Neo-loxP targeting cassette was inserted at the beginning of the second exon of the $Ca_v3.2$ channel, right after the initiation codon of the gene **Figure 19A**. In this mouse, GFP expression depends only on the activity of the $Ca_v3.2$ channel promoter. That is why GFP protein in these animals permits the identification of cells where the calcium channel gene promoter is active and at the same time evaluation of the $Ca_v3.2$ channel's role can be done because of the stop codon inserted at the end of the GFP sequence, which in theory should produce a knock-out of the $Ca_v3.2$ ionic channel.

ES cells transfected with the targeting vector were screened for positive clones using Southern blot. The insertion to the upstream sequences of the targeting site was analysed using the 5´End probe and digestion of clones´ genomic DNA with the restriction enzyme

BamHI. The wild type locus was identified by the 8.2 kb band, while insertion of the GFP-loxP-Neo-loxP targeting cassette would increase the size of the band to 11.2 kb **Figure 19B**.
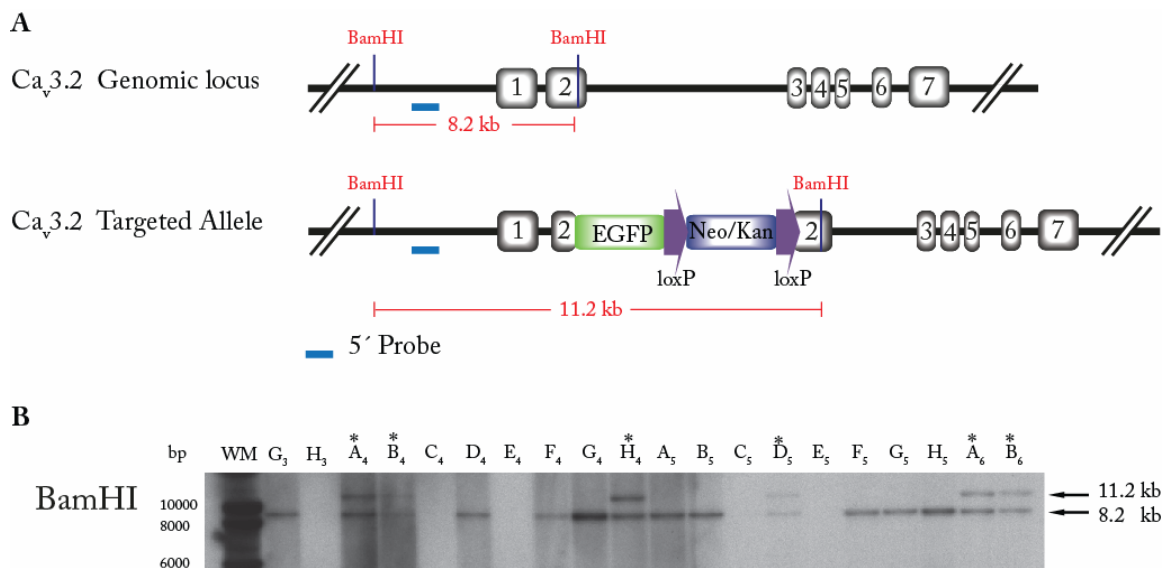
Figure 19. Screening of Ca$_v$3.2^{GFP} ES positive clones using the 5´End probe. (A) Representation of Ca$_v$3.2 wild type allele and *Ca$_v$3.2^{Cre}* knock-in allele and the band produced when BamHI is used to digest DNA. The 5´ probe (in blue) binds at the beginning of the DNA sequence. (B) Example of a western blot from ES cell DNA after electroporation with GFP-*LoxP-Neo-LoxP* targeting cassette. The wild type allele is recognized by the presence of a 8.2 kb band while the transformed allele shows a 11.2 kb band. * = *Ca$_v$3.2^{GFP}* positive clone.

The positive ES clones found with the 5' End probe were subsequently evaluated with the 3´End probe to check for correct recombination at the downstream region of the insertion site. Because the Neo cassette used to produce the targeting cassettes for both knock-in animals had the same sequence, EcoRI restriction enzyme could also be used to analyze *Ca$_v$3.2^{GFP}* ES positive clones. As expected, all the ES clones showed the 12 kb band indicating that a recombination event had occurred in the Ca$_v$3.2 locus **Figure 20**.

A

Ca$_v$3.2 Genomic locus

Ca$_v$3.2 Targeted Allele

3´ Probe

B
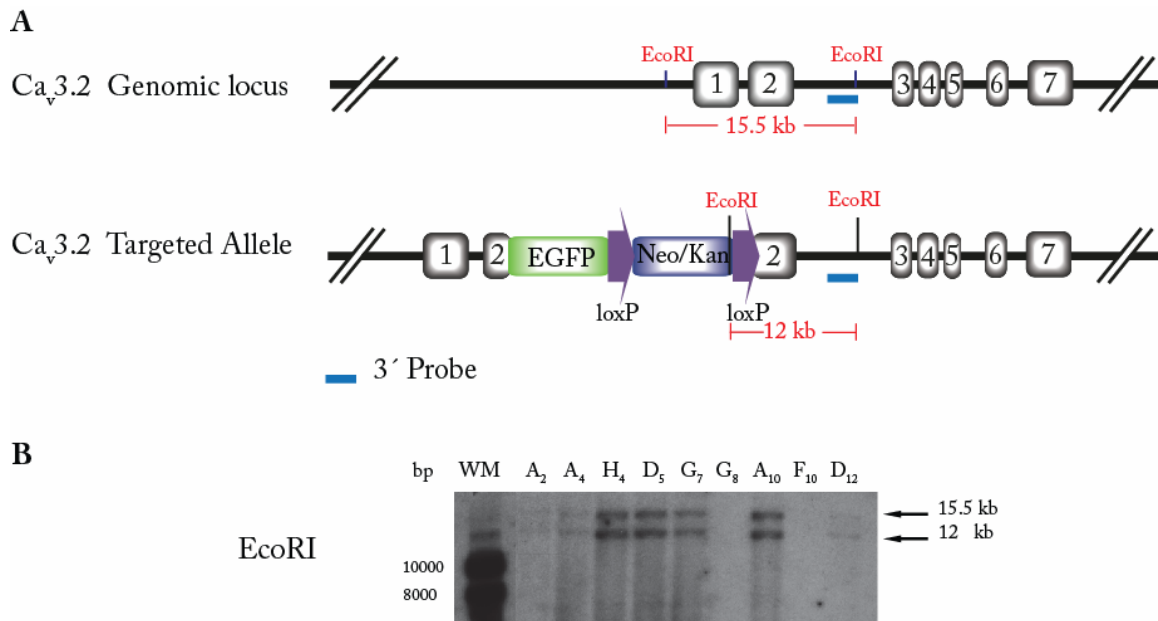
Figure 20. 3´End probe ES clones Southern blot analysis in Ca$_v$3.2^{GFP}. (A) Shows the design of the 3´End probe (in blue) that will screen for correct insertions to the left side of the insertion site of the targeting cassette. (B) Southern blot analysis of ES clones where the wild type band (15.5 kb) and the knock-in allele band (12 kb) are shown for positive clones when EcoRI restriction enzyme is used. * = positive ES clone.

Potential random recombination events in the genome of the mouse was evaluated by hybridization of EcoRI digested DNA of the ES clones with a Neo probe **Figure 21**. When the correct homologous recombination event occurs a unique 1.9 kb size band is visualized in the Southern blot. Only one ES clone (G$_8$) out of nine seemed to have any random insertions of the targeting cassette **Figure 21**. Two clones were selected and used for blastocyst injection and the chimeras obtained were bred with C57BL/6N mice. The animals were genotyped by Southern blot until the second generation. Subsequent genotyping was made by conventional PCR for GFP and wild type allele as described in material and methods.
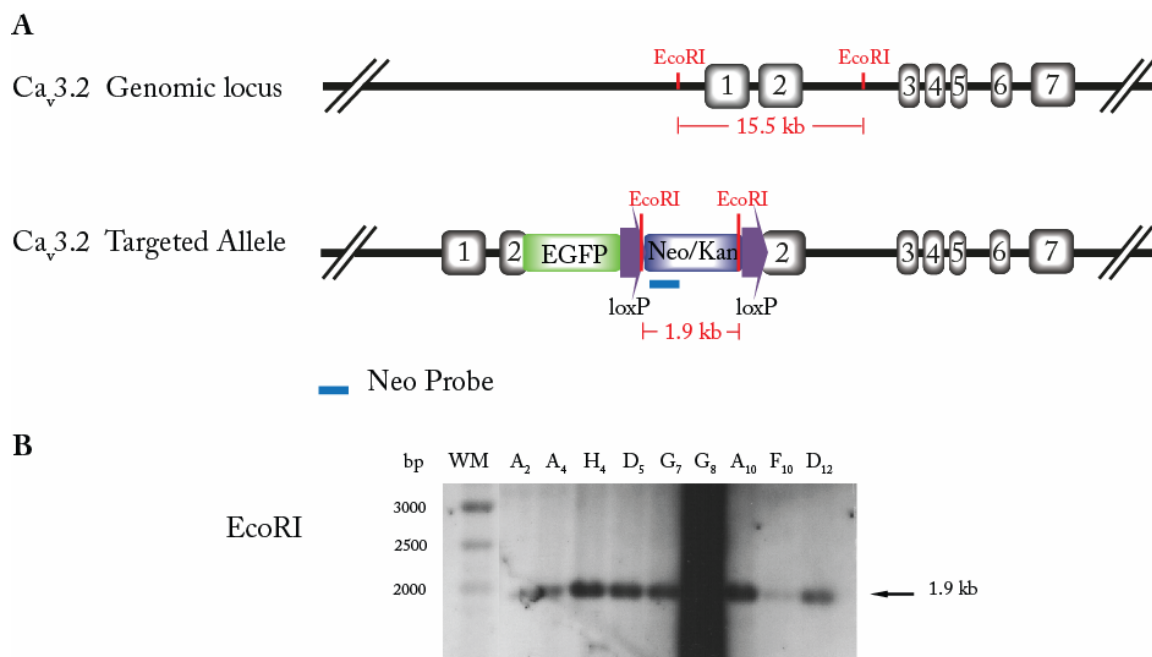
Figure 21. Random homologous recombination events in Ca$_v$3.2^{GFP} ES clones. (A) Neo probe (in blue) was designed to bind to the beginning of the sequence of the positive selection marker. A single and correct insertion of the targeting cassette would produce a 1.9 kb band. (B) Southern blot analysis of ES clones selected previously with 5´End and 3´End probe were used to test for single targeting cassette insertion.

1.3.4. Characterization of *Ca$_v$3.2^{GFP}* knock-in mouse

The T-type calcium channel subunits 3.1, 3.2 and 3.3 are known to play an important role in the function of excitable cells (Cain and Snutch, 2010; Iftinca, 2011). However, identification of the distinct physiological function of each channel subtype has been hampered due to the absence of specific channel blockers to dissect out single currents and the fact that high similarity between subunit sequences does not allow the production of specific antibodies for each T-type channel subtype. That is why the *Ca$_v$3.2^{GFP}* knock-in reporter mouse gives a very good opportunity to determine the spatiotemporal expression of the calcium channel. An immunostainig analysis of tissues slices from brain, spinal cord and DRGs of perfused *Ca$_v$3.2^{GFP}* adult animals was carried out to visualize GFP expressing cells because the fluorescence signal coming from the GFP expressed in such a tissues was not strong enough for detection.

1.3.4.1. GFP expression analysis in the central nervous system of *Ca_v3.2^{GFP}* knock-in mice

In the brain of *Ca_v3.2^{GFP}* homozygous adult animals, expression of GFP protein was observed only in the dentate gyrus (DG) of the hippocampus and in the axons located in the internal capsule, which contains both ascending and descending axons that run between the cerebral cortex and the pyramids of the medulla **Figure 22**. Although the pattern of staining in the hippocampus could be confused with cells of the Cornu Ammonis area 3 (CA), it is important to clarify that the nerve ending signal of the growth associated protein (GAP-43) was inserted in the GFP sequence of the cassette and this signal will send the GFP to the cytoplasmic face of the plasma membrane of axon terminals in the brain (Mosevitsky, 2005). Therefore, if cells of the CA3 region were positive, its axon projections would produce positive staining in the CA1 region and instead what can be observed in the figure is the bundle of axons that form the mossy fibers of the dentate granule cells.
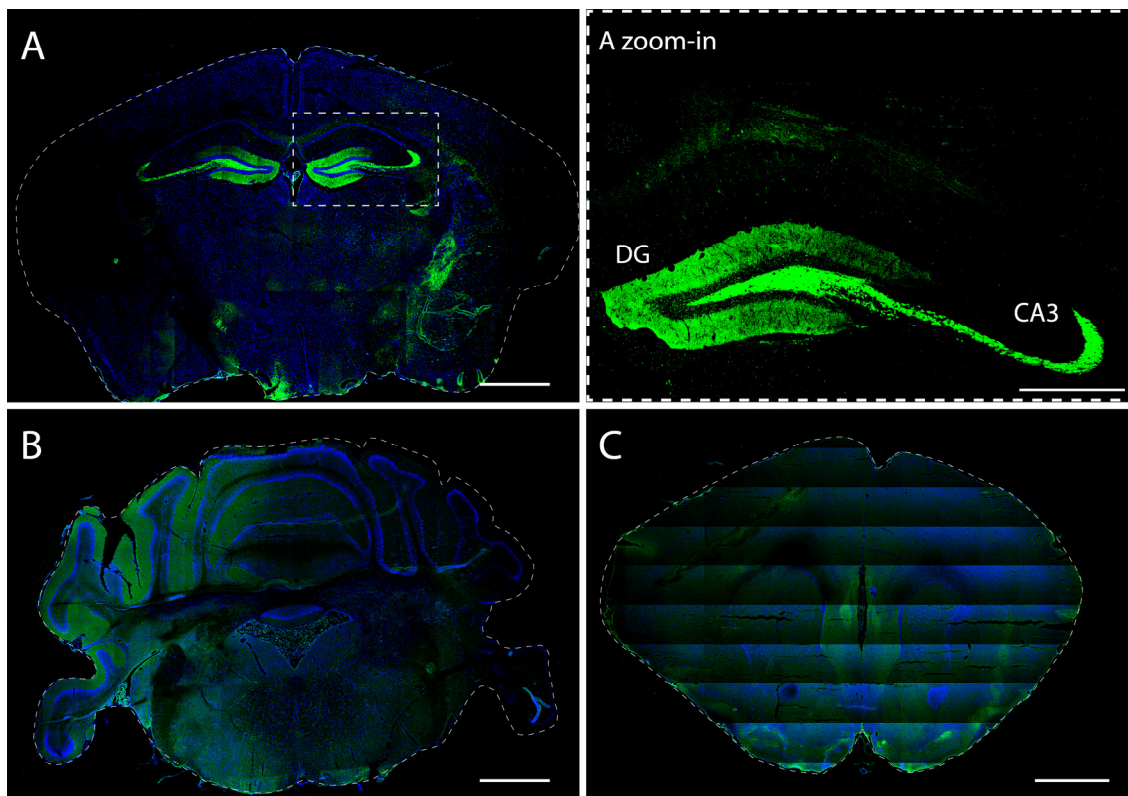
Figure 22. GFP expression pattern in brain of Ca_v3.2^{GFP} knock-in mice. GFP immunostaining of coronal sections of *Ca_v3.2^{GFP}* knock-in mice show staining only in hippocampus and in the internal capsule (A and zoom-in square). Cerebellum, hindbrain (B) and olfactory areas (C) do not show positive staining (B-C). Scale bar 1mm. (zoom-in scale bar 500 μm).

Expression of GFP in other regions of the brain was not observed. However, there is evidence of $Ca_v3.2$ channel expression in stratium, hypothalamus, thalamus and brain cortex (Chen et al., 2010; McRory et al., 2001; Talley et al., 1999). It is possible that levels of GFP in these regions are too low to detect with immunostaining. Hence, I decided to do qPCR to quantify GFP mRNA, and western blot to check GFP protein levels.

Absolute quantification of GFP mRNA in brain was done interpolating the cycle threshold obtained for every sample in the real time PCR into the standard curve made using different dilutions of pEGFP-N3 ranging from 50 to 5×10^8 plasmid molecules vs. cycle threshold (Ct) **Figure 23A**. Taking into account that real time PCR is so sensitive that as few as 50 molecules of GFP could be detected; total RNA samples were treated with DNAse before reverse transcription to eliminate interferences in the assay coming from genomic DNA.

GFP mRNA expression was measured in different brain regions of postnatal $Ca_v3.2^{GFP}$ homozygous animals and cDNA of Bl6 adult mice was used as a negative control. The results show GFP expression in hippocampus, olfactory bulbs, cerebellum, brain cortex, thalamus and the rest of the brain stem. However, notice that the number of GFP molecules in hippocampus was much higher compared with those from the other regions in the brain **Figure 23B**.

Figure 23. qPCR Analysis of GFP mRNA in Brain of $Ca_v3.2^{GFP}$ knock-in mice. (A) The calibration standard curve for GFP quantification using TaqMan Assay. The plotshows Cycle threshold (Ct) vs. $\log_{10}$ of GFP copies or molecules (n=2). (B) Bar graph showing the amount of GFP molecules per µg of total RNA used for reverse transcription. The amount of GFP molecules in the hippocampus was compared to those from other regions in the brain, (***P $\leq$ 0.001) Dunnet's multiple comparison test. Bars represent mean $\pm$ SD, (n=3).

According to the previous results, GFP's mRNA is expressed in different regions of the brain but GFP protein expression can be detected in the brain only in the hippocampus when using immunostaining. Although it could be explained due to the high levels of GFP messenger expression seen in this region, it is important to remember that real time PCR determines the amount of mRNA and determination of the GFP mRNA translated into protein in brain by means of a different method than immunostaining is necessary. Western blot analysis of GFP expression was performed because it permits quantification of proteins and is a much more sensitive than indirect immunostaining. In this case a rabbit polyclonal anti-GFP antibody was used to visualize the 27kDa GFP band present on the membranes **Figure 24A**. As described in materials and methods, BCA quantification of total protein in brain samples from P(0) $Ca_v3.2^{GFP}$ homozygous mice was made so that equal amounts of total protein could be loaded for protein separation on SDS-gels, and comparison of GFP expression levels between samples could be possible. Densitometry analysis of western blots was performed using the software ImageJ. The software transforms every band selected for quantification into a profile plot of the average intensity from the top to the bottom of the selection. The peaks in the profile plot correspond to the dark bands in the original image and integration of the area under the curve for each peak is how the intensity for each band is calculated. Comparison of the band intensity obtained for GFP protein in western blot in different regions of brain shows that the amount of GFP protein expressed in hippocampus is much higher than the amount expressed in cerebellum, cortex, olfactory bulb, thalamus and the rest of the brain stem **Figure 24B**. These results are very similar and confirm those obtained by real time PCR showing (**Figure 23B**) that detection limit is the reason why GFP can not be visualised in brain cortex using immunostaining.

Figure 24. Western blot analysis of GFP expression in brain of Ca$_v$3.2^{GFP} knock-in mice. (A) Representative western blots showing a GFP protein band at 27 kDa in different regions of the brain. Protein extract from HEK cells transfected with pEGFP-N3 was used as a positive control. (B) Densitometry quantification of GFP in brain. Arbitrary units (AU) from the hippocampus were compared to those from the other regions of the brain. (*P $\leq$ 0.05; ***P $\leq$ 0.001) Dunnet´s multiple comparison test. Data presented as mean $\pm$ SD, (n=3).

1.3.4.2. Ca$_v$3.2 promoter activation in the development of the peripheral nervous system

In order to obtain a complete understanding of the spatiotemporal activity of the Ca$_v$3.2 channel promoter in the peripheral nervous system of the mouse, immunofluorescence stainings using GFP antibody were made in spinal cord and DRG of *Ca$_v$3.2^{GFP}* homozygous mice during development at embryonic stages 9.5, 13.5, 16.5 and 18.5, as well as in postnatal stages.

In the embryonic mouse, GFP could be detected in stages as early as embryonic day 9.5 (E9.5) at the roof plate, some cells at the dorsal ventricular zone of the spinal cord and in some of the neural crest cells migrating to form the DRG later on at E10.5. Some positive staining was also observed in the epidermis **Figure 25A**. At E13.5 after the DRG is formed, GFP expression starts in few cells of the DRG, and a very strong fluorescent signal is observed at the ventral side of the spinal cord **Figure 25B**. As development progress the expression of GFP increases in the DRG at E16.5 and the number of labeled cells remains the same at E18.5. On the other hand, during the same period of time, the fluorescent signal seen at the ventral spinal cord in previous stages reduces its intensity and area until it disappears at E18.5 **Figure 25C** and **D** respectively. Bl6 embryos were used as a negative control for GFP staining.
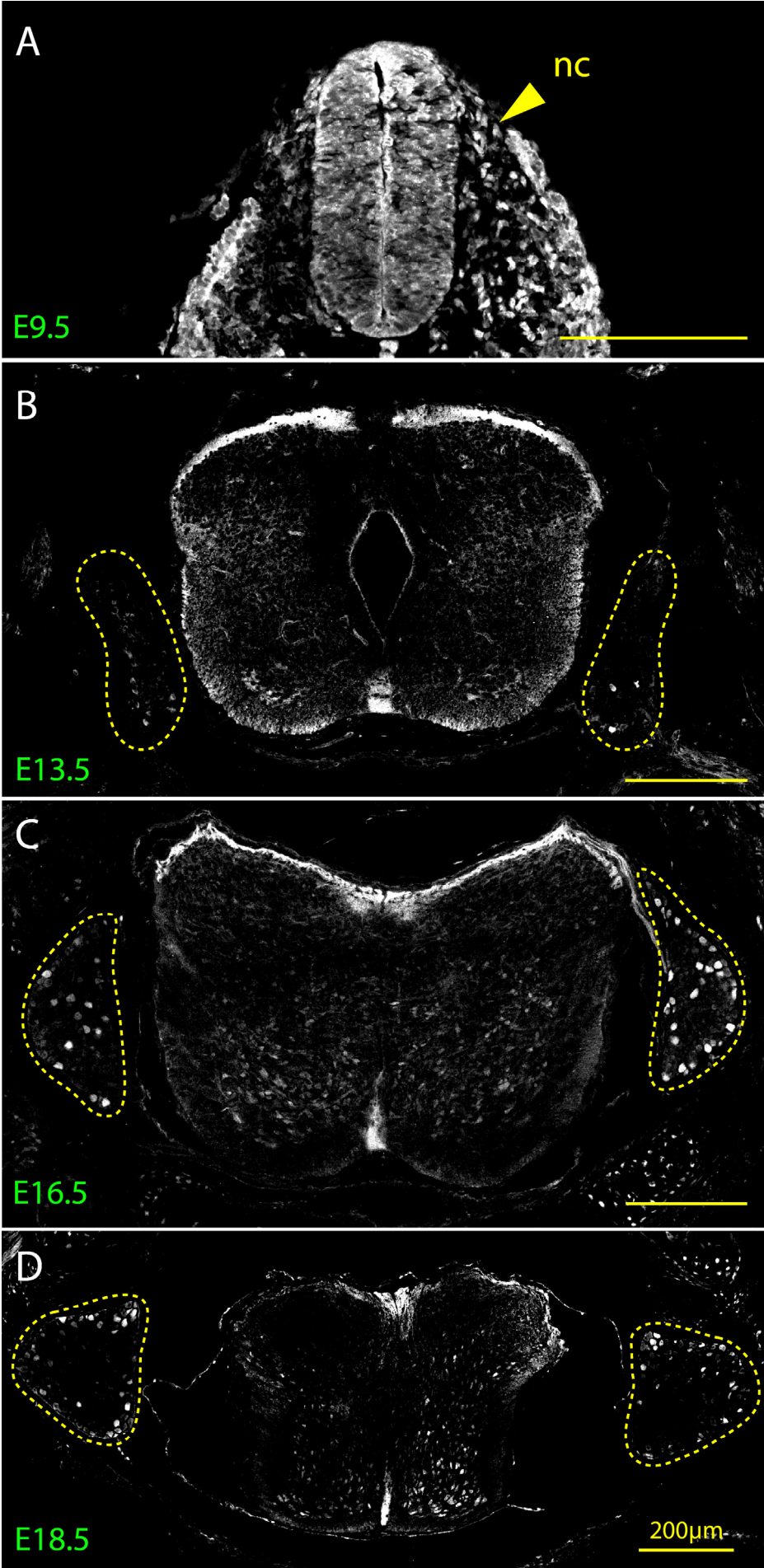
Figure 25. GFP expression during development in spinal cord and DRG of *Ca$_v$3.2^{GFP}* knock-in mice. At E9.5 (A), GFP is expressed in some cells of the neuronal crest (nc) is indicated by arrow head, and in the spinal cord. At E13.5 (B) a few cells of the DRG are GFP positive while the staining at the dorsal side of the spinal cord is stronger. At E16.5 (C) the number of GFP positive cells increases in the DRG, but staining in the spinal cord is becoming weaker. Finally at E18.5 (D) GFP expression in the DRG seems constant while the positive staining has almost disappeared in the spinal cord. The dashed lines indicate the borders of the DRG. Scale bar 200 μm.

Immunostaining for GFP was also tested in DRGs and spinal cord slices of 4 weeks old *Ca$_v$3.2^{GFP}* homozygous mice as well as at stage P0. Unfortunately, no positive GFP staining could be detected at these ages. To test if the Ca$_v$3.2 channel is down regulated postnatally, GFP expression was measured in DRGs at stages E16.5, E18.5 and P0 using real time PCR and western blot. Absolute quantification of GFP mRNA molecules by real time PCR showed no significant difference between the stages measured **Figure 26A** and **B**.
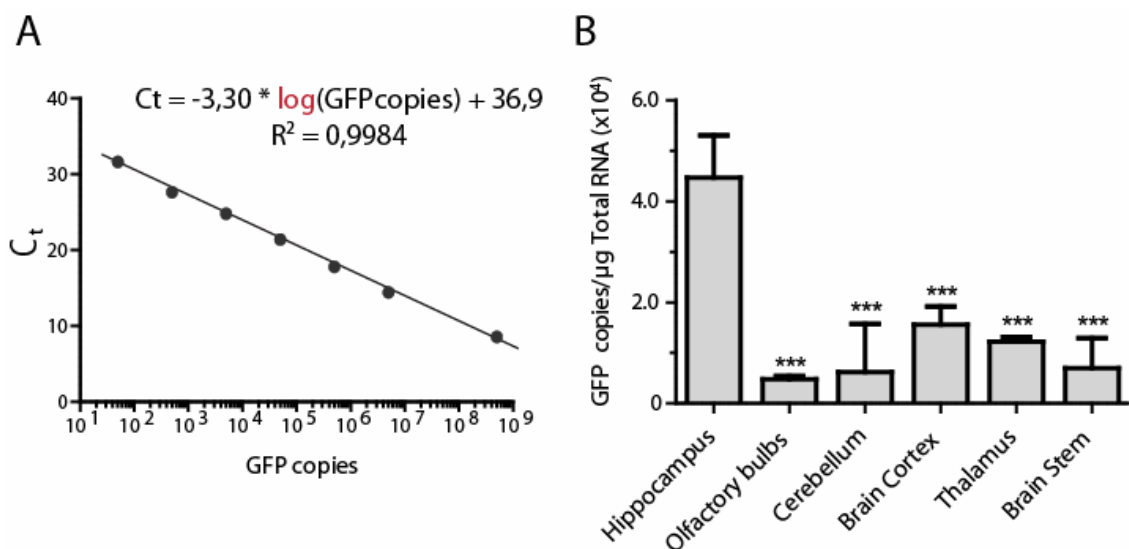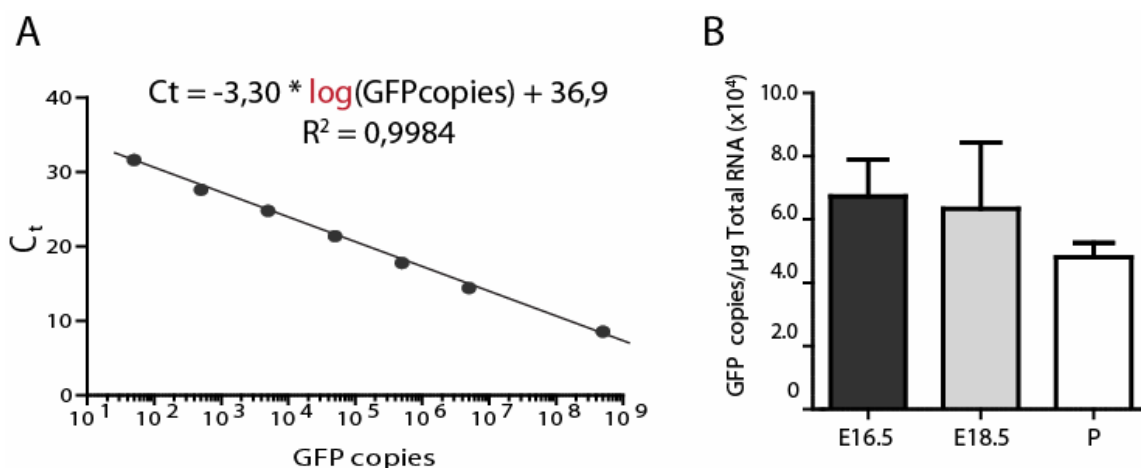

Figure 26. qPCR Analysis of GFP mRNA in DRGs of *Ca$_v$3.2^{GFP}* knock-in mice. (A) The calibration standard curve for GFP quantification using TaqMan Assay. Cycle threshold (Ct) was plot vs. log$_{10}$ of GFP copies or molecules (n=3). (B) Quantification of GFP molecules per μg of total RNA used for reverse transcription showed no difference in GFP mRNA expression in development compared with postnatal stages (P0). Tukey´s multiple comparison test. Bars represent mean $\pm$ SD, (n=3).

According to a western blot analysis GFP protein is expressed in postnatal (P0) DRG cells **Figure 27A**, and quantification of GFP protein expression levels obtained in western blot by densitometry did not show a difference between the embryonic stages measured and P(0) **Figure 27B**. E18.5 is the latest stage at which GFP protein can still be visualised in

DRG slices by immunostaining and the GFP expression seems to be at about the same levels as in P0 according to the results obtained by real time PCR and western blot. Hence DRG slices from E18.5 embryos were used to characterise the subpopulation of sensory neurons to which GFP positive cells in $Ca_v3.2^{GFP}$ homozygous mice belong.
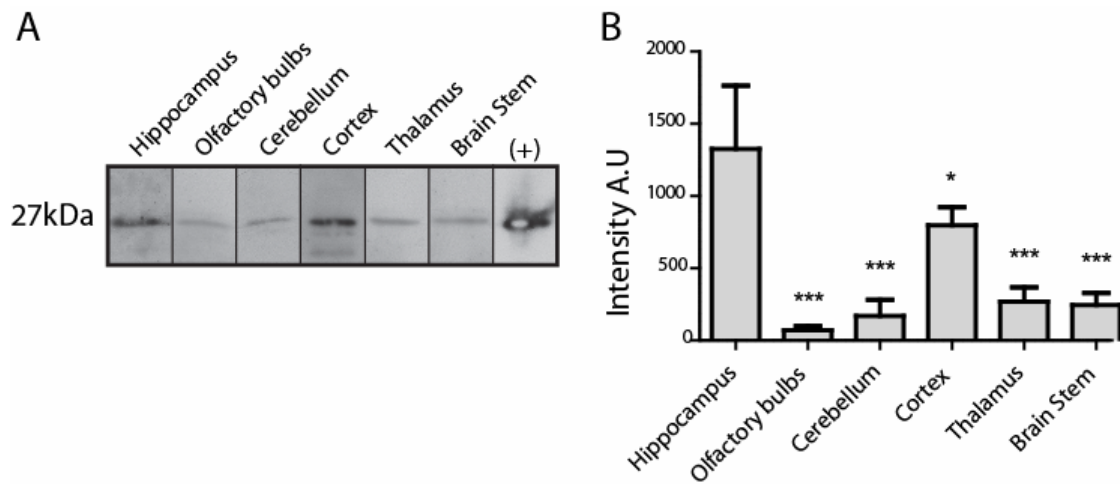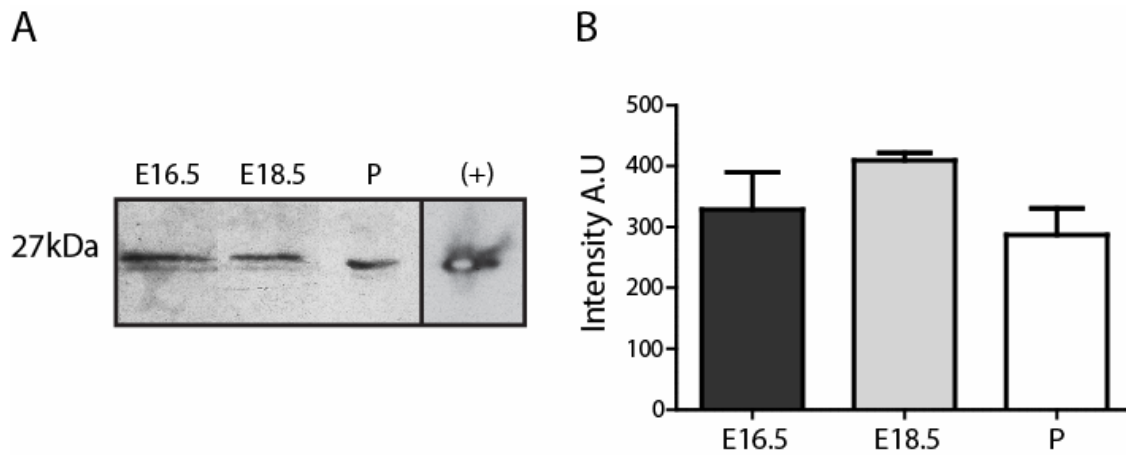

Figure 27. Western blot analysis of GFP expression in DRGs of $Ca_v3.2^{GFP}$ knock-in mice. (A) Representative western blots from DRGs showing GFP protein band at 27 kDa. Protein extract from HEK cells transfected with pEGFP-N3 was used as a positive control. (B) Densitometry of western blots was done to compare GFP protein expression between embryonic stages E16.5, E18.5 and postnatal stage (P0). Tukey's multiple comparison test. Data presented as mean $\pm$ SD, (n=2).

1.3.4.3. Characterization of GFP⁺ DRG cells in $Ca_v3.2^{GFP}$ knock-in mice

Because the calcium channel subunit 3.2 was identified previously in our laboratory as a potential molecular marker for D-hair mechanoreceptors (Shin et al., 2003), the GFP⁺ cells observed in DRGs of the $Ca_v3.2^{GFP}$ knock-in mouse should express molecular markers characteristic of Aδ-low threshold mechanoreceptors (LTMR). Expression of receptors for neurotrophic factors in the DRG was used to characterize GFP⁺ cells since they have become the standard for sensory neurons subtype's identification because of their roles on neuronal specification and survival (Ernfors et al., 1992; Marmigère and Ernfors, 2007). For example, knock-out of one of TrkB receptor's ligands, the neurotrophin-4 (NT-4) causes loss of about 95% of D-hair mechanoreceptors in adult animals (Stucky et al., 2002). As expected, co-immunostaining analysis in DRGs of E18.5 $Ca_v3.2^{GFP}$ homozygous embryos showed co-expression of GFP and TrkB in about 45% of the GFP⁺ cells **Figure 28Q**. However not all TrkB positive cells in the DRG expressed detectable GFP **Figure 28I-L**. At the same stage the molecular marker for propioceptive neurons TrkC (Ernfors et al., 1994) was observed in 55% of the GFP⁺ cells **Figure 28Q** but not all TrkC

expressing cells were positive for GFP **Figure 28M-P**. Since small diameter unmyelinated nociceptors can be classified neurochemically into peptidergic and non-peptidergic nociceptor, the nerve growth factor receptor TrkA was used to identify the first subtype **Figure 28A-D** (Molliver et al., 1995) and Isolectine B_4 (IB_4) for the second (Silverman and Kruger, 1990). Quantification of the immunostaining shows only 13% of GFP^+ cells were $TrkA^+$ **Figure 28Q** and there was no co-expression of GFP and IB_4 **Figure 28E-H**. A total of three embryos and three DRG per embryo were analysed for quantification.
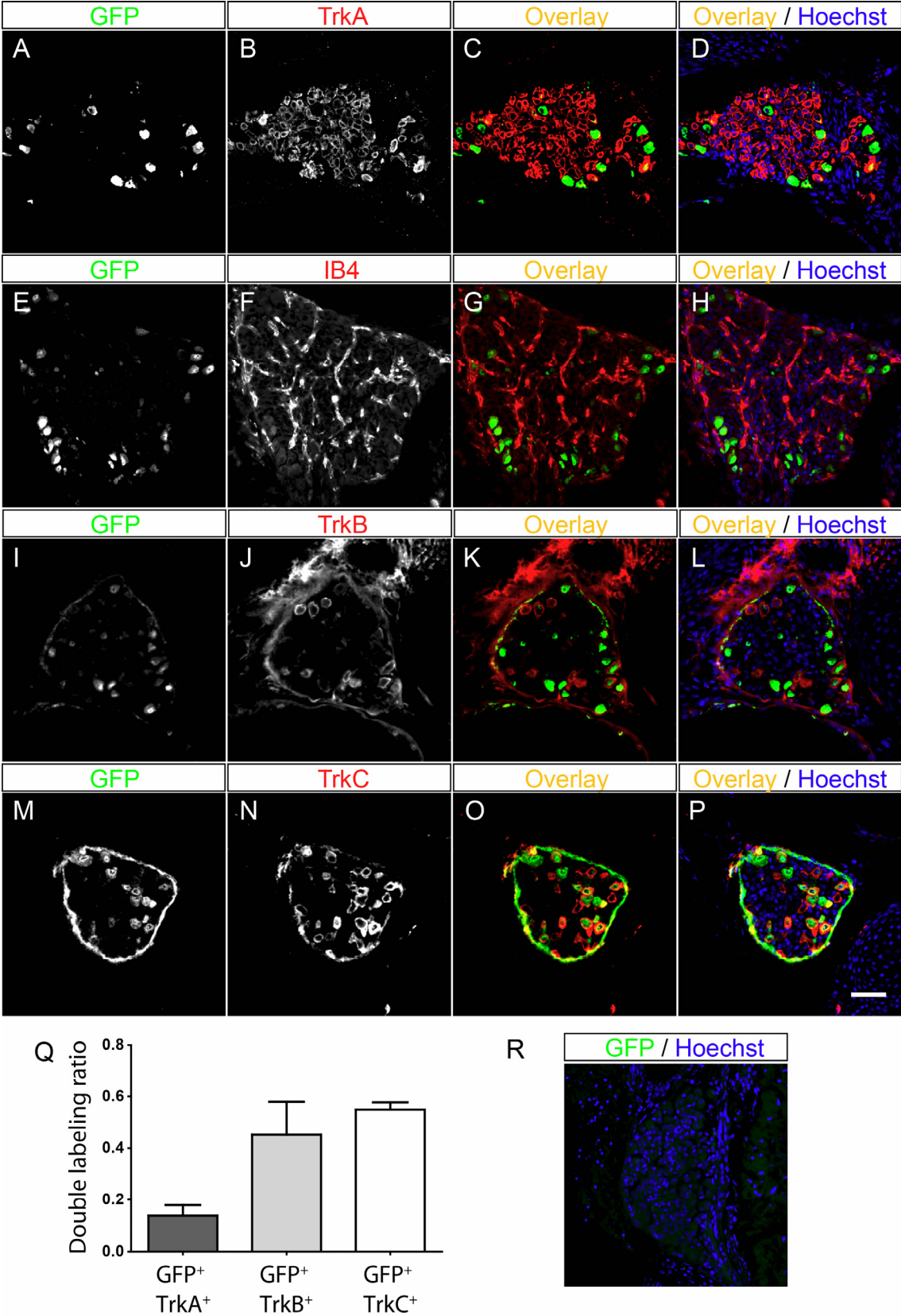
Figure 28. Double immunostainings for characterization of GFP+ cells in DRG of _Ca$_v$3.2^{GFP}_ knock-in mouse. DRGs double immunostaining of GFP with TrkA (A-D) and IB$_4$ (E-H), which are molecular markers for nociceptors; GFP with TrkB (I-L), and GFP with TrkC (M-P) in embryos at E18.5 stage. Blue staining represents cell nucleus labelled with Hoesch. Scale bar 50μm. (Q) Bar plot showing quantification of double immunostainings. The ordinate represents GFP+

cells co-expressing one of the molecular markers used divided by the total number of GFP$^+$ cells in the DRG. n=3 animals, and 3 DRGs were examined per animal, error bars indicate SD. (R) Example of Bl6 E18.5 DRG section used as a negative control for GFP antibody staining.

1.4.   DISCUSSION

The T-type currents produced by the low-voltage activated calcium channels are activated at small positive changes of the cell's resting membrane potential and inactivate rapidly in a voltage dependent manner (Chemin et al., 2002; Nowycky et al., 1985; Perez-Reyes et al., 1998). These properties are especially important for cell excitability, so that when a weak depolarization of the cell membrane activates T-type channels, the calcium influx produces a further depolarization until activation of sodium channels occurs, and in consequence action potentials are fire at very low thresholds (Llinás and Sugimori, 1980; Llinás and Yarom, 1981). Because of this way of function, it is believed that the individual electrophysiological properties of T-type calcium channels likely determine the firing patterns of excitable cells and the specific combinations of T-type isoforms could be crucial to action potential burst physiology in vivo (Cain and Snutch, 2010). So far, one bottle neck in the determination of the individual roles of T-type channel subtypes ($Ca_v3.1$, $Ca_v3.2$ and $Ca_v3.3$) in neuronal behaviour, has been the lack of subtype specific pharmacological tools and the impossibility to distinguish between cells expressing a specific T-type channel subtype in cell culture (Cribbs et al., 1998; Snutch et al., 2005; Xie et al., 2007). I used a knock-in genetic approach in order to investigate the expression pattern of the $Ca_v3.2$ channel in the nervous system of mice as well as to produce a model to investigate the channels´ role in the physiology of these neurons.

1.4.1. $Ca_v3.2$ channel expression in Central Nervous System

Description of the mRNA expression pattern of T-type calcium channels subunits 3.1, 3.2 and 3.3 had been previously described in rats using in-situ hybridization (Craig et al., 1999; Kase et al., 1999; Talley et al., 1999) as well as evaluation of the subcellular distribution of the T-type calcium channel subunit variants by immunostaining using polyclonal antibodies against each of the Ca_v3 T-type subunits (McKay et al., 2006). When comparing the results obtained from the *$Ca_v3.2^{Cre}$* knock-in mouse after breeding with a reporter line, and the previous studies mentioned above, there was brod agreement about the expression pattern of the T-type calcium channel subunit 3.2 in the brain. Thus, expression of the $Ca_v3.2$ ionic channel was confirmed in the olfactory system, hippocampus, amygdale, cerebral cortex, hypothalamus and thalamus of the mouse brain. However, it is important to note that the *$Ca_v3.2^{Cre}$*; *Rosa26* *$^{(LacZ)}$* mouse does not give real time information about the calcium

channels' promoter activity, nor a sense of how strong the activation of the promoter could be at the cellular level, because after DNA recombination the expression of the reporter protein (ß-gal) does not depends on the $Ca_v3.2$ promoter but on Rosa26. Nonetheless, one big advantage of using the Cre knock-in mouse is that cells having a weak activity of the $Ca_v3.2$ promoter can be still detected, since very little of CRE recombinase is needed to remove the stop signal preventing the reporter protein (ß-gal) from expression. Also, CRE expression does not need to be constant because, as explained before, after recombination ß-gal expression depends on Rosa26. To overcome the inconvenience regarding the temporal activation of the $Ca_v3.2$ promoter when using the $Ca_v3.2^{Cre}$ mouse, the following solutions could be taken: first to use an inducible CRE recombinase system which would allow recombination to proceed at a specified time (Feil et al., 1997; Metzger et al., 1995), second to make local injections of a Cre-dependent reporter virus in the brain (Gradinaru et al., 2010; Wall et al., 2010) or third to express a reporter protein directly under the $Ca_v3.2$ channel promoter which was done here using a new $Ca_v3.2^{GFP}$ knock-in mouse.

On the other hand, the promoter activity pattern obtained in brains of $Ca_v3.2^{GFP}$ knock-in mice differed in many aspects from that observed with the $Ca_v3.2^{Cre}$ mouse and from previous reports. In $Ca_v3.2^{GFP}$ mice, the $Ca_v3.2$ calcium channel promoter seems to be strongly active only in the granular cells of the dentate gyrus of the hippocampus as observed by the strong GFP signal obtained at the mossy fibers, and in some of the axons located in the internal capsule. Nevertheless, when the GFP mRNA and protein were quantified by qPCR and western blot respectively, $Ca_v3.2$ calcium channel expression could also be observed in other regions of the brain including cerebellum, brain cortex, olfactory bulb, brain stem and thalamus. It is important to note that the expression levels of GFP observed with those techniques were much higher in hippocampus than in the rest of the brain indicating differential strength of the $Ca_v3.2$ promoter activity. These findings suggest that the $Ca_v3.2$ calcium channel could contribute to the formation of T-type currents in many different regions of the brain, but may play a more prominent role in the hippocampal neurons under physiological conditions. Thus, in order to understand the functional role of the $Ca_v3.2$ channel in the physiology of a given brain region, discussion of the expression pattern obtained is more relevant in the context of the electrophysiological properties of the cells where T-type calcium currents have been observed.

1.4.1.1. Thalamocortical Network

Indication of the role of the Ca$_v$3.2 calcium channel in the oscillatory behaviour of the thalamus came initially from the fact that high levels of its mRNA was observed in the reticular thalamic nucleus (RT) (Talley et al., 1999). The RT is the inhibitory component in the thalamocortical network. It receives excitatory in-put from the cortex and the relay neurons (RE) of the thalamus, and delivers inhibitory out-put to the RE. Depending on the electrical stimulus received, RE and RT neurons have the possibility to change between tonic and burst firing modes. This is what is known as the oscillatory activity of the thalamus. The voltage dependent activity of the T-type calcium channel is crucial for burst and tonic firing, and in turn the firing mode would depend on the resting membrane potential of the cell (Llinás and Steriade, 2006). Recently, evidence for a role of the Ca$_v$3.2 channel in the intrinsic firing properties of the thalamus comes from the finding that the neurons of the RT in the Ca$_v$3.2 knock-out mouse lose tonic firing regularity as well as show decreased numbers of burst firing epochs (Liao et al., 2011). However, taking into account that the knock-out of the Ca$_v$3.2 does not abolish burst nor tonic firing in RT and that poor levels of GFP protein were found by western blot in the thalamus of *Ca$_v$3.2^{GFP}* homozygous; it could be suggested that the role of the subunit 3.2 is secondary in the thalamus due to the weak activity of its promoter and/or that the Ca$_v$3.3 subtype can support the underlying neuronal firing in RT neurons. In contrast, there is evidence indicating that an increase in the activity of the Ca$_v$3.2 channel within the thalamocortical network can have strong deleterious effects in brain function. In rats from Strasbourg (GAERS) which are an animal model for absence epilepsy; absence seizures are related to an increase in the expression levels of Ca$_v$3.2 mRNA in the RT of these animals, which in turn changes the oscillatory bursting patterns because of the elevated T-type calcium currents in these cells (Becker et al., 2008; Powell et al., 2009; Talley et al., 2000). In addition, several gain-of-function mutations found in the Ca$_v$3.2 ortholog gene (CACNA1H) in humans are also associated with generalized idiopathic epilepsy (IGE) (Chen et al., 2003; Heron et al., 2004), and the characterization of some of those mutations in HEK cells show an increase in the activation and deactivation kinetics of the channel (Khosravani et al., 2005). Although, it is well establish that IGEs show a polygenic origin involving different types of voltage activated ionic channels, all the literature presented above suggests that the CACNA1H gene is an active locus involved in this kind of neurological disorders.

1.4.1.2. Hippocampus

The $Ca_v3.2^{GFP}$ knock-in mice showed that the strongest activation of the $Ca_v3.2$ promoter takes place in the granule cells of the dentate gyrus (DG) in the hippocampus. The immunostainings against GFP showed a very strong signal located in the mossy fibers. Mossy fibers are the axon projections of the granule cells going into the polymorphic layer to innervate the inhibitory interneurons and mossy cells, and continue until they reach the apical dendrites of the pyramidal cells of the CA3 cells (Ribak et al., 1985). This result highly differs from previous studies showing expression of the T-type calcium channel subunit 3.2 in the CA3 and CA1 fields of the hippocampus (McKay et al., 2006; Talley et al., 1999). As explained before, injection of CRE dependent reporter virus in the brain of the $Ca_v3.2^{Cre}$ mouse could help to clarify if the lack of GFP in the CA fields of the hippocampus is due to no activity of the $Ca_v3.2$ promoter in these cells or that the promoter is weakly expressed in these cells and then produces low levels of GFP in the $Ca_v3.2^{GFP}$ mouse.

The hippocampus is associated with contextual, temporal and spatial learning and memory (Smith and Mizumori, 2006). In such cognitive processes, the function of the dentate gyrus is still confusing since organisms such as birds, which have an exquisite spatial memory needed for hoarding food at thousands of distinct locations every year and retrieving it after months (Healy et al., 2005), do not seem to have an dendate gyrus-like structure in their hippocampal formation (Montagnese et al., 1996; Srivastava et al., 2007; Tömböl et al., 2000). Nevertheless, in mammals, the specific involvement of the DG in spatial pattern separation has been determined using hippocampus-dependent behavioural tasks after impairment of the DG (Gilbert et al., 2001; Lee and Solivan, 2010; Morris et al., 2012; Xavier et al., 1999). Some of those tasks are the hidden-platform version of the water maze, and contextual conditioning or trace fear conditioning tests (TFC). The first behavioural task measures the ability of mice to learn to navigate to a submerged platform by using distal, spatial cues in the room. The TFC test involves learning of a new environment as a context by applying a mild foot shock to the animal that will produce freezing. After training, freezing behaviour is expected when the animal is expose once again to the context in the absence of the shock (Mizuno and Giese, 2005). Testing of $Ca_v3.2$ knock-out mice in hippocampus-dependent behavioural tasks was used recently by Chen and colleagues to determine the role of the $Ca_v3.2$ channel in the function of the hippocampus (Chen et al., 2012). The T-type subunit 3.2 seemed to be needed for memory retrieval in the context and passive avoidance tasks because homozygous $Ca_v3.2$ knockout

animals performed normally in the Morris water-maze but were impaired in the context-cued TFC. The mechanisms mediating this phenotype could be the change in synaptic plasticity observed in $Ca_v3.2^{-/-}$ mice. Excitatory post synaptic potentials (EPSP) recorded from hippocampal slices did not showed expression of the late-phase of hippocampal long term potentiation (LTP) at CA1synapses (Chen et al., 2012). With new technologies such as optogenetics available, the $Ca_v3.2^{Cre}$ mouse is a very good model that could be used to dissect the role of the cells expressing $Ca_v3.2$ channel in hippocampus physiology by directly manipulating the excitability of the neurons with light using Cre dependent virus expressing channelrhodopsin or halorhodopsin (Deisseroth, 2011; Zhang et al., 2010).

On the other hand, up-regulation of the Ca_v3 channels in the hippocampus seems to be also involved in epilepsy. After induction of status epilepticus with pilocarpine treatment, an increase of the T-type Ca^{2+} currents was observed in the CA1 neurons of the hippocampus, which in turn produced a change from regular firing into burst firing. However, although the high sensitivity to Ni^{2+} found in the T-type currents gave reason to speculate that the up regulation of the subunit 3.2 would be responsible for the changes in the intrinsic electrical properties of CA1 cells, there was no determination of mRNA or protein expression levels in the hippocampus of the animals after treatment with policarpine (Su et al., 2002).

1.4.1.3. Other regions of the brain

According to the results obtained by western blot from the brains of $Ca_v3.2^{GFP}$ homozygous mice, GFP expression was observed in the olfactory bulb (OB) and in the cerebellum. However, since the GFP expression levels were very low when compared with hippocampus, and the olfactory bulb and cerebellum receive input from the brain cortex where GFP was also detected; it could be possible that the GFP observed in the western blots is produced by the axons projecting from the brain cortex into these two regions. Evidence supporting this hypothesis is the lack of positive staining against ß-gal in the olfactory bulb of the $Ca_v3.2^{Cre}$;$Rosa26^{(LacZ)}$ mouse. Nevertheless, expression of the $Ca_v3.2$ has been shown in the olfactory bulb (Talley et al., 1999) and T-type currents have been observed in the granular interneurons (GC) which contribute to GC-mediated lateral inhibition in the OB (Pinato and Midtgaard, 2003). The lateral inhibition of GC to the principal excitatory neurons of the bulb, the mitral and tufted cells (M/TCs) is proposed as a mechanism for controlling the gain of GC output via persistent excitatory input. This statement suggest the T-type channels as an essential element in gating the entry of

olfactory information to the cortex (Egger et al., 2003, 2005). In addition, T-type currents are involved in action potential generation in olfactory receptor cells, and contribute to enhance odor sensitivity by lowering the threshold of spike generation (Gautam et al., 2007; Kawai and Miyachi, 2001). Although no evident phenotype in the olfaction abilities of the $Ca_v3.2^{GFP}$ and $Ca_v3.2^{Cre}$ homozygous knock-in mice was observed. The animals could still be used to evaluate the specific contribution of the subunit 3.2 in the electrical properties of olfactory neurons because, as described in material and methods, the insertion of GFP or Cre sequence causes the knock-out of the $Ca_v3.2$ channel.

In cerebellum, activation of the $Ca_v3.2$ ion channel was observed in both $Ca_v3.2^{GFP}$ and $Ca_v3.2^{Cre}$ animals. These results agree with previous reports where antibody staining against ion channel $Ca_v3.2$ showed positive staining in purkinje cells (PCs) and deep cerebellum cells (McKay et al., 2006; Molineux et al., 2006) but contradict a previous in situ-hybridization experiment where no signal against $Ca_v3.2$ mRNA was detected in cerebellum (Talley et al., 2000). The difference in the expression pattern between $Ca_v3.2$ channel protein and mRNA could be due to the existence of different splice variants.

Another interesting result was that not all purkinje cells in the cerebellar cortex of $Ca_v3.2^{Cre};Rosa26^{(LacZ)}$ mouse were ß-gal positive. This would suggest that probably not all purkinje cells would have the same electrical properties. However, so far there is no evidence of difference between the T-type currents found in purkinje cells. In addition, the properties of the T-type currents produced by the PCs such as Ni^{2+} sensitivity, fast inactivation kinetics and slow deactivation kinetics are more characteristic of $Ca_v3.1$ currents than either $Ca_v3.2$ or $Ca_v3.3$ (Kaneda et al., 1990). It could also be a consequence of having a weak activity of the $Ca_v3.2$ promoter in cerebellum as shown by the GFP western blots in $Ca_v3.2^{GFP}$ animals. In conclusion, although T-type currents are involved in the production of low voltage activated calcium spikes in the dendrites of purkinje cells (Isope and Murphy, 2005), the subunit 3.1 has a dominant role in this process (Hildebrand et al., 2009) and the role of the $Ca_v3.2$ channel in the production of dendritic action potentials in PCs is yet to be explored.

1.4.1.4. $Ca_v3.2$ promoter activity during spinal cord development

The use of a genetic knock-in approach such as the $Ca_v3.2^{GFP}$ and $Ca_v3.2^{Cre}$ mice made it possible to determine for the first time how the $Ca_v3.2$ gene changes its spatiotemporal expression during development. According to the GFP immunostaining obtained from

*Ca$_v$3.2^{GFP}* mouse spinal cord, the Ca$_v$3.2 channel promoter activates in stages as early as E9.5 in the roof plate and in some of the cells at the dorsal ventricular zone. From stage E13.5 to E.16 the GFP signal is located at the dorsal root entry zone of the spinal cord, suggesting that the positive labelling observed is coming from the axon projection of sensory neurons of the dorsal root ganglia (DRG) waiting to enter the dorsal horn to innervate the spinal neurons. Moreover, later on GFP is strongly expressed in the dorsal column at stage E18.5 and it makes part of the Dorsal Column-Medial Lemniscus System (DCML) that is the sensory pathway used by the sensory afferents to transmit fine touch, vibration and conscious propioception from the nerve end organs to the cerebral cortex (Nógrádi and Vrbová, 2000). The fact that no spinal neurons were GFP positive from stages E13.5 to E18.5 in the *Ca$_v$3.2^{GFP}* mice contradicted the mRNA expression pattern previously reported by Talley and colleagues (Talley et al., 2000). In their study, mRNA expression of the three T-type calcium channel subunits were found in the grey matter of the spinal cord, with subunit 3.1 having the highest expression over subunits 3.2 and 3.3. Also, Ca$_v$3.2 mRNA was restricted to lamina I-II of the dorsal horn (Talley et al., 2000). One explanation for this discrepancy could be that the GAP-43 signal in the sequence of GFP that was introduced to localize the protein at the axon terminals would make the GFP staining appears in the axons of the projection neurons and/or interneurons of the spinal cord. In the first case GFP from the axons of the projection neurons running through the spinothalamic tract would show some positive staining in the lateral white matter of the spinal cord (Todd, 2010), but no staining was observed in those regions. In the second case, if interneurons of the spinal cord were positive, GFP signal should have been observed in the gray matter of the spinal cord but that was not observed. In contrast, ß-gal staining in the *Ca$_v$3.2^{Cre};Rosa26$^{(LacZ)}$* mouse spinal cords showed activation of CRE recombinase in lamina I-X, but the reason for this broad staining could be the early activation of Ca$_v$3.2 promoter at E9,5. At this developmental stage the dorsal neural progenitor cells that will give rise to the dorsal spinal neurons are still dividing (Briscoe et al., 2000) and at the same time it will cause early removal of the transcription stop signal in the Rosa26 locus and the expression of ß-gal in all the neurons born after E9.5, a similar staining pattern was also observed when using another mouse reporter line as the Ca$_v$3.2^{Cre};Tau$^{(mGFP)}$. The importance of the early activation of the Ca$_v$3.2 promoter for the spinal cord development has not been addressed yet.

T-type currents have been shown to be involved in intracellular Ca^{2+} rise observed in projection neurons of the spinal cord after nociceptive afferent stimulation (Ikeda et al.,

2003). This activity-dependent sensitization is believed to be the synaptic mechanism underlying long term potentiation (LTP), which is a potential cellular mechanism of afferent induced hyperalgesia (Ikeda et al., 2003). However, as mentioned before the subunit 3.1 is strongly expressed in spinal neurons and could be responsible for the T-type currents observed in projection neurons (Ku and Schneider, 2011).

1.4.2. $Ca_v3.2$ channel expression in Sensory Nervous System

1.4.2.1. $Ca_v3.2$ promoter activation during DRG development

GFP stainings in early embryos from $Ca_v3.2^{GFP}$ mice showed that activation of the $Ca_v3.2$ promoter in some of the trunk neural crest cells (NCCs) occurred already at stage E9.5. Although NCCs can generate DRG and sympathetic neurons(Serbedzija et al., 1990), the GFP⁺ NCCs observed at E9.5 do not seem to be progenitors of sympathetic neurons because no ß-gal activity was found in the sympathetic chain of E11.5 $Ca_v3.2^{Cre}$;Tau$^{(mGFP)}$ mice embryos, nor in later stages of development. In contrast, the same embryos already showed ß-gal activity in almost all the cells of the DRG, confirming that the early activation of the promoter took place in some of the NCCs that give rise to sensory neurons or in dividing neuronal precursos in the DRG. The Neural crest cells can also generate endoneural fibroblast and melanocytes (Opdecamp et al., 1997), but the characterization of non neuronal cell types was beyond the scope of the present study.

At E13.5 when the three waves of DRG neurogenesis are complete (Ma et al., 1999), activation of the $Ca_v3.2$ promoter is observed in very few sensory neurons in the $Ca_v3.2^{GFP}$ embryos, and as development continues the GFP⁺ cell population rises and reaches 7% of the total DRGs at E16.5 and remains constant at E18.5. The progressive activation of the $Ca_v3.2$ promoter in a specific subpopulation of sensory neurons after neurogenesis, suggests that the transcriptional regulation of the $Ca_v3.2$ ionic channel depends on sensory subtype specification and not on neurogenic origin. During sensory neuron differentiation expression of intrinsic transcription factors together with growth factor receptors such as Trks are essential to regulate the genes defining the functionalities of sensory types during cell diversification (Liu and Ma, 2011). That is why DRG sensory neuron types can be delineated by expression of TrkA, TrkB and TrkC receptors, which serve as receptors for nerve growth factor (NGF), neurotrophin-4 and neurotrophin-3 respectively, and are necessary for cell survival during nerve target innervation (Marmigère and Ernfors, 2007).

Characterization of DRG subtype cells in $Ca_v3.2^{GFP}$ embryos at E18.5 revealed that the majority of the GFP$^+$ cells in this stage express TrkB and TrkC and a low percentage of them express TrkA. There is high probability that GFP$^+$/TrkB$^+$ and GFP$^+$/TrkC$^+$ cells in the DRG could have developed from the early TrkB/C sensory linage expressing Runx3/Shox2 transcription factors (Kramer et al., 2006; Levanon et al., 2002; Scott et al., 2011), and not from the early Ret (eRet$^+$/MafA$^+$) population (Bourane et al., 2009; Luo et al., 2009). This idea is supported by a recent study evaluating the role of the transcription factor cMaf in sensory neurons. cMaf acts upstream of MafA and its knock-out causes specific alterations in the physiological properties of Aß fiber mechanoreceptors without any deleterious effect on Aδ-fibers, in addition the expression of the Ca$_v$3.2 ionic channel in the mutants was unchanged (Wende et al., 2012). Nevertheless co-stainings of GFP and MafA$^+$ is needed to confirm this assumption.

On the other hand, to find out the progenitors for the GFP$^+$/TrkA$^+$ DRG cells of $Ca_v3.2^{GFP}$ mice without using molecular markers for TrkA$^+$ is much more difficult. TrkA$^+$ DRG cells develope in two waves, the first generated from the Ngn2-dependent wave of neurogenesis and being Cux2$^+$ which produces Aδ-fibers (Bachy et al., 2011), and the second generated from the Ngn1-dependent wave of neurogenesis and being Cux2$^-$ (Averill et al., 1995). The only marker for nociceptors used in $Ca_v3.2^{GFP}$ embryos was IB$_4$. IB$_4$$^+$/TrkA$^+$ nociceptors belong to the Ngn1/Cux2$^-$ lineage and although no co-expression with GFP was observed at E18.5 it can not be discarded that GFP$^+$/TrkA$^+$ cells found at E18.5 could developed from them because CGRP, Ret, TrpM8 and TH are also molecular markers used to label other TrkA$^+$ sublineage developing form the same progenitors. Thus a further characterization needs to be done to answer this question.

1.4.2.2. DRG cells subtype expressing Ca$_v$3.2 ion channel

Recently, advances have been made in the morphological and physiological characterization of some sensory neuron subtypes using genetic labelling in mice (Bourane et al., 2009; Li et al., 2011; Wende et al., 2012). In those studies, genes with an expression pattern restricted to a subpopulation of sensory neurons in the DRG, are used to express reporter proteins or Cre recombinases to identify and characterize the properties of sensory neuron subtypes. In this work I used a similar strategy and make use of the Ca$_v$3.2 promoter as a reporter system to characterize the molecular and electrophysiological properties of putative D-hair receptors. These ultrasensitive mechanoreceptors are rapidly adapting, slowly conducting Aδ-fibers with extremely low mechanical threshold (Brown and Iggo,

1967; Milenkovic et al., 2008). The $Ca_v3.2$ promoter was chosen because previous studies showed that its expression pattern in the DRG is restricted to D-hair afferents (Shin et al., 2003), and knock-out of this ion channel in mice produces impairment of D-hair afferent physiological properties without disturbing the function of other mechanoreceptor or nociceptors (Wang and Lewin, 2011). However, the use of TrkA, TrkB and TrkC as molecular markers to identify nociceptors, mechanoreceptors and propioceptors respectively, revealed that GFP$^+$ sensory neurons found in $Ca_v3.2^{GFP}$ knock-in animals are a more heterogeneous cell population as perhaps expected. To find GFP$^+$/TrkB$^+$ DRG cells was expected since signalling of NT-4 through TrkB is required for D-hairs survival in mature mice (Airaksinen et al., 1996; Stucky et al., 2002). Enriched TrkB expression in D-hair receptors was observed by Shin and colleagues (Shin et al., 2003) and more recently it was proposed that TrkB could be a molecular marker for D-hair receptors (Li et al., 2011a). In this study Li and colleagues generated the TrkB^{tauEGFP} knock-in mouse to visualize TrkB expressing cells in the DRG. Immunostaining analysis showed that GFP$^+$ cells in the DRG from TrkB^{tauEGFP} mice are medium size cells which do not express the TH marker for C-low threshold afferents, or IB$_4$ marker for nociceptors, nor cRet. Characterization of these cells physiological properties by intracellular recordings using the ex-vivo skin-nerve preparation, classified them as rapidly adapting, low threshold mechanoreceptors with intermediate conduction velocity. Finally, analysis of innervation of hairy skin showed GFP signal in longitudinal lanceolate endings associated with zigzag and awl/auchene hair follicle of the trunk (Li et al., 2011a). Although all these are characteristics of D-hair receptors, previous studies do not support expression of TrkB restricted to Aδ-fibers. Indeed, there exist a TrkB$^+$/MafA$^+$/cRet$^+$ sensory subtype at birth that are rapidly adapting, low threshold mechanoreceptors which Aß-fibers that seem to innervate Meissner corpuscles and/or lanceolate endings (Bourane et al., 2009; Luo et al., 2009). In addition, the development of Meissner corpuscles is compromised in TrkB null animals (Abdo et al., 2011; González-Martınez et al., 2004; Ichikawa et al., 2000; Perez-Pinera et al., 2008; Scott et al., 2011). Unfortunately, Li and colleagues (Li et al., 2011a) did not show staining of glaborous skin to confirm absence of GFP$^+$ nerve endings innervating Meissner corpuscles in the TrkB^{tauEGFP} mouse. More evidence of possible expression of TrkB by LTM Aß-fibers is coming from the other TrkB high affinity ligand, brain-derived neurotrophic factor (BDNF). Lack of BDNF affects the mechanical thresholds of slowly adapting mechanoreceptors (SAM) suggesting that the TrkB receptor could also be expressed in SAM that innervate Merkel cells and/or Ruffini corpuscles (Carroll et al.,

1998). Thus characterization of a molecular marker for D-hair receptors requires an extensive analysis of end sensory organs innervation in the glaborous and hairy skin.

Co-expression of TrkC receptor with GFP in the DRGs of $Ca_v3.2^{GFP}$ animals was somewhat surprising because this molecular maker is normally used to identify propioceptors which are big size heavily myelinated Aα/β-fibers innervating muscles spindle and golgi tendon organs (Hasegawa and Wang, 2008; Klein et al., 1994; Moqrich et al., 2004). However, disruption of TrkC's ligand, neurotrophin-3 (NT-3), produces more sensory neuron loss than TrkC knock-out animals (Ernfors et al., 1994; Liebl et al., 1997), including D-hair receptors which are reduced to 50% in early postnatal development (Airaksinen et al., 1996; Stucky et al., 2002). D-hair receptors lost in the NT-3 knock-out could be caused by the lost of the $TrkB^+/TrkC^+$ subpopulation of sensory neurons during development. Expression of T-type calcium currents in propioceptive neurons has not been observed so far. In this case, confirmation of $Ca_v3.2^+/TrkC^+$ DRGs subtype is necessary using the $Ca_v3.2^{Cre}$ mouse. Because the $Ca_v3.2$ promoter activates early in development, evaluation of Cre activation in postnatal stages could be done by transfection of $Ca_v3.2^{Cre}$ DRGs with a cre dependent reporter vector or infection of newborns with a Cre dependent reporter AAV virus.

In DRGs of $Ca_v3.2^{GFP}$ animals, a small proportion of GFP^+ cells were also $TrkA^+$ indicating that the $Ca_v3.2$ calcium channel promoter is also active in some nociceptors. Initially the $Ca_v3.2$ ion channel was though to modulate pain processing because of its expression pattern in regions required for pain transmission including medium- and small-size sensory neurons and in post-synaptic neurons in lamina I-II in the spinal cord (Talley et al., 2000). Moreover, silencing $Ca_v3.2$ with anti-sense oligonucleotides and $Ca_v3.2$ null animals showed a pronociceptive effect in pain models of noxious mechanical stimuli, chemical pain and neuropathic pain (Bourinet et al., 2005; Choi et al., 2006). These studies did not identify the specific subtype of nociceptive neurons responsible for the pronociceptive effect, but Nelson and colleagues (Nelson et al., 2005) reported that after treatment of acute dissociated DRG cells with the redox agent L-cysteine, a high-density T-type currents subpopulation of sensory neurons "T-rich" was observed, which were capsaicin-sensitive and IB_4 positive and could be involved in pain behaviour (Nelson et al., 2005; Todorovic et al., 2001). However, the $GFP^+/TrkA^+$ DRG cells observed in $Ca_v3.2^{GFP}$ animals in the present study were IB_4 negative. It could be possible that other Ca_v3 channel subtype acounts for the $IB_4^+/$ T-rich subpopulation or that the exposure of DRG cells to hyperalgesia inducers such as redox compounds causes up-regulation of the $Ca_v3.2$ ionic

channel that in turn increases the mechanical excitability of IB_4^+ nociceptors by decrease of the mechanical threshold at which these cells fire action potentials. Thus, although not directly shown, up-regulation of $Ca_v3.2$ channels seem to contribute to sensitization of nociceptors underlying pain pathologies. Over expression of $Ca_v3.2$ ionic channels under pathological condition has also been observed in brain neurons after seizure episodes in epilepsy (Su et al., 2002). However, under physiological conditions the $Ca_v3.2$ channel is necessary to maintain D-hairs afferent mechanosensitivity as well as the number of spikes that this mechanoreceptor fires during the dynamic phase of mechanical stimulation (Wang and Lewin, 2011). The cellular mechanisms involved in the exquisitely high mechanical sensitivity of D-hair afferents is still unknown, but analysis of the electrical properties of neurons with a rosette type neuritis morphology that require NT-4 for survival as D-hair afferents do, reveals that the T-type calcium currents expressed in these sensory neurons act as an amplifier of depolarization events producing a decrease in the current threshold for action potential generation (Dubreuil et al., 2004). Unfortunately, the strength of the GFP signal in DRG of $Ca_v3.2^{GFP}$ animals was not enough for visualization of the neurons in cell culture, and characterization of the electrophysiological properties of these cells could not be done. Nevertheless, I used action potential properties such as shape, half peak duration and after hyperpolarization recovery time of DRGs cells in culture from $Ca_v3.2^{Cre}$;Tau$^{(mGFP)}$ animals to classify the GFP$^+$ sensory neurons into nociceptors or mechanoreceptors (Djouhri et al., 1998; Hu and Lewin, 2006; Lechner et al., 2009; Petruska et al., 2000). The finding of an equal proportion of GFP$^+$ cells that had action potential characteristics of nociceptors or mechanoreceptors only confirmed the early activation of the $Ca_v3.2$ promoter, and a possible heterogeneous modality within these cells. Determination of CRE recombinase activation in adult DRG cells could still be done as explained before, transfecting DRG cells with a cre dependent reporter plasmid. However there is a technical impediment in this strategy since transfection of sensory neurons normally affects negatively the quality of the plasma membrane and patch clamp recordings are very difficult to perform.

1.4.2.3. Innervation of sensory end-organs in the skin

In addition to the intrinsic properties of the sensory afferents underlying their responses to mechanical stimulation, their association with end organs also determines sensory modality at which every single primary afferent produces a response (Montagna, 1977). That is why analysis of skin innervation of the $Ca_v3.2$ animals was very important. Skin innervation in

Ca$_v$3.2^{Cre};Tau$^{(mGFP)}$ showed that from all the sensory end organs evaluated, including hair follicles, Meissner corpuscle, free nerve endings and Merkel cells, only Merkel cells seem not to be innervated by GFP$^+$ sensory afferents; and considering that the Ca$_v$3.2 channel promoter activates very early in development in the DRG progenitors, the skin innervation pattern observed in Ca$_v$3.2^{Cre};Tau$^{(mGFP)}$ animals indicates that the Ca$_v$3.2 channel expression might occur in a specific subpopulation of those progenitors. This is an interesting finding because together with Ruffini endings, Merkel cells are the only encapsulated sensory organs innervated by slowly adapting receptors (Iggo and Andres, 1982; Maricich et al., 2009; Montagna, 1977). Thus, the Ca$_v$3.2 ionic channel could be expressed in sensory neurons coding information of dynamic stimuli rather than in afferents detecting indentation applied on the skin. On the other hand, Ca$_v$3.2 ionic channel might play a different role in not excitable DRG precursor cells.

2. Part II: SCREENING FOR MOLECULAR CANDIDATES FOR A TETHER PROTEIN REQUIRED FOR MECHANOTRANSDUCTION

2.1. INTRODUCTION

As described in Part I, psychophysical studies together with electrophysological recordings of the sensory neurons innervating the skin have shown how sensory neurons respond specifically to different stimuli modalities. Anatomical studies have showed us how the sensory system is topographically organized in order to convey the coded information to the brain, and have described the morphology of sensory nerve endings that subserve different sensory modalities. Although we now have a more complete picture of how somatosensation works, its molecular basis is still not clear in mammals. At the cellular levels, sensory neurons need to be able to transform mechanical stimuli into electrical signals but the identities of the molecules responsible for this function are still unknown. Models for mechanotransduction have emerged from studies in invertebrates, and from studying the molecular complex involved in hearing. Forces acting on cells are also indispensable for other diverse physiological cellular process such as morphogenesis (Collins et al., 2012; Niziolek et al., 2012), differentiation (Cui et al., 2012; Sun et al., 2012), and osmosensation (Lechner et al., 2011), to name just a few. Although it is not clear if the mechanosensitive channels involved in these cellular processes are the same as those in mechanosensation, the discovery of molecules involved mechanotransduction has not been easy for many reasons. One difficulty may be that mutations in mechanotransduction genes may be lethal in mice. Other difficulties are that the sensory cells or their receptor endings are extremely sparse and therefore difficult to isolate for biochemical analysis. In addition, the rarity of the cells and the low number of transducing molecules per cell makes the collection of suitable numbers for biochemical studies difficult. Even when some candidate genes for mechanotransduction are found, probably the most difficult task will be assaying the function of the candidates in heterologous systems. To provide the mechanical stimulation to the system by changing osmotic pressure or by manipulating the membrane physically is not a problem but unfortunately, in such heterologous systems, mechanical stimulation does not always activate many eukaryotic channels that are candidate mechanosensory receptors, and then it is difficult to determine if those proteins are not

mechanical activated channels or if they need other proteins to function which are not known and expressed in the native system.

2.1.1. Molecular model for mechanotransduction in invertebrates

The nematode Caenorhabditis elegans (C. elegans) is one of the best anatomically and genetically characterized multicellular organisms. All this available information together with its simple body plan, transparency and different behavioural responses to mechanical stimulation makes C. elegans a powerful model to study sensory mechanotransduction. The best characterized behaviour is the response to a gentle mechanical stimulus delivered transversely along the body of the animal by means of an eyelash hair attached to a toothpick, this is called the gentle touch response (Chalfie et al., 1985; Herman, 1996). Other mechanosensitive behaviours include the nose touch response in which the animal reverses when by normal locomotion it collides with an obstacle in a nose-on fashion (Kaplan and Horvitz, 1993; Riddle, 1997), and the tap withdrawal reflex where the worms retreat in response to a tap on the cell culture plate (Chiba and Rankin, 1990; Wicks and Rankin, 1997). C.elegans also responds to harsh mechanical stimuli and it is independent from functional touch cells, harsh stimuli are delivered by poking with a platinum wire (Li et al., 2011b; Riddle, 1997).

In *C. elegans* six sensory neurons sense touch and can be distinguished from other neurons because they are packed with 15-protofilament microtubules, their sensory processes are closely attached to the body wall and have a prominent extracellular matrix (Chalfie and Sulston, 1981). Genetic screens that allowed the isolation of touch-insensitive nematode mutants permitted the identification of genes involved in the function of these cells and the proposal of a molecular model for a mechanotransducing complex. The model suggests a transduction complex of four proteins: the degenerin/epithelial Na^+ channel (DEG/ENaC) formed by the subunits MEC-4 and MEC-10, and two accessory subunits the prohibitindomain protein MEC-2 and the paraoxonase-like protein MEC-6 **Figure 29a**. MEC-4 and MEC-10 are expressed in sensory neurons and their mutation produces touch insensitive worms (Driscoll and Chalfie, 1991; Huang and Chalfie, 1994). Loss of MEC-4 activity abolishes the mechanosensitive current expressed in *C. elegans* touch receptor neurons under mechanical stimulation of the worm (Brown et al., 2007; O'Hagan et al., 2005). MEC-10 seems to play a regulatory role in the channel complex that is essential for full sensitivity of gentle touch and may mediate its effect via the MEC-2 accessory subunit (Arnadóttir et al., 2011). On the other hand, MEC-2 and MEC-6 are not

channel pore forming subunits but transmembrane proteins that colocalize and interact with MEC-4 and MEC-10 (Zhang et al., 2004). Both proteins increase the channel activity by promoting its active state (Brown et al., 2008; Chelur et al., 2002; Goodman et al., 2002). MEC-2 is associated with the inner leaflet of the plasma membrane and binds to the N-terminal domain of MEC-4 through its PHB domain (Huang et al., 1995; Huber et al., 2006). Palmitoylation of MEC-2 seems to modulate its direct binding to cholesterol and these two characteristics are likely to tune the MEC-2 association with MEC-4/10 (Huber et al., 2006). In vivo, wild type MEC-6 is required for proper localization of the channel complex in a punctuate pattern along touch-sensory neuron processes (Chelur et al., 2002).

Other proteins required for functioning of touch neurons in *C. elegans* are cytoskeleton and extracellular matrix proteins. The α-tubulin MEC-12 and β-tubulin MEC-7 are needed to form the touch-neuron specific 15-filament microtubules (Fukushige et al., 1999; Savage et al., 1989). Genetic or chemical disruption of any of these proteins results in the elimination of the large diameter microtubules causing a decrease in the cell diameter and lost of mechanical sensitivity in the worm, however if microtubules have a direct or indirect effect on mechanotransduction is still unknown (Chalfie and Sulston, 1981). Three protein components of the extracellular matrix have been found to be required for mechanotransduction in *C. elegans*. One of those proteins is MEC-5 which is a collagen made by the epidermal cells that surround sensory neurons, and mutations in its Gly-X-Y repeats produces touch insensitivity (Du et al., 1996). Mec-1 encodes an EGF/Kunitz domain protein secreted protein without a transmembrane domain, and mutations in this gene also produce touch insensitivity but do not affect process attachment (Emtage et al., 2004), and MEC-9 a protein with multiple EGF and Kunitz domains, is also an extracellular matrix protein, and mutations in this gene also abolish mechanosensitivity. In addition, MEC-9 interacts with MEC-5 and it has been proposed but not directly shown that one or both proteins interact with the degenerin channel (Du et al., 1996).
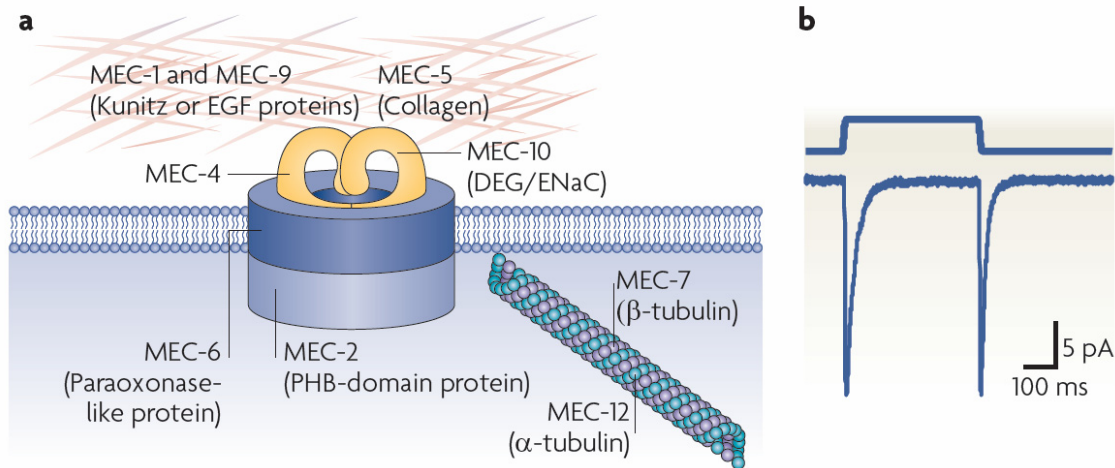
Figure 29. The *C. elegans* molecular models for mechanotranstruction. a. The molecular model for mechanotransduction is composed of the transduction channel subunits MEC-4 and MEC-6, the cytoskeletal proteins MEC-6, MEC-2 and MEC-7, and the extracellular matrix proteins MEC-1, MEC-5 and MEC9. b. Electrophysiological response of a sensory neuron to mechanical stimulation in the worm, the indentation produces a rapidly adapting inward current at the on-set and off-set of the force. Taken from Chalfie (2009).

Drosophila melanogaster is also an attractive model for studying mechanotransduction because it is possible to combine genetic manipulations with electrophysiological recordings from mechanoreceptor neurons (Kernan et al., 1994). Another advantage of *Drosophila* as a model is that it combines two experimental organisms in a single species, the larva and the adult fly and, both include the same major classes of external sensory organs. *Drosophila* has two types of sense organs both including mechanosensitive neurons (Kernan, 2007; Suster and Bate, 2002). The Type I organs are external ciliated mechanosensory receptors distributed trough the fly's body such as chordotonal organs and bristles **Figure 30A**. Chordotonal organs are stretch receptors attached to the skin or cuticle in the Johnston's Organ, function as the fly's ear, and also contribute to propioception feedback on limb position and locomotion, while bristles serve as principal propioceptors and touch receptors. Type I organs are normally innervated by one sensory type I neuron which has a single dendrite or sensory process and a modified cilium or outer segment at its distal tip. Three surrounding support cells enclose the sensory process and construct structures that differentiate the two types of organs **Figure 30B** and **C**. Movement or compression of the ciliated dendrite relative to surrounding structures causes the opening of cation channels and an inrush of K^+, leading to neuronal depolarisation. This can readily be recorded during the deflection of individual adult bristles (Corfas and Dudai, 1990). Type II or multidendritic neurons are located internally and are not associated with any other

specialized cell or structure. Their sensory endings vary in complexity from dipolar dendrites to extensive dendritic arborisation, some sense painful stimuli such as pinching or heat, and others function as propioceptors (Tracey et al., 2003).
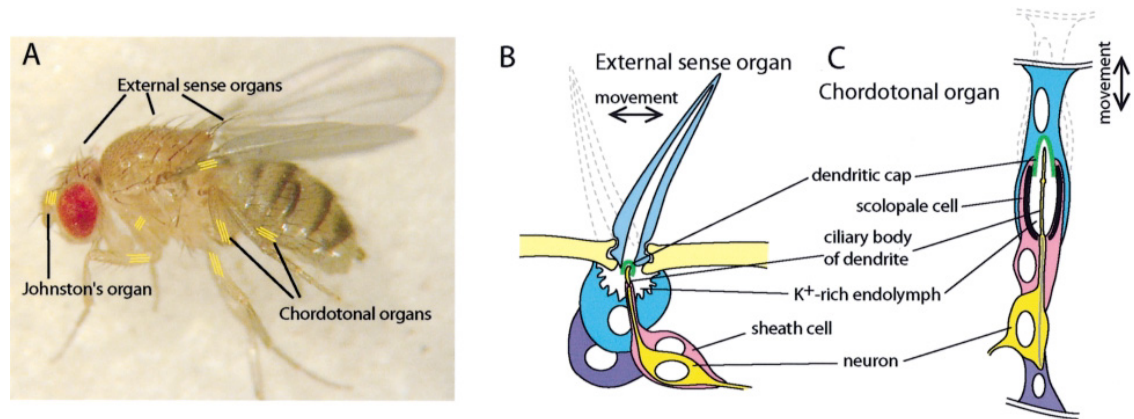
Figure 30. Type I sensory organs in _Drosophila_. A. _Drosophila Melanogaster_ photograph indicating the location of the type I sense organs. B. Representation of a bristle, supporting cells are painted in pink, purple and blue. Movement of the hair causes change of tension in the cilia. C. Chordotonal Organ showing supporting cells and the direction of the movement that causes stretch of the cilia. Taken from Jarman (2002).

Drosophila as well as _C. elegans_ are amenable organisms for genetic manipulation. The first candidate genes for touch sensitivity were screened in larvae followed by behavioural and electrophysiological analysis of mechanically insensitive mutants (Kernan et al., 1994). This screening identified the no mechanoreceptor potential C (NompC) as the first mechanotransduction channel in _Drosophila_. NompC is a TRPN1 (Transient receptor potential) cation channel formed by six transmembrane domains and an ion pore loop that is required for normal mechanosensitive currents in the fly hair bristles, also null NompC mutants have larval crawling deficits and adult flies showed severe uncoordination (Walker et al., 2000). Later, studies supported a role for NompC in sensation showing that TRPN1 localize to the distal tips of sensory dendrites in chordotonal and bristle mechanoreceptors where mechanical signals impinge on the sensory cilia (Cheng et al., 2010; Lee et al., 2010), and that NompC expression in heterologous systems allows the generation of mechanically activated currents (Yan et al., 2013). Other TRP channels involved in sensory transduction in _Drosophila_ are the vanilloid receptor subfamily (TRPV) proteins nanchung (NAN) and inactive (IAV), which are required for hearing but not touch (Gong et al., 2004; Kim et al., 2003).

On the other hand the Type II multidendritic neurons seem to subserve nociception rather than gentle touch in larvae, and also other ionic channels are reported as transducers in those neurons. The TRPA channel which is expressed in these neurons is involved in thermal and mechanical nociception (Hwang et al., 2012), and the mutants were initially called painless because the larvae do not react to noxious thermal stimuli in the nocifensive escape locomotion (NEL) behavior test (Tracey et al., 2003). When performing NEL, larvae rotate around the anterior posterior axes in a corkscrew-like manner. in mechanically induced escape behaviour assay . On the other hand, the pickpocket gene which is encoded by a DEG/ENaC subunit is required in the larva for mechanical nociception but not for thermal nociception nor gentle touch in highly branched class IV multidendritic sensory neurons (Zhong et al., 2010). TRP and DEG/ENaC channels have conserved function in *C. elegans*, where they are involved in harsh-touch and gentle touch detection respectively (Li et al., 2011b), however the nociceptive function of these ion channels in mammals is not conserved. Only recently the family of transmembrane proteins Piezo which are evolutionary conserved among animals, plants and other eukaryotic species were identified as components of the mechanical activated channels in mammals and seem to have the same function in invertebrates. The knockout of the single Piezo member in *Drosophila,* the Dmpiezo produced severe reduction of behavioral responses to noxious mechanical stimulation in larvae, while response to noxius thermal stimulus was unchanged as well as the response to gentle touch from ciliated neurons. Because knockout adult flies were viable, fertile and did not show a lack of coordination or a defect in bristle mechanoreceptor potential, a role for this channel in biological processes such as propioception and locomotion is excluded. In addition, transfection of Dmpiezo in human cell lines showed expression of mechanically activated currents indicating that Dmpiezo does not require accessory proteins to function (Kim et al., 2012).

Cytoskeleton proteins involved in mechanotransduction also had been proposed in *Drosophila.* A DNA microarray screening identified a unique doublecortin-domain-containing echinoderm- microtubule-associated protein (DCX-EMAP) as a candidate for a mechanoreceptor-specific protein in flies. DCX-EMAP localizes exclusively to sub-compartments of the sensory cilia, and mutants are uncoordinated and deaf. In addition, the mechanically evoked action potentials recorded in the ear are absent (Bechstedt et al., 2010). Regarding the extracellular matrix, NompA has been suggested as a candidate for the extracellular component that tethers the ion channel. It is expressed by Type I sensory supporting cells and is a key component of the dendritic caps of bristles and chordotonal

organs. Its mutation causes detachment of the dendrite from the bristle that in turn produces the lack of transepithelial potentials (Chung et al., 2001). A crucial step in identifying mechanosensory mutants is to establish that behavioral phenotypes are caused for defects in proteins needed for transduction rather than central processing or motor output, however as commented before regarding adult flies, the mechanosensitive currents can be directly measured from the sensory receptors allowing the selection of potential candidates.

Then, in *Drosophila* three different types of ionic channels are involved in mechanotransduction, Dmpiezo, DEG/ENaC and TRP channels. The gating mechanisms by which these channels function is still unknown, and no direct interaction with extracellular matrix or cytoskeleton proteins had been demonstrated so far. However, as mention previously, the only component of the extracellular matrix proved necessary for mechanotrotransduction in *Drosophila* is NompA which is localized at the surroundings of the sensory cilia, and NompC is expressed at the distal tips of the sensory cilia in tactile bristles (Lee et al., 2010).

2.1.2.   Molecular models for mechanotransduction in mammals

2.1.2.1. Molecular model for Hearing

In mammals, hair cells in the inner ear are probably the best characterized mechanosensor. Located in the organ of Corti, each hair cell contains at the apical surface its mechanichanically sensitive organelle, the hair bundle, which is composed of dozens of stereocillia **Figure 31B**. The cell bodies of the hair cells form tight connections with support cells that in the base are adhered at their basal surface to the basilar membrane. At the apical surface the stereocillia bundle are attached to the tectorial membrane which is an extracellular matrix structure **Figure 31A**. Hair cells allow the perception of sound by transducing sound-inducing vibrations into electrical signals. In the process of hearing, vibrations produced by sound waves are transferred to the cochlea where they are transformed into liquid pressures that induce vibrations in the basilar membrane. The differential displacement of the stereocillia bundle relative to the tectorial membrane is what starts the transduction process. Gradual changes in the features of the organ of Corti such as the height of the stereocillia, and the width and thickness of the basilar membrane (Lim, 1980) ensures that hair cells at different positions within the Cochlea are tuned to

different frequencies (Liberman, 1982). At the molecular level, the transduction mechanisms of hearing are based on a gating spring model **Figure 32A**. The elastic gating spring which is stretched in response to mechanical stimuli opens the transducing channel leading to the influx of Ca^{2+} and K^+ ions into the stereocillia (Corey and Hudspeth, 1983). The current generated by the mechanical stimulation in the stereocillia decays despite the persistence of an excitatory stimulus. This adaptation that is important to maintain receptor's sensitivity to new stimuli is bimodal and is fit by two time constants, one fast in the range of milliseconds and one 10 times slower. Fast and slow adaptation are regulated by calcium in a different way (Crawford et al., 1989). Slow adaptation is though to depend on active motor elements such as myosin, which is attached to the upper part of the tip-link end (Assad and Corey, 1992; Gillespie and Cyr, 2004; Stauffer and Holt, 2007), while the mechanism underlying the calcium dependence on fast adaptation is unknown.
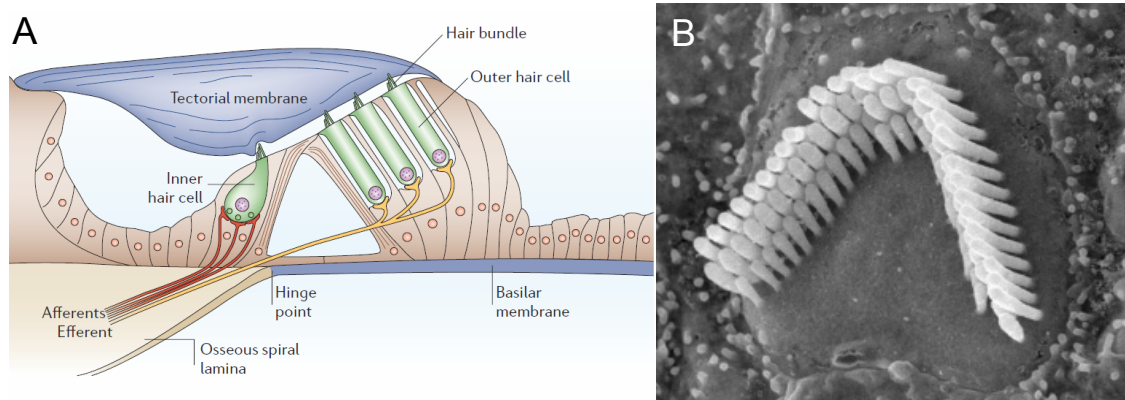
Figure 31. Hearing system in mammals. A. Organ of Corti showing the main cell components involved in sound transduction: the inner and outer hair cells, hair bundle and tectorial membrane. B. Electron microscopy photograph of hair bundle after removal of the tectorial membrane. Taken from Fettiplace and Hackney (2006).

The mechanosensitive channel in hair cells has not been identified. However it's location has been determined by analyzing the Ca^{2+} influx in the stereocillia at the lower tip-link end (Beurg et al., 2009). On the other hand, the tip-link is formed in the upper part by Cadherin 23 (CDH23) homodimers, and in the lower part by Protocadherein 15 (PCDH15) homodimers (Ahmed et al., 2006; Kazmierczak et al., 2007; Siemens et al., 2004). This tip-link is sensitive to Ca^{2+} depletion and treatment of the stereocillia with a calcium quelator such as BAPTA, abolishes the tip-link as well as transducer currents (Michel et al., 2005). Another protein besides cadherins and ionic channels that is potentially involved in mechanotransduction in hair cells is harmonin (Boëda et al., 2002;

Verpy et al., 2000). Harmonin localizes to the upper part of the tip-link end where it interacts with CDH23 through its PDZ2 domain and F-actin through its coiled-coil and PST domains **Figure 32B**. In addition, mutations in those domains demonstrated that harmonin is necessary for regulation of mechanotransduction, and is required for the sensitivity of hair bundles to displacement (Grillet et al., 2009). Myosin 1C and 7A also have been shown to be involved in mechanotransduction of hearing but their effect could be indirect since they are also required for protein transport (García et al., 1998; Kros et al., 2002).
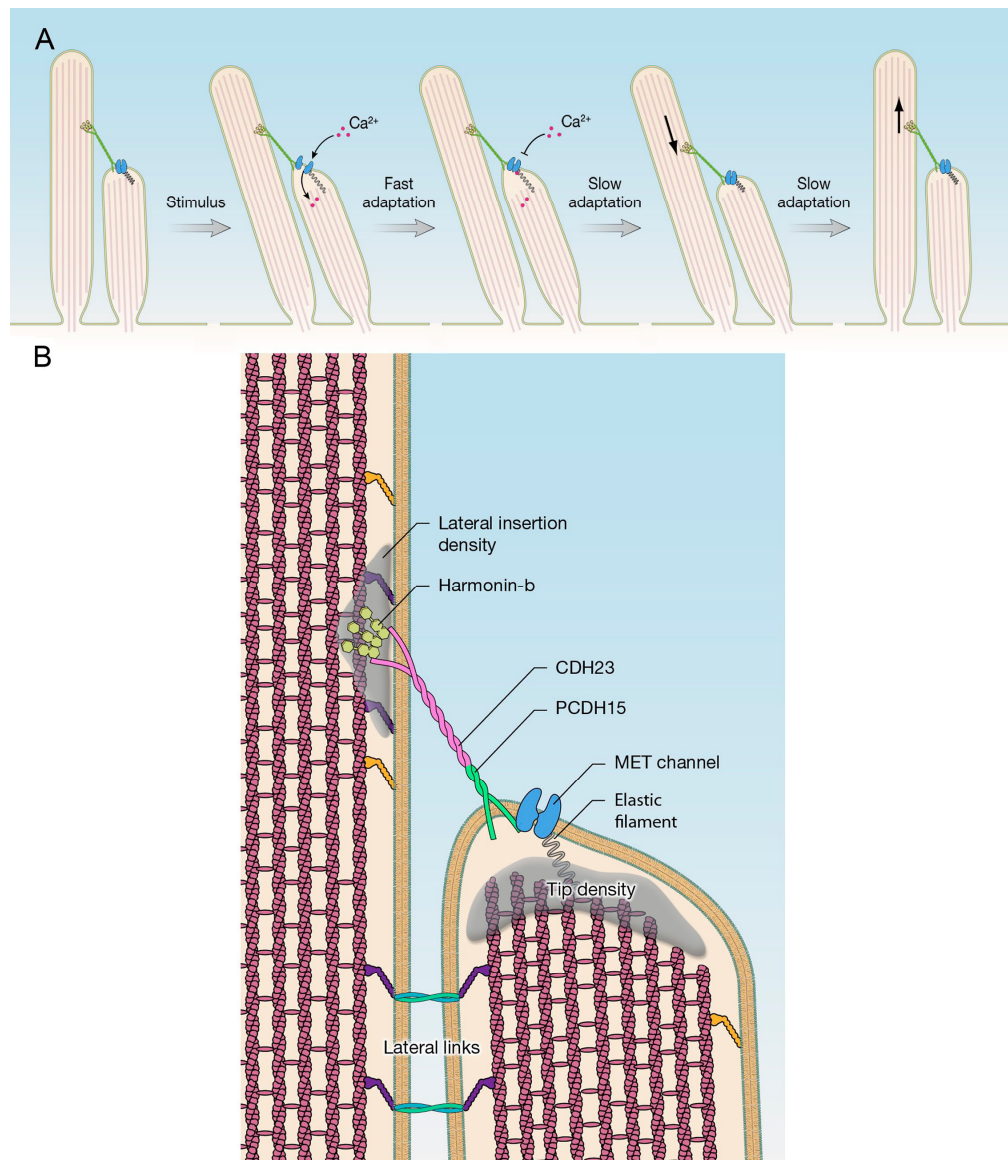
Figure 32. Molecular model for mammalian hearing. A. Mechanically generated currents in hair bundles show adaptation that is Ca^{2+} dependent. Fast adaptation is probably due to the ability of the sensitive ionic channel or proteins close to it to bind Ca^{2+}, while slow adaptation depends on molecular motors at the top of the tip-link end. B. Proteins involved in the transduction complex and its location in the stereocillia of the hair bundles. Taken from Schwander et al. (2010).

2.1.2.2. Molecular model for cutaneous mechanotransduction

In DRG cells DEG/ENaC channels were also initially proposed as the mechanically sensitive channel in mammals, but disruption of their isoforms, the acid sensing ion channels (ASICs) in mice showed only subtle changes in touch evoked responses even when it was shown that ASICs are expressed at the sensory ending organs (Drew et al., 2004; Duggan et al., 2002; García-Añoveros et al., 2001; Price et al., 2000, 2001). In contrast, they seem to subserve other biological process such as regulation of blood pressure (Lu et al., 2009) and pH sensing (Xie et al., 2002). As mention previously, TRP channels had been involved in touch mechanotransduction in *C. elegans* and *Drosophila*. In mammals, TRP orthologues such as TRPV4 work as an osmotic sensor in mice (Lechner et al., 2011; Liedtke and Friedman, 2003), and TRPA1 is required for mechanical nociception in an specific subset of visceral afferents (Brierley et al., 2009). Deletion of the genes for these channels leads to a modulation of mechanotransduction but does not abolish the response of sensory neurons to mechanical stimuli. The recently discovered family of Piezo channels, Piezo1 and Piezo2, had shown to be necessary for the expression of mechanically activated currents in heterologous systems such as cell lines. Piezo2 is expressed in 20% of DRG neurons and is co-expressed with peripherin or neurofilament 200, and some co-express the nociceptive marker TRPV1. In addition in these cells, Piezo2 is supporting expression of RA currents which makes it a potential candidate for touch and pain sensation (Coste et al., 2010, 2012). Nevertheless, the final proof is to come with the generation of the Piezo2 knock-out mouse.

The only component form the touch sensory complex in *C. elegans* that is also conserved in mammals is MEC-2. In mice, its homologue STOML3 is involved in tactile driven behaviours, and RAM are unresponsive in SLP3 [-/-] animals (Lapatsina et al., 2012; Wetzel et al., 2007). Our laboratory demonstrated that proteins of the extracellular matrix that are normally enriched and expressed in the basal lamina of the skin as laminins have a big effect on mechanosensitivity. In DRG cell culture, RA currents are supported by laminin-111 but not in substrates coated with laminin-332 (Chiang et al., 2011). In addition, laminin-111 supports mechanosensitivity because of the existence of a protein tether that links this extracellular matrix with the sensory neuron neurites in vitro. The tether protein was visualized using transmission electron microscopy (TEM) of cultured sensory neurons on dishes covered with laminin-111. The tether protein is not present when DRG cells are cultured on laminin-332, and its selective cleavage using the proteinase furin abolishes RA mechanically activated currents (Hu et al., 2010). This findings support a tether model for

touch transduction where the mechanically sensitive channel is gated by a protein binding to the extracellular matrix **Figure 33**.
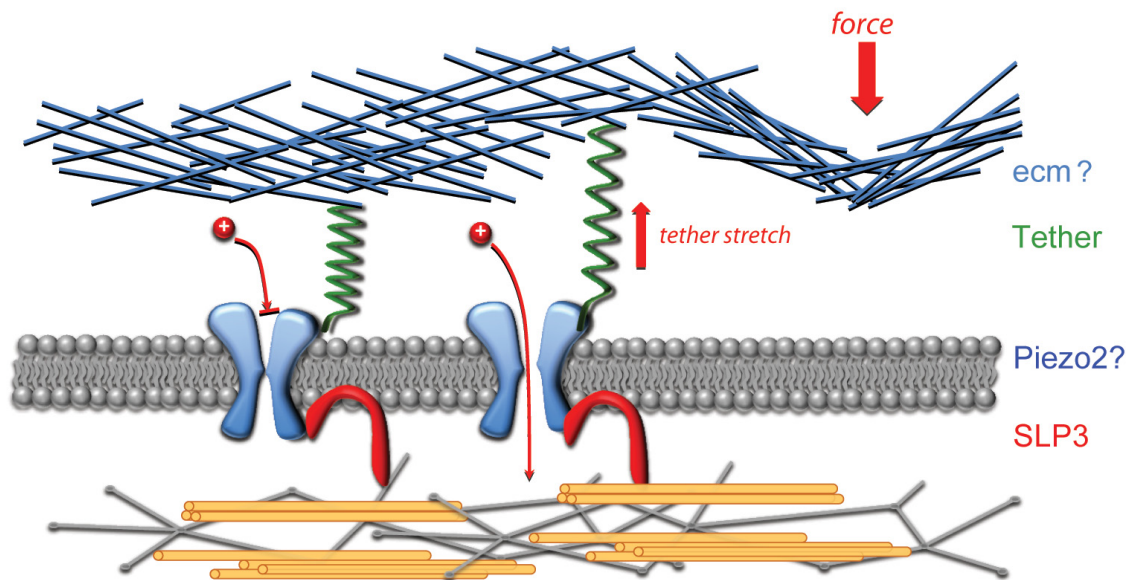
Figure 33. Model for touch mechanotransduction in mammals. The mechanical force applied to the skin is transferred to the sensitive ionic channel by the tether protein. Changes in the tether stretch cause the channel to open. SLP3 modulates channels function and probably mediates indirect interaction with the cytoskeleton. Modified from Lechner and Siemens (2011).

2.1.3.   Part II Aims

98

The main goal of the second part of my project was to identify the tether protein expressed in DRG cells and required for expression of RA currents in these cells, and to test its functionality as a gating spring of the mechanically sensitive channel. According to the biochemical properties of the tether protein described in the table 2. Characterization of the tether protein should include:

- Visualization of the protein as a tip-link about 100 nm long between the extracellular matrix and the neurites of DRG cells in culture.

- Molecular manipulation of the protein and functionality testing using electrophysiological techniques.

- Knock-out of the protein should abolish RA currents in DRG cells.

Table 2. Biochemical characteristics of the tether protein in vitro

Characteristic	Description
100 nm long Tip-link	The 100 nm link is observed using TEM in the interface between neurites of DRG but not in mechanically insensitive SCG cell cultures.
Cleavage site RX(K/R)R	Treatment of DRG cells in culture with Furin or Blisterase proteinase abolishes only RA currents and whashings of the proteinase and recovery of the cell culture after 30 h re-establishes RA currents expression.
The tether protein binds to Laminin-111	The 100 nm protein-link is observed in DRG cells cultured on laminin-111 but not on cells cultured on laminin-322 and RA currents are also expressed in neurites growing on laminin-111 but not on neurites growing on laminin-332.
The tether protein is not an integrin	Treatment of DRG cell cultures with a blocking antibody (CD29) against the α1 subunit of integrins does not abolish RA currents.
Ca^{2+} insensitive	Treatment of DRG cell cultures with a calcium chelator such as BAPTA does not abolish RA currents.
The tether protein is not a GPI-anchored protein	Treatment of DRG cell cultures with the enzyme phosphatidylinositol-specific phospholipase-C (PIPLC) to cleave glycosil phosphatidylinositol –anchored proteins (GPI-anchored) did not have an effect on the kinetics of mechanically activated currents in these cells.

(Hu et al., 2010)

2.2. MATERIALS AND METHODS

2.2.1. Preface

2.2.1.1. Chemicals

Name	Supplier
Amaxa necleofactor	Lonza AG
Cacodylate	Electron Microscopy Sciences
Dodecenylsuccinic anhydride (DDSA)	Polysciences
DMP	Polysciences
Gelatin	Sigma
Glycogen	Invitrogen
Laminin 332	Invitrogen
Laminin (EHS-derived matrix)	Invitrogen
Lead Citrate	Serva
Nadic Methyl Anhydride (NMA)	Polyscience
Osmium Tetroxide	Sigma-Aldrich
PetriPerm35 petridish	VivaScience AG
Polly Bed 8i	Polysciences
Polyethylenimine (PEI)	Polysciences, cat. no. 23966
Polydimethylsiloxane (PDMS)	
Propylene oxide	Polysciences Inc.
Ruthenium red	Sigma-Aldrich
Silicon Masters	Institute of Photonic Technology, Jena, Germany
Toluidine blue	Sigma
Uranyl acetate	Serva

2.2.1.2. Primers

Name	Sequence 5'-3'
Igsf10_L	GGATTCAAAAGCAAGACAGAAGA
Igsf10_R	TGAGGGAGATCAGCAAGCA
RIKEN5430411k18_L	TGAGCAGATGGCCGTACA
RIKEN5430411k18_R	TTCATTCATCTCTACTCGCTGGT
Stab1_L	ACCCAAAGAAGCATGGAGAG
Stab1_R	CACACAGACCGTGGACACA
Coagulation F8_L	AGATACACTTACCCTGTTCCCATT
Coagulation F8_R	ACCCCAAGACCCATAGACCT
Notch3_L	AGCTGGGTCCTGAGGTGAT
Notch3_R	AGACAGAGCCGGTTGTCAAT
Apc2_L	GAGCAGATCCGAGCCTACTG
Apc2_R	CTCGATTGGGACAGGAGTTT

RIKEN6720466o15_L	TGCATGGACAAAGCAAGAAG
RIKEN6720466o15_R	GCAAAACCTCCGTTATCCAG
Tecta_L	TTGACGGGAAGGAAATTGAC
Tecta_R	TCGACGAAGGAACTGTCCTC
Plxnb1_L	TGTGCGCAGCTACCAGTG
Plxnb1_R	CCATGGGACTGGGTGTGT
Dmb1_L	CCGACTTTGACAATAACACCAC
Dmb1_R	AATAGCCCATGGACTGAAGG
Pkhd1l1_L	AGACATTGGGAGTACGTGAGG
Pkhd1l1_R	TCCAGACCACAGGAATAGGC
Adamts20_L	TACAGCTGGGGACTGCTACA
Adamts20_R	TTCATCCCAGTTCCTGCTAAG
Pcsk5_L	AGACTTAGGAACGTGTCAGATGG
Pck5_R	CAGTGGCCTTGGTCATCAAT
Col5a_L	CTACATCCGTGCCCTGGT
Col5a_R	CCAGCACCGTCTTCTGGTAG
Celsr1_L	GGCAGTCATGACCTTGGACTA
Celsr1_R	AGCTGATTCCCAATCTGCAC
C3_L	ACCTTACCTCGGCAAGTTTCT
C3_R	TTGTAGAGCTGCTGGTCAGG
Thsd7a_L	GGGACGTGACGTGCTTAAA
Thsd7a_R	TCTTGCTGGCAAAGCTGA
Pcnxl3_L	ACCCCACCGTTCTCTGGT
Pcnxl3_R	TAGACTCCGCTCCCTTAGC
Clstn2_L	CTCTCTTCCAAAGTCCAGTGC
Clstn2_R	GACCATGATGTAGGCATCCAC
RIKEN4931403E03_L	CTATGCTCAGAGAACACTCCTCAG
RIKEN4931403E03_R	GAAGTAGGGCTGTCTTGTAGGG
Slit2_L	TCGAGCCAGCTATGACACC
Slit2_R	TTCCATCATTGATTGTCTCCAC
Slit1_L	GGGGACTGGAGGTTCTCACT
Slit1_R	GAACAGGTGGTTGGAGTGC
Madd_L	GCAGCCTCCTCCGAGATT
Madd_R	ACTGAGCAAGAAGCCAGCAT
Adamts12_L	CCTTGTGGAGAATGGCAAGT
Adamts12_R	CACCTCCTCCACAGGACCTA
Robo1_L	AGGGAAGCCTACGCAGATG
Robo1_R	TGGACAGTGGGCGATTTTAT
Scrib_L	CCACCACGGAAGAAGATGAC
Scrib_R	GTTATTGGCCTGGTCAAACG
Svep1_L	TAAGCCAGCTCAACCTCTGG
Svep1_R	CTGGCCAGCAACTTCACC
Frem2_L	AGGCCACCGTGTCATAA
Frem2_R	TCTCTTTGAATTGCATTTTAGGC
Fbn2_L	AAGAGGGTTCTCTCTGGATGC
Fbn2_R	CCCATCACACTCATCGACAT
Odz1_L	ACATCTATGGACAGAAGGTTTGG
Odz1_R	GGGCACATCTCATATTCATATCC
Odz2_L	GATCAAAGGCAAAGTCACCAT
Odz2_R	AGGAGATTCCTTCCGTGGAC

Odz3_L	CGGACGCATATAATCAGAAAGTC
Odz3_R	GCACGACTCGTACTCGTATCC
Odz4_L	ACATCCCACTGGAAACCAGA
Odz4_R	GAGGTTGTCGTGCAATGTCC

2.2.1.3. Primary antibodies

Name	Concentration/dilution	Application	Supplier
rabbit anti-Frem2	1:400	ICC/IF, IHC	Santa Cruz
rabbit anti-Slit1	1:400	ICC/IF, IHC	Abcam
rabbit anti-Scribble	1:400	ICC/IF, IHC	Abcam
rabbit anti-Pcsk5	1:400	ICC/IF, IHC	Abcam
mouse anti-Tecta	1:100	ICC/IF, IHC	Abnova
anti-Ten-m4	1:200	ICC/IF, IHC	Molekulare Neurophysiologie, Universität München

2.2.1.4. Immunogold secondary antibodies (Gold particle 10nm)

Name	Concentration/dilution	Supplier
Goat anti-rabbit	1:400	AURION
Goat anti-mouse	1:400	AURION

2.2.1.5. Enzymes

Name	Source
Furin	Invitrogen

2.2.1.6. Cell culture media

Name	Compositiom
HEK293 growth medium	DMEM (or Minimum Essential Medium, a Modification [a-MEM]), 100 units/ml penicillin, 100 μg/ml streptomycin, 4 mM L-glutamine,10% fetal bovine serum
CHO growth medium	F-12 medium, 100 units/ml penicillin, 100 μg/ml streptomycin, 10% fetal bovine serum
N2A growth medium	Opti-MEM 50%, F12 medium 50%, 100 units/ml penicillin, 100 μg/ml streptomycin, 10% fetal bovine serum.

2.2.2. METHODS

2.2.2.1. Molecular Biology

Extraction of mRNA from animal tissues, cDNA preparation and conventional cloning were done using the same protocols described in material and methods part I.

2.2.2.2. qRT-PCR of tether candidates

Reactions of 20 μL final volume were set for real time qPCR. 2 μL of cDNA or water was added to a mix containing 0.4 μM final concentration primers, 0.2 μL of corresponding probe from the mouse Universal Probe Library from Roche and 10 μL of 2X universal PCR master mix from Applied Biosystems. The samples were set up in a 96-well plate and run in ABI Prism 7700 (Applied Biosystems). A two step protocol used was as followed: 95°C for 10 min, then 95°C for 10 seconds and 60°C for one min, 40 cycles. For quantification, cDNA from three C57BL/6N animals 4-6 weeks old were used and the samples were run in duplicates. Normalization of expression was done using the HRTP housekeeping and for the samples Cycle threshold (CT) values below 35 were considered positive.

2.2.2.3. Cloning of candidate proteins to tether

The protein candidates selected were cloned into pEGFP-N3 or pCherry-N3 plasmid using conventional cloning. Each candidate protein cloned in these vectors produces a fusion protein with a fluorescent tag at the C-terminal end. Because the candidate proteins have a long coding sequence ranging from 5-12 kb, when needed the full length sequence of each candidate was divided into three to four fragments, and primers were designed to amplify each fragment. cDNA fragments amplified by PCR from DRG cDNA were cloned in sequential steps into pEGFP-N3 or pCherry-N3 vector until full length was achieved. The constructs obtained were sent for sequencing to control possible mutations and frame shifts. For PCR reaction Phusion polymerase and the follow protocols were used:

Standard PCR mix. for Phusion®	**Cycling protocol for Phusion®**
20-100ng of template	Initial denaturation: 98°C 30sec.
1x HF or GC buffer	Denaturation: 98°C 15sec
0.2mM dNTPs	Annealing: primer-dependent 20-30sec
0.4µM primer 3´	Extension: 72°C 30sec/kb
0.4µM primer 5´	Cycles: 25–35
1U of Phusion®	Final extension 72°C 10min
H_2O to 50µl reaction volume.	Storage: 4°C

2.2.2.4. Cell Biology

2.2.2.4.1. Transfection of N2A cells with Polyethylenimine (PEI)

N2A cells were split one day before transfection, and 1:3 dilution was plated in a new well of a 12- well plate containing PLL-Laminin coated glass coverslips. The next day, the cell medium was changed 3-4 h before transfection. Transfecton reactives were brought to room temperature under the hood. Then 4 µg of plasmid were added to 400 µL Serum-free medium (Opti-mem), vortexed for a few seconds, followed by the addition of 16 µl of sterile PEI (1mg/mL). The mixture was vortexed briefly and incubated at room temperature for 5-15 min. 30 uL of mix was added per well and as a negative control mixed with pEGFP-N3 or pCherry-N3 plasmid. The plate was briefly swirled and the cells

were incubated overnight at 37°C in a humidified incubator. The next day positive transfected cells were observed using fluorescence microscopy.

2.2.2.4.2. Hek and CHO cell transfection with Fugene HD

Hek cells that are 50-80% confluent in a 24-well culture dish were transfected using Fugene HD transfection reagent following the manufacturer's instructions. A ratio of 6:1 of Fugene HD reagent (μl) to DNA (μg) respectively was used. For every construct, 1.5 μl of Fugene HD and 0.25 μg DNA were added and mixed in 23.5 μl of OPTI-Mem medium. The mix was incubated at room temperature for 30 min and then added to the cells. The cell culture was observed under a fluorescence microscope 48 h after transfection.

2.2.2.4.3. Transfection of DRG cells

DRG cell transfections were made using the amaxa® system. After digestion with trypsin and trituration as described in cell culture methods, the cells were centrifuged at 1000 g for 3 min and resuspended into 100 μL of Nucleofector® solution. 3μg of the construct DNA were combined with the cell suspension and transfered into the transfection cuvette. After the cells were transfected with the program A-33, 500 μL of RPMI medium supplemented with 5% horse serum were added to the cuvette and the cells were plated on 35mm Ø dish precoated with PLL and laminin. The medium was changed after 4 hours for DMEM-F12 medium, and the cell culture was evaluated under the microscope after 24-48 hours of transfection.

2.2.2.4.4. Immunostaining of cultivated neurons

DRG or SCG cells cultured on PLL-Laminin coated coverslips were washed three times with 1X PBS for 10 minutes each and fixed with 4% paraformaldehyde for 20 min at room temperature. Then washed again for three times with PBS for 10 minutes and blocked with 3% normal goat serum in PBS for 1h at room temperature. Primary antibody incubation in blocking solution (3% normal goat serum) was done overnight at 4°C. Next, unbound primary antibody was washed out three times with PBS for 10 minutes. Secondary antibody incubation (1:500 dilution in blocking solution) was made at room temperature for 30 minutes. After washings with PBS, the coverslips were mounted in aqua PolyMout (Polysciences Inc). Images were acquired with a Olympus 1X81 Microscope.

2.2.2.4.5. Microcontact Printing

Printing of perpendicular crossing stripes of laminin and laminin/laminin-332 (10:1) on glass coverslips was made as previously described by von Philipsborn and colleagues (von Philipsborn et al., 2006)(Chiang et al., 2011). Polydimethylsiloxane (PDMS) stamps were prepared by pouring well-mixed PDMS prepolymer on a silicon master with a stripe pattern of mirror image on it. A small piece of glass was place on top of the PDMS, fixed with metal weights and polymerized at 60 °C overnight. Then the PDMS was cut-out and each stamp was ready to use to print the pattern on clean glass coverslips. Each PDMS stamp was cover with a solution of either laminin (20μg/mL) or laminin/laminin-332 (20μg/mL and 2.3μg/mL) and incubated for 30 min at 37° C in a humidified incubator. After incubation, the stamps were washed with ultrapure ddH$_2$O and dried with N$_2$. Meanwhile, glass coverslips were carefully cleaned with subsequent washes of ethanol:ddH$_2$O (1:1), ethanol:acetone (1:1), ethanol 100% and dried with N$_2$. To improve adherence of the protein to the glass, the coverslip surface was activated in a plasma cleaner oven. Next, the coverslip was immediately placed on top of the laminin coated PDMS stamp and then on top of the laminin/laminin-332 coated PDMS stamp taking care to print the second pattern in a perpendicular direction to the first one. To visualize the stripes printed on the glass 3μL (2μg/mL) of secondary antibody coupled to Alexa488 or Alexa350 (invitrogen) was added to 1 mL of the laminin or laminin/laminin-5 (10:1) solution before incubation with the PDMS stamps.

2.2.2.4.6. DRG Cell culture

DRGs dissected from one C57BL/6N mouse were digested with 1 mL Collagenase IV (1mg/mL Sigma Aldrich) and then treated with trypsin. Digested DRG´s were washed twice with growth medium (DMEM-F12 (Invitrogen) supplemented with L-glutamine (2μM, Sigma-Aldrich), Penicilin (200U/mL)-Streptomycin (200μM/mL)(both invitrogen) 10% fetal horse serum (Invitrogen)), triturated using fire-polished Pasteur pipettes and plated in a droplet of growth medium on a glass coverslip precoated with poly-L-lysin (20μg/cm², Sigma-Aldrich) and laminin (4μg/cm², invitrogen). To allow neurons to adhere, coverslips were kept for 3-4 hours at 37°C in a humidified incubator before being used for immunostaining experiments.

2.2.2.4.7. Immunogold labeling for Electron microscopy pre-embedding method

DRG neurons were isolated and cultivated on laminin-coated petriPERM dishes using standard culture conditions (Hu and Lewin 2006). After 24h, cells were washed with 1X PB (0.1M) and fixed with 4% PFA/0.2% glutaraldehyde solution for 15 min at room temperature followed by 2h incubation at 4°C. Then the cell culture was incubated in blocking buffer for 10 min at 4°C and primary antibody incubation was done the first day at room temperature and the second day at 4°C. Next, three times washing with PB was done and 10 minutes incubation in blocking buffer at room temperature. Gold-conjugated secondary antibody was used in a 1:50 dilution in incubation buffer for 2h at room temperature. Then the sample was washed three times with PB 5 minutes each and fixed again with 2.5% glutaraldehyde in 0.1M cacodylate buffer for 10 minutes at room temperature. The cells were washed twice with 0.1M cacodylate buffer followed by staining with OsO_4 in the presence of Ruthenium Red (Fluka) to enhance the electron density of extracellular proteins (Hasko and Richardson, 1988). The fixed samples were dehydrated through a series of graded ethanol exchanges and infiltrated in a mixture of Poly/BedR 812 epoxy resin and propylene oxide. Then it was embedded in Poly/BedR 812 epoxy resin. Embedded samples were randomly sectioned (50nm thick) and contrasted with uranyl acetate and lead citrate. Sections were examined with a Zeiss 910 electron microscope. Digital micrographs were taken with a 1k x 1k high speed slow scan CCD camera (Proscan) at an original magnification of 8000 to 12000 X and analyzed with iTEM software (Olympus Soft Imaging Solutions, Münster, Germany).

2.3. RESULTS

2.3.1. Screening of tether protein candidates

The search for tether protein candidates has not been an easy task. Approaches such as cell surface biotinylation assays and phage display technology were used without success. In cell surface biotinylation assays, membrane and extra-cellular proteins are label and purified, however once the sample was analysed using Mass spectrometry, a high contamination of peptides coming from the plate coating proteins such as laminin was observed as well as some intracellular proteins peptides. On the other hand, phage display is a technology to screen for candidate genes through protein-protein interactions. In this case a DRG cDNA phage display library is constructed using the T7 phage and the screening for potential candidates is done by rounds of incubation of the virus with laminin coated substrates followed by amplification of the bound viruses. In that way DNA sequences for laminin binding proteins could be obtained. Unfortunately the cloning capacity of T7 phage is too small and the cloning of long sequences was desired since the tether observed in TEM experiments is approx. 100 nm long (Hu et al., 2010). Nevertheless the main problem was that the auto-ligation of the phage is more efficient than the ligation of foreign cDNA sequence fragments, and in most cases, empty phages were obtained. Because of all these disadvantages we decided to use a bioinformatics approach to search for long proteins containing a minimum of one furin site in the mouse genome. Then a Phython script was created by Christian Sommer to search for proteins containing the cleavage site RX(K/R)R in the gene bank. Initially a list of 11302 proteins was obtained and making use of The Database for Annotation, Visualization and Integrated Discovery (DAVID) the proteins were classified according to their localization to the extracellular matrix and sequence size **Appendix I**. In addition, the expression pattern of the proteins in this pre-selection list was checked in the DRG using gene paint (www.genepaint.org) and from those showing staining signal in the DRG 34 final proteins were selected to measure mRNA expression in the DRG vs. SCG using real time PCR.

2.3.2. Selection of tether protein candidates

The mRNA expression levels for 34 proteins selected (Table 3.) was tested in dorsal root ganglia (DRG) and superior cervical ganglia (SCG). According to the previous electron

microscopy analysis of DRG and SCG cultures in our laboratory, the tether protein is absent in SCG cultures (Hu et al., 2010). After quantification of mRNA by qPCR using HRPT as housekeeping gene, six proteins were selected as promising candidates. All of them are long proteins expressed in DRG but not in SCG, have a minimum of one furin site and are membrane proteins or extracellular matrix proteins (Table 4).

Table No. 3. qPCR DRG vs. SCG cDNA

GENE	DRG		SCG	
	Mean	SEM	Mean	SEM
Igsf10	0.482	0.044	0.336	0.006
RIKEN 5430411k18	0.497	0.071	0.359	0.041
Stab1	0.519	0.034	0.482	0.019
coagulaion F8	0.387	0.012	0.090	0.041
Notch3	0.602	0.072	0.309	0.023
Apc2	0.177	0.013	0.037	0.015
RIKEN 672066o15	0.823	0.137	0.340	0.049
Tecta	0.287	0.041	N.E.D	---
Plxnb1	0.660	0.053	0.541	0.002
Dmbt1	N.E.D	---	N.E.D	---
Pkhd1l1	0.361	0.008	0.109	0.016
Adamts20	0.163	0.069	0.068	0.037
Pcsk5	0.388	0.325	N.E.D	---
Col5a1	N.E.D	---	0.469	0.158
Celsr1	0.464	0.071	0.401	0.040
Clstn2	0.673	0.034	0.276	0.080
RIKEN 4931403E03	0.103	0.016	0.178	0.028
Slit2	0.568	0.043	0.230	0.070
Slit1	0.234	0.025	N.E.D	---
Madd	0.405	0.151	0.391	0.119
Adamts12	N.E.D	---	N.E.D	---
Robo1	0.414	0.069	0.378	0.102
Scrib	0.188	0.066	N.E.D	---
Svep1	0.572	0.010	0.360	0.178
Frem2	0.362	0.062	N.E.D	---
Fbn2	0.322	0.085	0.308	0.038
Odz1	0.718	0.111	0.398	0.186
Odz2	0.656	0.010	0.526	0.190
Odz3	0.686	0.048	0.510	0.076
Odz4	0.280	0.059	N.E.D	---
C3	0.232	0.021	0.300	0.018
Thsd7a	0.992	0.049	0.995	0.010
Pcnxl3	0.595	0.217	0.439	0.022
Strc3	N.E.D	---	N.E.D	---

* N.E.D = No expression detected

Table No.4. Candidates to tether protein description

Gene	Protein Name	Transcript Length (bp)	Protein Length (aa)	Furin Sites No.
Ten-m4	odd Oz/ten-m homolog 4	10633	2771	1
Frem2	Fras1 related extracellular matrix protein 2	12368	3160	1
Pcsk5	Proprotein convertase subtilisin/kexin type 5	5208	1877	1
Scrib	Scribbled homolog	5547	1612	1
Tecta	Tectorin alpha	7355	2155	1
Slit1	Slit homolog 1	5236	1531	2

In addition, the protein sequence of each candidate was analysed using the web-based tool SMART (Simple Modular Architecture Research Tool). This bioinformatic tool allows the prediction of protein archuitectures within the protein sequence as domains based on sequence similarities using the algoritm BLAST. After SMART processing of the sequence it also provides a description of domain function when known **Figure 34**.

Ten-m4   Odd Oz/ten-m homolog 4 (Drosophila)

Pfam Ten_N — Teneurin Intracellular region

EGF — Epidermal growth factor like domain

Pfam RHS_repeat — RHS repeat: domain involved in binding carbohydrates

Frem2   Fras1 related extracellular matrix protein 2

RPT — Internal Repeat domain

CA — Cadherin repeats: Cadherin domains occur as repeats in the extracellular regions which are thought to mediate cell-cell contact when bound to calcium

Calx beta — Domain in Na-Ca exchangers and integrin subunit beta4: This domains are normally used to expel calcium from cells and is also present in the cytoplasmic tail of mammalian integrin-beta4, which mediates the bi-directional transfer of signals across the plasma membrane.

Pcsk5   Proprotein convertase   subtilisin/kexin type 5

PDB — PDB domain: Pro-hormone convertase domain

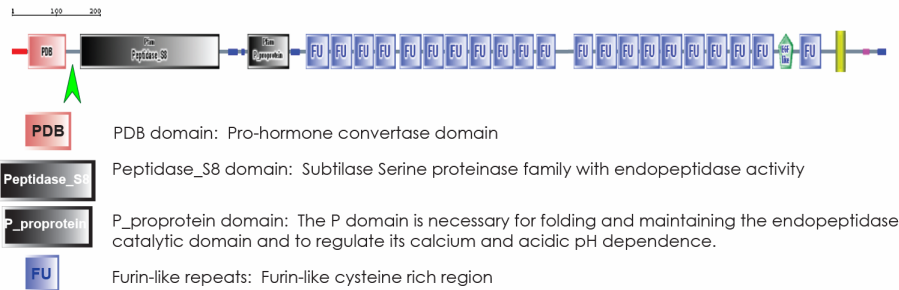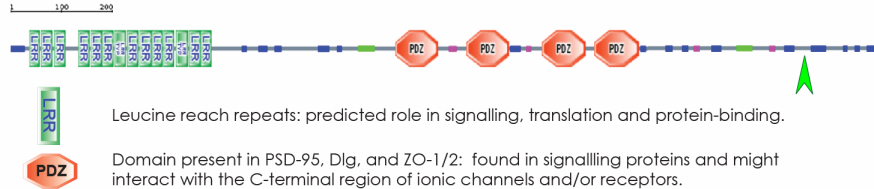**Peptidase_S8** — Peptidase_S8 domain: Subtilase Serine proteinase family with endopeptidase activity

P_proprotein — P_proprotein domain: The P domain is necessary for folding and maintaining the endopeptidase catalytic domain and to regulate its calcium and acidic pH dependence.

FU — Furin-like repeats: Furin-like cysteine rich region

Scrib   Scribbled homolog (Drosophila)

LRR — Leucine reach repeats: predicted role in signalling, translation and protein-binding.

PDZ — Domain present in PSD-95, Dlg, and ZO-1/2: found in signallling proteins and might interact with the C-terminal region of ionic channels and/or receptors.

Tecta   Tectorin alpha

NIDO — Nido domain: Extracellular domain of unknown function in nidogen, a protein enriched in basement membranes.

VWC — von Willebrand factor (vWF) type C domain: domain involved in protein-binding.

VWD — von Willebrand factor (vWF) type D domain: domain required for protein multimerisation.

C8 — This domain contains 8 conserved cysteine residues and is found in disease-related proteins including von Willebrand factor, Alpha tectorin, Zonadhesin and Mucin.

ZP — Zona pellucida (ZP) domain: ZP proteins are responsible for sperm-adhesion fo the zona pellucida.

Slit1   Slit homolog 1 (Drosophila)

LamG — Laminin G domain

FOLN — Follistatin-N-terminal domain-like: Follistatin binds to activin and is a specific inhibotor of the biosynthesis and secretion of pituitary follicle stimulating hormone

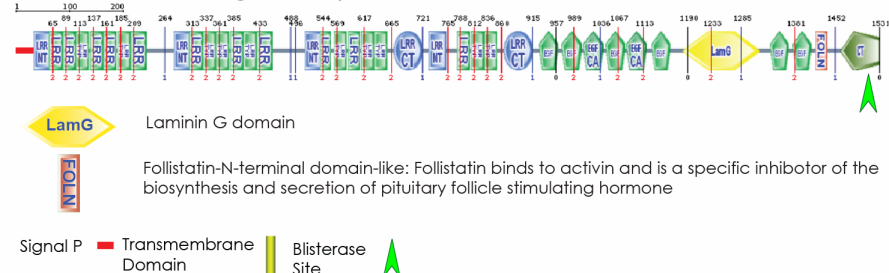Signal P   ▬ Transmembrane Domain   ▌ Blisterase Site

Figure 34. SMART sequence analysis. The figure shows a representation of domain protein architecture for each candidate tether protein. In addition detailed cartoons of the domain symbols are shown with a functional description. Scale bar 200 aa.

2.3.3. Immunostaining of the tether candidates in DRG and SCG cell culture

In the nematode worm *Caenorhabditis elegans (C.elegans)* the components of the mechanosensory channel complex localize to discrete puncta along the axon of the touch neuron (Chelur et al., 2002; Emtage et al., 2004; Zhang et al., 2004). Considering that, the tether protein should be part of the mechanosensory complex because it is expected to link the extracellular matrix directly to the mechanosensitive channel in the tethered gating channel model. It was also expected that immunostaining of the protein candidates might show a patchy like signal pattern in the neurites of sensory neurons cultured on laminin. The immunostaining was made without permeabilization because the labelling of protein in the extracellular part of the neurite was the main goal. Indeed, every candidate protein exhibited a patchy like staining pattern in the neurites of DRG cells and no signal was observed in SCG cells **Figure 35**.
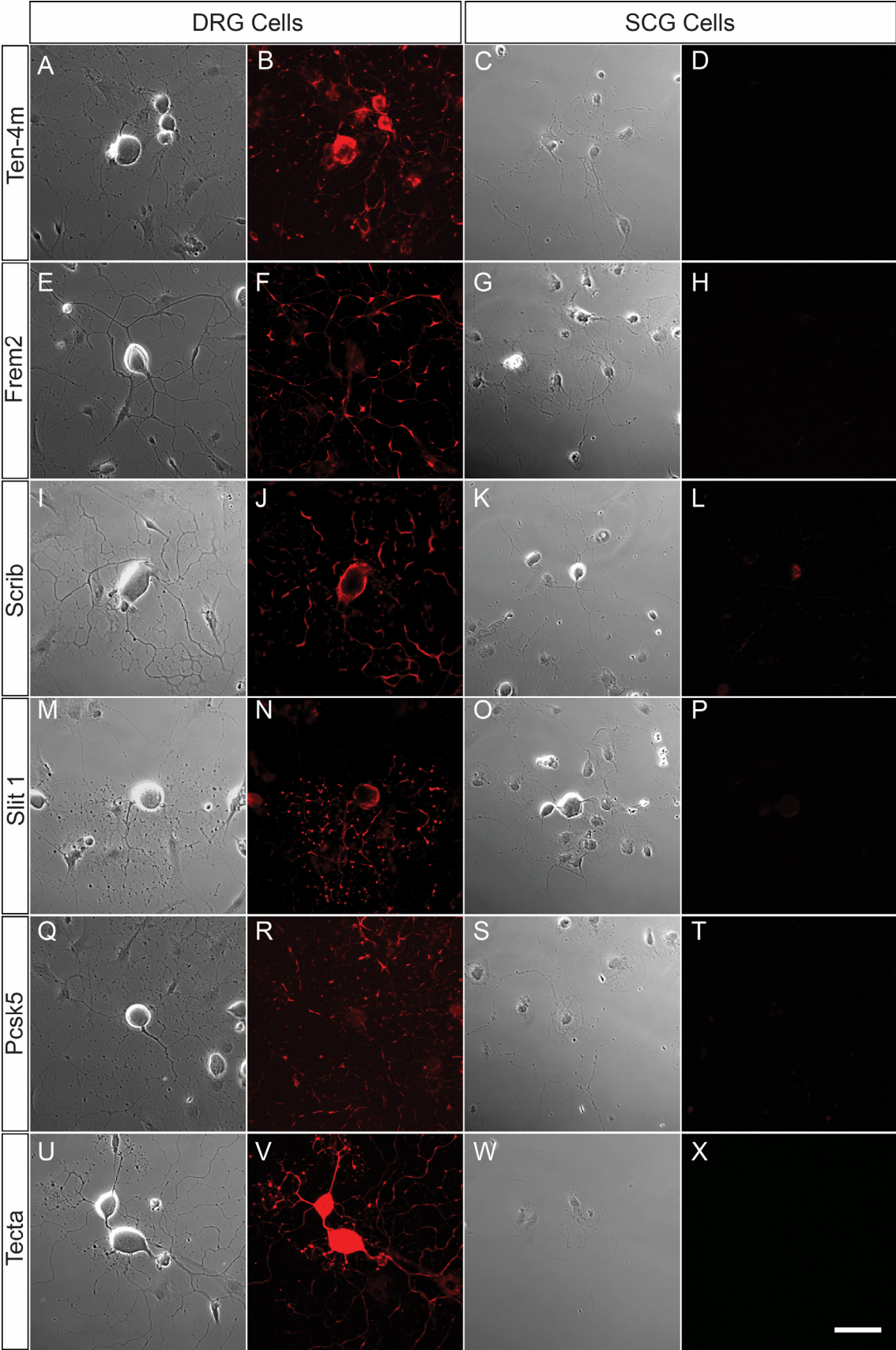
Figure 35. DRG and SCG cell culture immunostaining. A patchy-like expression pattern of the tether candidates is observed in the neurites of DRG cells, and no staining is observed in the non-mechanosensitive SCG neurons. The cells were cultured on plates coated with laminin. A-D

were stained with Ten-m4 antibody, E-F with Frem2, I-L with Scrib, M-P with Slit 1, Q-T with Pcsk5 and U-X with Tecta. Scale bar 50 μL.

2.3.4. Microcontact printing

Laminins are large extracellular glycoproteins that are components of all basement membranes. Laminin-111 and laminin-332 are present in the basement membrane of the skin and have an impact on neurite outgrowth as well as local regulation of mechanotransduction (Chiang et al., 2011; Edgar et al., 1988). Experiments in our laboratory have shown that substrates like laminin-111 support mechanosensitive currents while laminin-332 suppresses rapidly adapting (RA) activated currents. In addition, a 100 nm long tether protein is observed in neurites from DRG cells cultured on laminin-111 or EHS-laminin but not on laminin-332. Based on the previous results, one could suggest that the tether candidates should localize to neurites growing on lamminin-111. To test this hypothesis microcontact printing was used and DRG cells were cultured on grid patterns with laminin stripes in one direction crossed with stripes of laminin/laminin-332 mix at 90° to the laminin stripe **Figure 36**. Although neurite outgrowth occurred along both stripes, immunostaining with antibodies against the tether candidates revealed patchy-staining only in neurites growing on laminin stripes and no fluorescence was detected on neurites growing on laminin/laminin-332 stripes. In addition, staining against Scrib and Slit-1 showed a tendency to localize at the crossing points of the substrate pattern, at these cross road points bifurcation or trifurcation of neurites occurs **Figure 36O** and **Figure 36Y** (see Chiang et al 2011). This experiment did not enable us to identify any of the proteins as non-tether candidates and without proteins that are localized equally to neuritis on laminin or laminin/laminin-332 stripes it is not possible to know if only these six proteins are transported to neurites grown on laminin stripes or if somehow membrane and/or extracellular matrix proteins are in general repressed on laminin/laminin-332 substrates.
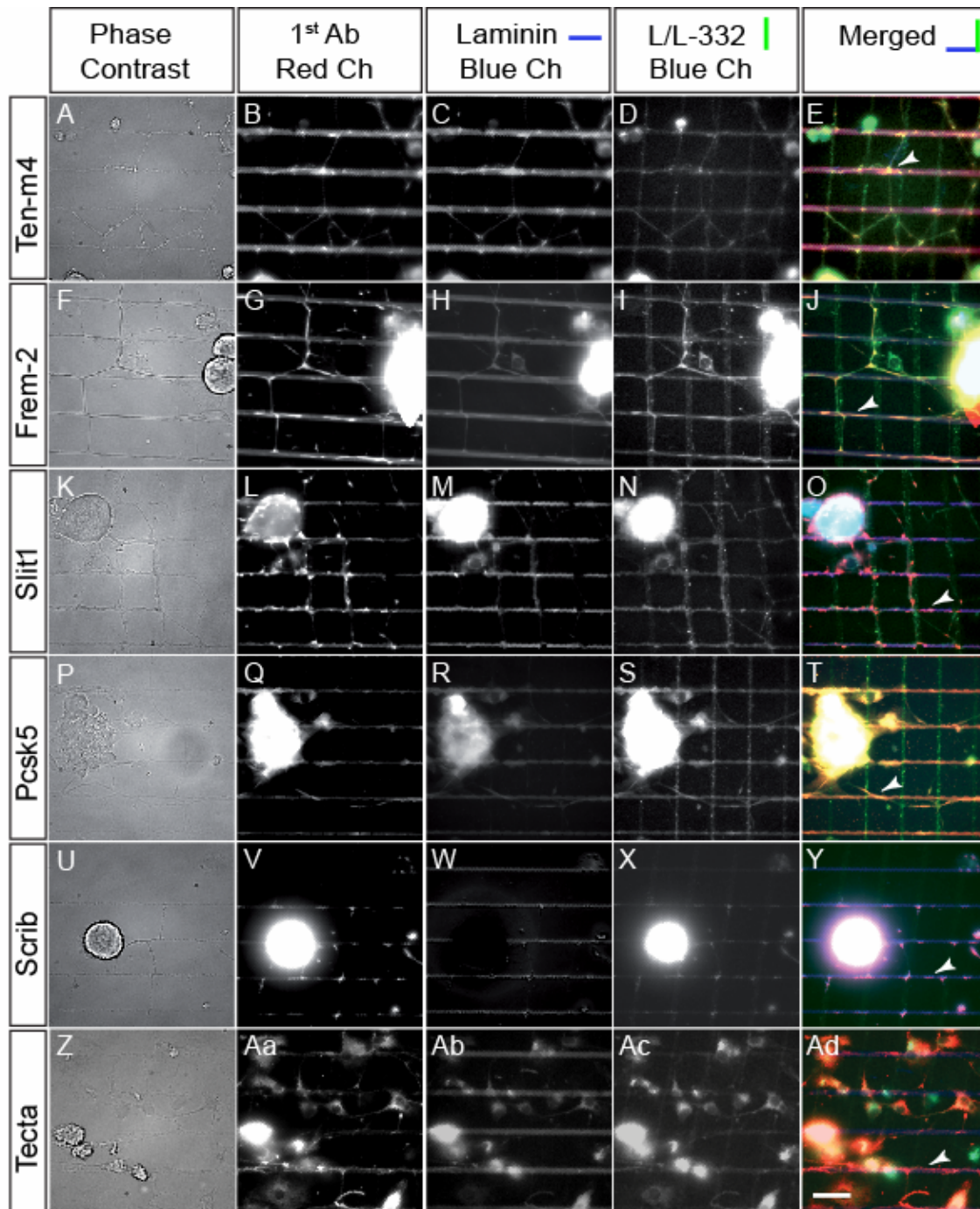
Figure 36. DRG cells cultured on microcontact printing of laminin. Immunofluorescence of the candidate tether proteins in DRG cells cultured on a grid pattern of laminin stripes stained with goat-antimouse alexa 488 (vertical-green channel) and laminin/laminin-322 stained with goat-antirabbit alexa 350 (horizontal-blue channel). Immunostaining with antibodies against the candidates was made in the red channel using alexa 633. Ten-m4 A-E, Frem2 F-J, Slit-1 K-O, Pcsk5 P-T, Scrib U-Y and Tecta Z-Ad. Arrow heads indicate some examples where neurites are growing on the laminin stripe. Scale bar 25 μL.

2.3.5. Cloning and expression of tether candidate proteins

Binding between neurites of DRG cells cultured and laminin and the extracellular matrix is essential for the activation of RA currents (Hu et al., 2010). Then, manipulation of the molecular properties of the tether protein should affect the activation of RA currents or at least modulate its kinetics. For this reason the full length cDNA was cloned in pEGFP-N3 or pCherry-N3 plasmid so that after cell transfection, positive cells could be visualized immediately. Five out of six proteins could be cloned and after sequencing, each clone was tested for expression in HEK cells using Fugine HD. The expression of Scrib, Pcsk5, Slit-1 and Tecta in HEK293 cells was successful as observed by the fluorescence signal **Figure 37**. Nonetheless, transfection efficiency of the tether candidate constructs was lower compared with the positive control which is HEK293 cells transfected with the backbone vector pEGFP-N3 or pCherry-N3 **Figure 37A, B, E and F**. It is probably due to the size of the construct since cell cultures transfected with Scrib, Pcsk5 and Slit-1 which are all encoded by very large cDNAs (~ 5 kb) showed more positive transfected cells than cultures transfected with Tecta that has a sequence about 7.5 kb long and showed very low transfection efficiency. Transfection of cells with the Frem2 construct did not work but this was the longest full length sequence of all candidates with 12 kb. Transfection of cell lines with the Frem2 construct was possible only when the transfection method was changed to PEI. The explanation proposed is the buffer effect caused by the mixture of primary, secondary, and tertiary amines characteristic of polymers such as PEI. The positive charged particles formed by the interaction of DNA and PEI are brought into the cell via endocytosis, once the endosome compartmens are inside the cell occurs an influx of protons causing swelling, rupture and release of the carrier and nucleic acids into the cytoplasm within about four hours. This mechanism makes PEI more efficient for the transfection of mammalian cells when compared to cationic lipid-based vectors (Campeau et al., 2001; Llères et al., 2004; Ogris et al., 2001; Tros de Ilarduya et al., 2010).

This experiment also allowed us to examine the subcellular localization of the expressed proteins. Most of the candidates showed cytoplasmic expression, and only Scrib expression was restricted to the cell membrane in HEK293 cells **Figure 37 C and D**. Next, transfection of mouse DRG cells with the candidate protein constructs by electroporation was the goal, but unfortunately the transfection efficiency was extremely low and the viability of the cells after transfection was very poor. This experimental problem limited the chance of testing the functionality of the candidate proteins in native

systems. Thus, other methodologies were used to find the tether protein such as immunogold labelling that allows the identification and visualization of the tether protein at the interface between neurite and extracellular matrix, and expression of the constructs in mechanically sensitive heterologous systems such as N2A cells.
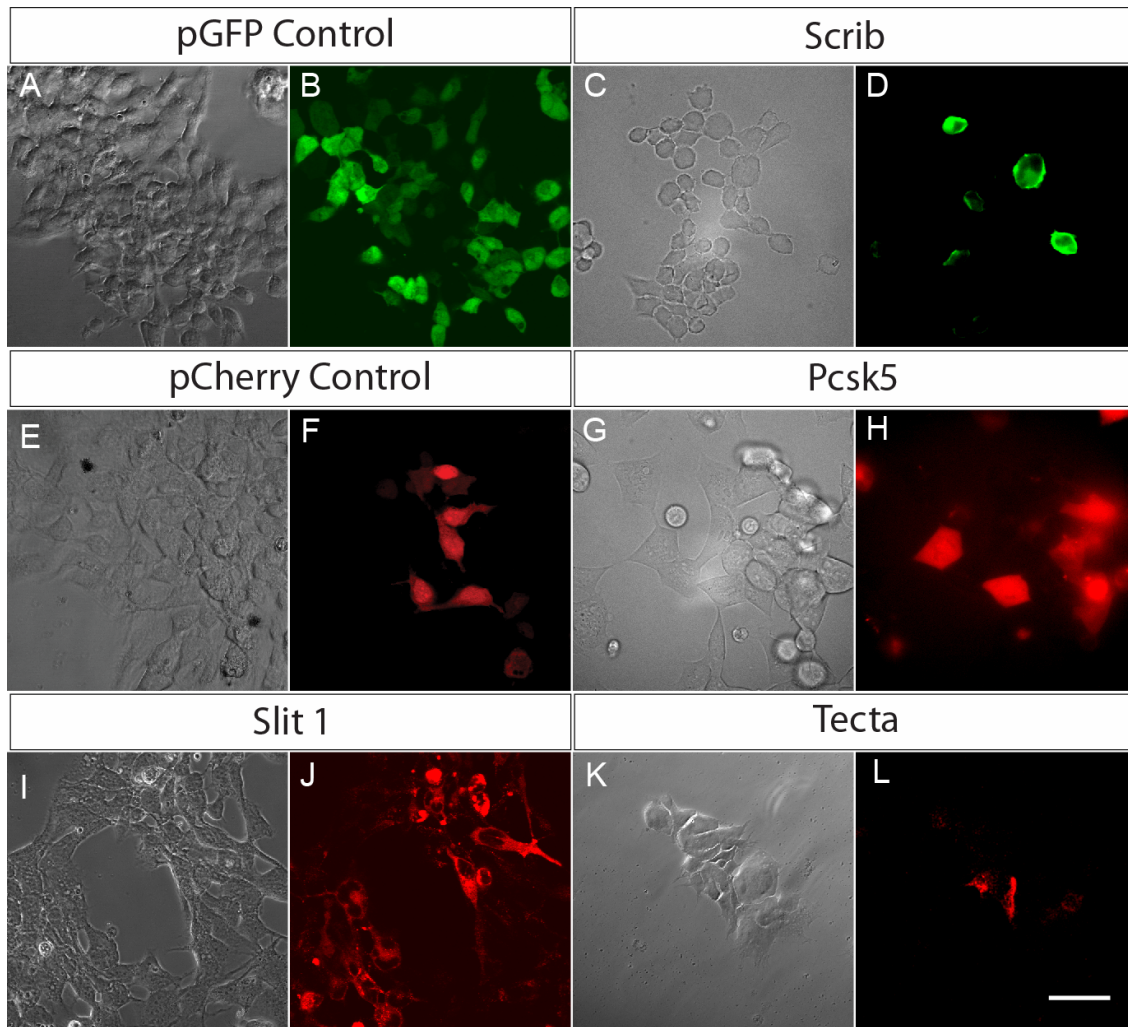

Figure 37. Transfection of the candidate proteins into HEK293 cells. Expression of the candidate proteins fused with a fluorescent tag in HEK293 cells. A-B show expression of pEGFP-N3 and E-F show expression of pCherry-N3. C-D, show membrane localization of the Scrib protein expressed in HEK293 cells. G-H, Show cytoplasmic expression of Pcsk5, as well as I-J for Slit-1 and K,L for Tecta. Scale bar 50 μL.

2.3.6. Immunogold labelling in cultured DRG cells

A direct method of identifying the tether protein is by immunogold labelling the protein in DRG cell culture with a gold conjugated antibody followed by visualization of the gold particle using transmission electron microscopy. However, although the primary antibodies used so far against the tether candidates worked fine in immunofluorescence,

this is no guarantee that they would also work for electron microscopy. Only antibodies against Scrib and Slit-1 worked as can be observed in the **Figure 38**, the 10 nm gold particles were located at the extracellular part of the neurite membrane but they did not colocalize with the tether protein, so these proteins can probably be discarded as potential candidates. Regarding the other candidates, new antibodies were needed to test their localization in the cell membrane.
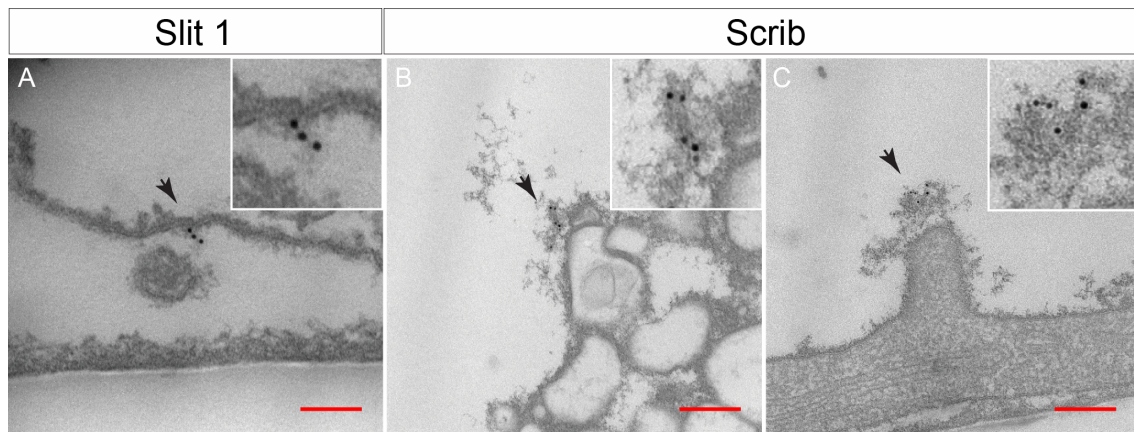

Figure 38. Immunogold labelling of protein candidates in DRG cell culture. A. Slit-1 immunogold labelling stains in the interface between neurites and extracellular matrix but is not located together with the tether protein scale bar 100nm. B-C, Scrib immunogold labelling shows gold particles located on the top of the cell soma B, and a neurite C, but was never found at the tether protein. Scale bar in B and C 200 nm. Gold particles 10 nm.

2.3.7. Primary antibody production by genetic immunization

Primary antibodies against Frem2 were produced by GENOVAC using a new technique called genetic immunization. This methodology had been successful in the production of antibodies against difficult antigens such as multi-membrane spanning proteins. The Frem2 sequence used for genetic immunization was from the 1300-2300aa. This region is located to the extracellular part of the cell membrane close to Frem2's transmembrane domain, and contains the five tandem repeats of the Calx-beta domain. Upon receiving medium supernatants from GENOVAC the antibody screening was made by immunostaining of CHO transfected cells with the Frem2 construct. Only supernatants that stained the cells positive for Frem2 transfection were selected and a western blot was made to test antibody specificity. Frem2 has two protein variants of 351 kDa and 296kDa, and western blots of protein extracts from CHO cells transfected with Frem2 construct showed that the monoclonal antibodies obtained recognized only the 351kDa Frem2 variant and that in cell culture both Frem2 variants are produced as shown by incubation of

the membrane with antibody against the fluorescent tag **Figure 39**. In the future experiments with these antibodies are going to be used for immunogold labelling of DRG cells in culture but the secondary antibody will be conjugated to an ultra small gold particle instead a 10 nm gold particle. Ultra small gold particles will improve antibody penetration as well as better access of the antibody to the antigen. However, establishing of this methodology is time consuming and will require minimum six months before any satisfactory result can be produced.
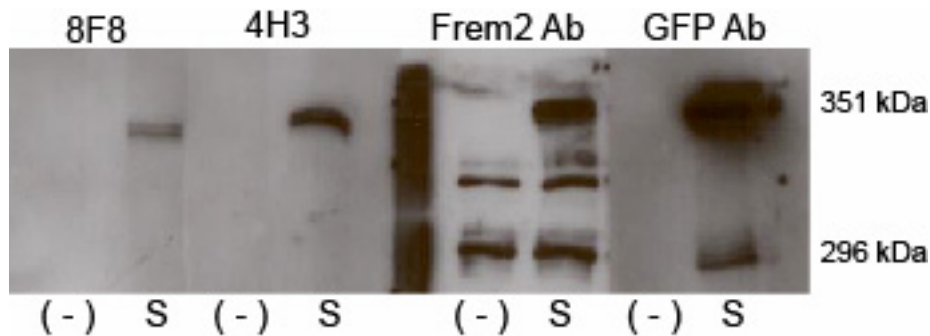

Figure 39. Frem2 monoclonal antibody western blot. Primary antibody clones 8F8 and 4H3 were tested for specificity using a western blot of protein extracts from CHO cells transfected with the Frem2 construct. The same samples were run four times and the membranes were incubated with the different antibodies, the supernatants 8F8, 4H3, Frem2 primary antibody from Santa Cruz and antibody against the GFP tag.

2.3.8. Mechanical activated current properties of N2A cells transfected with Frem2

Recently it was discovered that the mouse neuroblastoma cells Neuro2A (N2A) express mechanosensitive currents similar to those recorded from primary sensory neurons in culture and that the ion channel underlying the activation of the current is the Piezo1 channel (Coste et al., 2010). Taking advantage of the fact that cell lines are easier to transfect that primary DRG cells and that N2A cells express Piezo1, I wanted to see if Frem2 could affect the kinetic properties of the mechanosensitive currents expressed in N2A cells including activation time constant (τ_1), inactivation time constant (τ_2), latency which is the time between the mechanical stimulation and the activation of the current, and mechanical threshold which is the minimal displacement applied to the cell in order to produce a current. Transfected N2A cells with the Frem2 construct were recorded in whole-cell mode, and mechanosensitive currents were produced by stimulation of the cell soma with a glass probe driven by a nanomotor. As a negative control, N2A cells transfected with pEGFP-N3 were used. No difference was observed between Frem2 transfected N2A and the controls in any of the parameters measured **Figure 40**. That

suggest that in these cells the presence of a tether protein is not necessary for the generation of mechanically activated currents or that in DRG cells the tether protein could be associated with a mechanically activated ion channel different from Piezo1.
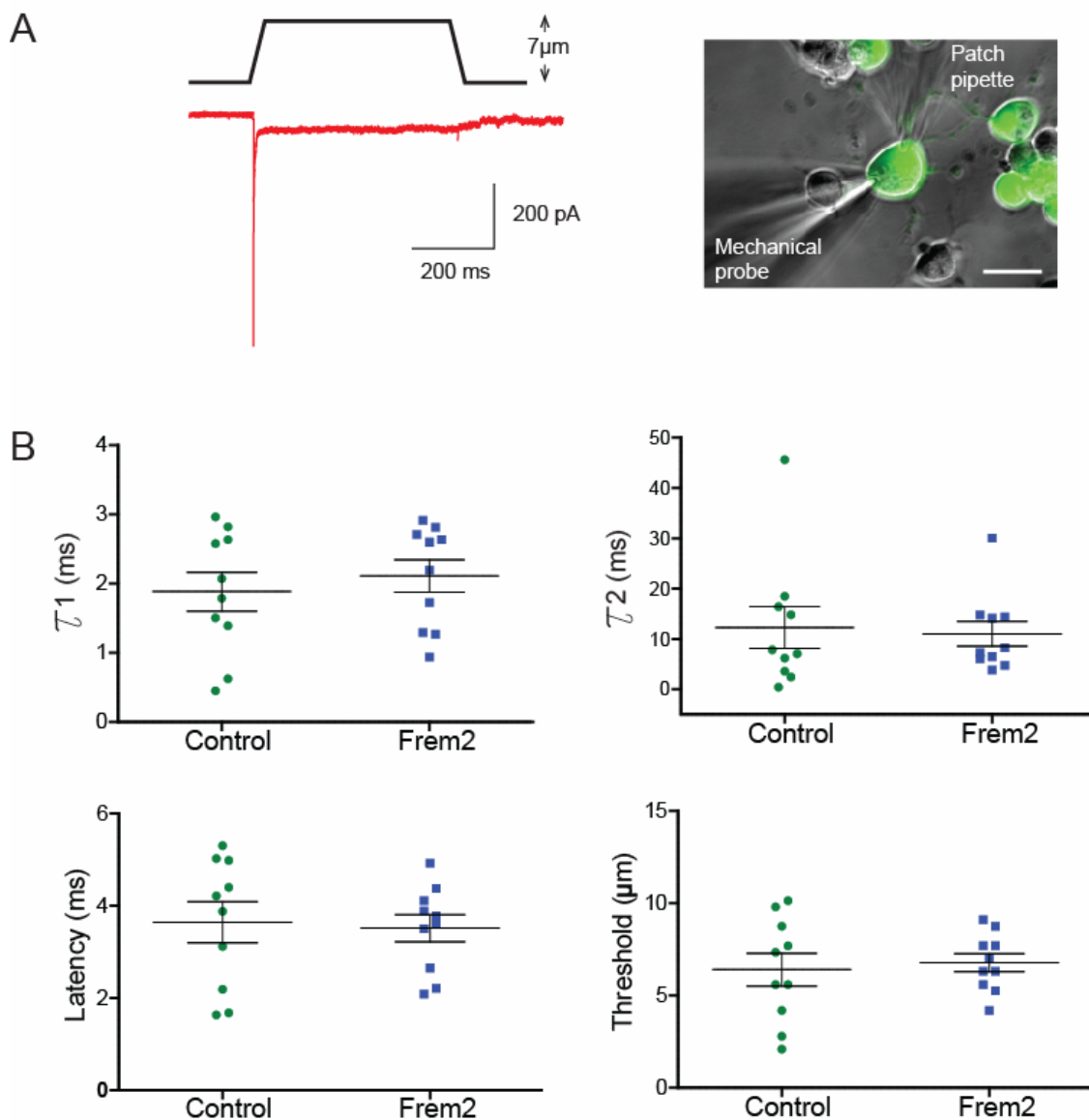

Figure 40. Effect of Frem2 in the kinetics of mechanically activated currents expressed in N2A cells. A. The left panel shows a representative mechanosensitive current expressed in N2A cells and the type of mechanical stimulus applied. The right panel shows a Frem2 transfected N2A cell being recorded in whole-cell mode and stimulated by a glass probe driven by the nanomotor, scale bar 25 μm. B. Kinetic properties of mechanically activated currents expressed in N2A cells transfected with the Frem2 construct or pEGFP-N3 vector. Each dot represent the mean of the parameter measured per cell, n=10 cells.

2.4. DISCUSSION

2.4.1. Biological function of tether candidates

Each promising candidate selected was a known protein the expression of which had been observed in nervous system or other tissues. In most cases, the function of these proteins had been evaluated in the central nervous system where they have been shown to have an effect in axon targeting, axon branching or cell adhesion. If the tether protein has a function in any of these biological processes, it was not directly relevant for us as the furin treatments made in cultured DRG cells were performed after cell adhesion and when the neurites are already grown. However, no detachment of cells or neurites is observed when sensory neruons are treated with furin or blisterase as recordings using mechanical stimulation were made after such treatments (Hu et al., 2010). This suggests that furin sensitive tethers are at least not directly involved in cell adhesion. Background published data on the proteins selected as possible candidates could help to evaluate their potential as possible components of the mammalian mechanotransducing complex in sensory neurons.

2.4.1.1. Slit-1

Slit-1 is part of the Slit family of proteins which are secreted glycopreteins and are predominantly expressed in the nervous system. Slit-1 is involved in cell migration as a molecular guidance cue, and its function depends on its post-translational modification (Howell et al., 2007). For example, the N-terminal fragment of Slit, Slit-N promotes the branching of axons of the dorsal root ganglion, whereas the full-length Slit antagonizes this activity (Chen et al., 2001; Wang et al., 1999). In addition Slit-1 promotes regenerative neurite outgrowth of DRG cells in vitro by binding to the Robo receptor (Zhang et al., 2010b). Thus Slit-1 seems to be very important in the physiology of axon growth and axonal targeting as reported by Xiao and colleagues where they showed that the specificity by which retina axon projections innervate their target lamina the midbrain tectum in the zebra fish is mediated by Slit-1 bound to Type IV collagen (Xiao et al., 2011). It is interesting to note that Slit-1 is directing the projection of axons based on an extracellular guidance system because when the localization of Slit-1 was observed in the neurites of cultured DRG cell using immunogold labelling, the gold particles where observed in the interface neurite-extracellular matrix which validates this methodology and shows that the

gold particles can penetrate these small spaces. At the same time, the absence of a direct interaction observed with laminin, that the gold particles are not co-localized with the tether protein and its clear function in axon guidance, exclude Slit-1 as a potential tether candidate.

2.4.1.2. Pcsk5

Pcsk5 belongs to the proprotein convertases family (PCs). PCs cleave proteins precursors as prohormones, proreceptors, growth factors, adhesion molecules, and viral glycoproteins at basic sites during their transit to the secretory pathway and/or at the cell surface (Essalmani R, et al. 2007). The knock-out of Pcsk5 in mice produces embryonic lethality between stages E4.5 and E7.5 probably because of maternal deficit of Pcsk5 which is needed for embryo implantation (Essalmani et al., 2006). Specific inactivation of Pcsk5 in endothelial cells results in cardiovascular hypotrophy associated with decreased collagen deposition (Marchesi et al., 2011). Pcsk5 cell surface localization and the fact that the majority of protein precursers cleaved by Pcsk5 are adhesion proteins including integrin α chain and the neural adhesion protein L1 suggest that this proteinase is involved in extracellular matrix modification (Kalus et al., 2003; Lehmann et al., 1996). Thus, although not directly, Pcsk5 could play a role in mechanostransduction through the modification of the ECM in the basement membrane, however this theory is still elusive.

2.4.1.3. Tecta

α- Tectorin is an extracellular matrix protein of the inner ear involved in hearing. In homozygous mice for a targeted deletion (ΔENT) in the gene encoding α-Tectorin, deafness is observed because the tectorial membrane lacks all non-collagenous components and is completely detached from the organ of Corti and the spiral limbus (Legan PK et al. 2000). In addition, the mutations of the TECTA gene in humans support its function in hearing, and as an important component in the maintenance of the tectorial membrane in the inner ear (Xia et al., 2010). Studies in sensory neurons in *C. elegans* show that dex-1 and dyf-7 which encode a Tectorin-like protein par, act as a dendritic tip for anchoring of the sensory dendrite during cell body migration (Heiman MG, et al. 2009). Despite Tecta's function in cell adhesion, its specific function in sensory neurons is still unknown. It is not a promising candidate to tether proteins because despite its hearing phenotype, no touch deficit has been observed in the Tecta knock-out mouse.

2.4.1.4. Scrib

Scrib is involved in cell polarization and in maintaining normal cell-cell contacts in epithelial cells through its PDZ domain (Javier, 2008; Yates et al., 2013). In the nervous system Scrib is required for neuronal tube closure during development (Murdoch et al., 2003), and in the adult brain Scrib regulates dendritic spine morphology where it influences actin cytoskeleton (Moreau et al., 2010). In DRG cells in culture, expression of Scrib was observed in the extracellular part of the membrane in the cell soma or on top of the neurites. Although the function of Scrib in DRG cells has not been addressed, its location on top of neurites instead in the extracellular matrix-neurite interface excludes Scrib as an interesting tether candidate.

2.4.1.5. Ten-m4

Ten-m4 belongs to the teneurin family of proteins which are expressed in distinct and often interconnected areas of the developing nervous system. They are large proteins that have a molecular weight ~300 kDa and are classified as type II transmembrane glycoproteins (Baumgartner et al., 1994; Levine et al., 1994). Teneurin-4 is involved in determining the anterior-posterior axis in mice in early development (Lossie et al., 2005). In the spinal cord Ten-m4 regulates myelination in oligodendrocytes (Suzuki et al., 2012), and in the avian embryo Ten-m4 helps to generate the complex epithelial-mesenchymal cross-talk necessary for the normal development of the limbs, and it binds to the gama-1 subunit of laminin in these tissues (Kenzelmann-Broz et al., 2010). In general Teneurins seem to have a role in axon bundling, pathfinding and patterning within the nervous system, and pattern formation in certain non-neuronal tissues during development (Mosca et al., 2012; Young and Leamey, 2009). In the central nervous system the absence of Ten-m4 caused by transgene insertion in mice results in tremors and severe hypomyelination of small-diameter axons, and it reduces oligodendrocyte differentiation especially in the spinal cord of the CNS (Suzuki et al., 2012). So far, no studies have been made about what role Ten-m4 could play in DRG cells. Ten-m4 match the characteristics found currently for the tether protein, it has a furin site, most of the sequence of the protein is located extracellularly, it is expressed in DRG and not in SCG, it seems to interact with laminin-1 in the extracellular matrix and it is a large protein which looks very similar to the tether when the recombinant protein is observed with electron microscopy (Feng et al., 2002). Unfortunately it has proven difficult to clone and there are no good commercially available

antibodies. Ten-m4 remains as an interesting candidate and efforts are going to continue in order to obtain the antibodies for immunogold labelling.

2.4.1.6. Frem2

Frem2 is an extracellular matrix protein detected in epithelial basement membranes of newborn and adult mice, using immunofluorescence and electron microscopy (Pavlakis et al., 2008; Petrou et al., 2007). Frem2 has been functionally implicated in embryonic dermal-epidermal adhesion as deduced from the appearance of sub-epidermal blisters in mouse mutants compromising the function of Fras1, Frem1 and/or Frem2 proteins (Jadeja et al., 2005; Timmer et al., 2005). Assembly of Frem2 with Fras1 is required for their stable localization at the basement membrane that prevents detachment of the skin observed in Fraser-syndrome disease where the expression or the function of any of these proteins is compromised (Kiyozumi et al., 2006). Frem2 was a very promising tether candidate taking into account the tight relation of Frem2 with the extracellular matrix. Immunogold labelling of the protein in the base membrane of the skin shows a structure of about 200nm long very similar to the tether protein observed in the neurites of cultured DRG cells (Petrou et al., 2007). In addition, Frem2 has two furin domains located at the extracellular part of the protein, and one furine site is located very close to the transmembrane domain which would certainly abolish its function after cleavage. Although, expression of Frem2 in N2A cells did not showed any modulation of the kinetic properties of mechanical activated currents in these cells, it is important to highlight that piezo1 is the channel responsible for expression of mechanosensitive currents in N2A cells, and in DRG cells it is piezo2 that has been proposed to be responsible for expression of RA currents (Coste et al., 2010). In addition, piezo2 is observed only in 20% of cultured DRG cells but RA-currents are expressed in about 31% of cells in the DRG (Hu and Lewin, 2006), and overlap of some piezo2 positive DRG cells with the nociceptive marker TRPV1 suggested a role for this channel in noxious mechanosensation (Coste et al., 2010). A recent study supported this theory showing that knock-out of the orthologous Dmpiezo in *Drosophila* reduces the response of larvae to noxious mechanical stimulus while response to other noxious stimuli or touch were not affected (Kim et al., 2012). Then, there is a possibility that in DRG cells Frem2 could interact with piezo2 but it is not present in N2A cells or that Frem2 could also interact with another mechanically activated channel which has yet to be discovered and is neither present in N2A cells, or that at the end it does not play a role in mechanotransduction. Immunogold labelling using the monoclonal

antibodies produced and the measure of mechanical activated currents in DRG cultured cells of the gene trap mouse KST252 that produces a truncated Frem2 protein will help to elucidate the role of Frem2 in mechanosensation.

2.4.2.   Functional test for tether candidates

The use of a bioinformatics approach allowed the selection of some potential candidates according to the properties of the tether protein known so far (Hu et al., 2010). However, experiments still need to be done in order to prove that either one of the two remaining tether candidates (Frem2 and Ten m4) is indeed involved in mechanotransduction. After the cDNAs for the tether candidates were cloned, modification of the furin site would produce a protein resistant to furin treatment so that if one the candidate protein happens to be the tether, DRG cell culture transfected with it should also support the expression of RA currents after treatment with furin. Unfortunately, the difficulties found so far in characterizing function of these candidates in mechanotransduction have been technical in nature. For example, when transfecting primary sensory neurons with the cloned cDNAs for candidate tethers, the transfection efficiency was found to be extremely poor and after electroporation of DRG cells, the cell membrane is so damaged that recordings using patch clamp were not possible. Other transfection techniques suitable for primary neurons in cell culture are infection with viruses (Karra and Dahm, 2010), but in this case the vector capacity is normally no higher than 3 kb and Frem2 and Ten-m4 coding sequences are already twice as large. In addition viruses take some time to express the protein transfected in cell culture which is incompatible with the fact that DRG cells need to be patched within 30h after plating.

Another possible experiment to test the function of the tether candidates in sensory neurons could be to use blocking antibodies to prevent their binding to laminin. In theory if the tether protein is not able to bind to laminin the RA-current may not be maintained. In any case the antibody needs to bind to the laminin binding epitope of the candidate protein and that might not be so easy to find. A variant of this method could be to incorporate the antibody to extracellular matrix coating proteins that do not support mechanosensitive currents such as laminin-332 and expect appearance of RA currents in sensory neurons cultured on plates coated with such a mix. Nevertheless, the key experiment to test if Frem2 or Ten-m4 is required for the expression of RA currents in sensory neurons is to produce conditional knock-outs and test if the currents are still

pressent in DRG cells as well as to visualise the tether using TEM. In addition, the behaviour of these animals can be tested to detect any somatosensory deficit.

2.4.3. Other screening methods to identify tether candidates

Since the tether protein was discovered, we have made large efforts to determine its identity. Screening for tether protein candidates using cell surface biotinylation assays and phage display were tried without success. From the experience accumulated so far and in order to increase the probability of success, the need of biochemical approaches in combination with proteomics seems like a more promising approach. The tether is an extracellular matrix protein 100 ± 3 nm long, occurs with an average density of 4.9 ± 1.3 filaments per μm^2 of membrane, is cleaved by furin proteinase and binds to laminin (Hu et al., 2010). This information can be used to design experiment strategies to search for potential candidates. Mass spectrometry (MS) based proteomics allows the identification of the protein sequence of short peptides. However, to eliminate background, the protein sample should be pre-purified or treated using a method that makes use of the molecular properties of the tether protein such as its ability to bind to laminin or its furin cleavage site, or both simultaneously. For example, chemical cross-linking could be used to fix non-covalent protein-protein interaction between the tether and laminin in cultured sensory neurons followed by osmotic shock of the cells and wash out of the proteins not fixed to laminin. Depending on the cross-linker used, MS analysis of laminin-tether cross-linked peptides could be done (Gomes and Gozzo, 2010), or if the cross-linker is cleavable then only peptides with potential binding to laminin would be obtained. A recent MS approach developed by Kleifeld and colleagues (Kleifeld et al., 2010) named teminal amine isotopic labelling of substrates (TALES) uses reductive dimethylation of primary amines to positively select N-termini generated by digestion with a protease. DRG cells cultured on laminin can be digested with furin protease and after disruption of the cells by osmotic shock the proteins bound to laminin can be isolated and labelled with $(d(2)C^{13})$-formaldehyde for the protease-treated (heavy) or with $(d(0)C^{12})$- formaldehyde for the control cell culture without protease treatment (light). After trypsin treatment, removal of tryptic and C-terminal peptides is done with a polyglycerol aldehyde polymer and the sample is analysed by MS (Kleifeld et al., 2010). The advantage of this method is that the peptides produced by trypsin treatment of laminin, which are in a high concentration in the sample, are removed with the polymer and do not interfere with MS and only one purification step is needed.

Although the molecular properties of the tether protein we have so far are very useful to design strategies for its identification, still more information of the tether's nature is needed to narrow the spectra of candidates when a screening is made as well as to broad our experimental possibilities. For example, the finding of more specific protease cleavage sites in the tether protein that also produces abolishment of mechanotransduction. Also to find the tether's binding domain to laminin-111 would help to design more specific purification approaches and would also allow artificial manipulation of the tether protein in cell culture.

3. BIBLIOGRAPHY

Abdo, H., Li, L., Lallemend, F., Bachy, I., Xu, X.-J., Rice, F.L., and Ernfors, P. (2011). Dependence on the transcription factor Shox2 for specification of sensory neurons conveying discriminative touch. Eur. J. Neurosci. *34*, 1529–1541.

Ahmed, Z.M., Goodyear, R., Riazuddin, S., Lagziel, A., Legan, P.K., Behra, M., Burgess, S.M., Lilley, K.S., Wilcox, E.R., Riazuddin, S., et al. (2006). The tip-link antigen, a protein associated with the transduction complex of sensory hair cells, is protocadherin-15. J. Neurosci. *26*, 7022–7034.

Airaksinen, M.S., Koltzenburg, M., Lewin, G.R., Masu, Y., Helbig, C., Wolf, E., Brem, G., Toyka, K.V., Thoenen, H., and Meyer, M. (1996). Specific subtypes of cutaneous mechanoreceptors require neurotrophin-3 following peripheral target innervation. Neuron *16*, 287–295.

Arnadóttir, J., O'Hagan, R., Chen, Y., Goodman, M.B., and Chalfie, M. (2011). The DEG/ENaC protein MEC-10 regulates the transduction channel complex in Caenorhabditis elegans touch receptor neurons. J. Neurosci. *31*, 12695–12704.

Assad, J.A., and Corey, D.P. (1992). An active motor model for adaptation by vertebrate hair cells. J. Neurosci. *12*, 3291–3309.

Averill, S., McMahon, S.B., Clary, D.O., Reichardt, L.F., and Priestley, J.V. (1995). Immunocytochemical localization of trkA receptors in chemically identified subgroups of adult rat sensory neurons. Eur. J. Neurosci. *7*, 1484–1494.

Bachy, I., Franck, M.C.M., Li, L., Abdo, H., Pattyn, A., and Ernfors, P. (2011). The transcription factor Cux2 marks development of an A-delta sublineage of TrkA sensory neurons. Dev. Biol. *360*, 77–86.

Basbaum, A.I., Bautista, D.M., Scherrer, G., and Julius, D. (2009). Cellular and Molecular Mechanisms of Pain. Cell *139*, 267–284.

Batista, M.F., and Lewis, K.E. (2008). Pax2/8 act redundantly to specify glycinergic and GABAergic fates of multiple spinal interneurons. Dev Biol *323*, 88–97.

Baumgartner, S., Martin, D., Hagios, C., and Chiquet-Ehrismann, R. (1994). Tenm, a Drosophila gene related to tenascin, is a new pair-rule gene. EMBO J *13*, 3728–3740.

Bechstedt, S., Albert, J.T., Kreil, D.P., Müller-Reichert, T., Göpfert, M.C., and Howard, J. (2010). A doublecortin containing microtubule-associated protein is implicated in mechanotransduction in Drosophila sensory cilia. Nat Commun *1*, 11.

Becker, A.J., Pitsch, J., Sochivko, D., Opitz, T., Staniek, M., Chen, C.-C., Campbell, K.P., Schoch, S., Yaari, Y., and Beck, H. (2008). Transcriptional upregulation of Cav3.2 mediates epileptogenesis in the pilocarpine model of epilepsy. J. Neurosci. *28*, 13341–13353.

Bell, J., Bolanowski, S., and Holmes, M.H. (1994). The structure and function of Pacinian corpuscles: a review. Prog. Neurobiol. *42*, 79–128.

Beurg, M., Fettiplace, R., Nam, J.-H., and Ricci, A.J. (2009). Localization of inner hair cell mechanotransducer channels using high-speed calcium imaging. Nat. Neurosci. *12*, 553–558.

Birder, L.A., and Perl, E.R. (1994). Cutaneous sensory receptors. J Clin Neurophysiol *11*, 534–552.

Birnbaumer, L., Campbell, K.P., Catterall, W.A., Harpold, M.M., Hofmann, F., Horne, W.A., Mori, Y., Schwartz, A., Snutch, T.P., and Tanabe, T. (1994). The naming of voltage-gated calcium channels. Neuron *13*, 505–506.

Blake, D.T., Hsiao, S.S., and Johnson, K.O. (1997). Neural Coding Mechanisms in Tactile Pattern Recognition: The Relative Contributions of Slowly and Rapidly Adapting Mechanoreceptors to Perceived Roughness. J. Neurosci. *17*, 7480–7489.

Boëda, B., El-Amraoui, A., Bahloul, A., Goodyear, R., Daviet, L., Blanchard, S., Perfettini, I., Fath, K.R., Shorte, S., Reiners, J., et al. (2002). Myosin VIIa, harmonin and cadherin 23, three Usher I gene products that cooperate to shape the sensory hair cell bundle. EMBO J. *21*, 6689–6699.

Bourane, S., Garces, A., Venteo, S., Pattyn, A., Hubert, T., Fichard, A., Puech, S., Boukhaddaoui, H., Baudet, C., Takahashi, S., et al. (2009a). Low-Threshold Mechanoreceptor Subtypes Selectively Express MafA and Are Specified by Ret Signaling. Neuron *64*, 857–870.

Bourane, S., Garces, A., Venteo, S., Pattyn, A., Hubert, T., Fichard, A., Puech, S., Boukhaddaoui, H., Baudet, C., Takahashi, S., et al. (2009b). Low-Threshold Mechanoreceptor Subtypes Selectively Express MafA and Are Specified by Ret Signaling. Neuron *64*, 857–870.

Bourinet, E., Alloui, A., Monteil, A., Barrère, C., Couette, B., Poirot, O., Pages, A., McRory, J., Snutch, T.P., Eschalier, A., et al. (2005). Silencing of the Cav3.2 T-type calcium channel gene in sensory neurons demonstrates its major role in nociception. EMBO J. *24*, 315–324.

Brierley, S.M., Hughes, P.A., Page, A.J., Kwan, K.Y., Martin, C.M., O'Donnell, T.A., Cooper, N.J., Harrington, A.M., Adam, B., Liebregts, T., et al. (2009). The ion channel TRPA1 is required for normal mechanosensation and is modulated by algesic stimuli. Gastroenterology *137*, 2084–2095.e3.

Brisben, A.J., Hsiao, S.S., and Johnson, K.O. (1999). Detection of vibration transmitted through an object grasped in the hand. J. Neurophysiol. *81*, 1548–1558.

Briscoe, J., Pierani, A., Jessell, T.M., and Ericson, J. (2000). A homeodomain protein code specifies progenitor cell identity and neuronal fate in the ventral neural tube. Cell *101*, 435–445.

Brown, A.G., and Iggo, A. (1967). A quantitative study of cutaneous receptors and afferent fibres in the cat and rabbit. J. Physiol. (Lond.) *193*, 707–733.

Brown, A.L., Fernandez-Illescas, S.M., Liao, Z., and Goodman, M.B. (2007). Gain-of-function mutations in the MEC-4 DEG/ENaC sensory mechanotransduction channel alter gating and drug blockade. J. Gen. Physiol. *129*, 161–173.

Brown, A.L., Liao, Z., and Goodman, M.B. (2008). MEC-2 and MEC-6 in the Caenorhabditis elegans sensory mechanotransduction complex: auxiliary subunits that enable channel activity. J. Gen. Physiol. *131*, 605–616.

Brown, M.C., Engberg, I., and Matthews, P.B. (1967). The relative sensitivity to vibration of muscle receptors of the cat. J. Physiol. (Lond.) *192*, 773–800.

Burgess, P.R., and Perl, E.R. (1967). Myelinated afferent fibres responding specifically to noxious stimulation of the skin. J. Physiol. (Lond.) *190*, 541–562.

Cain, S.M., and Snutch, T.P. (2010). Contributions of T-type calcium channel isoforms to neuronal firing. Channels (Austin) *4*, 475–482.

Campeau, P., Chapdelaine, P., Seigneurin-Venin, S., Massie, B., and Tremblay, J.P. (2001). Transfection of large plasmids in primary human myoblasts. Gene Ther. *8*, 1387–1394.

Carbone, E., and Lux, H.D. (1984). A low voltage-activated, fully inactivating Ca channel in vertebrate sensory neurones. Nature *310*, 501–502.

Carroll, P., Lewin, G.R., Koltzenburg, M., Toyka, K.V., and Thoenen, H. (1998). A role for BDNF in mechanosensation. Nat. Neurosci. *1*, 42–46.

Caspary, T., and Anderson, K.V. (2003). Patterning cell types in the dorsal spinal cord: what the mouse mutants say. Nature Reviews Neuroscience *4*, 289–297.

Chalfie, M. (2009). Neurosensory mechanotransduction. Nat. Rev. Mol. Cell Biol. *10*, 44–52.

Chalfie, M., and Sulston, J. (1981). Developmental genetics of the mechanosensory neurons of Caenorhabditis elegans. Dev. Biol. *82*, 358–370.

Chalfie, M., Sulston, J.E., White, J.G., Southgate, E., Thomson, J.N., and Brenner, S. (1985). The neural circuit for touch sensitivity in Caenorhabditis elegans. J. Neurosci. *5*, 956–964.

Chelur, D.S., Ernstrom, G.G., Goodman, M.B., Yao, C.A., Chen, L., O' Hagan, R., and Chalfie, M. (2002). The mechanosensory protein MEC-6 is a subunit of the C. elegans touch-cell degenerin channel. Nature *420*, 669–673.

Chemin, J., Monteil, A., Perez-Reyes, E., Bourinet, E., Nargeot, J., and Lory, P. (2002). Specific contribution of human T-type calcium channel isotypes (alpha(1G), alpha(1H) and alpha(1I)) to neuronal excitability. J. Physiol. (Lond.) *540*, 3–14.

Chen, C.-C., Shen, J.-W., Chung, N.-C., Min, M.-Y., Cheng, S.-J., and Liu, I.Y. (2012a). Retrieval of context-associated memory is dependent on the Ca(v)3.2 T-type calcium channel. PLoS ONE *7*, e29384.

Chen, C.-C., Shen, J.-W., Chung, N.-C., Min, M.-Y., Cheng, S.-J., and Liu, I.Y. (2012b). Retrieval of context-associated memory is dependent on the Ca(v)3.2 T-type calcium channel. PLoS ONE *7*, e29384.

Chen, C.-L., Broom, D.C., Liu, Y., de Nooij, J.C., Li, Z., Cen, C., Samad, O.A., Jessell, T.M., Woolf, C.J., and Ma, Q. (2006). Runx1 determines nociceptive sensory neuron phenotype and is required for thermal and neuropathic pain. Neuron *49*, 365–377.

Chen, J.H., Wen, L., Dupuis, S., Wu, J.Y., and Rao, Y. (2001). The N-terminal leucine-rich regions in Slit are sufficient to repel olfactory bulb axons and subventricular zone neurons. J. Neurosci. *21*, 1548–1556.

Chen, W.-K., Liu, I.Y., Chang, Y.-T., Chen, Y.-C., Chen, C.-C., Yen, C.-T., Shin, H.-S., and Chen, C.-C. (2010). Ca(v)3.2 T-type Ca2+ channel-dependent activation of ERK in paraventricular thalamus modulates acid-induced chronic muscle pain. J. Neurosci. *30*, 10360–10368.

Chen, Y., Lu, J., Pan, H., Zhang, Y., Wu, H., Xu, K., Liu, X., Jiang, Y., Bao, X., Yao, Z., et al. (2003). Association between genetic variation of CACNA1H and childhood absence epilepsy. Ann. Neurol. *54*, 239–243.

Cheng, L., Samad, O.A., Xu, Y., Mizuguchi, R., Luo, P., Shirasawa, S., Goulding, M., and Ma, Q. (2005). Lbx1 and Tlx3 are opposing switches in determining GABAergic versus glutamatergic transmitter phenotypes. Nat. Neurosci. *8*, 1510–1515.

Cheng, L.E., Song, W., Looger, L.L., Jan, L.Y., and Jan, Y.N. (2010). The role of the TRP channel NompC in Drosophila larval and adult locomotion. Neuron *67*, 373–380.

Chiang, L.-Y., Poole, K., Oliveira, B.E., Duarte, N., Sierra, Y.A.B., Bruckner-Tuderman, L., Koch, M., Hu, J., and Lewin, G.R. (2011). Laminin-332 coordinates mechanotransduction and growth cone bifurcation in sensory neurons. Nature Neuroscience *14*, 993–1000.

Chiba, C.M., and Rankin, C.H. (1990). A developmental analysis of spontaneous and reflexive reversals in the nematode Caenorhabditis elegans. J. Neurobiol. *21*, 543–554.

Choi, S., Na, H.S., Kim, J., Lee, J., Lee, S., Kim, D., Park, J., Chen, C.-C., Campbell, K.P., and Shin, H.-S. (2006). Attenuated pain responses in mice lacking CaV3.2 T‑type channels. Genes, Brain and Behavior *6*, 425–431.

Chung, Y.D., Zhu, J., Han, Y., and Kernan, M.J. (2001). nompA encodes a PNS-specific, ZP domain protein required to connect mechanosensory dendrites to sensory structures. Neuron *29*, 415–428.

Collins, C., Guilluy, C., Welch, C., O'Brien, E.T., Hahn, K., Superfine, R., Burridge, K., and Tzima, E. (2012). Localized tensional forces on PECAM-1 elicit a global mechanotransduction response via the integrin-RhoA pathway. Curr. Biol. *22*, 2087–2094.

Corey, D.P., and Hudspeth, A.J. (1983). Analysis of the microphonic potential of the bullfrog's sacculus. J. Neurosci. *3*, 942–961.

Corfas, G., and Dudai, Y. (1990). Adaptation and fatigue of a mechanosensory neuron in wild-type Drosophila and in memory mutants. J. Neurosci. *10*, 491–499.

Coste, B., Mathur, J., Schmidt, M., Earley, T.J., Ranade, S., Petrus, M.J., Dubin, A.E., and Patapoutian, A. (2010). Piezo1 and Piezo2 are essential components of distinct mechanically activated cation channels. Science *330*, 55–60.

Coste, B., Xiao, B., Santos, J.S., Syeda, R., Grandl, J., Spencer, K.S., Kim, S.E., Schmidt, M., Mathur, J., Dubin, A.E., et al. (2012). Piezo proteins are pore-forming subunits of mechanically activated channels. Nature *483*, 176–181.

Craig, P.J., Beattie, R.E., Folly, E.A., Reeves, M.B., Priestley, J.V., Carney, S.L., Sher, E., Perez-Reyes, E., and Volsen, S.G. (1999). Distribution of the voltage-dependent calcium channel α1G subunit mRNA and protein throughout the mature rat brain. European Journal of Neuroscience *11*, 2949–2964.

Crandall, S.R., Govindaiah, G., and Cox, C.L. (2010). Low-threshold Ca2+ current amplifies distal dendritic signaling in thalamic reticular neurons. J. Neurosci. *30*, 15419–15429.

Crawford, A.C., Evans, M.G., and Fettiplace, R. (1989). Activation and adaptation of transducer currents in turtle hair cells. J. Physiol. (Lond.) *419*, 405–434.

Cribbs, L.L., Lee, J.H., Yang, J., Satin, J., Zhang, Y., Daud, A., Barclay, J., Williamson, M.P., Fox, M., Rees, M., et al. (1998). Cloning and characterization of alpha1H from human heart, a member of the T-type Ca2+ channel gene family. Circ. Res. *83*, 103–109.

Cribbs, L.L., Gomora, J.C., Daud, A.N., Lee, J.-H., and Perez-Reyes, E. (2000). Molecular cloning and functional expression of Cav3.1c, a T-type calcium channel from human brain. FEBS Letters *466*, 54–58.

Crunelli, V., Tóth, T.I., Cope, D.W., Blethyn, K., and Hughes, S.W. (2005). The "window" T-type calcium current in brain dynamics of different behavioural states. J. Physiol. (Lond.) *562*, 121–129.

Cui, X., Zhang, X., Guan, X., Li, H., Li, X., Lu, H., and Cheng, M. (2012). Shear stress augments the endothelial cell differentiation marker expression in late EPCs by upregulating integrins. Biochem. Biophys. Res. Commun. *425*, 419–425.

Deisseroth, K. (2011). Optogenetics. Nature Methods *8*, 26–29.

Djouhri, L., and Lawson, S.N. (2004). Abeta-fiber nociceptive primary afferent neurons: a review of incidence and properties in relation to other afferent A-fiber neurons in mammals. Brain Res. Brain Res. Rev. *46*, 131–145.

Djouhri, L., Bleazard, L., and Lawson, S.N. (1998). Association of somatic action potential shape with sensory receptive properties in guinea-pig dorsal root ganglion neurones. J Physiol *513*, 857–872.

Drew, L.J., Rohrer, D.K., Price, M.P., Blaver, K.E., Cockayne, D.A., Cesare, P., and Wood, J.N. (2004). Acid-sensing ion channels ASIC2 and ASIC3 do not contribute to mechanically activated currents in mammalian sensory neurones. J. Physiol. (Lond.) *556*, 691–710.

Driscoll, M., and Chalfie, M. (1991). The mec-4 gene is a member of a family of Caenorhabditis elegans genes that can mutate to induce neuronal degeneration. Nature *349*, 588–593.

Du, H., Gu, G., William, C.M., and Chalfie, M. (1996). Extracellular proteins needed for C. elegans mechanosensation. Neuron *16*, 183–194.

Dubreuil, A.-S., Boukhaddaoui, H., Desmadryl, G., Martinez-Salgado, C., Moshourab, R., Lewin, G.R., Carroll, P., Valmier, J., and Scamps, F. (2004). Role of T-Type Calcium Current in Identified D-Hair Mechanoreceptor Neurons Studied In Vitro. J. Neurosci. *24*, 8480–8484.

Duggan, A., Garcia-Anoveros, J., and Corey, D.P. (2002). The PDZ domain protein PICK1 and the sodium channel BNaC1 interact and localize at mechanosensory terminals of dorsal root ganglion neurons and dendrites of central neurons. J. Biol. Chem. *277*, 5203–5208.

Edgar, D., Timpl, R., and Thoenen, H. (1988). Structural requirements for the stimulation of neurite outgrowth by two variants of laminin and their inhibition by antibodies. J. Cell Biol. *106*, 1299–1306.

Egger, V., Svoboda, K., and Mainen, Z.F. (2003). Mechanisms of lateral inhibition in the olfactory bulb: efficiency and modulation of spike-evoked calcium influx into granule cells. J. Neurosci. *23*, 7551–7558.

Egger, V., Svoboda, K., and Mainen, Z.F. (2005). Dendrodendritic Synaptic Signals in Olfactory Bulb Granule Cells: Local Spine Boost and Global Low-Threshold Spike. J. Neurosci. *25*, 3521–3530.

Ellinor, P.T., Zhang, J.F., Randall, A.D., Zhou, M., Schwarz, T.L., Tsien, R.W., and Horne, W.A. (1993). Functional expression of a rapidly inactivating neuronal calcium channel. Nature *363*, 455–458.

Emtage, L., Gu, G., Hartwieg, E., and Chalfie, M. (2004). Extracellular proteins organize the mechanosensory channel complex in C. elegans touch receptor neurons. Neuron *44*, 795–807.

Ernfors, P., Merlio, J.-P., and Persson, H. (1992). Cells Expressing mRNA for Neurotrophins and their Receptors During Embryonic Rat Development. Eur. J. Neurosci. *4*, 1140–1158.

Ernfors, P., Lee, K.F., Kucera, J., and Jaenisch, R. (1994a). Lack of neurotrophin-3 leads to deficiencies in the peripheral nervous system and loss of limb proprioceptive afferents. Cell *77*, 503–512.

Ernfors, P., Lee, K.F., Kucera, J., and Jaenisch, R. (1994b). Lack of neurotrophin-3 leads to deficiencies in the peripheral nervous system and loss of limb proprioceptive afferents. Cell *77*, 503–512.

Ertel, E.A., Campbell, K.P., Harpold, M.M., Hofmann, F., Mori, Y., Perez-Reyes, E., Schwartz, A., Snutch, T.P., Tanabe, T., Birnbaumer, L., et al. (2000). Nomenclature of voltage-gated calcium channels. Neuron *25*, 533–535.

Essalmani, R., Hamelin, J., Marcinkiewicz, J., Chamberland, A., Mbikay, M., Chrétien, M., Seidah, N.G., and Prat, A. (2006). Deletion of the gene encoding proprotein convertase 5/6 causes early embryonic lethality in the mouse. Mol. Cell. Biol. *26*, 354–361.

Fallon, J.B., and Macefield, V.G. (2007). Vibration sensitivity of human muscle spindles and Golgi tendon organs. Muscle Nerve *36*, 21–29.

Feil, R., Wagner, J., Metzger, D., and Chambon, P. (1997). Regulation of Cre recombinase activity by mutated estrogen receptor ligand-binding domains. Biochem. Biophys. Res. Commun. *237*, 752–757.

Feng, K., Zhou, X.-H., Oohashi, T., Mörgelin, M., Lustig, A., Hirakawa, S., Ninomiya, Y., Engel, J., Rauch, U., and Fässler, R. (2002). All four members of the Ten-m/Odz family of transmembrane proteins form dimers. J. Biol. Chem. *277*, 26128–26135.

Fettiplace, R., and Hackney, C.M. (2006). The sensory and motor roles of auditory hair cells. Nature Reviews Neuroscience *7*, 19–29.

Fox, A.P., Nowycky, M.C., and Tsien, R.W. (1987). Kinetic and pharmacological properties distinguishing three types of calcium currents in chick sensory neurones. J. Physiol. (Lond.) *394*, 149–172.

Frank, E., and Sanes, J.R. (1991). Lineage of neurons and glia in chick dorsal root ganglia: analysis in vivo with a recombinant retrovirus. Development *111*, 895–908.

Fukushige, T., Siddiqui, Z.K., Chou, M., Culotti, J.G., Gogonea, C.B., Siddiqui, S.S., and Hamelin, M. (1999). MEC-12, an alpha-tubulin required for touch sensitivity in C. elegans. J. Cell. Sci. *112 (Pt 3)*, 395–403.

Fulton, J.F., and Pi-Suñer, J. (1928). A Note Concerning the Probable Function of Various Afferent End-Organs in Skeletal Muscle. Am J Physiol *83*, 554–562.

García, J.A., Yee, A.G., Gillespie, P.G., and Corey, D.P. (1998). Localization of myosin-Ibeta near both ends of tip links in frog saccular hair cells. J. Neurosci. *18*, 8637–8647.

García-Añoveros, J., Samad, T.A., Zuvela-Jelaska, L., Woolf, C.J., and Corey, D.P. (2001). Transport and localization of the DEG/ENaC ion channel BNaC1alpha to peripheral mechanosensory terminals of dorsal root ganglia neurons. J. Neurosci. *21*, 2678–2686.

Gautam, S.H., Otsuguro, K.-I., Ito, S., Saito, T., and Habara, Y. (2007). T-type Ca2+ channels mediate propagation of odor-induced Ca2+ transients in rat olfactory receptor neurons. Neuroscience *144*, 702–713.

Gilbert, P.E., Kesner, R.P., and Lee, I. (2001). Dissociating hippocampal subregions: double dissociation between dentate gyrus and CA1. Hippocampus *11*, 626–636.

Gillespie, P.G., and Cyr, J.L. (2004). Myosin-1c, the hair cell's adaptation motor. Annu. Rev. Physiol. *66*, 521–545.

Gomes, A.F., and Gozzo, F.C. (2010). Chemical cross-linking with a diazirine photoactivatable cross-linker investigated by MALDI- and ESI-MS/MS. J Mass Spectrom *45*, 892–899.

Gong, Z., Son, W., Chung, Y.D., Kim, J., Shin, D.W., McClung, C.A., Lee, Y., Lee, H.W., Chang, D.-J., Kaang, B.-K., et al. (2004). Two interdependent TRPV channel subunits, inactive and Nanchung, mediate hearing in Drosophila. J. Neurosci. *24*, 9059–9066.

González-Martınez, T., Germanà, G.P., Monjil, D.F., Silos-Santiago, I., de Carlos, F., Germanà, G., Cobo, J., and Vega, J.A. (2004). Absence of Meissner corpuscles in the digital pads of mice lacking functional TrkB. Brain Research *1002*, 120–128.

Goodman, M.B., Ernstrom, G.G., Chelur, D.S., O'Hagan, R., Yao, C.A., and Chalfie, M. (2002). MEC-2 regulates C. elegans DEG/ENaC channels needed for mechanosensation. Nature *415*, 1039–1042.

Gottmann, K., and Lux, H.D. (1990). Low- and high-voltage-activated Ca2+ conductances in electrically excitable growth cones of chick dorsal root ganglion neurons. Neurosci. Lett. *110*, 34–39.

Gottmann, K., Rohrer, H., and Lux, H.D. (1991). Distribution of Ca2+ and Na+ conductances during neuronal differentiation of chick DRG precursor cells. J. Neurosci. *11*, 3371–3378.

Gradinaru, V., Zhang, F., Ramakrishnan, C., Mattis, J., Prakash, R., Diester, I., Goshen, I., Thompson, K.R., and Deisseroth, K. (2010). Molecular and cellular approaches for diversifying and extending optogenetics. Cell *141*, 154–165.

Grillet, N., Xiong, W., Reynolds, A., Kazmierczak, P., Sato, T., Lillo, C., Dumont, R.A., Hintermann, E., Sczaniecka, A., Schwander, M., et al. (2009). Harmonin mutations cause mechanotransduction defects in cochlear hair cells. Neuron *62*, 375–387.

Harper, A.A., and Lawson, S.N. (1985). Conduction velocity is related to morphological cell type in rat dorsal root ganglion neurones. J Physiol *359*, 31–46.

Hasegawa, H., and Wang, F. (2008). Visualizing mechanosensory endings of TrkC-expressing neurons in HS3ST-2-hPLAP mice. The Journal of Comparative Neurology *511*, 543–556.

Hasko, J.A., and Richardson, G.P. (1988). The ultrastructural organization and properties of the mouse tectorial membrane matrix. Hear. Res. *35*, 21–38.

Healy, S.D., de Kort, S.R., and Clayton, N.S. (2005). The hippocampus, spatial memory and food hoarding: a puzzle revisited. Trends Ecol. Evol. (Amst.) *20*, 17–22.

Herman, R.K. (1996). Touch sensation in Caenorhabditis elegans. Bioessays *18*, 199–206.

Heron, S.E., Phillips, H.A., Mulley, J.C., Mazarib, A., Neufeld, M.Y., Berkovic, S.F., and Scheffer, I.E. (2004a). Genetic variation of CACNA1H in idiopathic generalized epilepsy. Annals of Neurology *55*, 595–596.

Heron, S.E., Phillips, H.A., Mulley, J.C., Mazarib, A., Neufeld, M.Y., Berkovic, S.F., and Scheffer, I.E. (2004b). Genetic variation of CACNA1H in idiopathic generalized epilepsy. Ann. Neurol. *55*, 595–596.

Hess, P., Lansman, J.B., and Tsien, R.W. (1984). Different modes of Ca channel gating behaviour favoured by dihydropyridine Ca agonists and antagonists. , Published Online: 11 October 1984; | Doi:10.1038/311538a0 *311*, 538–544.

Hildebrand, M.E., Isope, P., Miyazaki, T., Nakaya, T., Garcia, E., Feltz, A., Schneider, T., Hescheler, J., Kano, M., Sakimura, K., et al. (2009). Functional coupling between mGluR1 and Cav3.1 T-type calcium channels contributes to parallel fiber-induced fast calcium signaling within Purkinje cell dendritic spines. J. Neurosci. *29*, 9668–9682.

Hippenmeyer, S., Vrieseling, E., Sigrist, M., Portmann, T., Laengle, C., Ladle, D.R., and Arber, S. (2005). A Developmental Switch in the Response of DRG Neurons to ETS Transcription Factor Signaling. PLoS Biol *3*.

Hjerling-Leffler, J., Marmigère, F., Heglind, M., Cederberg, A., Koltzenburg, M., Enerbäck, S., and Ernfors, P. (2005). The boundary cap: a source of neural crest stem cells that generate multiple sensory neuron subtypes. Development *132*, 2623–2632.

Horch, K.W., Tuckett, R.P., and Burgess, P.R. (1977). A Key to the Classification of Cutaneous Mechanoreceptors. Journal of Investigative Dermatology *69*, 75–82.

Howell, D.M., Morgan, W.J., Jarjour, A.A., Spirou, G.A., Berrebi, A.S., Kennedy, T.E., and Mathers, P.H. (2007). Molecular guidance cues necessary for axon pathfinding from the ventral cochlear nucleus. J. Comp. Neurol. *504*, 533–549.

Hu, J., and Lewin, G.R. (2006). Mechanosensitive currents in the neurites of cultured mouse sensory neurones. J. Physiol. (Lond.) *577*, 815–828.

Hu, J., Chiang, L.-Y., Koch, M., and Lewin, G.R. (2010). Evidence for a protein tether involved in somatic touch. EMBO J. *29*, 855–867.

Huang, M., and Chalfie, M. (1994). Gene interactions affecting mechanosensory transduction in Caenorhabditis elegans. Nature *367*, 467–470.

Huang, M., Gu, G., Ferguson, E.L., and Chalfie, M. (1995). A stomatin-like protein necessary for mechanosensation in C. elegans. Nature *378*, 292–295.

Huber, T.B., Schermer, B., Müller, R.U., Höhne, M., Bartram, M., Calixto, A., Hagmann, H., Reinhardt, C., Koos, F., Kunzelmann, K., et al. (2006). Podocin and MEC-2 bind cholesterol to regulate the activity of associated ion channels. Proc. Natl. Acad. Sci. U.S.A. *103*, 17079–17086.

Hwang, R.Y., Stearns, N.A., and Tracey, W.D. (2012). The ankyrin repeat domain of the TRPA protein painless is important for thermal nociception but not mechanical nociception. PLoS ONE *7*, e30090.

Ichikawa, H., Matsuo, S., Silos-Santiago, I., and Sugimoto, T. (2000). Developmental dependency of Meissner corpuscles on trkB but not trkA or trkC. Neuroreport *11*, 259–262.

Iftinca, M.C. (2011). Neuronal T-type calcium channels: what's new? Iftinca: T-type channel regulation. J Med Life *4*, 126–138.

Iggo, A., and Andres, K.H. (1982). Morphology of cutaneous receptors. Annu. Rev. Neurosci. *5*, 1–31.

Iggo, A., and Muir, A.R. (1969). The structure and function of a slowly adapting touch corpuscle in hairy skin. J Physiol *200*, 763–796.4.

Ikeda, H., Heinke, B., Ruscheweyh, R., and Sandkühler, J. (2003). Synaptic plasticity in spinal lamina I projection neurons that mediate hyperalgesia. Science *299*, 1237–1240.

Inoue, K., Ozaki, S., Shiga, T., Ito, K., Masuda, T., Okado, N., Iseda, T., Kawaguchi, S., Ogawa, M., Bae, S.-C., et al. (2002). Runx3 controls the axonal projection of proprioceptive dorsal root ganglion neurons. Nat. Neurosci. *5*, 946–954.

Isope, P., and Murphy, T.H. (2005). Low threshold calcium currents in rat cerebellar Purkinje cell dendritic spines are mediated by T-type calcium channels. J. Physiol. (Lond.) *562*, 257–269.

Jadeja, S., Smyth, I., Pitera, J.E., Taylor, M.S., van Haelst, M., Bentley, E., McGregor, L., Hopkins, J., Chalepakis, G., Philip, N., et al. (2005). Identification of a new gene mutated in Fraser syndrome and mouse myelencephalic blebs. Nat. Genet. *37*, 520–525.

Jarman, A.P. (2002). Studies of mechanosensation using the fly. Hum. Mol. Genet. *11*, 1215–1218.

Javier, R.T. (2008). Cell polarity proteins: common targets for tumorigenic human viruses. Oncogene *27*, 7031–7046.

Johnson, D., Jürgens, R., and Kornhuber, H.H. (1980). Somatosensory-evoked potentials and perception of skin velocity. Arch Psychiatr Nervenkr *228*, 95–100.

Johnson, K.O., Yoshioka, T., and Vega-Bermudez, F. (2000). Tactile functions of mechanoreceptive afferents innervating the hand. J Clin Neurophysiol *17*, 539–558.

Joksovic, P.M., Nelson, M.T., Jevtovic-Todorovic, V., Patel, M.K., Perez-Reyes, E., Campbell, K.P., Chen, C.-C., and Todorovic, S.M. (2006). CaV3.2 is the major molecular substrate for redox regulation of T-type Ca2+ channels in the rat and mouse thalamus. J. Physiol. (Lond.) *574*, 415–430.

Kalus, I., Schnegelsberg, B., Seidah, N.G., Kleene, R., and Schachner, M. (2003). The proprotein convertase PC5A and a metalloprotease are involved in the proteolytic processing of the neural adhesion molecule L1. J. Biol. Chem. *278*, 10381–10388.

Kaneda, M., Wakamori, M., Ito, C., and Akaike, N. (1990). Low-threshold calcium current in isolated Purkinje cell bodies of rat cerebellum. J. Neurophysiol. *63*, 1046–1051.

Kaplan, J.M., and Horvitz, H.R. (1993). A dual mechanosensory and chemosensory neuron in Caenorhabditis elegans. Proc. Natl. Acad. Sci. U.S.A. *90*, 2227–2231.

Karra, D., and Dahm, R. (2010). Transfection Techniques for Neuronal Cells. J. Neurosci. *30*, 6171–6177.

Kase, M., Kakimoto, S., Sakuma, S., Houtani, T., Ohishi, H., Ueyama, T., and Sugimoto, T. (1999). Distribution of neurons expressing alpha 1G subunit mRNA of T-type voltage-dependent calcium channel in adult rat central nervous system. Neurosci. Lett. *268*, 77–80.

Kawai, F., and Miyachi, E. (2001). Enhancement by T-type Ca2+ currents of odor sensitivity in olfactory receptor cells. J. Neurosci. *21*, RC144.

Kazmierczak, P., Sakaguchi, H., Tokita, J., Wilson-Kubalek, E.M., Milligan, R.A., Müller, U., and Kachar, B. (2007). Cadherin 23 and protocadherin 15 interact to form tip-link filaments in sensory hair cells. Nature *449*, 87–91.

Kenzelmann-Broz, D., Tucker, R.P., Leachman, N.T., and Chiquet-Ehrismann, R. (2010). The expression of teneurin-4 in the avian embryo: potential roles in patterning of the limb and nervous system. Int. J. Dev. Biol. *54*, 1509–1516.

Kernan, M.J. (2007). Mechanotransduction and auditory transduction in Drosophila. Pflugers Arch. *454*, 703–720.

Kernan, M., Cowan, D., and Zuker, C. (1994). Genetic dissection of mechanosensory transduction: mechanoreception-defective mutations of Drosophila. Neuron *12*, 1195–1206.

Khosravani, H., Bladen, C., Parker, D.B., Snutch, T.P., McRory, J.E., and Zamponi, G.W. (2005). Effects of Cav3.2 channel mutations linked to idiopathic generalized epilepsy. Ann. Neurol. *57*, 745–749.

Kim, D., Song, I., Keum, S., Lee, T., Jeong, M.J., Kim, S.S., McEnery, M.W., and Shin, H.S. (2001). Lack of the burst firing of thalamocortical relay neurons and resistance to absence seizures in mice lacking alpha(1G) T-type Ca(2+) channels. Neuron *31*, 35–45.

Kim, J., Chung, Y.D., Park, D.-Y., Choi, S., Shin, D.W., Soh, H., Lee, H.W., Son, W., Yim, J., Park, C.-S., et al. (2003). A TRPV family ion channel required for hearing in Drosophila. Nature *424*, 81–84.

Kim, S.E., Coste, B., Chadha, A., Cook, B., and Patapoutian, A. (2012). The role of Drosophila Piezo in mechanical nociception. Nature *483*, 209–212.

Kiyozumi, D., Sugimoto, N., and Sekiguchi, K. (2006). Breakdown of the reciprocal stabilization of QBRICK/Frem1, Fras1, and Frem2 at the basement membrane provokes Fraser syndrome-like defects. Proc. Natl. Acad. Sci. U.S.A. *103*, 11981–11986.

Kleifeld, O., Doucet, A., Keller, U. auf dem, Prudova, A., Schilling, O., Kainthan, R.K., Starr, A.E., Foster, L.J., Kizhakkedathu, J.N., and Overall, C.M. (2010). Isotopic labeling of terminal amines in complex samples identifies protein N-termini and protease cleavage products. Nature Biotechnology *28*, 281–288.

Klein, R., Silos-Santiago, I., Smeyne, R.J., Lira, S.A., Brambilla, R., Bryant, S., Zhang, L., Snider, W.D., and Barbacid, M. (1994). Disruption of the neurotrophin-3 receptor gene trkC eliminates la muscle afferents and results in abnormal movements. Nature *368*, 249–251.

Koltzenburg, M., Stucky, C.L., and Lewin, G.R. (1997a). Receptive properties of mouse sensory neurons innervating hairy skin. J. Neurophysiol. *78*, 1841–1850.

Koltzenburg, M., Stucky, C.L., and Lewin, G.R. (1997b). Receptive properties of mouse sensory neurons innervating hairy skin. J. Neurophysiol. *78*, 1841–1850.

Kramer, I., Sigrist, M., de Nooij, J.C., Taniuchi, I., Jessell, T.M., and Arber, S. (2006). A Role for Runx Transcription Factor Signaling in Dorsal Root Ganglion Sensory Neuron Diversification. Neuron *49*, 379–393.

Kros, C.J., Marcotti, W., van Netten, S.M., Self, T.J., Libby, R.T., Brown, S.D.M., Richardson, G.P., and Steel, K.P. (2002). Reduced climbing and increased slipping adaptation in cochlear hair cells of mice with Myo7a mutations. Nat. Neurosci. *5*, 41–47.

Ku, W., and Schneider, S.P. (2011). Multiple T-type Ca2+ current subtypes in electrophysiologically characterized hamster dorsal horn neurons: possible role in spinal sensory integration. J. Neurophysiol. *106*, 2486–2498.

Lallemend, F., and Ernfors, P. (2012). Molecular interactions underlying the specification of sensory neurons. Trends in Neurosciences *35*, 373–381.

Lamb, G.D. (1983). Tactile discrimination of textured surfaces: psychophysical performance measurements in humans. J. Physiol. (Lond.) *338*, 551–565.

Lambert, R.C., McKenna, F., Maulet, Y., Talley, E.M., Bayliss, D.A., Cribbs, L.L., Lee, J.H., Perez-Reyes, E., and Feltz, A. (1998). Low-voltage-activated Ca2+ currents are generated by members of the CavT subunit family (alpha1G/H) in rat primary sensory neurons. J. Neurosci. *18*, 8605–8613.

Lapatsina, L., Brand, J., Poole, K., Daumke, O., and Lewin, G.R. (2012). Stomatin-domain proteins. Eur. J. Cell Biol. *91*, 240–245.

Lawson, S.N. (2002). Phenotype and function of somatic primary afferent nociceptive neurones with C-, Adelta- or Aalpha/beta-fibres. Exp. Physiol. *87*, 239–244.

Lechner, S.G., and Siemens, J. (2011). Sensory transduction, the gateway to perception: mechanisms and pathology. EMBO Rep *12*, 292–295.

Lechner, S.G., Frenzel, H., Wang, R., and Lewin, G.R. (2009). Developmental waves of mechanosensitivity acquisition in sensory neuron subtypes during embryonic development. EMBO J. *28*, 1479–1491.

Lechner, S.G., Markworth, S., Poole, K., Smith, E.S.J., Lapatsina, L., Frahm, S., May, M., Pischke, S., Suzuki, M., Ibañez-Tallon, I., et al. (2011). The molecular and cellular identity of peripheral osmoreceptors. Neuron *69*, 332–344.

Lee, I., and Solivan, F. (2010). Dentate gyrus is necessary for disambiguating similar object-place representations. Learn. Mem. *17*, 252–258.

Lee, E.C., Yu, D., Martinez de Velasco, J., Tessarollo, L., Swing, D.A., Court, D.L., Jenkins, N.A., and Copeland, N.G. (2001). A highly efficient Escherichia coli-based chromosome engineering system adapted for recombinogenic targeting and subcloning of BAC DNA. Genomics *73*, 56–65.

Lee, J., Moon, S., Cha, Y., and Chung, Y.D. (2010). Drosophila TRPN(=NOMPC) channel localizes to the distal end of mechanosensory cilia. PLoS ONE *5*, e11012.

Lee, J.-H., Daud, A.N., Cribbs, L.L., Lacerda, A.E., Pereverzev, A., Klöckner, U., Schneider, T., and Perez-Reyes, E. (1999). Cloning and Expression of a Novel Member of the Low Voltage-Activated T-Type Calcium Channel Family. J. Neurosci. *19*, 1912–1921.

Leem, J.W., Willis, W.D., and Chung, J.M. (1993). Cutaneous sensory receptors in the rat foot. J. Neurophysiol. *69*, 1684–1699.

Lehmann, M., Rigot, V., Seidah, N.G., Marvaldi, J., and Lissitzky, J.C. (1996). Lack of integrin alpha-chain endoproteolytic cleavage in furin-deficient human colon adenocarcinoma cells LoVo. Biochem. J. *317 (Pt 3)*, 803–809.

Levanon, D., Brenner, O., Negreanu, V., Bettoun, D., Woolf, E., Eilam, R., Lotem, J., Gat, U., Otto, F., Speck, N., et al. (2001). Spatial and temporal expression pattern of Runx3 (Aml2) and Runx1 (Aml1) indicates non-redundant functions during mouse embryogenesis. Mech. Dev. *109*, 413–417.

Levanon, D., Bettoun, D., Harris-Cerruti, C., Woolf, E., Negreanu, V., Eilam, R., Bernstein, Y., Goldenberg, D., Xiao, C., Fliegauf, M., et al. (2002). The Runx3 transcription factor regulates development and survival of TrkC dorsal root ganglia neurons. EMBO J. *21*, 3454–3463.

Levine, A., Bashan-Ahrend, A., Budai-Hadrian, O., Gartenberg, D., Menasherow, S., and Wides, R. (1994). Odd Oz: a novel Drosophila pair rule gene. Cell *77*, 587–598.

Li, L., Rutlin, M., Abraira, V.E., Cassidy, C., Kus, L., Gong, S., Jankowski, M.P., Luo, W., Heintz, N., Koerber, H.R., et al. (2011a). The Functional Organization of Cutaneous Low-Threshold Mechanosensory Neurons. Cell *147*, 1615–1627.

Li, W., Kang, L., Piggott, B.J., Feng, Z., and Xu, X.Z.S. (2011b). The neural circuits and sensory channels mediating harsh touch sensation in Caenorhabditis elegans. Nat Commun *2*, 315.

Liao, Y.-F., Tsai, M.-L., Chen, C.-C., and Yen, C.-T. (2011). Involvement of the Cav3.2 T-type calcium channel in thalamic neuron discharge patterns. Mol Pain *7*, 43.

Liberman, M.C. (1982). The cochlear frequency map for the cat: labeling auditory-nerve fibers of known characteristic frequency. J. Acoust. Soc. Am. *72*, 1441–1449.

Liebl, D.J., Tessarollo, L., Palko, M.E., and Parada, L.F. (1997). Absence of sensory neurons before target innervation in brain-derived neurotrophic factor-, neurotrophin 3-, and TrkC-deficient embryonic mice. J. Neurosci. *17*, 9113–9121.

Liedtke, W., and Friedman, J.M. (2003). Abnormal osmotic regulation in trpv4-/- mice. Proc. Natl. Acad. Sci. U.S.A. *100*, 13698–13703.

Lim, D.J. (1980). Cochlear anatomy related to cochlear micromechanics. A review. J. Acoust. Soc. Am. *67*, 1686–1695.

Liu, Y., and Ma, Q. (2011). Generation of somatic sensory neuron diversity and implications on sensory coding. Current Opinion in Neurobiology *21*, 52–60.

Liu, P., Jenkins, N.A., and Copeland, N.G. (2003). A highly efficient recombineering-based method for generating conditional knockout mutations. Genome Res. *13*, 476–484.

Liu, Q., Tang, Z., Surdenikova, L., Kim, S., Patel, K.N., Kim, A., Ru, F., Guan, Y., Weng, H.-J., Geng, Y., et al. (2009). Sensory neuron-specific GPCR Mrgprs are itch receptors mediating chloroquine-induced pruritus. Cell *139*, 1353–1365.

Liu, Y., Yang, F.-C., Okuda, T., Dong, X., Zylka, M.J., Chen, C.-L., Anderson, D.J., Kuner, R., and Ma, Q. (2008). Mechanisms of compartmentalized expression of Mrg class G-protein-coupled sensory receptors. J. Neurosci. *28*, 125–132.

Llères, D., Weibel, J.-M., Heissler, D., Zuber, G., Duportail, G., and Mély, Y. (2004). Dependence of the cellular internalization and transfection efficiency on the structure and physicochemical properties of cationic detergent/DNA/liposomes. J Gene Med *6*, 415–428.

Llinás, R.R. (1988). The intrinsic electrophysiological properties of mammalian neurons: insights into central nervous system function. Science *242*, 1654–1664.

Llinás, R., and Sugimori, M. (1980). Electrophysiological properties of in vitro Purkinje cell dendrites in mammalian cerebellar slices. J. Physiol. (Lond.) *305*, 197–213.

Llinás, R., and Yarom, Y. (1981). Electrophysiology of mammalian inferior olivary neurones in vitro. Different types of voltage-dependent ionic conductances. J. Physiol. (Lond.) *315*, 549–567.

Llinás, R., and Yarom, Y. (1986). Oscillatory properties of guinea-pig inferior olivary neurones and their pharmacological modulation: an in vitro study. J Physiol *376*, 163–182.

Llinás, R.R., and Steriade, M. (2006). Bursting of thalamic neurons and states of vigilance. J. Neurophysiol. *95*, 3297–3308.

Löken, L.S., Wessberg, J., Morrison, I., McGlone, F., and Olausson, H. (2009). Coding of pleasant touch by unmyelinated afferents in humans. Nature Neuroscience *12*, 547–548.

Lossie, A.C., Nakamura, H., Thomas, S.E., and Justice, M.J. (2005). Mutation of l7Rn3 shows that Odz4 is required for mouse gastrulation. Genetics *169*, 285–299.

Lu, Y., Ma, X., Sabharwal, R., Snitsarev, V., Morgan, D., Rahmouni, K., Drummond, H.A., Whiteis, C.A., Costa, V., Price, M., et al. (2009). The ion channel ASIC2 is required for baroreceptor and autonomic control of the circulation. Neuron *64*, 885–897.

Lumpkin, E.A., and Caterina, M.J. (2007). Mechanisms of sensory transduction in the skin. Nature *445*, 858–865.

Luo, W., Enomoto, H., Rice, F.L., Milbrandt, J., and Ginty, D.D. (2009a). Molecular identification of rapidly adapting mechanoreceptors and their developmental dependence on ret signaling. Neuron *64*, 841–856.

Luo, W., Enomoto, H., Rice, F.L., Milbrandt, J., and Ginty, D.D. (2009b). Molecular Identification of Rapidly Adapting Mechanoreceptors and Their Developmental Dependence on Ret Signaling. Neuron *64*, 841–856.

Ma, Q., Fode, C., Guillemot, F., and Anderson, D.J. (1999). Neurogenin1 and neurogenin2 control two distinct waves of neurogenesis in developing dorsal root ganglia. Genes Dev. *13*, 1717–1728.

Macefield, V.G., Häger-Ross, C., and Johansson, R.S. (1996). Control of grip force during restraint of an object held between finger and thumb: responses of cutaneous afferents from the digits. Exp Brain Res *108*, 155–171.

Marchesi, C., Essalmani, R., Lemarié, C.A., Leibovitz, E., Ebrahimian, T., Paradis, P., Seidah, N.G., Schiffrin, E.L., and Prat, A. (2011). Inactivation of endothelial proprotein convertase 5/6 decreases collagen deposition in the cardiovascular system: role of fibroblast autophagy. J. Mol. Med. *89*, 1103–1111.

Maricich, S.M., Wellnitz, S.A., Nelson, A.M., Lesniak, D.R., Gerling, G.J., Lumpkin, E.A., and Zoghbi, H.Y. (2009). Merkel cells are essential for light-touch responses. Science *324*, 1580–1582.

Marmigère, F., and Ernfors, P. (2007). Specification and connectivity of neuronal subtypes in the sensory lineage. Nat. Rev. Neurosci. *8*, 114–127.

Marmigère, F., Montelius, A., Wegner, M., Groner, Y., Reichardt, L.F., and Ernfors, P. (2006). The Runx1/AML1 transcription factor selectively regulates development and survival of TrkA nociceptive sensory neurons. Nat Neurosci *9*, 180–187.

Maro, G.S., Vermeren, M., Voiculescu, O., Melton, L., Cohen, J., Charnay, P., and Topilko, P. (2004). Neural crest boundary cap cells constitute a source of neuronal and glial cells of the PNS. Nat. Neurosci. *7*, 930–938.

McCormick, D.A., and Bal, T. (1997). SLEEP AND AROUSAL: Thalamocortical Mechanisms. Annual Review of Neuroscience *20*, 185–215.

McGlone, F., and Reilly, D. (2010). The cutaneous sensory system. Neurosci Biobehav Rev *34*, 148–159.

McKay, B.E., McRory, J.E., Molineux, M.L., Hamid, J., Snutch, T.P., Zamponi, G.W., and Turner, R.W. (2006a). Ca(V)3 T-type calcium channel isoforms differentially distribute to somatic and dendritic compartments in rat central neurons. Eur. J. Neurosci. *24*, 2581–2594.

McKay, B.E., McRory, J.E., Molineux, M.L., Hamid, J., Snutch, T.P., Zamponi, G.W., and Turner, R.W. (2006b). Ca(V)3 T-type calcium channel isoforms differentially distribute to somatic and dendritic compartments in rat central neurons. Eur. J. Neurosci. *24*, 2581–2594.

McRory, J.E., Santi, C.M., Hamming, K.S., Mezeyova, J., Sutton, K.G., Baillie, D.L., Stea, A., and Snutch, T.P. (2001). Molecular and functional characterization of a family of rat brain T-type calcium channels. J. Biol. Chem. *276*, 3999–4011.

Metzger, D., Clifford, J., Chiba, H., and Chambon, P. (1995). Conditional site-specific recombination in mammalian cells using a ligand-dependent chimeric Cre recombinase. Proc Natl Acad Sci U S A *92*, 6991–6995.

Michel, V., Goodyear, R.J., Weil, D., Marcotti, W., Perfettini, I., Wolfrum, U., Kros, C.J., Richardson, G.P., and Petit, C. (2005). Cadherin 23 is a component of the transient lateral links in the developing hair bundles of cochlear sensory cells. Dev. Biol. *280*, 281–294.

Milenkovic, N., Wetzel, C., Moshourab, R., and Lewin, G.R. (2008). Speed and temperature dependences of mechanotransduction in afferent fibers recorded from the mouse saphenous nerve. J. Neurophysiol. *100*, 2771–2783.

Mizuno, K., and Giese, K.P. (2005). Hippocampus-dependent memory formation: do memory type-specific mechanisms exist? J. Pharmacol. Sci. *98*, 191–197.

Molineux, M.L., McRory, J.E., McKay, B.E., Hamid, J., Mehaffey, W.H., Rehak, R., Snutch, T.P., Zamponi, G.W., and Turner, R.W. (2006). Specific T-type calcium channel isoforms are associated with distinct burst phenotypes in deep cerebellar nuclear neurons. Proc. Natl. Acad. Sci. U.S.A. *103*, 5555–5560.

Molliver, D.C., Radeke, M.J., Feinstein, S.C., and Snider, W.D. (1995). Presence or absence of TrkA protein distinguishes subsets of small sensory neurons with unique cytochemical characteristics and dorsal horn projections. J. Comp. Neurol. *361*, 404–416.

Montagna, W. (1977). Morphology of Cutaneous Sensory Receptors. Journal of Investigative Dermatology *69*, 4–7.

Montagnese, C.M., Krebs, J.R., and Meyer, G. (1996). The dorsomedial and dorsolateral forebrain of the zebra finch, Taeniopygia guttata: a Golgi study. Cell Tissue Res. *283*, 263–282.

Moqrich, A., Earley, T.J., Watson, J., Andahazy, M., Backus, C., Martin-Zanca, D., Wright, D.E., Reichardt, L.F., and Patapoutian, A. (2004). Expressing TrkC from the TrkA locus causes a subset of dorsal root ganglia neurons to switch fate. Nat. Neurosci. *7*, 812–818.

Moreau, M.M., Piguel, N., Papouin, T., Koehl, M., Durand, C.M., Rubio, M.E., Loll, F., Richard, E.M., Mazzocco, C., Racca, C., et al. (2010). The planar polarity protein Scribble1 is essential for neuronal plasticity and brain function. J. Neurosci. *30*, 9738–9752.

Morris, A.M., Churchwell, J.C., Kesner, R.P., and Gilbert, P.E. (2012). Selective lesions of the dentate gyrus produce disruptions in place learning for adjacent spatial locations. Neurobiol Learn Mem *97*, 326–331.

Mosca, T.J., Hong, W., Dani, V.S., Favaloro, V., and Luo, L. (2012). Trans-synaptic Teneurin signalling in neuromuscular synapse organization and target choice. Nature *484*, 237–241.

Mosevitsky, M.I. (2005). Nerve ending "signal" proteins GAP-43, MARCKS, and BASP1. Int. Rev. Cytol. *245*, 245–325.

Müller, T., Brohmann, H., Pierani, A., Heppenstall, P.A., Lewin, G.R., Jessell, T.M., and Birchmeier, C. (2002). The homeodomain factor lbx1 distinguishes two major programs of neuronal differentiation in the dorsal spinal cord. Neuron *34*, 551–562.

Murdoch, J.N., Henderson, D.J., Doudney, K., Gaston-Massuet, C., Phillips, H.M., Paternotte, C., Arkell, R., Stanier, P., and Copp, A.J. (2003). Disruption of Scribble (Scrb1) Causes Severe Neural Tube Defects in the Circletail Mouse. Hum. Mol. Genet. *12*, 87–98.

Nelson, M.T., Joksovic, P.M., Perez-Reyes, E., and Todorovic, S.M. (2005a). The endogenous redox agent L-cysteine induces T-type Ca2+ channel-dependent sensitization of a novel subpopulation of rat peripheral nociceptors. J. Neurosci. *25*, 8766–8775.

Nelson, M.T., Joksovic, P.M., Perez-Reyes, E., and Todorovic, S.M. (2005b). The endogenous redox agent L-cysteine induces T-type Ca2+ channel-dependent sensitization of a novel subpopulation of rat peripheral nociceptors. J. Neurosci. *25*, 8766–8775.

Niziolek, P.J., Warman, M.L., and Robling, A.G. (2012). Mechanotransduction in bone tissue: The A214V and G171V mutations in Lrp5 enhance load-induced osteogenesis in a surface-selective manner. Bone *51*, 459–465.

Nógrádi, A., and Vrbová, G. (2000). Anatomy and Physiology of the Spinal Cord.

Nowycky, M.C., Fox, A.P., and Tsien, R.W. (1985). Three types of neuronal calcium channel with different calcium agonist sensitivity. Nature *316*, 440–443.

O'Hagan, R., Chalfie, M., and Goodman, M.B. (2005). The MEC-4 DEG/ENaC channel of Caenorhabditis elegans touch receptor neurons transduces mechanical signals. Nat. Neurosci. *8*, 43–50.

Oakley, R.A., Lefcort, F.B., Plouffe, P., Ritter, A., and Frank, E. (2000). Neurotrophin-3 promotes the survival of a limited subpopulation of cutaneous sensory neurons. Dev. Biol. *224*, 415–427.

Ogris, M., Steinlein, P., Carotta, S., Brunner, S., and Wagner, E. (2001). DNA/polyethylenimine transfection particles: influence of ligands, polymer size, and PEGylation on internalization and gene expression. AAPS PharmSci *3*, E21.

Olausson, H., Lamarre, Y., Backlund, H., Morin, C., Wallin, B.G., Starck, G., Ekholm, S., Strigo, I., Worsley, K., Vallbo, A.B., et al. (2002). Unmyelinated tactile afferents signal touch and project to insular cortex. Nat. Neurosci. *5*, 900–904.

Olausson, H., Cole, J., Rylander, K., McGlone, F., Lamarre, Y., Wallin, B.G., Krämer, H., Wessberg, J., Elam, M., Bushnell, M.C., et al. (2008). Functional role of unmyelinated tactile afferents in human hairy skin: sympathetic response and perceptual localization. Exp Brain Res *184*, 135–140.

Opdecamp, K., Nakayama, A., Nguyen, M.T., Hodgkinson, C.A., Pavan, W.J., and Arnheiter, H. (1997). Melanocyte development in vivo and in neural crest cell cultures: crucial dependence on the Mitf basic-helix-loop-helix-zipper transcription factor. Development *124*, 2377–2386.

Pavlakis, E., Makrygiannis, A.K., Chiotaki, R., and Chalepakis, G. (2008). Differential localization profile of Fras1/Frem proteins in epithelial basement membranes of newborn and adult mice. Histochem. Cell Biol. *130*, 785–793.

Perez-Pinera, P., García-Suarez, O., Germanà, A., Díaz-Esnal, B., de Carlos, F., Silos-Santiago, I., del Valle, M.E., Cobo, J., and Vega, J.A. (2008). Characterization of sensory deficits in TrkB knockout mice. Neurosci. Lett. *433*, 43–47.

Perez-Reyes, E., Cribbs, L.L., Daud, A., Lacerda, A.E., Barclay, J., Williamson, M.P., Fox, M., Rees, M., and Lee, J.H. (1998). Molecular characterization of a neuronal low-voltage-activated T-type calcium channel. Nature *391*, 896–900.

Petrou, P., Pavlakis, E., Dalezios, Y., and Chalepakis, G. (2007). Basement membrane localization of Frem3 is independent of the Fras1/Frem1/Frem2 protein complex within the sublamina densa. Matrix Biol. *26*, 652–658.

Petruska, J.C., Napaporn, J., Johnson, R.D., Gu, J.G., and Cooper, B.Y. (2000). Subclassified acutely dissociated cells of rat DRG: histochemistry and patterns of capsaicin-, proton-, and ATP-activated currents. J. Neurophysiol. *84*, 2365–2379.

Von Philipsborn, A.C., Lang, S., Bernard, A., Loeschinger, J., David, C., Lehnert, D., Bastmeyer, M., and Bonhoeffer, F. (2006). Microcontact printing of axon guidance molecules for generation of graded patterns. Nat Protoc *1*, 1322–1328.

Pinato, G., and Midtgaard, J. (2003). Regulation of granule cell excitability by a low-threshold calcium spike in turtle olfactory bulb. J. Neurophysiol. *90*, 3341–3351.

Powell, K.L., Cain, S.M., Ng, C., Sirdesai, S., David, L.S., Kyi, M., Garcia, E., Tyson, J.R., Reid, C.A., Bahlo, M., et al. (2009). A Cav3.2 T-Type Calcium Channel Point Mutation Has Splice-Variant-Specific Effects on Function and Segregates with Seizure Expression in a Polygenic Rat Model of Absence Epilepsy. J. Neurosci. *29*, 371–380.

Price, M.P., Lewin, G.R., McIlwrath, S.L., Cheng, C., Xie, J., Heppenstall, P.A., Stucky, C.L., Mannsfeldt, A.G., Brennan, T.J., Drummond, H.A., et al. (2000). The mammalian sodium channel BNC1 is required for normal touch sensation. Nature *407*, 1007–1011.

Price, M.P., McIlwrath, S.L., Xie, J., Cheng, C., Qiao, J., Tarr, D.E., Sluka, K.A., Brennan, T.J., Lewin, G.R., and Welsh, M.J. (2001). The DRASIC cation channel contributes to the detection of cutaneous touch and acid stimuli in mice. Neuron *32*, 1071–1083.

Reeh, P.W. (1986). Sensory receptors in mammalian skin in an in vitro preparation. Neurosci. Lett. *66*, 141–146.

Ribak, C.E., Seress, L., and Amaral, D.G. (1985). The development, ultrastructure and synaptic connections of the mossy cells of the dentate gyrus. J. Neurocytol. *14*, 835–857.

Riddle, D.L.D.L. (1997). C. elegans II (Cold Spring Harbor (NY): Cold Spring Harbor Laboratory Press).

Rifkin, J.T., Todd, V.J., Anderson, L.W., and Lefcort, F. (2000a). Dynamic expression of neurotrophin receptors during sensory neuron genesis and differentiation. Dev. Biol. *227*, 465–480.

Rifkin, J.T., Todd, V.J., Anderson, L.W., and Lefcort, F. (2000b). Dynamic expression of neurotrophin receptors during sensory neuron genesis and differentiation. Dev. Biol. *227*, 465–480.

Rugiero, F., Drew, L.J., and Wood, J.N. (2010). Kinetic properties of mechanically activated currents in spinal sensory neurons. J. Physiol. (Lond.) *588*, 301–314.

Savage, C., Hamelin, M., Culotti, J.G., Coulson, A., Albertson, D.G., and Chalfie, M. (1989). mec-7 is a beta-tubulin gene required for the production of 15-protofilament microtubules in Caenorhabditis elegans. Genes Dev. *3*, 870–881.

Schmelz, M., Schmidt, R., Weidner, C., Hilliges, M., Torebjork, H.E., and Handwerker, H.O. (2003). Chemical response pattern of different classes of C-nociceptors to pruritogens and algogens. J. Neurophysiol. *89*, 2441–2448.

Schmidt, R., Schmelz, M., Forster, C., Ringkamp, M., Torebjörk, E., and Handwerker, H. (1995). Novel classes of responsive and unresponsive C nociceptors in human skin. J. Neurosci. *15*, 333–341.

Schwander, M., Kachar, B., and Müller, U. (2010). Review series: The cell biology of hearing. J. Cell Biol. *190*, 9–20.

Scott, A., Hasegawa, H., Sakurai, K., Yaron, A., Cobb, J., and Wang, F. (2011). Transcription factor short stature homeobox 2 is required for proper development of tropomyosin-related kinase B-expressing mechanosensory neurons. J. Neurosci. *31*, 6741–6749.

Scroggs, R.S., and Fox, A.P. (1992). Calcium current variation between acutely isolated adult rat dorsal root ganglion neurons of different size. J. Physiol. (Lond.) *445*, 639–658.

Serbedzija, G.N., Fraser, S.E., and Bronner-Fraser, M. (1990). Pathways of trunk neural crest cell migration in the mouse embryo as revealed by vital dye labelling. Development *108*, 605–612.

Shin, J.-B., Martinez-Salgado, C., Heppenstall, P.A., and Lewin, G.R. (2003). A T-type calcium channel required for normal function of a mammalian mechanoreceptor. Nature Neuroscience *6*, 724–730.

Siemens, J., Lillo, C., Dumont, R.A., Reynolds, A., Williams, D.S., Gillespie, P.G., and Müller, U. (2004). Cadherin 23 is a component of the tip link in hair-cell stereocilia. Nature *428*, 950–955.

Silverman, J.D., and Kruger, L. (1990). Selective neuronal glycoconjugate expression in sensory and autonomic ganglia: relation of lectin reactivity to peptide and enzyme markers. Journal of Neurocytology *19*, 789–801.

Smith, D.M., and Mizumori, S.J.Y. (2006). Hippocampal place cells, context, and episodic memory. Hippocampus *16*, 716–729.

Snutch, T.P., Leonard, J.P., Gilbert, M.M., Lester, H.A., and Davidson, N. (1990). Rat brain expresses a heterogeneous family of calcium channels. Proc Natl Acad Sci U S A *87*, 3391–3395.

Snutch, T.P., Peloquin, J., Mathews, E., and McRory, J. (2005). Molecular Properties of Voltage-Gated Calcium Channels - Madame Curie Bioscience Database - NCBI Bookshelf.

Soriano, P. (1999). Generalized lacZ expression with the ROSA26 Cre reporter strain. Nat. Genet. *21*, 70–71.

Splawski, I., Yoo, D.S., Stotz, S.C., Cherry, A., Clapham, D.E., and Keating, M.T. (2006). CACNA1H mutations in autism spectrum disorders. J. Biol. Chem. *281*, 22085–22091.

Srinivasan, M.A., and Dandekar, K. (1996). An investigation of the mechanics of tactile sense using two-dimensional models of the primate fingertip. J Biomech Eng *118*, 48–55.

Srivastava, U.C., Chand, P., and Maurya, R.C. (2007). Cytoarchitectonic organization and morphology of the cells of hippocampal complex in strawberry finch, Estrilda amandava. Cell. Mol. Biol. (Noisy-le-grand) *53*, 103–120.

Stanfield, C.L. (2012). Principles of Human Physiology, Books a la Carte Plus MasteringA&P with eText -- Access Card Package (Benjamin Cummings).

Stauffer, E.A., and Holt, J.R. (2007). Sensory transduction and adaptation in inner and outer hair cells of the mouse auditory system. J. Neurophysiol. *98*, 3360–3369.

Stucky, C.L., Shin, J.-B., and Lewin, G.R. (2002). Neurotrophin-4: A Survival Factor for Adult Sensory Neurons. Current Biology *12*, 1401–1404.

Su, H., Sochivko, D., Becker, A., Chen, J., Jiang, Y., Yaari, Y., and Beck, H. (2002). Upregulation of a T-type Ca2+ channel causes a long-lasting modification of neuronal firing mode after status epilepticus. J. Neurosci. *22*, 3645–3655.

Sun, Y., Villa-Diaz, L.G., Lam, R.H.W., Chen, W., Krebsbach, P.H., and Fu, J. (2012). Mechanics regulates fate decisions of human embryonic stem cells. PLoS ONE *7*, e37178.

Suster, M.L., and Bate, M. (2002). Embryonic assembly of a central pattern generator without sensory input. Nature *416*, 174–178.

Suzuki, N., Fukushi, M., Kosaki, K., Doyle, A.D., de Vega, S., Yoshizaki, K., Akazawa, C., Arikawa-Hirasawa, E., and Yamada, Y. (2012). Teneurin-4 is a novel regulator of oligodendrocyte differentiation and myelination of small-diameter axons in the CNS. J. Neurosci. *32*, 11586–11599.

Takashima, Y., Ma, L., and McKemy, D.D. (2010). The development of peripheral cold neural circuits based on TRPM8 expression. Neuroscience *169*, 828–842.

Talley, E.M., Cribbs, L.L., Lee, J.-H., Daud, A., Perez-Reyes, E., and Bayliss, D.A. (1999). Differential Distribution of Three Members of a Gene Family Encoding Low Voltage-Activated (T-Type) Calcium Channels. J. Neurosci. *19*, 1895–1911.

Talley, E.M., Solórzano, G., Depaulis, A., Perez-Reyes, E., and Bayliss, D.A. (2000a). Low-voltage-activated calcium channel subunit expression in a genetic model of absence epilepsy in the rat. Brain Res. Mol. Brain Res. *75*, 159–165.

Talley, E.M., Solórzano, G., Depaulis, A., Perez-Reyes, E., and Bayliss, D.A. (2000b). Low-voltage-activated calcium channel subunit expression in a genetic model of absence epilepsy in the rat. Brain Res. Mol. Brain Res. *75*, 159–165.

Timmer, J.R., Mak, T.W., Manova, K., Anderson, K.V., and Niswander, L. (2005). Tissue morphogenesis and vascular stability require the Frem2 protein, product of the mouse myelencephalic blebs gene. Proc. Natl. Acad. Sci. U.S.A. *102*, 11746–11750.

Todd, A.J. (2010). Neuronal circuitry for pain processing in the dorsal horn. Nat Rev Neurosci *11*, 823–836.

Todorovic, S.M., Jevtovic-Todorovic, V., Meyenburg, A., Mennerick, S., Perez-Reyes, E., Romano, C., Olney, J.W., and Zorumski, C.F. (2001). Redox Modulation of T-Type Calcium Channels in Rat Peripheral Nociceptors. Neuron *31*, 75–85.

Tömböl, T., Davies, D.C., Németh, A., Alpár, A., and Sebestény, T. (2000). A golgi and a combined Golgi/GABA immunogold study of local circuit neurons in the homing pigeon hippocampus. Anat. Embryol. *201*, 181–196.

Tracey, W.D., Jr, Wilson, R.I., Laurent, G., and Benzer, S. (2003). painless, a Drosophila gene essential for nociception. Cell *113*, 261–273.

Treede, R.D., Meyer, R.A., Raja, S.N., and Campbell, J.N. (1992). Peripheral and central mechanisms of cutaneous hyperalgesia. Prog. Neurobiol. *38*, 397–421.

Tros de Ilarduya, C., Sun, Y., and Düzgüneş, N. (2010). Gene delivery by lipoplexes and polyplexes. Eur J Pharm Sci *40*, 159–170.

Tsien, R.W., Lipscombe, D., Madison, D.V., Bley, K.R., and Fox, A.P. (1988). Multiple types of neuronal calcium channels and their selective modulation. Trends in Neurosciences *11*, 431–438.

Vallbo, A.B., Olausson, H., and Wessberg, J. (1999). Unmyelinated afferents constitute a second system coding tactile stimuli of the human hairy skin. J. Neurophysiol. *81*, 2753–2763.

Verpy, E., Leibovici, M., Zwaenepoel, I., Liu, X.Z., Gal, A., Salem, N., Mansour, A., Blanchard, S., Kobayashi, I., Keats, B.J., et al. (2000). A defect in harmonin, a PDZ

domain-containing protein expressed in the inner ear sensory hair cells, underlies Usher syndrome type 1C. Nat. Genet. *26*, 51–55.

Walker, R.G., Willingham, A.T., and Zuker, C.S. (2000). A Drosophila mechanosensory transduction channel. Science *287*, 2229–2234.

Wall, N.R., Wickersham, I.R., Cetin, A., De La Parra, M., and Callaway, E.M. (2010). Monosynaptic circuit tracing in vivo through Cre-dependent targeting and complementation of modified rabies virus. Proc. Natl. Acad. Sci. U.S.A. *107*, 21848–21853.

Wang, R., and Lewin, G.R. (2011). The Cav3.2 T-type calcium channel regulates temporal coding in mouse mechanoreceptors. J Physiol *589*, 2229–2243.

Wang, K.H., Brose, K., Arnott, D., Kidd, T., Goodman, C.S., Henzel, W., and Tessier-Lavigne, M. (1999). Biochemical purification of a mammalian slit protein as a positive regulator of sensory axon elongation and branching. Cell *96*, 771–784.

Wen, X., Li, Z., Chen, Z., Fang, Z., Yang, C., Li, H., and Zeng, Y. (2006). Intrathecal administration of Cav3.2 and Cav3.3 antisense oligonucleotide reverses tactile allodynia and thermal hyperalgesia in rats following chronic compression of dorsal root of ganglion. Acta Pharmacol. Sin. *27*, 1547–1552.

Wende, H., Lechner, S.G., Cheret, C., Bourane, S., Kolanczyk, M.E., Pattyn, A., Reuter, K., Munier, F.L., Carroll, P., Lewin, G.R., et al. (2012). The Transcription Factor C-Maf Controls Touch Receptor Development and Function. Science *335*, 1373–1376.

Wetzel, C., Hu, J., Riethmacher, D., Benckendorff, A., Harder, L., Eilers, A., Moshourab, R., Kozlenkov, A., Labuz, D., Caspani, O., et al. (2007). A stomatin-domain protein essential for touch sensation in the mouse. Nature *445*, 206–209.

Wicks, S.R., and Rankin, C.H. (1997). Effects of tap withdrawal response habituation on other withdrawal behaviors: the localization of habituation in the nematode Caenorhabditis elegans. Behav. Neurosci. *111*, 342–353.

Wilson, S.R., Gerhold, K.A., Bifolck-Fisher, A., Liu, Q., Patel, K.N., Dong, X., and Bautista, D.M. (2011). TRPA1 is required for histamine-independent, Mas-related G protein-coupled receptor-mediated itch. Nat Neurosci *14*, 595–602.

Xavier, G.F., Oliveira-Filho, F.J., and Santos, A.M. (1999). Dentate gyrus-selective colchicine lesion and disruption of performance in spatial tasks: difficulties in "place strategy" because of a lack of flexibility in the use of environmental cues? Hippocampus *9*, 668–681.

Xia, A., Gao, S.S., Yuan, T., Osborn, A., Bress, A., Pfister, M., Maricich, S.M., Pereira, F.A., and Oghalai, J.S. (2010). Deficient forward transduction and enhanced reverse transduction in the alpha tectorin C1509G human hearing loss mutation. Dis Model Mech *3*, 209–223.

Xiao, T., Staub, W., Robles, E., Gosse, N.J., Cole, G.J., and Baier, H. (2011). Assembly of lamina-specific neuronal connections by slit bound to type IV collagen. Cell *146*, 164–176.

Xie, J., Price, M.P., Berger, A.L., and Welsh, M.J. (2002). DRASIC contributes to pH-gated currents in large dorsal root ganglion sensory neurons by forming heteromultimeric channels. J. Neurophysiol. *87*, 2835–2843.

Xie, X., Van Deusen, A.L., Vitko, I., Babu, D.A., Davies, L.A., Huynh, N., Cheng, H., Yang, N., Barrett, P.Q., and Perez-Reyes, E. (2007). Validation of high throughput screening assays against three subtypes of Ca(v)3 T-type channels using molecular and pharmacologic approaches. Assay Drug Dev Technol *5*, 191–203.

Yan, Z., Zhang, W., He, Y., Gorczyca, D., Xiang, Y., Cheng, L.E., Meltzer, S., Jan, L.Y., and Jan, Y.N. (2013). Drosophila NOMPC is a mechanotransduction channel subunit for gentle-touch sensation. Nature *493*, 221–225.

Yates, L.L., Schnatwinkel, C., Hazelwood, L., Chessum, L., Paudyal, A., Hilton, H., Romero, M.R., Wilde, J., Bogani, D., Sanderson, J., et al. (2013). Scribble is required for normal epithelial cell-cell contacts and lumen morphogenesis in the mammalian lung. Dev. Biol. *373*, 267–280.

Young, T.R., and Leamey, C.A. (2009). Teneurins: important regulators of neural circuitry. Int. J. Biochem. Cell Biol. *41*, 990–993.

Zhang, F., Gradinaru, V., Adamantidis, A.R., Durand, R., Airan, R.D., de Lecea, L., and Deisseroth, K. (2010a). Optogenetic interrogation of neural circuits: technology for probing mammalian brain structures. Nat Protoc *5*, 439–456.

Zhang, H.Y., Zheng, L.F., Yi, X.N., Chen, Z.B., He, Z.P., Zhao, D., Zhang, X.F., and Ma, Z.J. (2010b). Slit1 promotes regenerative neurite outgrowth of adult dorsal root ganglion neurons in vitro via binding to the Robo receptor. J. Chem. Neuroanat. *39*, 256–261.

Zhang, S., Arnadottir, J., Keller, C., Caldwell, G.A., Yao, C.A., and Chalfie, M. (2004). MEC-2 Is Recruited to the Putative Mechanosensory Complex in C. elegans Touch Receptor Neurons through Its Stomatin-like Domain. Current Biology *14*, 1888–1896.

Zhong, L., Hwang, R.Y., and Tracey, W.D. (2010). Pickpocket is a DEG/ENaC protein required for mechanical nociception in Drosophila larvae. Curr. Biol. *20*, 429–434.

4. APPENDIX

4.1. Apendix I. List of candidate proteins to tether protein.

REFSEQ PROTEIN	Gene Name	SEQUENCE LENGTH (aa)	Blisterase Site No.
NP_073725	SUSHI, VON WILLEBRAND FACTOR TYPE A, EGF AND PENTRAXIN DOMAIN CONTAINING 1	3567	3*
NP_031489	AORTIC PREFERENTIALLY EXPRESSED GENE 1	3262	7*
NP_660258	ALSTROM SYNDROME 1 HOMOLOG (HUMAN)	3251	2* towards C-term
NP_766450	FRAS1 RELATED EXTRACELLULAR MATRIX PROTEIN 2	3160	2 beginning and end, only end is accesible
NP_031525	ATAXIA TELANGIECTASIA MUTATED HOMOLOG (HUMAN)	3066	2* middle
NP_034311	FIBRILLIN 2	2907	2 beginning and end
NP_035986	ODD OZ/TEN-M HOMOLOG 2 (DROSOPHILA)	2764	middle*2
NP_035985	ODD OZ/TEN-M HOMOLOG 1 (DROSOPHILA)	2731	1*
NP_035987	ODD OZ/TEN-M HOMOLOG 3 (DROSOPHILA)	2715	2*
NP_780438	SERINE/ARGININE REPETITIVE MATRIX 2	2703	11
XP_919034	IMMUNOGLOBULIN SUPERFAMILY, MEMBER 10	2594	1
NP_109620	LPS-RESPONSIVE BEIGE-LIKE ANCHOR	2579	2
XP_921375	RIKEN CDNA 5430411K18 GENE	2572	1
NP_619613	STABILIN 1	2571	1 after signal peptide
XP_126005	POLYCYSTIC KIDNEY DISEASE 1 LIKE 1	2520	1 maybe intracellular
NP_082158	CAPICUA HOMOLOG (DROSOPHILA)	2510	2 sites both intracellular
NP_034567	HUMAN IMMUNODEFICIENCY VIRUS TYPE I ENHANCER BINDING PROTEIN 2	2430	2 sites both intracellular
NP_780447	RAP1 INTERACTING FACTOR 1 HOMOLOG (YEAST)	2419	3* middle
NP_0010179 85	EXPRESSED SEQUENCE AU020772	2323	2* beginning and middle
NP_032003	COAGULATION FACTOR VIII	2319	2* middle prob extra
NP_032742	NOTCH GENE HOMOLOG 3 (DROSOPHILA)	2318	6* end and middle outside but 2 inside
XP_489612	RIKEN CDNA 5730405K23 GENE	2274	1* towards end

NP_035919	ADENOMATOSIS POLYPOSIS COLI 2	2274	1* towards C term, perhaps outside
NP_035935	DEATH INDUCER-OBLITERATOR 1	2256	4* beginning and end
NP_061218	GOLGI AUTOANTIGEN, GOLGIN SUBFAMILY A, 4	2238	3* all structually inaccesible
NP_808547	RIKEN CDNA 6720466O15 GENE	2193	1* at the beginning
NP_038878	ATP-BINDING CASSETTE, SUB-FAMILY A (ABC1), MEMBER 7	2159	1* in middle but masked
NP_033373	TECTORIN ALPHA	2155	1*site at end but extra
NP_853522	POLYCYSTIC KIDNEY DISEASE 1 LIKE 3	2151	1* site but intra
NP_940810	TUDOR DOMAIN CONTAINING 6	2134	1* middle
NP_038703	SPECTRIN BETA 1	2128	2 but both inaccesible
NP_766363	PLEXIN B1	2119	1* towards end in putative cytoplasmic domain
NP_035737	TENASCIN C	2110	4* only two accesinble beginning and end
NP_031795	DELETED IN MALIGNANT BRAIN TUMORS 1	2085	1* just before TM extra but inaccesible
NP_034950	MULTIPLE PDZ DOMAIN PROTEIN	2055	1* at end
NP_112451	DOWN SYNDROME CELL ADHESION MOLECULE	2013	3* but all intra or TM
NP_742120	CILIARY ROOTLET COILED-COIL, ROOTLETIN	2009	4* all structurally inaccesible
NP_035059	NOTCH GENE HOMOLOG 4 (DROSOPHILA)	1964	2* intracellular
NP_619615	POLYCYSTIC KIDNEY AND HEPATIC DISEASE 1-LIKE 1	1944	1* in large protein towards end
NP_803180	A DISINTEGRIN-LIKE AND METALLOPEPTIDASE (REPROLYSIN TYPE) WITH THROMBOSPONDIN TYPE 1 MOTIF, 20	1906	2* at beginning
XP_129214	PROPROTEIN CONVERTASE SUBTILISIN/KEXIN TYPE 5	1877	!* at beginning
NP_056549	PROCOLLAGEN, TYPE V, ALPHA 1	1838	1* towards end but extra
NP_536707	STEREOCILIN	1809	1* site
NP_032935	PERIPLAKIN	1755	no accesible site
NP_034536	HEMOLYTIC COMPLEMENT	1680	1* middle
NP_034016	CADHERIN EGF LAG SEVEN-PASS G-TYPE RECEPTOR 1	1671	2* extracellular
NP_033908	COMPLEMENT COMPONENT 3	1663	1* middle
XP_287555	GENE MODEL 837, (NCBI)	1645	1* extra, but inaccesible
NP_671753	ATP-BINDING CASSETTE TRANSPORTER SUB-FAMILY A MEMBER 9	1623	2*start and end
NP_694785	ATP-BINDING CASSETTE, SUB-FAMILY A (ABC1), MEMBER 8A	1620	1* at start

NP_659117	PECANEX-LIKE 3 (DROSOPHILA)	1620	1* in extra or intra cell loop
NP_038879	ATP-BINDING CASSETTE, SUB-FAMILY A (ABC1), MEMBER 8B	1620	1* at start
NP_598850	SCRIBBLED HOMOLOG (DROSOPHILA)	1612	1* at end prob not extra
NP_062286	ROUNDABOUT HOMOLOG 1 (DROSOPHILA)	1612	1 in middle proba in extra
NP_780710	EXPRESSED SEQUENCE AI605170	1600	1* at beginning
NP_035966	LAMININ GAMMA 3	1581	
NP_663502	MAP-KINASE ACTIVATING DEATH DOMAIN	1577	1* near beginning
NP_066379	ATP-BINDING CASSETTE, SUB-FAMILY C (CFTR/MRP), MEMBER 9	1546	1* site near beginn intra or extra
NP_941991	LATROPHILIN 3	1537	1* site but intra
NP_056563	SLIT HOMOLOG 1 (DROSOPHILA)	1531	1* inaccesible towards end
NP_848919	SLIT HOMOLOG 2 (DROSOPHILA)	1521	2*middle and end both inaccesible
NP_056616	NEUROPATHY TARGET ESTERASE	1470	1*at end
NP_032507	LAMININ, ALPHA 2	1457	
NP_067352	VPS10 DOMAIN RECEPTOR PROTEIN SORCS 1	1426	
NP_064303	LATENT TRANSFORMING GROWTH FACTOR BETA BINDING PROTEIN 1	1389	
NP_032424	INTEGRIN ALPHA 7	1379	
NP_035962	INSULIN RECEPTOR-RELATED RECEPTOR	1378	
NP_038593	INTEGRIN ALPHA 3	1378	
NP_059088	CADHERIN EGF LAG SEVEN-PASS G-TYPE RECEPTOR 2	1375	
NP_071707	TENASCIN R	1358	
NP_032507	LAMININ, ALPHA 2	1355	
NP_032425	INTEGRIN, ALPHA E, EPITHELIAL-ASSOCIATED	1323	
NP_808507	TENASCIN N	1306	
XP_144060	RIKEN CDNA 4931403E03 GENE	1300	1*in middle
NP_071714	CALSYNTENIN 2	1296	1* after signal peptide
NP_058062	CONTACTIN ASSOCIATED PROTEIN 1	1285	
NP_058615	PROCOLLAGEN, TYPE V, ALPHA 3	1285	
NP_032511	LAMININ, GAMMA 2	1257	
NP_783574	A DISINTEGRIN-LIKE AND METALLOPEPTIDASE (REPROLYSIN TYPE) WITH THROMBOSPONDIN TYPE 1 MOTIF, 2	1256	
NP_032510	LAMININ, BETA 3	1253	
NP_899014	PHOSPHOLIPASE C-LIKE 3	1247	
NP_795904	RIKEN CDNA C030017F07 GENE	1242	
NP_569715	PROTOCADHERIN 18	1222	
NP_059074	PROTOCADHERIN 12	1191	
XP_919694	RIKEN CDNA 4931403E03 GENE	1188	

NP_080957	RIKEN CDNA 0610010D24 GENE	1184	
NP_775561	CARTILAGE INTERMEDIATE LAYER PROTEIN, NUCLEOTIDE PYROPHOSPHOHYDROLASE	1180	
NP_033100	MACROPHAGE STIMULATING 1 RECEPTOR (C-MET-RELATED TYROSINE KINASE)	1178	
NP_796347	HYPOTHETICAL PROTEIN 5330438O12	1173	
NP_062332	NEPHROSIS 1 HOMOLOG, NEPHRIN (HUMAN)	1168	
NP_579933	GLUTAMATE RECEPTOR, IONOTROPIC, DELTA 2 (GRID2) INTERACTING PROTEIN 1	1159	
NP_777365	INTERPHOTORECEPTOR MATRIX PROTEOGLYCAN 2	1140	
NP_848919	SLIT HOMOLOG 2 (DROSOPHILA)	1134	
NP_032538	LOW DENSITY LIPOPROTEIN RECEPTOR-RELATED PROTEIN 1	1133	
NP_035344	PROTEIN TYROSINE PHOSPHATASE, RECEPTOR TYPE, U	1130	
NP_742050	A DISINTEGRIN-LIKE AND METALLOPETIDASE (REPROLYSIN TYPE) WITH THROMBOSPONDIN TYPE 1 MOTIF, 16	1128	
NP_079972	SORTILIN-RELATED VPS10 DOMAIN CONTAINING RECEPTOR 3	1127	
NP_062683	MEMBRANE-BOUND TRANSCRIPTION FACTOR PEPTIDASE, SITE 1	1126	
NP_033076	RET PROTO-ONCOGENE	1115	
NP_766054	A DISINTEGRIN-LIKE AND METALLOPEPTIDASE (REPROLYSIN TYPE) WITH THROMBOSPONDIN TYPE 1 MOTIF, 18	1114	
NP_034834	LEPTIN RECEPTOR	1095	
NP_112455	TOLL-LIKE RECEPTOR 9	1092	
NP_056563	SLIT HOMOLOG 1 (DROSOPHILA)	1053	
NP_033009	PROTEIN TYROSINE PHOSPHATASE, RECEPTOR TYPE, K	1053	
NP_766532	INTEGRIN, ALPHA E, EPITHELIAL-ASSOCIATED	1052	
NP_598530	RIKEN CDNA 1500004I01 GENE	1038	
NP_666258	LEPTIN RECEPTOR	1038	
NP_569722	GLUTAMATE RECEPTOR, IONOTROPIC, NMDA3B	1035	
NP_033010	PROTEIN TYROSINE PHOSPHATASE, RECEPTOR TYPE,	1024	

	M		
NP_032740	NOTCH GENE HOMOLOG 1 (DROSOPHILA)	1022	
NP_536685	CADHERIN EGF LAG SEVEN-PASS G-TYPE RECEPTOR 3	1021	
NP_783572	RIKEN CDNA 2310046A13 GENE	1003	
NP_032509	LAMININ, BETA 2	1003	
NP_032617	MET PROTO-ONCOGENE	104	
NP_0010013 22	A DISINTEGRIN-LIKE AND METALLOPEPTIDASE (REPROLYSIN TYPE) WITH THROMBOSPONDIN TYPE 1 MOTIF, 13		
NP_0010144 23	RIKEN CDNA 5033411B22 GENE		
NP_0010251 56	CYSTEINE RICH BMP REGULATOR 2 (CHORDIN LIKE)		
NP_031592	BACULOVIRAL IAP REPEAT-CONTAINING 6		
NP_031758	PROCOLLAGEN, TYPE XVII, ALPHA 1		
NP_031815	CHONDROITIN SULFATE PROTEOGLYCAN 3		
NP_031857	DELETED IN COLORECTAL CARCINOMA		
NP_031964	EPH RECEPTOR A6		
NP_032019	FIBRILLIN 1		
NP_032055	FMS-LIKE TYROSINE KINASE 4		
NP_032198	GLUTAMATE RECEPTOR, IONOTROPIC, NMDA2D (EPSILON 4)		
NP_032403	LEUCINE-RICH REPEATS AND IMMUNOGLOBULIN-LIKE DOMAINS 1		
NP_033100	MACROPHAGE STIMULATING 1 RECEPTOR (C-MET-RELATED TYROSINE KINASE)		
NP_033126	REPETIN		
NP_033766	AE BINDING PROTEIN 1		
NP_034243	EPIDERMAL GROWTH FACTOR		
NP_034251	EUKARYOTIC TRANSLATION INITIATION FACTOR 2 ALPHA KINASE 3		
NP_034439	GNAS (GUANINE NUCLEOTIDE BINDING PROTEIN, ALPHA STIMULATING) COMPLEX LOCUS		
NP_034439	GNAS (GUANINE NUCLEOTIDE BINDING PROTEIN, ALPHA STIMULATING) COMPLEX LOCUS		
NP_034643	INSULIN-LIKE GROWTH FACTOR I RECEPTOR		
NP_034718	JAGGED 2		
NP_034742	KINASE INSERT DOMAIN PROTEIN RECEPTOR		
NP_034742	KINASE INSERT DOMAIN PROTEIN RECEPTOR		
NP_035838	VON WILLEBRAND FACTOR HOMOLOG		
NP_038593	INTEGRIN ALPHA 3		
NP_038850	JAGGED 1		

4.2.   LIST OF FIGURES

4.3.   LIST OF TABLES

DECLARATION

This project was conducted and finished in the group of "Molecular physiology of somatic sensation" in the Max Delbrück Zentrum für Molekulare Medizin under the supervision of Prof. Dr. Gary R. Lewin. This thesis is submitted to the Department of Biology, Chemistry and Pharmacy of Freie Universität Berlin to obtain the academic degree of Doctor rerum naturalium (Dr. rer. nat). It has not been submitted for any other degree of any examining body. Except where specifically mentioned, it is all the work of the author.

Berlin, 2013